Molecular Expression of Recombinant Apoptin *in planta* and Preliminary Evaluation of Biological Characteristics of Plant-Made Apoptin on Cancerous Cells

CHAN XIAO YING

Thesis submitted to The University of Nottingham

for the degree of Doctor of Philosophy

FEBRUARY 2017

Abstract

Apoptin, a potential anticancer candidate, selectively kills tumour or transformed cells but remains harmless to normal and non-transformed cells. Besides, apoptin-induced apoptosis is independent of p53 apoptosis pathway, which is always mutated in cancer cells during tumorigenesis or after radiotherapy. This has made apoptin becoming more pharmacological valuable. In this study, the general aim was to develop a plant-derived apoptin which offers a safer and more cost-effective treatment for cancer patients. The scope of the study focused on the production of recombinant apoptin in a plant-based system and preliminary bioactivity evaluation of the purified plant-derived apoptin on human lung cancer adenocarcinoma A549 cells. Recombinant apoptin was expressed in *Nicotiana benthamiana* as apoptin alone, in fusion to green fluorescent protein (GFP) as well as in fusion to lichenase (Lic) to increase the expression of recombinant protein in soluble fraction. Recombinant apoptin was also in fusion to H22 single chain antibody and epidermal growth factor (EGF) in order to target recombinant H22-apoptin and EGF-apoptin to cancer cells overexpressed with immunoglobulin G (IgG) receptor (CD64) and EGF receptors. Expression of recombinant apoptin was detected in *N. benthamiana* successfully, however, high amount of soluble protein was obtained in plants infiltrated with recombinant GFP-apoptin (gene casette: PR-GFP-VP3-HK) and EGF-apoptin (gene casette: PR-EGF-CatAd-VP3-HK) that targeted the recombinant proteins to endoplasmic reticulum (ER). Protein purification using immobilised metal affinity chromatography (IMAC) recovered recombinant GFP-apoptin (GFP-VP3-HK) and EGF-apoptin (EGF-CatAd-VP3-HK) at a low purity when recombinant proteins were purified in a non-denaturing condition. Host cell protein contamination was not able to be removed when second chromatography and acid precipitation method were used. However, recombinant GFP-apoptin (GFP-VP3-H) and lichenase-apoptin (Lic-VP3-H) without targeted to specific cellular compartment were purified at a good purity using IMAC. Recombinant GFP-VP3-H extracted in a denaturing condition was successfully refolded without an addition of chemical additives while recombinant Lic-VP3-H required triton to refold the protein. In cell-based study, enzyme-linked immunosorbent assay (ELISA) showed that apoptin interacted with EGF receptors as well as A549 cells which finding is the first of its kind in report but with an unverified speculation. On the other hand, nuclear localisation activity and a few apoptosis-associated morphological features were observed in cells microinjected with recombinant GFP-VP3-H. Meanwhile, recombinant EGF-VP3-HK showed a dose-dependent growth inhibitory effect at higher concentration and caused the loss

of mitochondrial membrane potential (MMP) in treated A549 cells. However, internalisation of recombinant EGF-VP3-HK requires a further study for confirmation. Considering the findings on MMP and caspase 3/7 assays were not convincing enough, further evaluations are necessitated in order to verify the apoptosis events induced by the recombinant GFP-VP3-H and EGF-VP3-HK. Nonetheless, this study has heralded a new milestone for apoptin research by which its protein has been successfully produced in plants and some preliminary biological characteristics have been explored at a certain extent.

Acknowledgements

Foremost, I would like to express my greatest appreciation to my principle supervisor, Professor Sandy Loh Hwei San, who guided me through the whole study. I would like to thank for her kindness to share valuable time and knowledge with me during these 5 years of study. I had also been acquired a lot of chances for learning and developing myself in addition to the expertise required for the laboratory works.

I would also like to extend my sincere gratitude to my co-supervisors, Professor Vidadi Yusibov, Dr Konstantin Musiychuk and Dr Yoko Shoji, who had contributed their valuable time and technical guidance in this project. The financial support provided by Fraunhofer Center for Molecular Biotechnology FhCMB (USA) is highly appreciated. Besides, I would also like to present my gratitude to all colleagues from Molecular Engineering and Expression, Protein Biochemistry and Immunology groups in FhCMB, who had always been giving unlimited support and help when I performed my study in the laboratory.

A great appreciation is also conveyed to Dr Song Jia Ling from University of Delaware, USA. She had shared her time, expertise and knowledge on microinjection with me when I performed microinjection work in her laboratory. It is a great pleasure to meet and learn from her although it was just a short period of time.

I am also grateful to Ministry of Higher education (MOHE) since this project is also partially sponsored by MyBrain 15 scheme. The scholarship provided by MOHE had given me a relatively stable life.

Last but not least, I would like to thank all my friends from The University of Nottingham providing me companionship and support throughout the 5 years of study.

List of Abbreviations

A. tumefaciens	*Agrobacterium tumefaciens*
NNK	4-(methylnitrosamino)-1-(3-pyridyl)-1-butanone
z-DEVD	amino acid aspartate-glutamate-valine-aspartate
APC/C	anaphase-promoting complex/cyclosome
Ang	angiopoietin
AIF	Apoptosis-inducing factor
AMV	Avian Myeloblastosis Virus
bp	base pair
BSE	bovine spongiform encephalopathy
MCF-7	breast tumour
CAD	caspase-activated DNAse
CPPs	cell penetrating peptides
CAV	Chicken Anemia Virus
CTB	cholera toxin B
CRM1	chromosomal maintenance 1
CP	coat protein
CAIs	codon adaptation indices
HT29	colon carcinoma
CV	column volume
CCU	cytosolic cleavable unit
Da	Dalton

dpi	days post infiltration
DD	death domain
DED	Death effector domain
DISC	death-inducing signaling complex
DEDAF	DED associated factor
°C	degree celsius
DNA	deoxyribonucleic acid
DIC	differential interference contrast
ENC	effective number of codons
ELP	elastin like protein
ER	endoplasmic reticulum
ECU	endosomal cleavable unit
Ent	enterokinase
ELISA	enzyme-linked immunosorbent assay
EGF	epidermal growth factor
EGFR	epidermal growth factor receptors
FSK-1	epidermal keratinocytes
KDEL	ER retention signal
E. coli	Escherichia coli
FasL	Fas ligand
FADD	Fas-associated death domain protein
FBS	fetal bovine serum

VH25	fibroblasts cell
FL-SEM	fluorescence scanning electron microscope
GST	glutathione S-transferase
g	gram
GFP	green fluorescent protein
GuHCl	Guanidium hypochloride
HepG2	hepatoma
HCP	host cell proteins
HIV	Human immunodeficiency virus
HPV	Human papillomavirus
HUVEC	human umbilical cord vascular endothelial cells
Hip-1	Huntingtin-interacting protein 1
HIC	hydrophobic interaction chromatography
IMAC	immobilised metal affinity chromatography
IF	immunofluorescence
CD64	immunoglobulin G (IgG) receptor
importins	IMPs
inHg	inch Mercury
IBDV	Infectious Bursal Disease Virus
IEX	ion-exchanged chromatography
G401	kidney rhabdoid tumour
k	kilo

KRAS	Kirsten rat sarcoma viral oncogene
LB	Left border
LRR	leucine rich region
LRS	leucine rich regions
Lic	lichenase
Lic-VP3-H	Lichenase-apoptin
l	litre
ALK	lymphoma kinase
MBP	maltose binding proten
MTS	membrane transfer sequence
MET	mesenchymal epithelial transition factor
mRNA	messenger RNA
m	milli
MMP	mitochondrial membrane potential
M	Molar
Cos-7	monkey SV40-transformed kidney cells
MP	movement protein
MALS	multi-angle light scattering
K562	myeloid leukemia
N. benthamiana	Nicotiana benthamiana
NSCLC	non-small cell lung cancer
NES	nuclear export signal

NLS	nuclear localization signal
Saos-2	osteosarcoma
ORFs	overlapping open reading frames
PBS-T	PBS-Tween
PTD	peptide transfer domains
Ppil3	peptidyl-prolyl isomerase–like 3
PBS	phosphate-buffered saline
PI3	phosphatidylinositol 3 kinase
PAH	polycyclic aromatic hydrocarbons
PES	polyethersulfone
PCR	polymerase chain reaction
PTGS	post transcriptional gene silencing
PML	promyelocytic leukemia protein
PI	Propidium iodide
PTD4	protein transduction domain 4
bcl-2	proto-oncogenes
REF	rat embryo fibroblasts
xg	rcf (relative centrifugal force)
EGF-VP3-HK	recombinant EGF-apoptin
GFP-VP3-H	recombinant GFP-apoptin
RE	Restriction enzyme
RPC	reverse phase chromatography

rpm	Revolutions per minute
RB	Right border
RISC	RNA-induced silencing complex
SEC	size exclusion chromatography
SLCC	small lung cell carcinoma
HSMC	smooth muscle cells
H_2SO_4	sulphuric acid
TMV	tobacco mosaic viral
PR1a	tobacco pathogenesis related protein 1a
TP	total protein extract
TSP-T	total soluble protein with 0.5% triton
TAT	trans-activator protein
TRAIL	tumor necrosis factor-related apoptosis-inducing ligand
TNF-R	tumour necrosis factor receptor
TNF-α	tumour necrosis factor α
p53	Tumour suppressor gene
UPR	unfolded protein response
VEGF	vascular endothelial growth factor
VP1	Viral Protein 1
VP2	Viral Protein 2
VP3	Viral Protein 3
V	Voltage

v	volume
w	weight

List of figures

List of tables

Table of contents

Chapter 1

Introduction

Chicken Anemia Virus (CAV), a member of Gyrovirus, was first isolated in Japan in year 1979. Severe anemia, atrophy of lymphoid as well as hemorrhages are the symptoms observed during viral infection (Noteborn[b] and Koch, 1994). Viral Protein 3 (VP3) of CAV, a non-structural 14 kDa small protein, is the main candidate responsible for the destruction of erythroblastoid cells and cortical thymocytes that leads to anemia and immunodeficiency symptoms. Depletion of both erythroblastoid cells and cortical thymocytes was found to be the result of apoptosis induced by VP3. Due to the induction of apoptosis by VP3 in CAV infected or transformed chicken cells, VP3 was named "apoptin" by Noteborn and his colleagues in 1995. Other than transformed or CAV susceptible chicken cells, tumourigenic and transformed mammalian cells are also susceptible to apoptin (Noteborn *et al*., 1998). However, most of the normal and non-transformed mammalian cells are not susceptible to apoptin. Apoptin consists of 121 amino acids and three important functional regions are found on this small protein, including a leucine rich region (LRR), a bipartite nuclear localisation signal (NLS) and a nuclear export signal (NES).

To date, more than 70 cancer cell lines are susceptible to apoptin, including breast tumour (MCF-7), osteosarcoma (Saos-2), small lung cell carcinoma (SLCC), hepatoma (HepG2), kidney rhabdoid tumour (G401), myeloid leukemia (K562), colon carcinoma (HT29) and etc (Noteborn *et al*., 1998). Some mechanistic studies of apoptin-induced apoptosis in cancer cells had been reported. Most of the studies showed that apoptosis induced by apoptin was independent of extrinsic apoptosis pathway; but instead it involved in intrinsic apoptosis pathway (Los *et al.*, 2009). Loss of mitochondrial membrane potential, release of cytochrome *c* and activation of caspase cascade, which are the underlying apoptosis events of intrinsic pathway, were observed in cancer cells undergoing an apoptin-induced apoptosis. Apoptin-induced apoptosis does not require the functional tumour gene suppressor p53 but it is regulated by anti-apoptotic proteins Bcl-2 family in most cell lines (Los *et al.*, 2009). Tumour gene suppressor p53 is always mutated in tumourigenic cells, which leads to inefficiency of radiotherapy and chemotherapy on cells that require a functional p53. Hence, apoptin-induced apoptosis which is independent of p53 pathway has made apoptin a great anticancer candidate particularly for cells with malfunctioning p53. The Bcl-2 family proteins include pro-apoptotic (such as Bax, BAD, and Bak) and anti-apoptotic groups (Bcl-2 and Bcl-xL) of proteins and the balance among these 2 groups of proteins determines the fate of cells (Elmore, 2007). Increasing availability of pro-apoptotic group of proteins leads induction of apoptosis via mitochondria-mediated apoptosis pathway; however, increasing availability of anti-apoptotic group of proteins inhibit apoptosis triggered by mitochondria- mediated apoptosis pathway,

Plant molecular pharming is production of pharmaceutical recombinant proteins via genetic engineering approach by using plant as expression host. In relative to other expression hosts, several advantages such as ease in scaling up, high protein expression level, low production cost, low risk of contamination by pathogenic agents and capability of post translational modifications, have made plant an attractive expression system (Fischer *et al*., 1999). Up to date, various kinds of plant-derived therapeutic proteins are available and many of them are important for defeating the life-threatening pandemic diseases. For example, ZMapp, released by Mapp Biopharmaceutical Inc (San Diego, USA) in year 2014, was a chimeric monoclonal antibody raised against the surface glycoprotein of Ebola produced in *Nicotiana benthamiana* (Davidson *et al*., 2015). This product has successfully saved numerous lives from death, which caused by Ebola infection that was originated from the outbreak in West Africa. In comparison with the laborious and time consuming stable transformation, production of high protein expression level within a short period could be achieved via transient expression. By using the deconstructed or agroinfiltration approach, leaf tissues are infiltrated with agrobacterial transformants bearing the recombinant foreign gene sequences. *Agrobacterium* is delivered into intercellular space of mesophyll cells by using syringe or vacuum infiltration. Vacuum infiltration, serving as a feasible and effective delivery tool, is currently widely adopted by manufacturers such as Medicago Inc (USA), Fraunhofer Center for Molecular Biotechnology (FhCMB, USA), Kentucky Bioprocessing (USA) and Icon Genetics (Germany).

Cancer is a disease caused by uncontrolled proliferation of transformed body’s cells. This disease leads to the death of estimated ~ 8.2 million of people in the world in 2012 (GLOBOCAN, 2012). The most common types of cancers in men and women include lung, breast, colorectal, stomach and prostate cancers. There are numerous factors that lead to the development of cancer including exposure to physical carcinogens (such as ultraviolet and ionizing radiation), chemical carcinogens (such as nicotine from cigarettes or presence of heavy metal in drinking water), biological pathogenic agents (such as Human papillomavirus, HPV) and obesity. Non-small cell lung cancer (NSCLC) is one of the most common types of lung cancer and patients suffer from NSCLC accommodates 80-85% of lung cancer disease (American Cancer Society, 2016). The primary reason leads to the lung carcinogenesis is cigarette smoking. Various kind of carcinogens, such as polycyclic aromatic hydrocarbons (PAH) and 4-(methylnitrosamino)-1-(3-pyridyl)-1-butanone (NNK), are present in the cigarette smoke and can induce DNA mutation in cigarette smoker as well as second-hand smokers (Hecht, 2012). To date, available treatments for lung cancer disease include surgery, radiofrequency ablation, radiotherapy, chemotherapy and immunotherapy. Numbers of cancer markers for NSCLS have also been determined, including epidermal growth factors (EGF), anaplastic lymphoma kinase (ALK), Kirsten rat sarcoma viral oncogene (KRAS), and etc. Identification for the cancer markers could accelerate the development of diagnosis for NSCLS and verify the disease in the earlier stage.

NSCLS is the most common type of lung cancer and only ~ 30% of patients survive for 1 year after diagnosed with lung cancer disease (CancerReasrch UK, 2016). Side effects such as nausea, hair loss, breathing difficulty, loss of appetite, vomiting, fatigue and etc have caused patients to suffer after treatments, such as surgery, radiotherapy and chemotherapy. Especially, some of the patients could not get rid off the side effects, including breathing difficulty and long term chest pain, for the rest of the life after they received the surgery to remove lung tissues, where the tumour was located. Suicide cases are always observed especially when patients could not stand for the pain after treatments. Study of Cipriano *et al*., (2011) showed that the liability cost for lung cancer patients was ~ $1,617 to $2,004 per month if the patient received chemo-radiotherapy in year of 2000. The cost for treatments is a huge burden for patients especially for patients who are not allowed to work due to their health problem.

Apoptin, a potential anticancer candidate, showing a great selective killing activity in cancer cells have attracted great interest from researchers. Apoptin is always delivered into mammalian cells in DNA form or in recombinant protein form. Apoptin delivered into mammalian cells in DNA form requires the employment of human viral vectors or non-viral vectors (such as bacteria or transfection reagents) (Rollano Peñaloza *et al*., 2014; Zhuang *et al*., 1995); however, disadvantages of viral vector delivery approach include potential for development of replication competent virus as well insertional mutagenesis. Meanwhile, recombinant apoptin protein, which is a relatively safer delivery approach, is delivered into mammalian cells via microinjection or animal models via cell penetrating peptides (CPPs) (Guelen *et al*., 2004; Zhang *et al*., 2003). Most of the recombinant apoptin was currently produced in *Escherichia coli (*Leliveld *et al*., 2003; Guelen *et al*., 2004; Sun *et al*., 2009). Besides, recombinant apoptin was also produced in human umbilical vein endothelial cells (HUVEC) (Ma *et al.,* 2012). However, high production cost as well as potential contamination of animal pathogens and toxin compounds are huge drawback for the production of recombinant protein in both bacterial and human cell line system. However, there are very scarce reports detailing the production of recombinant apoptin in plants. Plants are currently developed as one of the important biofactories for therapeutic protein production. Trastuzumab, a plant-derived anticancer antibody drug, has shown effectives in reducing size and growth of breast cancer tumours. Besides, PlantForm, manufacturer of Trastuzumab, also claimed that the production cost for plant-based system was 90% lower than that of conventional production approach (Generic and Biosimilars Initiative, 2013). Hence, the main goal of current study is to evaluate the feasibility of production for recombinant apoptin in a cost-effective plant-based expression system. Development of the cost-effective plant-derived apoptin is expected to reduce the overall cost for a cancer treatment making it affordable to needy and hence could save more lives (Fischer *et al*., 1999; Gleba *et al*., 2005). Low risk of contamination by animal pathogens as well as free of co-infection by mammalian viral vectors during drug delivery are also the main drivers to opt for production of recombinant apoptin in plant-based system (Fischer *et al*., 1999). Hence, optimisations for recombinant apoptin expression and protein purification process were the main focuses at current stage of study in order to obtain a high amount of recombinant protein. Besides, additional study for the preliminary assessment on bioactivity of recombinant apoptin was also performed using human lung cancer cells. The result might provide some understanding of bioactivities of plant-made apoptin on human cells and suggestion for improvement on the production of plant-made apoptin in future study.

In order to optimise the expression level of recombinant apoptin in *Nicotiana benthamiana*, several groups of gene cassettes were designed by which details are described in Chapter 3. Gene cassettes, including apoptin alone, apoptin in fusion to C-terminal of GFP (GFP-apoptin) and apoptin in fusion to lichenase (lichenase-apoptin), were designed in order to optimise the expression of recombinant proteins. Signal peptide (PR1a), which directs the recombinant protein into endoplasmic reticulum (ER) space, and ER retention signal (KDEL) were also added to apoptin, GFP-apoptin and lichenase-apoptin gene cassettes in order to accumulate the recombinant proteins in specific cellular compartments. For targeting therapy purpose, recombinant apoptin was in fusion to C-terminal of H22 single chain antibody and epidermal growth factor (EGF). A molecular adaptor CatAd, a kind of CPPs developed from immunotoxin, was inserted between apoptin and H22 single chain antibody as well as apoptin and EGF. All gene cassettes were cloned into high expression tobacco mosaic viral (TMV) vector and binary vector (pGR-DN).

Chapter 4 describes the delivery of agrobacterium transformed with the respective recombinant vectors into 4-5-week-old *N. benthamiana* using vacuum infiltration approach. Expression profiles of recombinant apoptin were assessed using Western blotting analysis. Leaf tissues infiltrated with high expression recombinant vectors harbouring apoptin gene sequences were harvested and used for subsequent downstream processing, including immobilised metal affinity chromatography (IMAC), ion-exchanged chromatography (IEX), hydrophobic interaction chromatography (HIC) as well as size exclusion chromatography (SEC) which are deduced in Chapter 5.

Subsequently, Chapter 6 describes the preliminary bioactivity of purified recombinant apoptin (GFP-apoptin and EGF-apoptin) which was investigated on human lung cancer A549 cells. Interaction between recombinant apoptin and A549 cells as well as EGF receptors was evaluated using enzyme-linked immunosorbent assay (ELISA). Then, recombinant GFP-apoptin was delivered into A549 cells using microinjection approach. Cell viability, localisation of apoptin, mitochondrial membrane potential (MMP) and activation of caspase 3/7 activities were examined after recombinant GFP-apoptin was microinjected into A549 cells. On the other hand, recombinant EGF-VP3-HK was directly applied to A549 cultures. Cell viability, localisation of apoptin, MMP and activation of caspase 3/7 activities were also assessed in the recombinant EGF-VP3-HK treated A549 cells.

Hence, the ultimate goal for the study is to produce a safe and cost-effective recombinant apoptin as an anticancer drug candidate by using plant-based expression platform via the agroinfiltration strategy. The specific objectives of this study were: (i) to design and construct gene cassettes for the development of recombinant apoptin vector variants; (ii) to evaluate protein expression profiles of *N. benthamiana* receiving recombinant apoptin vector variants via agroinfiltration; (iii) to purify recombinant apoptin extracted from *N. benthamiana*; and (iv) to provide a preliminary evaluation of *in vitro* bioactivity of recombinant apoptin on human lung cancer cells.

Chapter 2

Literature Reviews

Table of Contents

2.1 Viral Protein 3 (VP3) of Chicken Anemia Virus (CAV)

2.1.1 Overview of CAV and apoptin

The Chicken Anemia Virus (CAV), first isolated in Japan, causes anemia, lymphoid atrophy, hemorrhages and increased mortality in young chickens during infection (Yuasa et al., 1979). Destruction of hemocytoblasts in bone marrow as well as depletion of lymphocytes and thymocytes in thymic cortex are the major characteristics of a CAV viral infection (Adair, 2000; Jeurissen et al., 1992) which directly led to development of severe anemia and immunodeficiency in young chickens. This also causes vaccination failure and concurrent infection by other infectious diseases such as Marek's disease virus, Infectious Bursal Disease Virus (IBDV) and lentogenic Newcastle disease virus (Notebornb and Koch, 1994).

As a member of Gyrovirus in the family of Circoviridae, CAV is a non-enveloped and icosahedral virus with only 23-25 nm in diameter (Noteborn[b] and Koch, 1994). Circular viral genome comprises 2.3 kilobases (kb) single strand DNA and the virus replicates via circular double-stranded replicative intermediate (Noteborn[b] and Koch, 1994; Prasetyo *et al*., 2009). Unlike other Circoviridae members, all three partially and completely overlapping open reading frames (ORFs) (Figure 2.1 -a) encoding for three viral proteins of CAV are coded on the antigenomic (minus) strand of DNA. An unspliced polycistronic mRNA is generated during transcription (Prasetyo *et al*., 2009). Viral Protein 1 (VP1) of CAV, 50 kDa, encodes for capsid protein of the virus. The sixty capsid protein subunits are clustered into 12 pentagonal trumpet-shaped units to form the three-dimension shape of virus (Figure 2.1 -b) (Crowther *et al*., 2003). On the other hand, the 24 kDa Viral Protein 2 (VP2) is a dual specificity protein phosphatase and it plays an important role in viral replication as well as cellular regulation in infected lymphocytes (Peter *et al*., 2002). The main candidate responsible for the destruction and cell death of lymphocytes via induction of apoptosis in infected chicken is the smallest 14 kDa non-structural Viral Protein 3 (VP3) of CAV. With this apoptosis-inducing ability, VP3 is thus renamed as 'Apoptin' by Noteborn[b] and Koch (1994).

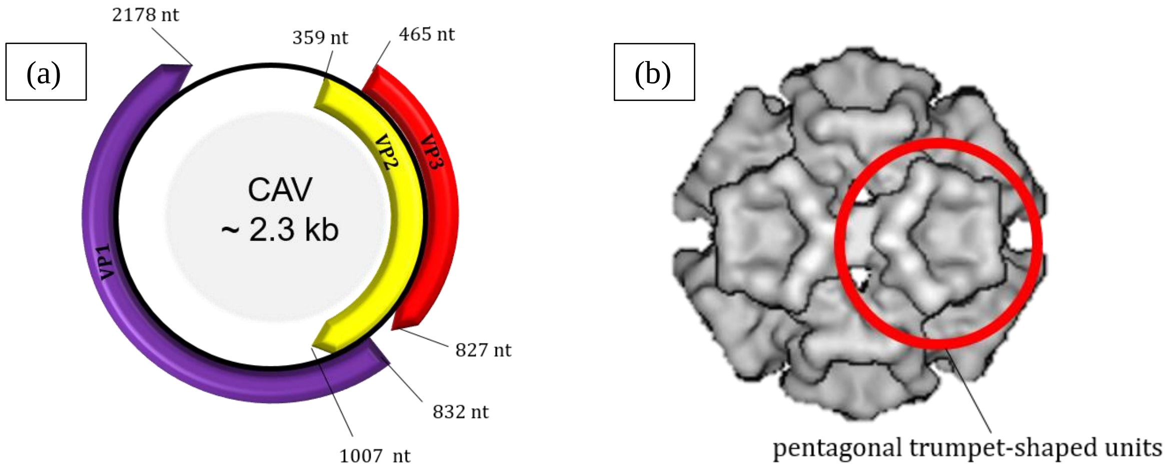

Figure 2.1: Schematic diagram of genome and 3-D morphological structure of CAV. (a) Circular CAV genome encoding three partially or almost completely overlapping ORFs, which are VP1, VP2 and VP3. (b) Three-dimensional structure of CAV with petagonal trumpet shaped subunits. Sources are partly adopted from Artimo et al. (2012); Prasetyo et al. (2009) and Crowther et al., (2003).

2.1.2 Structure and functional regions of apoptin

Apoptin, a basic protein, consists of 121 amino acids with no similarity in sequence to any other known proteins (Noteborn[b] and Koch, 1994). It is rich in proline, serine and threonine, harbouring two proline rich stretches, two positively charged regions and a leucine rich region.

Bipartite nuclear localisation signals NLS1 and NLS2, located on amino acids 82-88 and 111-121, from apoptin have been reported that these two regions play a crucial role in the accumulation of apoptin in nucleus and in the cell killing effectiveness of apoptin on transformed cells (Figure 2.2) (Danen-van Oorschot *et al*., 2003; Poon *et al*., 2005). Translocation of apoptin from cytoplasm into nucleus is believed to be modulated by importins (IMPs), a karyopherin which recognises specific short nuclear localisation sequence (Kuusisto *et al*., 2008). In addition, the nuclear export signal (NES) located on amino acid at the 97-105 position, which is recognised by the chromosomal maintenance 1 (CRM1) exportin, is responsible for the reduced nuclear accumulation of apoptin in normal cell lines (Kuusisto *et al*., 2008; Poon *et al*., 2005). A hydrophobic leucine rich region (LRR) on amino acids position 33-46, is a weak apoptosis inducing region on apoptin. This region may enhance nucleus retention and is also the main site for the binding of a number of interacting proteins (Poon *et al*., 2005; Los *et al*., 2009). In addition, LRR region is also responsible for the multimerisation activity of apoptin. In the study of Leliveld[b] *et al*. (2013), biologically active recombinant MBP-apoptin was in multimerised state and comprised of ~ 30-40 monomers.

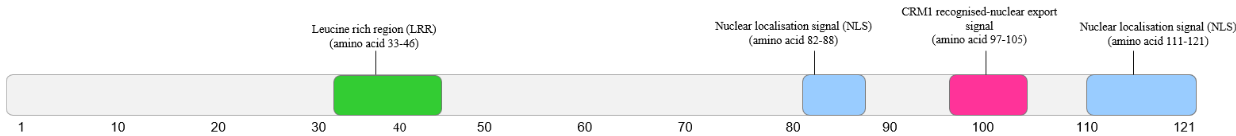

1	MDALQEDTPP	GPSTVFRPPT	SSRPLETPHC	REIRIGIAGI
41	TITLSLCGCA	NARAPTLRSA	TADNSESTGF	KNVPDLRTDQ
81	PKPPSKKRSC	DPSEYRVSKL	KESLITTTPS	RPRTAKRRIK
121	L			

Figure 2.2: Schematic diagram of functional regions and amino acids of apoptin. Apoptin contains a leucine rich region (located on amino acids 33-46), a bipartite nuclear localisation signal (NLS) (located on amino acids 82-88 and 111-121) and a CRM1 recognised nuclear export signal (NES). The representative apoptin nucleotide sequence of is based on the sequence of a Malaysia isolate (GenBank accession number: AAB86420.1) reported by Mohd-Azmi et al. (1997).

2.1.3 Bioactivity of apoptin in mammalian cells

Apoptin-induced apoptosis was initially reported in transformed chicken lymphoblastoid T cells (MDCC-MSBI) and myeloid cells (LSCC-HD11) but not in normal chicken embryo fibroblasts (Noteborn[a] *et al*., 1994). In year 1995, apoptin was first reported to induce apoptosis in human osteosarcoma cells (Zhuang *et al*., 1995). To date, apoptin has been widely exploited as antitumour agents due to its selective killing effect on tumour cells and transformed cells but not on normal or primary cells. More than 70 human cancer cell lines have shown apoptotic effect in response to apoptin drug. This includes breast tumour (MCF-7), osteosarcoma (Saos-2), small lung cell carcinoma (SLCC), hepatoma (HepG2), kidney rhabdoid tumour (G401), myeloid leukemia (K562), colon carcinoma (HT29) and other cells (Los *et al*., 2009; Noteborn *et al*., 1998; Sun *et al*., 2003; Zhuang *et al*., 1995). Apoptin also induced apoptosis in some non-tumorigenic transformed cell lines, such as monkey SV40-transformed kidney cells (Cos-7), avian myeloblastosis virus (AMV) transformed cells and Adenovirus-5-transformed baby rat kidney cell. However, no apoptosis effect is observed in T cells, smooth muscle cells (HSMC), epidermal keratinocytes (FSK-1), fibroblasts cell (VH25) and human umbilical-cord vascular endothelial cells (HUVEC) (Noteborn *et al*., 1998). Detailed mechanism of apoptin-induced apoptosis is still not clear; whereas, protein structure and sequence of apoptin have been studied exclusively in order to understand each regions of this protein that contributes to apoptosis effect.

2.1.4 Apoptosis and mechanisms of apoptin-induced apoptosis

2.1.4.1 Apoptosis

Apoptosis (or programmed cell death) refers to “falling off of petals from a flower” or “of leaves from a tree in autumn” in ancient Greek. It was first used by John Kerr in 1972 to illustrate distinct morphological features of apoptotic bodies formation and phagocytosis as well as lysosomal degradation of apoptotic bodies by phagosomes (Kerr *et al.*, 1972). Various kinds of diseases and physiological development involve apoptosis process, for example, Alzheimer’s (Cotman and Anderson, 1995; De-la Monte *et al*., 1997), Parkinson’s (Mochizuki *et al*., 1996) and diabetes (Russell *et al.*, 1999). Besides, apoptosis also plays roles in cell number control (Hall *et al*., 1994), elimination of self-reactive lymphocytes (Parijs *et al*., 1998), and removal of cellular stresses (induced by irradiation or drugs) and DNA damage cells (Enoch and Norbury, 1995). In addition, arisen of several types of cancers could be also traced to malfunction of apoptosis signalling molecules, especially p53 deficient cells, which cause most of the cancerous cells resistant to chemotherapeutic drugs (Wattel *et al.*, 1994).

Characteristics of apoptotic cells include round in cell shape, shrinkage in cell size and the loss in contact with neighbouring cells (Lawen, 2003). Within the dense cytoplasm, organelles are more tightly packed while endoplasmic reticulum (ER) stretches and vesicles are budded off from cisternae. In nucleus, condensation of chromatin and degradation of genomic DNA by endonucleases to form “laddering DNA” features in agarose gel analysis can be observed (Walker *et al*., 1994; Walker *et al.,* 1999). At later stage of apoptosis, plasma membrane blebs and cell content is separated into several membrane spheres shielded apoptotic bodies that are various in size. These apoptotic bodies, with recognition site for phagocytic cells, are subsequently degraded and digested by macrophages, parenchymal cells or neoplastic cells

(Elmore, 2007). Apoptosis process does not release cell content into intercellular compartment, hence, this cell death mechanism does not result in inflammation.

There are two important pathways, the intrinsic and extrinsic pathways, that regulate apoptosis process, and both pathways work non-independently by sharing some signaling molecules. Extrinsic pathway, also named as receptor-mediated pathway, involves triggering of receptors that reside on plasma membrane to induce apoptosis. Numerous kinds of receptors, including Fas, tumor necrosis factor receptor (TNF-R) family and granzyme B/perforin system, are available to bind to ligands, such as FasL, apoptosis ligand 2 (Apo 2) and tumor necrosis factor-related apoptosis-inducing ligand (TRAIL), in order to initiate formation of death-inducing signaling complex (DISC) and downstream caspase cascades (Ashkenazi, 2008). For instance, binding of FasL (Fas ligand) to Fas receptor leads to the binding of adaptor Fas-associated death domain protein (FADD) to Fas receptor via death domain (DD), which is available on both Fas and FADD. Death effector domain (DED) of FADD allows the binding of pro-caspase 8, which contains the same domain. Subsequently, pro-caspase 8 is activated to active caspase 8 that responsible to activate other apoptosis elements. Hence, DISC is the complex of Fas, FasL, FADD and pro-caspase 8 (Lawen, 2003). Active caspase 8 is responsible to activate caspase 3, cleave Bid protein, produce truncated Bid protein that travels into mitochondria and leads to the release of cytochrome c, which initiates intrinsic apoptosis events.

Instead of depending on receptors, intrinsic pathway is induced by intracellular signals (such as Bax and Bak proteins) that subsequently leads to mitochondrial-mediated apoptosis process. Opening of mitochondrial permeability transition pore and loss of the mitochondrial transmembrane potential occur in order to release two main groups of pro-apoptotic proteins (Elmore, 2007). Cytochrome C, Smac/DIABLO and serine protease HtrA2/Omi are the first main group of pro-apoptotic proteins that are important to initiate apoptosis cascades. ‘Apoptosome’, a signaling molecule to activate caspase-9, forms when cytochrome C, a key element binding to WD40 repeat of Apaf-1, is released from mitochondria and subsequently results in the activation and oligomerisation of Apaf-1 into a wheel-shaped oligomeric complexes in the presence of dATP (Riedl and Salvesen, 2007). Second group of pro-apoptotic proteins are Apoptosis-inducing factor (AIF), endonuclease G and Caspase-Activated DNase (CAD) (Elmore, 2007). This group of proteins translocate into nucleus and eventually lead to

DNA fragmentation (Daugas *et al*., 2000; Li *et al*., 2001; Van Loo *et al*., 2001; Widlak, 2000). A simple overview diagram of intrinsic and extrinsic pathway is shown in Figure 2.3**.**

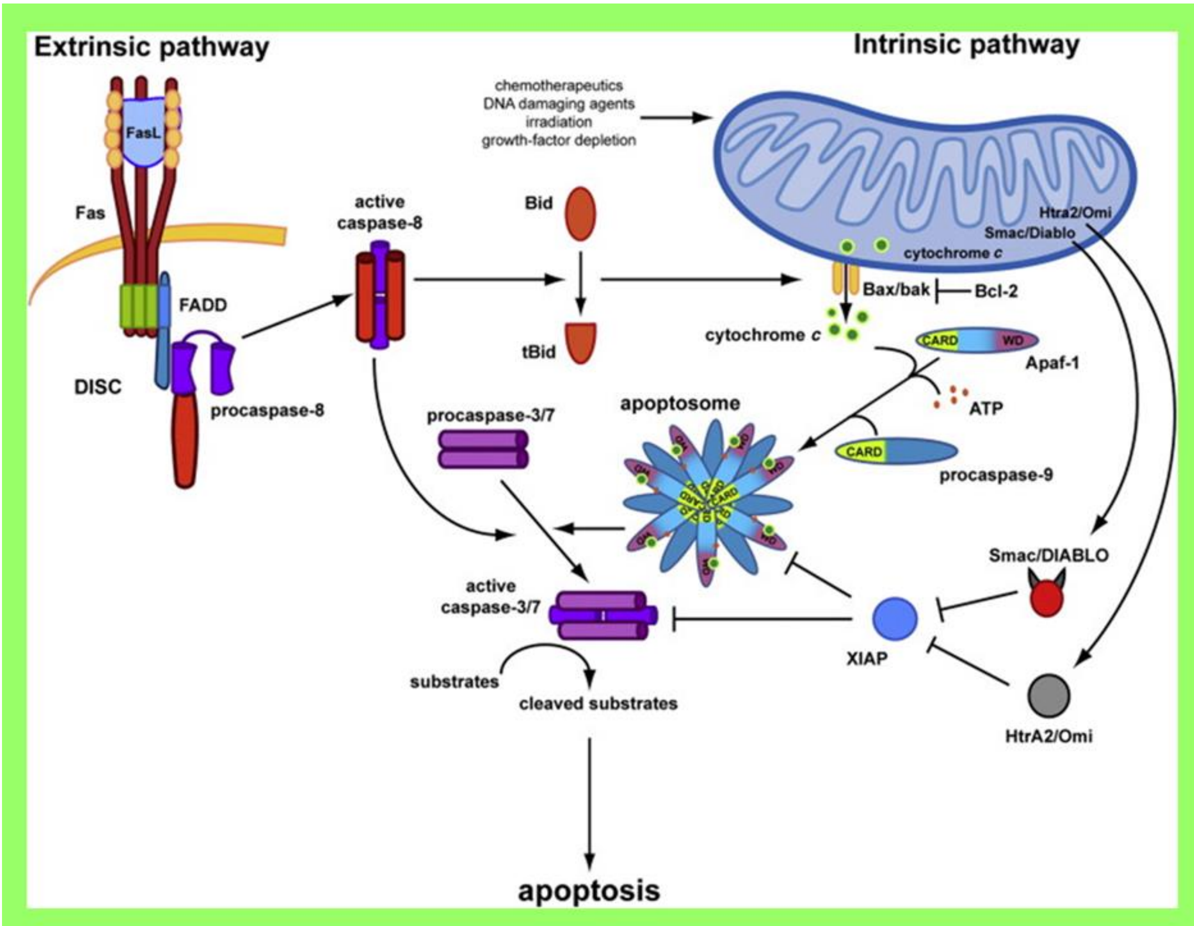

Figure 2.3: Schematic diagram for intrinsic and extrinsic pathway of apoptosis. Extrinsic apoptosis pathway involves receptors on plasma membrane. For example, binding of FasL to Fas causes the formation of DISC complexes, which is important for the activation of caspase 8 (Lawen, 2003). Active caspase 8 is responsible to activate caspase 3 and produce truncated Bid protein, a messenger that translocates into mitochondria and initiates intrinsic apoptosis events. For intrinsic apoptosis pathway, increasing permeability of mitochondrial membrane results the release of cytochrome c and formation of apoptosome. Apoptosome is important for the activation of caspase 9, which subsequently activate caspase 3, 6 and 7. Schematic diagram is adopted from Lamkanfi and Dixit (2010).

Both intrinsic and extrinsic pathways are equivalently important for induction of apoptosis, whereas, both pathways are also regulated by several kinds of regulator proteins. For example, tumor suppressor protein p53, a nuclear DNA-binding phosphoprotein, is a transcriptional factor that regulates cell cycle, DNA repair and apoptosis (Bellamy, 1997). Apoptosis induced by p53 may be caused by DNA damage, inappropriate oncogene activation, cytokines or heat shock. Another group of apoptosis regulator is Bcl-2 family proteins, which contain pro-apoptotic and anti-apoptotic two independent categories, and ratio between these two categories of proteins is key to determine the fate of cells (Gross *et al*., 1999; Oltval *et al*., 1993). With the understanding of apoptosis pathway, various kind of drugs are designed in order to target desired signaling molecules or pathway to regulate apoptosis process of diseased cells.

2.1.4.2 Mechanisms of apoptin-induced apoptosis

To date, complete mechanism of apoptin-induced apoptosis is not fully explained but several proteins interacting with apoptin has been reported. Although there is no concrete data proving that apoptin-triggered cell death is induced by extrinsic pathway, Guelen and his colleagues (2004) has found that apoptin partial colocalised with FADD and resulted in formation of death effector filaments (DEFs), which was formed when proteins containing death domains are overexpressed. Besides, apoptin also interacts with DED associated factor (DEDAF) and partial colocalised with this protein in osteosarcoma cells (Danen-van Oorschot *et al.*, 2004). However, apoptin has also been observed working independently of extrinsic pathway, which induced significant apoptotic effect on Caspase-8 deficient and truncated FADD overexpressing cells (Maddika *et al*., 2005). Hence, relation between apoptin-induced apoptosis and extrinsic apoptosis pathway still remained controversial and more studies need to be carried out to clarify the association between apoptin and extrinsic pathway.

In contrast, apoptin was believed triggering apoptosis via intrinsic pathway. Apoptin successfully causes loss of mitochondrial membrane potential (MMP) (Maddika *et al*., 2005). Cytochrome c, AIF and caspase-3 are detected within cytosol of apoptin-treated cells; in addition, Nur77 is suggested as the nucleo-cytoplasmic signal transmitting candidate between nucleus and mitochondria since apoptin is reported triggering apoptosis independently of p53 (Maddika *et al*., 2005; Zhuang *et al.*, 1995).

Instead of intrinsic and extrinsic pathways, PI3-K/Akt signaling pathway is triggered by apoptin. PI3 (phosphatidylinositol 3 kinase), a lipid kinase, is responsible to catalyse phosphorylation of inositol ring of phosphoinositides; while, Akt is a serine/threonine kinase that is activated by PI3 (Maddika *et al*., 2007). PI3 was reported involving in proliferation differentiation and cells. Maddika and his colleagues (2010) proved that apoptin binds to SH3 domain of p85, a subunit of PI3-K, via proline-rich region (amino acid 80-90). They suggested that PI3-K is responsible for apoptin localisation and cytotoxic activity of apoptin. Increasing expression level and translocation of Akt into nucleus upon treatment of apoptin have also been reported by Maddika and his co-workers (2007). Akt is suggested involving in phosphorylation activities of apoptin within nucleus, in which phosphorylation of apoptin on Threonine (108 amino acid) of apoptin is crucial to trigger cell death in tumour cells (Poon *et al*., 2005; Rohn *et al*., 2002).

Besides, peptidyl-prolyl isomerase–like 3 (Ppil3) also interacts with apoptin and localisation of apoptin is associated with amount of Ppil3 (Huo *et al*., 2008). In tumour cells, Ppils is expressed in low level and apoptin is localized into nucleus; whereas, high protein amount of Ppil3 in normal cells cause distribution of apoptin in cytoplasm. Furthermore, Hippi, a protein interacting with Huntingtin-interacting protein 1 (Hip-1), is suggested responsible for suppression of apoptosis within normal cells by retention of apoptin in cytoplasm (Cheng *et al*., 2003). Interaction between APC1, a subunit of the anaphase-promoting complex/cyclosome (APC/C), and apoptin is also reported. Binding of apoptin with APC/C causes APC/C complex disruption and degradation, which eventually results G2/M cell cycle arrest and induction of apoptosis (Teodoro *et al*., 2004). In addition, apoptin was reported to initiate apoptosis independent of p53, a tumour suppressor protein (Zhuang *et al*., 1995). p53 is always mutated during tumour development and causes poor response to anticancer therapies that require functional p53. Therefore, apoptin is a potential anticancer drug that do not require functional p53 for its action. Bcl-2, an anti-apoptotic protein, does not inhibit activity of apoptin, on the contrary, apoptosis is stimulated by overexpression of this protein in the study of Noteborn *et al*., 1998. In the study of Burek *et al*. (2006), a contrary result was observed. They reported that apoptin-induced apoptosis was inhibited in MCF-7 cells overexpressed with Bcl-2 and Bcl-x_L. Therefore, effect of Bcl-2 protein to apoptin-induced apoptosis is yet to confirmed.

In addition, researchers also studied apoptin-induced apoptosis in relation to the translocation of apoptin into nucleus of tumour cells and interaction of apoptin with nuclear compartments. Nucleo-cytoplasmic shuttling of apoptin is responsible by importins (IMPs) and exportins CRM-1, which are nuclear envelope-embedded multi protein channels (Kuusisto *et al.*, 2008; Poon *et al.*, 2005). Both transport receptors recognise NLS or NES signal embedded in apoptin sequence and translocate apoptin into nucleus of tumour cell but apoptin remains in cytoplasm of normal cells. Within the nucleus, apoptin is able to form DNA-apoptin superstructure, which consists 20 multimeric apoptin complexes and 3 kb of DNA. Formation of DNA-apoptin superstructure interrupts chromosomal organization and it is suggested that apoptin may plays role in regulating transcription of genes involving in apoptosis activities (Lelived[c] *et al.*, 2003). Besides, it is also interesting to note that apoptin is also colocalised with promyelocytic leukemia protein (PML) bodies, which plays roles in viral replication, tumour progression, apoptosis and cell cycle regulation. It was found that apoptin was sumoylated before being targeted to PML. Nevertheless, interaction between apoptin and PML is suggested not responsible for apoptosis but for CAV viral replication (Los, 2009). A summary of cellular proteins interacting with apoptin is listed Table 2.1.

Table 2.1: List of cellular proteins interacting with apoptin.

Molecules	Biological effects
Extrinsic Pathway	
Fas-associated death domain protein (FADD) and DEDAF	Apoptin is colocalised with FADD as well as DEDAF and induces formation of death effector filaments (DEFs); However, apoptin-mediated apoptosis is also suggested independent of extrinsic pathway. Hence, interaction between apoptin and extrinsic pathway molecules requires for further investigation.
Intrinsic Pathway	
Nur77	Maddika and his colleagues showed that apoptin induced apoptosis via intrinsic pathway by releasing cytochrome c, AIF, caspase 3 and Nur77 as the nucleo-cytoplasms transmitting signal.
Phosphorylation Pathway	
Akt and PI3K	Apoptin interacts with the SH3-domain of the p85 regulatory subunit of PI3K and activates PI3K. This event leads to sustained Akt activation and nuclear translocation of Akt.
Others	
Peptidyl-prolyl isomerase-- like 3 (Ppil3)	Interaction between apoptin and Ppil3 may favor its cytoplasmic localisation.
Hip-interacting	In normal cells, apoptin colocalises with Hippi in the cytoplasm;

protein (Hippi)	whereas apoptin migrates to the nucleus in tumour cells while Hippi remains in the cytoplasm.
APC1 (subunit of anaphase-promoting complex/cyclosome)	Interaction between apoptin and APC1 may lead to mitotic cell cycle arrest and apoptosis.
Nucleus	
Promyelocytic leukemia protein (PML)	SUMOylated apoptin interacts with PML in PML nuclear bodies. However, the disruption of interaction between PML and apoptin does not affect apoptin's cytotoxicity.
Importin-β1	Importin-β1 plays a role in nuclear localisation of apoptin by translocating apoptin through the nuclear pore complex.
CRM1	CRM1 is involved in nuclear exportation of apoptin
DNA	Formation of DNA-apoptin superstructure molecules was observed in the study of Leliveld *et al.* (2003). Apoptin interacts with genomic DNA of cancerous cells and the interaction is suggested involving in regulation of the transcription of genes involving in apoptosis activity.

2.1.5 Cancer

2.1.5.1 Overview of cancer

Cancer is a disease characterised by the formation of tumours due to uncontrolled proliferation of transformed body's cells that are induced by genetic mutation (Cancer Research UK, 2010; Golan *et al.*, 2005; Rang *et al.*, 2007). According to GLOBOCAN (2012), death of 8.2 million people in the world is due to cancer and 14.1 million of new cases are being detected. The most common cancers among men and women include lung, breast, colorectum, stomach and prostate. In South-East Asia, death from cancer accumulated more than 1 million people and more than 1 million new cases has been diagnosed (GLOBOCAN, 2012). In Malaysia, nearly 7000 new cancer cases have been reported in Peninsular Malaysia between year 2003-2005 (MAKNA, 2013). Among these cases reported in Malaysia, the most common cancers are breast cancer (18%), large bowel cancer (11.9%) and lung cancer (7.4%).

A numbers of risk factors have been identified that lead to the formation of this malignancy. In particularly, physical and chemical carcinogens that inevitably present around human beings or existing in the environment are the major causes for cancer. Physical carcinogens, such as ultraviolet and ionizing radiation, can induce irreversible DNA damage and mutation that lead to development of skin cancer (Gruijl, 1999; Gruijl *et al.*, 2001; Kvam and Tyrrell, 1997). In addition, polycyclic aromatic hydrocarbons (PAH), an active component of cigarettes, is also recognised as the carcinogen that promotes lung cancer in smokers (American Cancer Society, 2016). According to WHO (2013), 22% of global cancer deaths and 71% of global lung cancer deaths are due to the usage of tobacco. Besides, several types of cancers, including liver, lung, bladder and kidney, are initiated by inorganic arsenic that is available in drinking water (Chen *et al.*, 1992). Biological agents, including virus, bacteria and parasites, are also another risk factor for stimulation of cancer. Human papillomavirus (HPV) has become a nightmare for women as this virus has successfully caused invasive cervical cancer and led to presence of estimated 528,000 new cases globally (GLOBOCAN, 2012; Walboomers *et al*., 1999). Recently, obesity and lack of physical exercise are also suggested to correlate with cancer incidences (Calle and Thun, 2004; Michaud *et al*., 2001; Wolk *et al*., 2001). Mechanisms of obesity induced tumorigenesis are related to insulin resistance and resultant chronic hyperinsulinaemia, increased bioavailability of steroid hormones and localised inflammation (Calle and Kaaks, 2004). Moreover, aging is also another major risk factor that is responsible for cancer incidences. Continuous and prolonged exposure to carcinogens as well as less effective cellular repair mechanisms make people more susceptible to malignancy as they are growing older (Dix and Cohen, 1980).

2.1.5.2 Pathogenesis of Cancer

Development of cancer is a complex and multistep process (Weinberg, 2007). Instead of cell proliferation, maturation and differentiation occurred in normal cells, cancerous cells are uncontrollably dividing, resisting for maturation and differentiation, invading the underlying tissues as well as spreading to other part of body via circulatory system.

Uncontrolled proliferation of cancerous cells

Uncontrolled proliferation is the main characteristic of cancerous cells. This may be due to the over-expression of growth factors and abnormal activity of mutated receptors in the absence of ligands (Rajkumar, 2001). For example, Guo and his colleagues (2003) have showed that overexpression of vascular endothelial growth factor (VEGF) can promote the cell proliferation of breast cancer *in vivo*. Besides, over-proliferation of cancerous cells could be also due to the cells are resistant to apoptosis. Mutation occurs on several genes involved in apoptosis pathway, such as proto-oncogenes (bcl-2) (Coultas and Strasser, 2003) and tumour suppressor genes (p53) (Greenblatt *et al*., 1994), directly inhibit apoptosis activity of cancerous cells. To prevent the end of DNA replication and cell senescence, telomerase activity is re-activated in 85-95% of most common cancers (Shay, 1997). Telomerase is a ribonucleoprotein enzyme. This enzyme involves in synthesising hexameric repeats (TTAGGG) on telemetric end, which is only detected in human during blastocyst stage embryogenesis. A portion of telomere is eroded in each round of cell division because DNA polymerase cannot easily replicate the last few nucleotides on DNA (Rang *et al*, 2007). This causes the DNA to become non-functional and thus lead to cell senescence. Thus, re-activation of telomerase is important to compensate telomeric loss in each round of cell division. In order to gain enough nutrients for tumours enlargement, tumours also induce angiogenesis. Angiogenesis is a process for development of new blood vessels in response to induction of growth factors (Rang *et al*, 2007). For example, VEGF and angiopoietin (Ang) play a vital role as the survival factor to maintain survival of endothelial cells to form new vessels and this kind of cells is normally killed by angiogenesis inhibitors by the induction of apoptosis (Carmeliet and Jain, 2000).

Less of differentiation

Another important characteristic of cancerous cells is differentiation of cells into varying degrees of different tumours. Normal cells are differentiated into specialised cell types after cell division and maturation. However, cancerous cells are less mature over time because they lost most of the genetic materials during each round of replication. Undeniably, this makes the cells more primitive and malfunctioned, but the cells tend to reproduce more rapidly. Based on this characteristic, severity of cancer can be classified into low, medium and high grade (Cancer Research UK, 2010). Cancer cells look normal and replicate slowly for low severity of cancer; whereas, cancer cells are less differentiated and more abnormal as well as proliferating in higher speed for high severity of cancer. This is a useful indicator for doctor to judge the severity of the disease and decide for the treatments for patients.

Invasiveness and Metastasis

Tumours require more space and nutrients for enlargement as the benign tumours grow and expand. Hence, angiogenesis becomes a part of tumour growth in order to provide essential nutrients. As new blood vessels are formed, they become a new entryway for tumour cells to pass into circulation system and metastases to other parts of the body (Folkman and Shing, 1992). According to Liotta (1986), tumour cells require three important steps to invade the underlying cell layers, including binding to the matrix collagen of basement membrane, secreting of hydrolytic enzymes

to degrade the matrix and tumour locomotion into region of matrix modified by proteolysis.

According to Weinberg (2007), tumours are basically classified into two categories based on their degree of aggressive growth, including benign and malignant tumours. Benign tumours are local and slow growing tumours that are harmless. They may cause certain degree of damage if located on vital body organs, such as brain. On the other hand, malignant tumours are capable to spread and invade nearby tissues as well as other parts of body organs to form secondary tumours (metastases).

2.1.5.3 Case study: Lung cancer

In study by GLOBOCAN (2012), lung cancer is the most common cancer in the world and approximately 1.8 million of new cases was estimated in 2012. In general, incidence rate of lung cancer is high in men (about 1.2 million) and lower in women (about 0.6 million). More than 50% of lung cancer patients were diagnosed with lung cancer at stage IV. Generally, there are several factors that induce lung carcinogenesis. Tobacco smoking is the main risk for lung carcinogenesis and it causes 80% death for lung cancer (American Cancer Society, 2016). Cigarette smoke contains lung carcinogens, including polycyclic aromatic hydrocarbons (PAH) and 4-(methylnitrosamino)-1-(3-pyridyl)-1-butanone (NNK), that are responsible for induction of DNA mutation especially in *TP53 and* Kirsten rat sarcoma viral oncogene *(KRAS)* (Hecht, 2012). Hence, there is also high risk for secondhand smokers to develop lung cancer. Besides, lung carcinogenesis could also be developed due to exposure to polluted air condition, asbestos and radon (American Cancer Society, 2016).

Non-small cell lung cancer (NSCLC) and small cell lung cancer (SCLC) are two common types of lung cancer and NSCLC accommodates 80-85% of lung cancer (American Cancer Society, 2016). Majority of lung cancer are adenocarcinoma (40% of lung cancer) following by squamous carcinoma (25-30% of lung cancer) and large cell carcinoma (10-15% of lung cancer). Several cancer markers or molecular alterations have been identified in NSCLS and these assist the identification of the correct treatment. Epidermal growth factor receptor (EGFR) mutations are one of the molecular alterations observed in lung carcinogenesis. Overexpression of EGFR and improper activation of EGFR tyrosine kinase domain induce hyperactivation of downstream pro-survival signaling pathways (Gazdar, 2009). Besides, rearrangement of anaplastic lymphoma kinase (ALK), mutation on KRAS and overexpression of mesenchymal epithelial transition factor (MET) are also molecular alterations occurred in NSCLC (Dara *et al*., 2012).

To date, there are several treatments available for NSCLC including surgery, radiofrequency ablation, radiotherapy, chemotherapy, targeted therapy and immunotherapy (American Cancer Society, 2016). Surgery and radiofrequency ablation are direct method to remove tumours. Surgery for NSCLC is categorised into pneumonectomy (removal of entire lung), lobectomy (removal lobe of lung), segmentectomy or wedge resection (removal part of lobe of lung) and sleeve resection (removal of tumourigenic region in large broncus and rejoining with remaining lobes) (American Cancer Society, 2016). Radiofrequency ablation is treatment for tumours located on the outer edges of lung. This therapy requires penetration of probe through the patient’s skin and tumours are destroyed by the high-energy radio waves. Radiofrequency ablation is also applied if patients cannot tolerate surgery (American Cancer Society, 2016).

Radiotherapy is used if the tumours are not completely cleared by surgery or patients cannot tolerate surgery. Radiotherapy uses high energy rays, such as x-rays, gamma rays, or protons, to kill tumour cells. There are two types of radiotherapy including external radiotherapy and non-commonly used internal radiation therapy. External radiotherapy is applied from outside of body; while non-commonly used internal radiation therapy requires a piece of small source radioactive material to be implanted or taken by patients via oral delivery as well as injection to allocate radioactive elements near to tumour cells for effective killing activity. Internal radiation therapy is commonly used for treating bronchus tumours (American Cancer Society, 2016). Patients may feel tired, weak, skin soreness and hair fall after radiotherapy (Cancer Research UK, 2013).

Chemotherapy is the use of cytotoxic drugs to destroy cancerous cells either via mouth or injection. Chemotherapy drugs are commonly used for treating NSCLC including Paclitaxel, Cisplatin, Carboplatin and others. Instead of killing actively dividing cells randomly and causing various side effects, targeted therapy treats NSCLC by targeting drugs towards specific pathway or cancer markers found on NSCLC. For example, Erlotinib, Afatinib and Gefitinib are EGFR inhibitors that disturb activity of EGFR, which are overexpressed on NSCLC (Paez *et al.*, 2004). Targeting drugs including ALKk inhibitors (Crizotinib, Ceritinib and Alectinib) (Ivana and David, 2016) and anti-angiogenesis monoclonal antibodies (such as Bevacizumab and Ramucirumab) (Das and Wakelee, 2014) are also used to treat NSCLC.

2.1.6 Current study of apoptin with efficient delivery approaches

Induction of apoptin-induced apoptosis in human cancer cells was first reported in 1995 (Zhuang *et al*., 1995) and diverse researches on apoptin-induced apoptosis was carried out after the report in human mammalian cell lines as well as in mice model. Based on previous studies, apoptin is a selective tumour killer since the protein selectively induces apoptosis in human transformed and tumorigenic cells but remains harmless to primary as well as non-transformed cells (Rollano Peñaloza *et al*., 2014). A huge variety of cancer cells have non-functional p53. p53 tumour suppressor pathway-based chemotherapeutic compounds as well as ionizing radiation are not effective in this condition. However, apoptin-induced apoptosis is independent of p53 tumour suppressor pathway. Therefore, apoptin is an attractive and potential anticancer candidate for cancer therapy.

Delivery of apoptin into intracellular space of cells is a challenge for apoptin-based therapy since apoptin does not harbour cell penetrating peptide (CPP). Various kinds of delivery approaches have been established including employment of viral vectors, bacteria and direct apply of recombinant apoptin in fusion to CPPs. The most common delivery method of apoptin is by using viral vectors. Human viral vectors, including non-replicative viruses, replication-deficient viruses, non-oncolytic lentiviral vectors as well as oncolytic viruses, have been used to deliver apoptin gene into intracellular space of mammalian cells (Rollano Peñaloza *et al*., 2014). The most commonly used viral vectors for delivery of apoptin is adenoviral vector. Adenoviral vector is a high potential viral vector for gene delivery since the vector is able to transduce non-mitotic cells, easily grown in high titers and non-integrated into host genome. Apoptin delivered by adenoviral vector was tested in various cancer cells, including a xenogeneic tumor (HepG2) in Balb/Cnu/nu mice (Pietersen *et al*., 1999), *in-vitro* prostate cancer cells (LNCaP) (Vida *et al*., 2016) and *in-vitro* cholangiocarcinoma cell lines (Pietersen *et al*., 2004). Other potential viral vector candidates, including replication deficient fowlpox viral vector (tested in human hepatoma cell line (HepG2) and xenogeneic mouse hepatoma (H22) in C57BL/6 mice) (Li *et al.*, 2006), lentiviral vector regulated by surviving promoter (tested in SW480, Hela and MCF-7 cell lines and xenogeneic tumor (SW480) (athymic NCR-nu/nu) nude mice) (Feng *et al*., 2013) and newcastle disease viral vector (tested in SMMC7721, A549 cell lines and xenogeneic tumor (Hep-2) in mice) (Wu *et al*., 2012), were also reported for delivery of apoptin.

Besides, non-viral vector approach was also applied to transfer apoptin into tumour cells, including transfection reagents, nanoparticles and *Salmonella typhimurium*. The most common delivery tools for apoptin *in vitro* are transfection reagents, such as DEAE-dextran, calcium phosphate precipitation and lipofection (Zhuang *et al*., 1995). Besides, nanoparticles were also used to deliver apoptin, such as chitosan (Liu *et al*., 2008) and polyamidoamine dendrimer (Bae *et al*., 2016). *S. typhimurium*, a biological delivery tool as well as a potential cancer therapeutic agent, selectively accumulates in tumour tissue and it is also actively against p53-deficient tumours (Guan *et al*., 2013). Recently, apoptin-induced apoptosis was reported when apoptin was delivered into human laryngeal cancer cell line (Hep-2). Significant reduction in tumour growth as well as tumour microvessel density was also observed when apoptin was delivered into xenogeneic tumor (Hep-2) in BALB/c nude mice.

Instead of delivering apoptin in DNA form using vectors, protein form of apoptin could also be used. Currently, most of recombinant apoptin was produced in *Escherichia coli* expression system (Leliveld *et al*., 2003; Guelen *et al*., 2004; Sun *et al*., 2009). Preparation of recombinant apoptin in mammalian system was also reported by Ma *et al.* (2012) using human umbilical vein endothelial cells (HUVEC). Expression of recombinant apoptin in plants, *Nicotiana benthamiana*, was reported by Lacorte *et al*. (2007); however, no subsequent study was reported for bioactivity of plant-made apoptin in mammalian cells. Purified recombinant apoptin from *E. coli* expression system, recombinant MBP-apoptin, successfully induced apoptosis in human bone osteosarcoma (Saos-2) cells. However, MBP-apoptin was delivered into mammalian cells using microinjection since the protein could not directly pass through plasma membrane. In order to design a feasible delivery way for long term study of recombinant apoptin, cell-penetrating peptides (CPPs) have been employed to assist protein penetrating plasma membrane. Trans-acting activator of transcription (Tat) protein from HIV, harbouring a protein transduction domain, was in fusion to apoptin (Guelen *et al*., 2004). Significant cell killing effect was observed when recombinant Tat-apoptin was applied in Saos-2, HSC-3 cancer cells and human premyelocytic leukemia HL-60 cells (Guelen *et al*., 2004; Lee *et al*., 2012). Besides, protein transduction domain 4 (PTD4) in fusion to apoptin, harvested from *E. coli* expression system, also harboured cell killing activity in human hepatocarcinoma HepG2 cells and restrained xenogeneic tumour growth in BALB/c nude mice (Sun *et al*., 2009). To date, no clinical study has been reported for apoptin; hence, effort for understanding apoptin-induced apoptosis as well as a good apoptin-based therapy approach is important to promote apoptin towards a great anticancer drug.

2.2 Plant as Expression Host

2.2.1 Molecular Pharming

2.2.1.1 Overview of plant as expression host for production of recombinant therapeutic proteins

Molecular pharming is production of pharmaceutical recombinant proteins, such as vaccines and antibodies, in specific host using genetic engineering approach (Marsian and Lomonossoff, 2016). Various kinds of expression hosts have been developed for the efficient production of recombinant proteins, such as prokaryotic system (*E. coli* and *Bacillus subtilis*), yeast (*Saccharomyces cerevisiae*), insect (*Spodoptera frugiperd*a), mammalian cell lines (COS cells and CHO cells) and plants (*N. benthamiana*). Presence of pros and cons are always available for each of this expression systems; therefore, study should be performed and compared between the expression system in order to choose for the best expression host that gives the satisfied yield. For cell-based culture, recombinant protein can be produced within hours or days. Therefore, this production system, especially *E. coli*, becomes the most fascinated choice to produce large volume of targeted product within short period of time. However, expensive instruments and high maintenance cost for culture, fermentor and reactor have made production difficult to be scaled up. Besides, several critical problems are also arisen from this system, such as contamination of endotoxin in purified product, formation of inclusion body and lack of post-translational modification system, and this has led to the development for alternative expression hosts (Yina *et al*., 2007). Mammalian cell expression system, as one of the alternative cell-based system, possess complete post-translational modification system; whereas, potential of mammalian viral contamination in purified product has also induced severe safety issue (Van der Pol and Tramper, 1998). As a result, plant-based expression system is highly gaining attention from researchers recently since all problems discussed above can be avoided using plants as expression host.

Numbers of persuasive reasons using plant as alternative expression platform have driven researchers to focus on the establishment of this system. First, plant-based expression can be easily scaled up since plants can be grown in huge quantity in field. Plants require only simple and inexpensive sources for growing such as sunlight, mineral salt, water and soil (Fischer *et al*., 1999). There was estimated less than $50 required for 1 gram production of purified recombinant protein by Gleba *et al*., (2005). Besides, high expression level of recombinant protein could be obtained in plants. It was reported that milligrams or grams of recombinant proteins could be harvested within a month and 100 kg of products are possible collected less than a year (Gleba *et al.*, 2005). In addition, potential infectious or pathogenic microbes are relatively lower in plant-based system. Besides, presence of oncogenic sequences and viral contaminants, which are always the drawbacks of using mammalian viral vectors, could be also avoided by using plants (Fischer *et al*., 1999). Available of post translational modification system in plants is also another important reason for choosing plants as expression host, especially for the production of functional recombinant proteins that require proper folding. Production of improper folding protein in microbes (such as *E. coli*) has led to the formation of insoluble protein. In order to refold misfolded recombinant proteins, sophisticated and expensive downstream procedures are required to attain functional structure of proteins (Verma *et al.*, 1998). On the way, expression of recombinant proteins in edible plant organs, such as seeds, could also eliminate the use of needles for delivery of the desired drug to human body. Instead of using leafy plants (such as tobacco), cereal seeds (such as maize, rice, wheat and barley) and some edible fruits as well as vegetables (potato, carrot and banana) have already been exploited to produce numbers of therapeutic drugs such as human serum albumin, tumour necrosis factor α (TNF-α) and antibodies (Fischer *et al*., 2004).

2.2.1.2 Current status of plant-derived therapeutic proteins

In 1986, human growth insulin, first plant-based recombinant therapeutics, was produced in sunflower and tobacco. By year 2011, there were more than 20 plant-derived therapeutic proteins undergoing preclinical and clinical trials (Yao *et al*., 2015). To date, several plant-derived therapeutic proteins have been commercialised in the market for research use as well as for human application. In year 2004, Sigma Aldrich announced that they would distribute tobacco-derived aprotinin, which was a protease inhibitor produced by Large Scale Biology Corporation using GENEWARE technology (Outsourcing-Phama.com). Conventionally, aprotinin was extracted from lung of bovine; however, high cost as well as contamination of animal pathogens, such as bovine spongiform encephalopathy (BSE), were a concern of using this natural aprotinin. By using GENEWARE technology, which employing a full virus tobacco mosaic virus (TMV)-

based expression system, high amount of aprotinin was harvested (at ~ 150 to 300 mg/kg) and the risk for animal pathogen contamination is also low (Pogue *et al*., 2010).

In year 2012, ELELYSO™, recombinant taliglucerase alfa produced from carrot cells, was the first FDA approved plant-derived therapeutic proteins for the treatment of Gaucher disease for adult (Yao *et al*., 2015). In addition, ZMapp, a chimeric monoclonal antibody against surface glycoprotein of Ebola produced in tobacco, was released by Mapp Biopharmaceutical Inc (San Diego, USA) in year 2014 (Davidson *et al*., 2015). ZMapp successfully saved several patients from death caused by Ebola disease although the drug has not been approved by FDA. In year 2015, an outbreak of Middle East respiratory syndrome coronavirus (MERS-CoV) has killed 35% of infected patient. Plant Biotechnology Inc. (California, USA) reported that they have produced a tobacco-derived immunoadhesin (DPP4-Fc), by fusion of cell surface protein dipeptidyl peptidase 4 (DPP4) of MERS-CoV to constant region of human immunoglobulin (SBIRSource, 2014). The recombinant protein prevents the infection of MERS-CoV by binding to MERS-CoV spike (S) glycoprotein. However, they claimed that high amount of recombinant protein is required to achieve 50% of inhibitory effect.

2.2.2 Plant transformation strategies

2.2.2.1 Stable transformation and transient expression

Stable transformation is a term for description regarding integration of foreign genes into recipient host genome and stably of integrated genes inherited by the progeny (Lico *et al*., 2008). There are numerous techniques available for plant stable transformation, including agrobacterium mediated transformation, biolistic, protoplast fusion, microinjection, employment of silicon carbide and tissue electroporation. The most commonly used stable transformation technique is agrobacterium-based transformation. In agrobacterium-based transformation approach, foreign genes are cloned on disarmed Ti plasmid, which is later delivered into host plants by agrobacterium (such as *Agrobacterium tumefaciens* and *Agrobacterium rhizogene*) (Gelvin, 2003). Agrobacterium-mediated transformation has been used widely in crops, such as soy bean, corn, rice and wheat (Nishimura *et al*., 2007; Sparks *et al*., 2014). However, agrobacterium transformation is naturally available for dicotyledonous plants and favourable for transformation of monocotyledonous plants. Thus, direct gene transfer approach, using biolistic, protoplast fusion, microinjection, employment of silicon carbide and tissue electroporation, is an alternative way to produce stable nuclear transformation for both monocotyledonous and dicotyledonous plants (Slater *et al*., 2003).

Stable transformation is time consuming and requires tedious steps in order to generate transgenic plants. However, transient expression system is able to produce high protein expression level in short period of time after transformation (Slater *et al*., 2003). Foreign genes do not integrate into plant genome in transient expression system and non-integrated DNA is eventually lost over time. In plant, full viral vector as well as agroinfiltration are two major delivery approaches employed for transient expression. By using full viral vectors, DNA form of viral vectors or RNA transcripts of viral vector, harbouring genes of interest, is mechanically inonculated on plant leaves with carborandum (Escobar *et al*., 2003). Wounding sites on leaf surface generated by carbodandum allows the entry of plant viruses. For agroinfiltration approach, agrobacterium, harbouring disarmed Ti plasmid with gene of interest, is infiltrated into intercellular space of leaf mesophyll and agrobacterium is subsequently transfer Ti plasmid into plant genome (Chen *et al*., 2013). Since no selection activity for transformed cells with antibiotics is performed in both approaches, the expression of recombinant proteins is only expected from the infected or infiltrated plants and no seeds with stable transgenes are collected. Hence, protein expression using this method does not generate progeny with stable transgene.

2.2.2.2 Agroinfiltration strategy

Agroinfiltration was initially used to study plant-virus interactions; however, this technique has been adopted recently for the production of recombinant proteins (Chen *et al*., 2013). By using agroinfiltration strategy, 2 common types of DNA vectors are available. General binary vector could be used for agroinfiltration by inserting an expression cassettes in T-DNA region of Ti plasmid. The second type of DNA vector involves the incorporation of partial or whole viral genome into T-DNA region of binary vector. Gene of interest is incorporated into the viral genome by inserting gene between viral elements, fusion to coat protein (CP) or replacing a non-essential viral element.

Agroinfiltration can be performed using syringe or vacuum infiltration approaches. Syringe infiltration requires simple syringe rather than sophiscated machine. Besides, small amount of bacterial cultures is required and expression of multiple gene constructs could be assessed by infiltrating multiple construct on the same leaf. By using syringe infiltration, small amount of bacterial culture is pressed on the abaxial of leaves to deliver bacteria into intercellular space of leaf mesophyll. On the other hand, vacuum infiltration delivers bacteria into intercellular space of leaf mesophyll by changing the pressure in the infiltration chamber. Since infiltration work is performed by submerging plant leaves into bacterial suspension. larger amount of bacterial suspension is required for vacuum infiltration. However, this approach can infiltrate large batches of plants in short period of time. In addition, infiltration work performed using vacuum infiltration is consistent and severe mechanical injury could also be reduced. Currently, this platform is applied in several biopharmaceutical companies that produced recombinant proteins in plants, including Medicago Inc (USA), Fraunhofer Center for Molecular Biotechnology (FhCMB, USA), Kentucky Bioprocessing (USA) and Icon Genetics (Germany).

2.2.2.3 Emerging agro-based transformation approaches

Although vacuum infiltration can efficiently infiltrate huge batches of plants, this approach is laborious and requires sophiscated machine. Hence, new delivery approaches are suggested to improve the current research challenge. In year 2008, Yang and his colleagues suggested delivery of agrobacterium into *N. benthamiana* using “root absorption” approach. They have successfully expressed recombinant GFP protein via this approach. From their study, expression of recombinant GFP in quadrifiliate phase and quinquefoliate phase is ~ 70% higher than in hexaphyllous phase. Seedling with root also showed higher expression of recombinant proteins. It is interesting to find that expression of recombinant GFP was ~60% higher when plants were not watered 7-10 days before inoculation.

Besides, air-brush approach to deliver agrobacterium into tobacco plants was also reported in 2015. Jin *et al*., (2015) successfully expressed recombinant GFP and human acidic fibroblast growth factor (ha FGF) in *N. benthamiana* using “air brush” method by employing carborandum and air-brush tube (pressure 75–80 psi). Similarly, recombinant protein has higher expression level in quadrifiliate phase and quinquefoliate phase. Highest expression of recombinant protein was harvested from plants infiltrated for 7-9 dpi. Development for new delivery strategy is encouraged since this can directly reduce the cost as well as difficulty of the work for infiltration.

Chapter 3

Construction of Gene Cassettes for the Development of Recombinant Apoptin Vector Variants

Table of Contents

3.1 Introduction

Viral Protein 3 (VP3) is a small protein derived from Chicken Anemia Virus (CAV). This protein is renamed as ‘apoptin’ since it causes the depletion of myeloid cells and thymocytes by triggering apoptosis during viral infection in young chicken (Noteborn and Koch, 1995). It is believed that apoptin is a potential anticancer agent because apoptin exhibits selective killing feature towards cancer or transformed cells but not primary or non-transformed cells (Noteborn *et al*., 1995). DNA transfection with transfection reagents or mammalian viral vectors is a common tool used in most of the studies to deliver apoptin gene into cancer cells *in vitro* and *in vivo* (Backendorf *et al*., 2008). Moreover, production of recombinant apoptin had rapidly been discovered with predominant recovery from *Escherichia coli* expression system (Leliveld[a] *et al*., 2003; Nogueira-Dantas *et al*., 2007).

Employment of plants as bioreactor to produce therapeutic drugs develops rapidly in both academia and industries. In comparison to other expression systems, plant-based system provides relatively more attractive benefits. These include low production cost, easy and scalable in production, short lead period and low risk of contamination with life-threatening biological agents (Fischer *et al*., 2004). With the advanced recombinant technology, high amount of recombinant proteins can be produced from plants with the creation of stable transformed lines or transient expression approach. Due to short incubation time and significantly high expression yield, transient expression is always a favourable method for large scale production of pharmaceutical products especially in an emergency situation (Gleba *et al*., 2005). Binary vectors and plant viral vectors are the two types of common vectors used in transient expression strategy to harbour gene of interest to be delivered into host plants. Due to several disadvantages of Ti plasmids originated from *Agrobacterium tumefaciens*, likewise the large molecular size leading to difficult manipulation in cloning activities, binary vectors have been developed to separate T-DNA region and *vir* genes that are important for transformation activities of *Agrobacterium* into two recombinant plasmids (Lee and Gelvin, 2008). Size reduction of recombinant plasmids enhances the transformation efficiency of foreign gene inserts with large molecular szie. The most commonly used binary vectors include pGreen, pBin19 and pPVP (Lee and Gelvin, 2008). More new binary vectors have been developed and modified based on these above mentioned binary vectors as vector backbones. On the other hand, plant viruses are also exploited and engineered to become compatible vectors for delivery of foreign DNA into plants. Expression of recombinant protein with ‘full virus’ strategy requires several weeks for systemic movement of virus to whole plants; however, efficient delivery of foreign DNA into whole plants can be obtained by using deconstructed viral vectors (Gleba *et al*., 2007). Some viral elements that are responsible for systemic infection of virus, for example coat proteins or movement proteins, are removed and functions of these viral elements could be complemented by *Agrobacterium* via agroinfection or agroinfiltration technique.

Yield and solubility are the two main challenges for recombinant protein expression following the successful delivery of transgene into host plants. In order to increase both yield and solubility of recombinant proteins, several approaches as mentioned below are always applied. First, codon sequences of foreign DNA could be optimised based on codon preferences of expression hosts. Codon optimisation removes rare codons and replaces synonymous codon sequences which are favourable by expression hosts; therefore, protein translation efficiency could be increased and yield of recombinant proteins could also be enhanced (Angov, 2011). Second, subcellular targeting is a way to accumulate recombinant proteins in a specific cell compartment in order to avoid high proteolytic activities occurring in cytoplasm. In plants, several subcellular compartments are always the preferred choices of researchers to store recombinant proteins, including endoplasmic reticulum (ER), vacuoles, apoplasts and chloroplasts (Streatfield, 2007). Third, fusion of recombinant proteins with large soluble protein molecules is an alternative way to enhance protein solubility. Large protein molecules, such as maltose binding protein (MBP) and glutathione S-transferase (GST), have always been used to increase solubility and correct folding of recombinant proteins (Terpe, 2003). Other than approaches mentioned above, protein expression may also be enhanced by inhibiting plant defense mechanisms by co-expression of recombinant protein with gene silencing suppressors, enhancing protein folding by co-expression with chaperones molecules as well as reducing proteolytic activity by co-expression of protease inhibitors (Feller *et al*., 2013; Kim *et al*., 2008). Nevertheless, these strategies do not necessary work well for all kinds of recombinant proteins and a good combination of these strategies should be investigated in order to achieve a better protein expression result.

Development of a functional recombinant apoptin from plant-based system was the ultimate aim of the study. Previous studies showed several challenges that were needed to be solved in order to develop apoptin as a therapeutical drug. Up to date, expression of recombinant apoptin in plants was only once reported by Larcote *et al.* (2007) and only scarce information was available for the production of apoptin in plant-based system. Recombinant apoptin produced in *E. coli* is always appeared in insoluble state, sophisticated purification and refolding processes are always required to recover the protein activities (Leliveld[a] *et al*., 2003). Uneven delivery of apoptin gene into cancer cells is one of the major issues when apoptin is delivered via DNA transfection method (Backendorf *et al*., 2008). Besides, risk of potential infection by the mammalian virus, which it is used as a delivery tool, and cytotoxic effect of transfection reagents are also two major concerns with DNA transfection approaches (Anson, 2004). Hence, potential of production for recombinant apoptin in plants was explored in this study and several improvements had been made for recombinant apoptin expression in order to move a step forward for the production of apoptin as anticancer agent.

In this chapter, design of apoptin gene cassettes and cloning of recombinant vectors are presented. In order to obtain high amount of soluble recombinant protein in *Nicotiana benthamiana*, optimisation was performed on codon sequences of apoptin to remove rare codons that might hamper expression of recombinant apoptin. Signal peptide (PR1a) and also ER retention signal were fused to apoptin sequence to redirect the accumulation of recombinant protein in apoplast and ER. Furthermore, green fluorescent protein (GFP) and a modified version of lichenase, a β-1,3-1,4-glucanase from *Clostridium thermocellum*, were fused to apoptin and it was believed that the fusion of large proteins was able to enhance the fraction of soluble protein. Sequences of single chain antibody H22 specifically binding to Fc gamma receptor I CD64+ and epidermal growth factor (EGF) that binds to EGF receptors were fused to apoptin sequence in order to target the action of apoptin towards cancer cells that overexpressed these receptors. A molecular adaptor was added between apoptin and tumor specific ligands to assist the internalisation of apoptin into cell cytosol. Besides, apoptin gene variants were co-expressed with ER stress proteins bZIP17, bZIP28 and bZIP60 to enhance expression of recombinant apoptin.

Hence, the specific objectives of this chapter were: (1) to optimise apoptin gene sequences based on the codon usage of *N. benthamiana*; (2) to design and construct apoptin gene cassettes harbouring apoptin gene with subcellular targeting signals, including signal peptide (PR1a) and ER retention signal (KDEL); (3) to construct apoptin gene cassettes in fusion with individual GFP and lichenase; (4) to construct apoptin gene cassettes in fusion with individual tumour specific ligands, namely H22 single chain antibody, EGF and the molecular adaptor CatAd; (5) to incorporate apoptin gene cassettes into vectors, pGR-D4, pGR-D and pGR-DN, and lastly, (6) to integrate apoptin gene cassettes into vector, pGR-DN that harboured bZIP17, bZIP28 and bZIP60.

3.2 Materials and Methods

3.2.1 General materials

3.2.1.1 Vectors

Two types of vectors, including binary vectors (pGR-D and pGR-DN) and plant viral vector (pGR-D4), were used in this study to harbour apoptin gene cassettes and deliver into *Nicotiana benthamiana* via *Agrobacterium*. Tobacco mosaic virus (TMV) based expression vector (pGR-D4) as well as binary vectors, pGR-D and pGR-DN were kindly provided by Fraunhofer Center for Molecular Biotechnology (FhCMB), United States of America (USA).

3.2.1.2 Synthetic gene cassettes

All apoptin/VP3 gene cassettes based on sequence of Mohd-Azmi *et al*. (1997) (Malaysia isolate) (GenBank accession number: AAB86420.1) was synthesised by GeneArt™ Gene Synthesis, Thermo Scientific (USA). Synthetic gene cassette, PR-VP3-HK was designed as apoptin gene in fusion to C-terminal of signal peptide PR1a and N-terminal of hexahistidine as well as endoplasmic reticulum (ER) retention signal (Appendix 3.1). Individual green fluorescent protein (GFP) and lichenase were also synthesised in fusion to N-terminal of apoptin gene with signal peptide PR1a, hexahistidine and ER retention signal resulting the synthetic gene cassettes, PR-GFP-VP3-HK (Appendix 3.2) and PR-Lic-VP3-HK (Appendix 3.3 Besides, synthetic gene sequences of red fluorescent protein, mCherryNuc (Appendix 3.4), H22 single chain antibody (Appendix 3.5) and epidermal growth factor (EGF) (Appendix 3.6), bZIP17 (Appendix 3.7), bZIP28 (Appendix 3.8), bZIP60 (Appendix 3.9) were also synthesised by Gene Synthesis, Thermo Scientific (USA). All synthetic genes were provided in pMAT which served as a holding vector.

Codon sequences of all synthetic genes were optimised based on the codon usage *N. benthamiana.* These synthetic genes are summarised in Table 3.1.

Table 3.1: List of synthetic genes.

No	Synthetic gene cassettes	Holding vector	Source of sequences	Appendix
2	PR-VP3-HK	pMAT:: PR-VP3-HK	GeneArtTM Gene Synthesis, Thermo Scientific (USA)	3.1
3	PR-GFP-VP3-HK	pMAT:: PR-GFP-VP3-HK	GeneArtTM Gene Synthesis, Thermo Scientific (USA)	3.2
4	PR-Lic-VP3-HK	pMAT:: PR-Lic-VP3-HK	GeneArtTM Gene Synthesis, Thermo Scientific (USA)	3.3
5	mCherryNuc	pMAT:: mCherryNuc	GeneArtTM Gene Synthesis, Thermo Scientific (USA)	3.4
6	H22	pMAT:: PR-HF-H22catADGM	GeneArtTM Gene Synthesis, Thermo Scientific (USA)	3.5
7	EGF	pMAT:: PR-HF-EGF-CatAD-Tau	GeneArtTM Gene Synthesis, Thermo Scientific (USA)	3.6
8	bZIP17	-	GeneArtTM Gene Synthesis, Thermo Scientific (USA)	3.7
9	bZIP28	-	GeneArtTM Gene Synthesis, Thermo Scientific (USA)	3.8
10	bZIP60	-	GeneArtTM Gene Synthesis, Thermo Scientific (USA)	3.9

3.2.1.3 Enzymes, kits and chemical reagents

Polymerase enzymes used in polymerase chain reaction (PCR) assays included Phusion® High Fidelity PCR Master Mix with HF Buffer (New England Biolabs (NEB)® Inc, USA), Platinum® PCR SuperMix High Fidelity (Thermo Scientific, USA) and Platinum® PCR SuperMix (ThermoFisher Scientific, USA). DNA ladder, namely 1 kb Plus DNA ladder (ThermoFisher Scientific, USA) was used in gel electrophoresis. Restriction enzyme (RE) digestion was performed using enzymes inculduing PacI, XhoI, BsrGI and NheI (NEB® Inc, USA). Ligation was performed using T4 ligase (NEB® Inc, USA) and ligation buffer (ThermoFisher Scientific, USA). Gel purification was performed using Zymoclean™ Gel DNA Recovery Kit (Zymo Research, USA). Purification of DNA was also carried out using DNA Clean and Concentrator™-5 (Zymo Research, USA). Plasmid purification was performed using Zyppy™ Plasmid Midiprep Kit (Zymo Research, USA). DNA gels were stained with ethidium bromide (ThermoFisher Scientific, USA).

3.2.1.4 Consumable labware supplies and specialised equipment

PCR was performed using Biometra T-Gradient (Biometra GmbH, Germany). DNA gel electrophoresis was carried out using DNA Plus gel electrophoresis system (USA Scientific, USA). Images of electrophoresed gels were captured using Kodak Capturing system with FOTO/Prep Transilluminator (Fotodyne Incorporated, USA). Concentration of DNA was measured using Nano Drop 1000 spectrophotometer (Thermo Scientific, USA).

3.2.1.5 DNA sequencing, primer synthesis and data analysis

Optimised DNA sequences were synthesised by GeneArt™ Gene Synthesis (Thermo Scientific, USA). Primers were synthesised by Integrated DNA Technologies (IDT, USA). DNA sequencing service was provided by Delaware Biotechnology Institute (DBI, USA).

Codon adaptation indices (CAIs) of sequences were compared using CAIcal server. DNA sequences and maps were analysed using SeqBuilder (DNASTAR, Inc, USA) and GENtle (University of Cologne, 2003). Sequencing data were analysed and aligned using SeqMan Pro (DNASTAR, Inc, USA), BioEdit and ClustalW2 Multiple sequence alignment.

3.2.2 Overview of design and construction of recombinant of apoptin vector variants

Synthetic apoptin gene in fusion to signal peptide from tobacco pathogenesis related protein 1a (PR1a), hexa-histidine tag and endoplasmic reticulum (ER) retention signal (gene cassettes: PR-VP3-HK, PR-GFP-VP3-HK and PR-Lic-VP3-HK) (Table 3.2) were released from holding vector, pMAT using restriction enzymes, PacI and XhoI before incorporated into pGR-D4 vector. Recombinant apoptin expressed from these three gene cassettes were expected accumulating in ER of plant cells. Besides, ER retention signal was removed and the resultant gene cassettes, PR-VP3-H, PR-GFP-VP3-H and PR-Lic-VP3-H (Table 3.2) were generated. Removal of ER retention signal would be expected resulting recombinant proteins entering in secretory pathway and subsequently secreted into apoplast. Further removal of signal peptide generated gene cassettes, VP3-H, GFP-VP3-H and Lic-VP3-H (Table 3.2). Recombinant apoptin expressed from these gene cassettes were expected accumulating in cell cytoplasm. To remove the fusion protein from apoptin after protein purification, an enterokinase site was incorporated between GFP and apoptin gene as well as lichenase and apoptin gene. Gene cassettes, PR-VP3-H, VP3-H, PR-GFP-VP3-H, GFP-VP3-H, PR-Lic-VP3-H and Lic-VP3-H were amplified from pMAT:: PR-VP3-HK, pMAT:: PR-GFP-VP3-HK and pMAT:: PR-Lic-VP3-HK accordingly by the relevant primers (Table 3.3 and Appendix 3.10) via single step PCR using Phusion® High Fidelity PCR Master Mix with HF Buffer as described in section 3.2.3. All PCR gene fragments were digested using PacI and XhoI before ligated to pGR-D4 vector.

Single chain antibody H22 and epidermal growth factor (EGF), for targeting to specific cell types, were also fused to N-terminal of apoptin gene with addition of signal peptide PR1a and ER retention signal. Instead of using full length apoptin gene sequence, truncated apoptin gene were also study while in fusion with H22 single chain antibody and EGF protein. A molecular adaptor was also incorporated between H22 single chain antibody and apoptin gene as well as EGF and apoptin gene. Therefore, gene cassettes, namely PR-H22-CatAd-VP3-HK, PR-H22-CatAd-VP3-40-121-HK, PR-H22-CatAd-VP3-60-121-HK, PR-H22-CatAd-VP3-80-121-HK, PR-EGF-CatAd-VP3-HK, PR-EGF-CatAd-VP3-40-121-HK, PR-EGF-CatAd-VP3-60-121-HK, PR-EGF-CatAd-VP3-80-121-HK were amplified from recombinant vectors, pMAT:: PR-HF-H22catADGM, pMAT:: PR-HF-EGF-CatAD-Tau and pMAT:: PR-GFP-VP3-HK with corresponding primers (Table 3.3 and Appendix 3.10) via fusion PCR using Platinum® PCR SuperMix High Fidelity (section 3.2.3). All PCR gene fragments were digested using PacI and XhoI before ligated to pGR-D4 vector.

Gene cassettes, PR-VP3-HK, PR-GFP-VP3-HK and PR-EGF-CatAd-VP3-HK (Table 3.2Table 3.) were released from pGR-D4 vector using restriction enzymes, PacI and XhoI before ligated to pGR-DN vector that harboured the sequences of ER stress proteins, i.e. bZIP17, bZIP28 and bZIP60 located downstream of apoptin expression cassettes driven by individual promoters.

Besides, gene cassettes, PR-GFP-VP3-HK, PR-GFP-VP3-H and GFP-VP3-H (Table 3.2) were also released from vectors, pMAT and pGR-D4 using restriction enzymes, PacI and XhoI before subcloned into binary vector, pGR-D. Recombinant GFP-apoptin was co-expressed with a red fluorescent protein (mCherry) in order to evaluate the localisation of recombinant apoptin in *N. benthamiana*. mCherry was fused to N-terminal of nuclear localisation signal (Nuc) and the expression of *mCherryNuc* was directed by a separate promoter located downstream of apoptin expression cassettes. Gene cassette, mCherryNuc was released from vector, pMAT:: mCherryNuc using BsrGI and NheI before ligated to pGR-D.

A schematic diagram is presented to illustrate the construction procedure of recombinant vectors in Figure 3.1.

Table 3.2: List of apoptin gene cassettes.

No	Name of backbone	Schematic diagrams of apoptin gene cassettes for the recombinant vector variants
1	pGR-D4	PR-VP3-HK 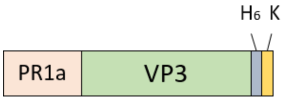
2	pGR-D4	PR-VP3-H 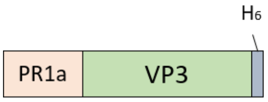
3	pGR-D4	VP3-H 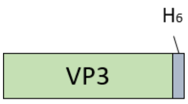
4	pGR-D4	PR-GFP-VP3-HK 
5	pGR-D4	PR-GFP-VP3-H 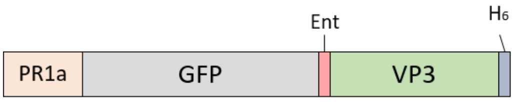
6	pGR-D4	GFP-VP3-H 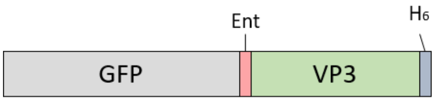

7	pGR-D4	PR-Lic-VP3-HK 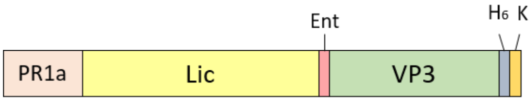
8	pGR-D4	PR-Lic-VP3-H 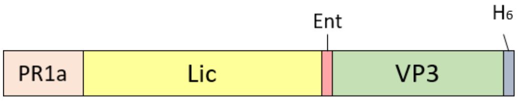
9	pGR-D4	Lic-VP3-H 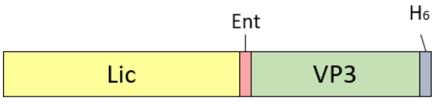
10	pGR-D4	PR-H22-CatAd-VP3-HK 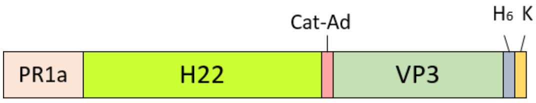
11	pGR-D4	PR-H22-CatAd-VP3-40-121-HK 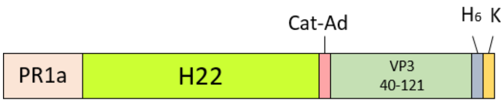
12	pGR-D4	PR-H22-CatAd-VP3-60-121-HK 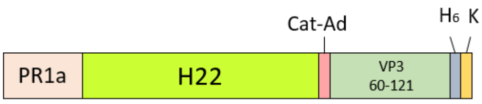
13	pGR-D4	PR-H22-CatAd-VP3-80-121-HK 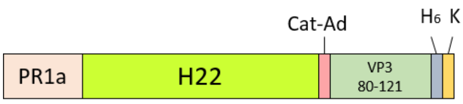
14	pGR-D4	PR-EGF-CatAd-VP3-HK 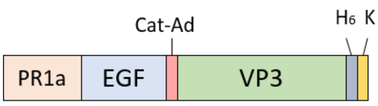
15	pGR-D4	PR-EGF-CatAd-VP3-40-121-HK 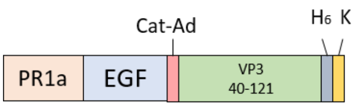

16	pGR-D4	PR-EGF-CatAd-VP3-60-121-HK 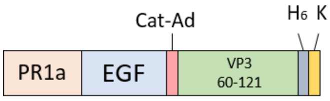
17	pGR-D4	PR-EGF-CatAd-VP3-80-121-HK 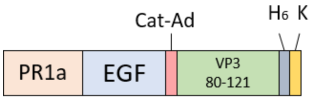
18	pGR-DN	PR-VP3-HK__bZIP17 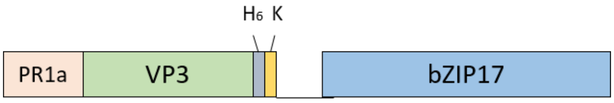
19	pGR-DN	PR-VP3-HK__bZIP28 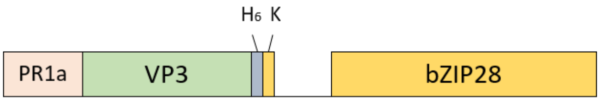
20	pGR-DN	PR-VP3-HK__bZIP60 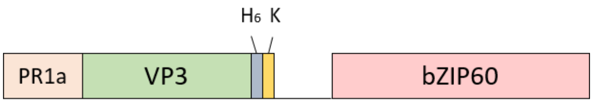
21	pGR-DN	PR-GFP-VP3-HK__bZIP17 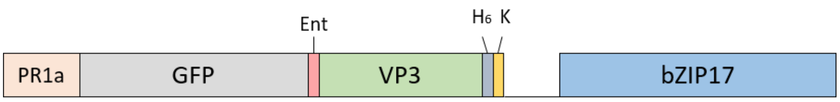
22	pGR-DN	PR-GFP-VP3-HK__bZIP28 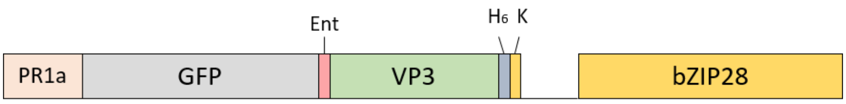
23	pGR-DN	PR-GFP-VP3-HK__bZIP60 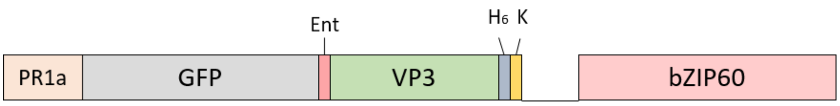
24	pGR-DN	PR-EGF-CatAd-VP3-HK__bZIP17 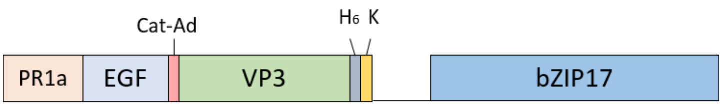

25	pGR-DN	PR-EGF-CatAd-VP3-HK__bZIP28 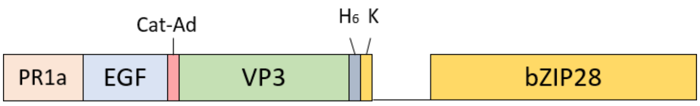
26	pGR-DN	PR-EGF-CatAd-VP3-HK__bZIP60 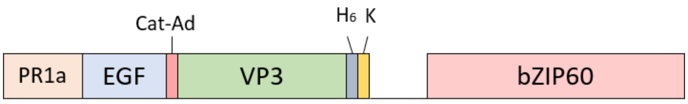
27	pGR-D	PR-GFP-VP3-HK__mCherryNuc 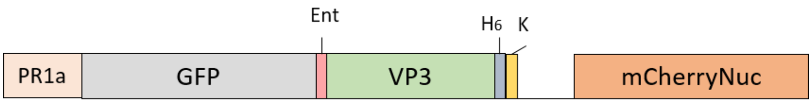
28	pGR-D	PR-GFP-VP3-H__mCherryNuc 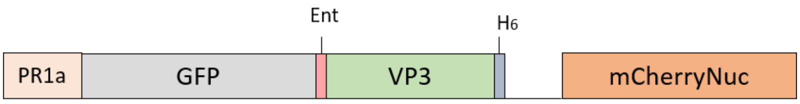
29	pGR-D	GFP-VP3-H__mCherryNuc 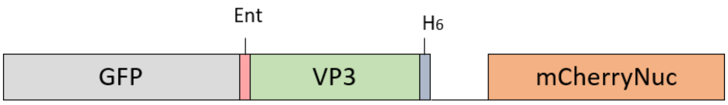

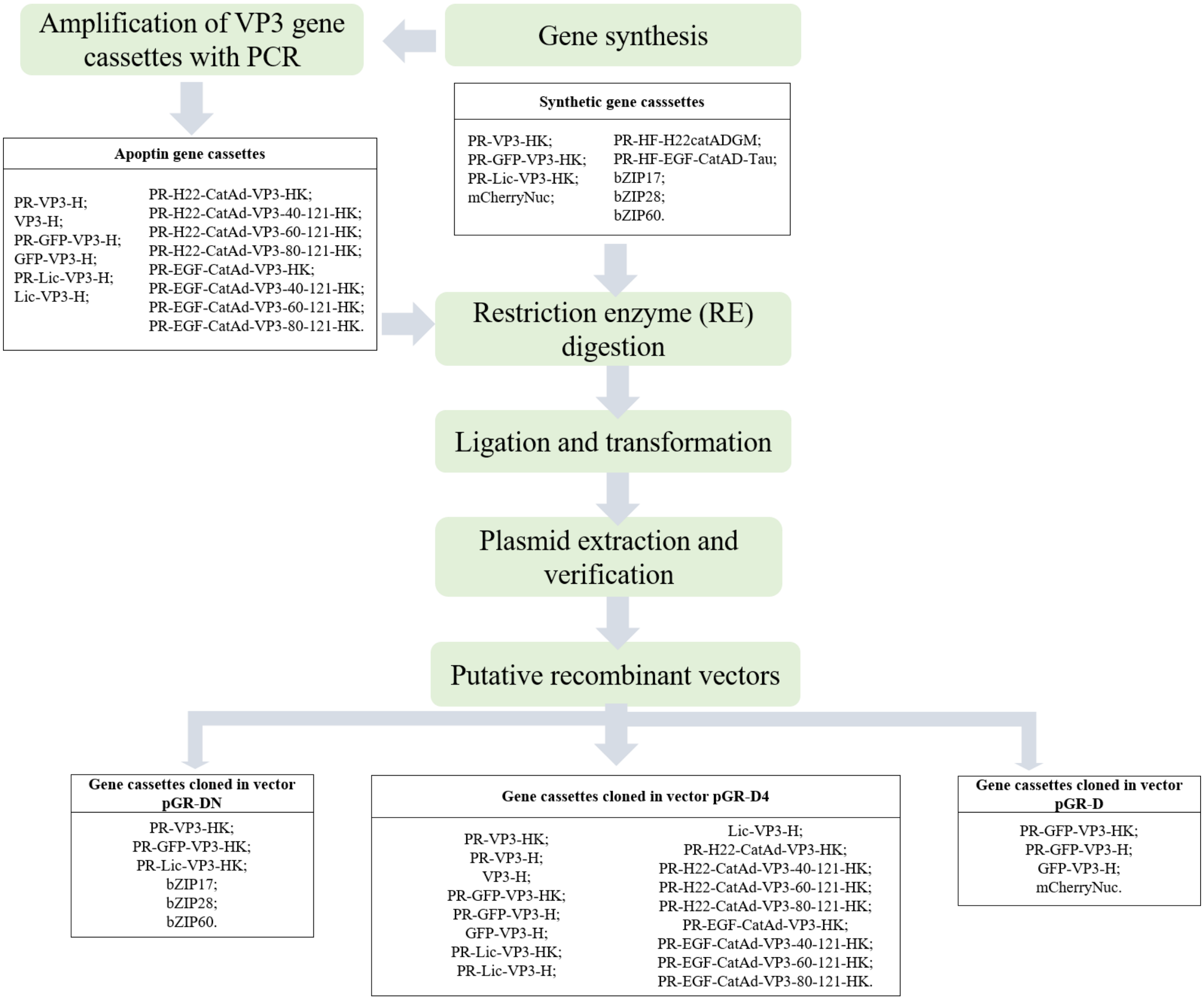

Figure 3.1: Schematic representation of construction process of all recombinant vectors under the study.

3.2.3 Polymerase chain reaction (PCR)

All PCR preparations were done as recommended by manufacturer. General PCR mixtures were prepared as described: 1X reaction buffer, 1 unit of polymerase, forward and reverse primers (0.6 µM each), 15 ng DNA template and topped up with distilled water to 50 µl. PCR programme was initiated at 94-98°C from 30 seconds to 5 minutes, followed by 35 cycles of denaturation at 94-98°C for 10-45 seconds, annealing at 40-70°C for 40 seconds and extension at 68-72°C with 1-2kb/minute. The mixtures were incubated at 68-72°C for an additional 5-10 minutes and stored at 4-10°C after the amplification processes had finished. Amplified fragments were analysed in 1% agarose gel electrophoresis, subsequently, gel images were captured and recorded. Specific conditions of PCR for each gene cassette are listed clearly in Table 3.3 and primer sequences in Appendix 3.10.

Table 3.3: PCR conditions for apoptin gene cassettes.

No	Gene cassettes	Templates	Parameters of PCR			
			Primers		Annealing temperature	Extension time
			Forward	Reverse		
1	PR-VP3-H	pMAT:: PR-VP3-HK	pVP3-F	VP3H-R	56°C	40 seconds
2	VP3-H	pMAT:: PR-VP3-HK	VP3-F	VP3H-R	56°C	40 seconds
3	PR-GFP-VP3-H	pMAT:: PR-GFP-VP3-HK	pVP3-F	gVP3H-R	56°C	40 seconds
4	GFP-VP3-H	pMAT:: PR-GFP-VP3-HK	gVP3-F	gVP3H-R	56°C	40 seconds
5	PR-Lic-VP3-H	pMAT:: PR-Lic-VP3-HK	pVP3-F	VP3H-R	56°C	40 seconds
6	Lic-VP3-H	pMAT:: PR-Lic-VP3-HK	LicVP3-F	VP3H-R	56°C	40 seconds
7	PR-H22-CatAd-VP3-HK	pMAT:: PR-HF-H22catADGM and pMAT:: PR-GFP-VP3-HK	PRH22-F; HCatVP3-F; YFE1-T-F	HCatVP3-R; VP3-HK_R	56-63°C	45-90 seconds
8	PR-H22-CatAd-VP3-40-121-HK	pMAT:: PR-HF-H22catADGM and pMAT:: PR-GFP-VP3-HK	PRH22-F; HCatVP3-40-121-F; YFE1-T-F	HCatVP3-40-121-R; VP3-HK_R	56-63°C	45-90 seconds
9	PR-H22-CatAd-VP3-60-121-HK	pMAT:: PR-HF-H22catADGM and pMAT:: PR-GFP-VP3-HK	PRH22-F; HCatVP3-60-121-F; YFE1-T-F	HCatVP3-60-121-R; VP3-HK_R	56-63°C	45-90 seconds
10	PR-H22-CatAd-VP3-80-121-HK	pMAT:: PR-HF-H22catADGM and pMAT:: PR-GFP-VP3-HK	PRH22-F; HCatVP3-80-121-F; YFE1-T-F	HCatVP3-80-121-R; VP3-HK_R	56-63°C	45-90 seconds
11	PR-EGF-CatAd-VP3-HK	pMAT:: PR-HF-EGF-CatAD-Tau and pMAT:: PR-GFP-VP3-HK	PREGF-F; ECatVP3-F; YFE1-T-F	ECatVP3-R; VP3-HK_R	56-63°C	45-90 seconds
12	PR-EGF-CatAd-VP3-40-121-HK	pGR-D4:: PR-EGF-CatAd-VP3-HK	YFE-1-T-F; ECatVP3-40-121-F;	ECatVP3-40-121-R; VP3-HK_R	56-63°C	45-90 seconds
13	PR-EGF-CatAd-VP3-60-121-HK	pGR-D4:: PR-EGF-CatAd-VP3-HK	YFE-1-T-F; ECatVP3-60-121-F;	ECatVP3-60-121-R; VP3-HK_R	56-63°C	45-90 seconds
14	PR-EGF-CatAd-VP3-80-121-HK	pGR-D4:: PR-EGF-CatAd-VP3-HK	YFE-1-T-F; ECatVP3-80-121-F;	ECatVP3-80-121-R; VP3-HK_R	56-63°C	45-90 seconds

3.2.4 DNA purification

Zymoclean^{TM} Gel DNA Recovery Kit was used to recover the DNA pieces from agarose gel. Three volumes of ADB buffer were added to each volume of agarose excised from the gel and the mixture was incubated at 55°C for 10 minutes until the gel slice was completely dissolved. Melted agarose solution was transferred to a Zymo-Spin™ column with collection tube following by 30-second centrifugation at 13, 000 rpm. The pass-through was discarded and 200 µl of DNA wash buffer was added to the column followed by 30-second centrifugation at 13, 000 rpm. The washing step was repeated before DNA bound to the column matrix was eluted with 15-20 µl of distilled water. Columns were further incubated for 5 minutes at room temperature before centrifuging at 13, 000 rpm for 1 minute. Elution step was repeated to acquire higher amount of DNA from column matrix.

RE-digested DNA was also purified by using DNA Clean and Concentrator^{TM}-5. Approximately 5 volumes of DNA Binding Buffer was added to 1 volume of DNA sample and mixed by vortexing. All mixtures were then transferred to Zymo-Spin^{TM} columns with collection tubes followed by centrifugation for 30 seconds. The pass-through was discarded and 200 µl of DNA Wash Buffer was added to the column followed by another centrifugation for 30 seconds. Washing step was repeated before addition of 8-10 µl of distilled water to the column matrix. Columns were incubated at room temperature for 5 minutes before centrifuging for 30 seconds to elute DNA from the column matrix.

Concentration and purity of all purified DNA products were then measured by Nano Drop 1000 spectrophotometer.

3.2.5 Restriction enzyme (RE) digestion

A general double RE digestion was prepared as below: 0.5-2 µg of vectors, 500 ng of gene cassettes from PCR, 1-10 units of enzymes, 1X reaction buffer, 1X BSA and topped up to 50 µl with distilled water. RE digestion for specific apoptin gene cassettes and vectors are listed clearly in Table 3.4.

Table 3.4: RE digestion details of apoptin gene cassettes and vectors.

No	Gene cassettes	RE		Incubation temperature	Incubation period
		1	2		
1	PR-VP3-H	PacI	XhoI	37°C	2 hours
2	VP3-H	PacI	XhoI	37°C	2 hours
3	PR-GFP-VP3-H	PacI	XhoI	37°C	2 hours
4	GFP-VP3-H	PacI	XhoI	37°C	2 hours
5	PR-Lic-VP3-H	PacI	XhoI	37°C	2 hours
6	Lic-VP3-H	PacI	XhoI	37°C	2 hours
7	PR-H22-CatAd-VP3-HK	PacI	XhoI	37°C	2 hours
8	PR-H22-CatAd-VP3-40-121-HK	PacI	XhoI	37°C	2 hours
9	PR-H22-CatAd-VP3-60-121-HK	PacI	XhoI	37°C	2 hours
10	PR-H22-CatAd-VP3-80-121-HK	PacI	XhoI	37°C	2 hours
11	PR-EGF-CatAd-VP3-HK	PacI	XhoI	37°C	2 hours
12	PR-EGF-CatAd-VP3-40-121-HK	PacI	XhoI	37°C	2 hours
13	PR-EGF-CatAd-VP3-60-121-HK	PacI	XhoI	37°C	2 hours
14	PR-EGF-CatAd-VP3-80-121-HK	PacI	XhoI	37°C	2 hours
15	mCherryNuc	BsrGI	NheI	37°C	2 hours
16	bZIP17	BsrGI	NheI	37°C	2 hours
17	bZIP28	BsrGI	NheI	37°C	2 hours
18	bZIP60	BsrGI	NheI	37°C	2 hours
19	pGR-D4	PacI	XhoI	37°C	2 hours
20	pGR-D	PacI	XhoI	37°C	2 hours
21	pGR-D	BsrGI	NheI	37°C	2 hours
22	pGR-DN	PacI	XhoI	37°C	2 hours
23	pGR-DN	BsrGI	NheI	37°C	2 hours

3.2.6 Ligation

All RE-digested inserts were ligated to the respective vectors, pGR-D4, pGR-DN or pGR-D at 3:1 molar ratio. Ligation mixtures were prepared with inserts (3X molar of vector), 20 ng of vectors, 0.5 µl of T4 ligase, 1X Ligation Buffer and topped up with distilled water to 10 µl. Mixtures were incubated at room temperature for at least 2 hours.

3.2.7 Transformation and selection of positive clones

Ten µl of ligation mixture was added into 100 µl of *Escherichia coli* competent cells (XLI-B strain) and incubated on ice for at least 20 minutes. *E. coli* competent cells were heat-shocked at 42°C for 45 seconds, subsequently, incubated on ice again for 2 minutes. Then, 400 µl of Luria Broth (LB) was added to the competent cells before bacterial suspensions were incubated at 37°C for at least an hour. After the incubation, bacterial suspensions were spread on LB agar plates containing 50 µg/ml kanamycin. All plates were incubated at 37°C overnight and PCR screening was performed to confirm the positive recombinant clones.

3.2.8 Plasmid extraction

Overnight bacterial cultures were purified using Zyppy^{TM} Plasmid Midiprep Kit. Forty ml of overnight cultures were pelleted at 6, 000 rpm for 10 minutes and 6 ml of distilled water was used to resuspend bacterial pellets. Pellets were vortexed and 1 ml of 7X Lysis Buffer (Blue) was added and followed by inverting the tubes for 2-4 times. Mixtures were incubated at room temperature for 2 minutes and 3.5 ml of cold Neutralisation Buffer (Yellow) was added subsequently. Then, mixtures were inverted for 4-6 times to mix thoroughly while samples turned yellow with precipitates observed as neutralisation was complete. All mixtures were transferred to Zymo-Midi Filter^{TM} columns, which were fixed onto a vacuum manifold, and vacuum was turned on to remove all the liquid lysate. All blue Zymo-Midi Filter^{TM} columns from the top of Zymo-Spin^{TM} V-E were discarded, nevertheless, Zymo-Spin^{TM} V-E columns were transferred to a collection tube and centrifuged at 13, 000 rpm for 30 seconds to remove any retained liquid. Then, 200 µl of Endo-Wash Buffer was added to Zymo-Spin^{TM} V-E columns and centrifuged at 13, 000 rpm for 30 seconds. Besides, 400 µl of Zyppy^{TM} Wash Buffer was also added to the columns and centrifuged at 13, 000 rpm for another 30 seconds. Washing step of the columns with Zyppy^{TM} Wash Buffer was repeated and the columns were centrifuged at 13, 000 rpm for additional 1 minute to remove any trace of buffer. Zymo-Spin^{TM} V-E columns were then transferred to new 1.5 ml microcentrifuge tubes and 150 µl of distilled water was added to the centre of the column. The column was incubated at room temperature for 5 minutes before centrifuging at 13, 000 rpm for 1 minute. Purity and concentration of DNA were measured using Nano Drop 1000 spectrophotometer.

3.2.9 Verification of recombinant vectors

Extracted recombinant vectors were verified by RE-digestion as illustrated in sections 3.2.3 and 3.2.5. Verified recombinant vectors were then sent for sequencing. Sequencing results were assembled using SeqMan Pro and sequences were aligned using Bioedit and ClustalW2 Multiple sequence alignment.

3.3 Results

3.3.1 Codon optimisation of apoptin gene

Codon sequences of apoptin gene cassettes were optimised based on codon usage of *Nicotiana benthamiana* in order to enhance the translation efficiency of recombinant protein. Codon adaptation index (CAI), a scoring or measure for codon adaptiveness in a gene sequence in reference to a given set of codon usage frequency analysed from highly expressed gene in a species and effective number of codons (ENC), a scoring for equal usage of synonymous codons in a gene, for native and optimised apoptin gene sequences are listed in Table 3.5.

Table 3.5: Codon adaptation index (CAI) and effective number of codons (ENC) for apoptin gene cassettes.

No	Source of gene sequences	Apoptin gene cassettes	CAI	ENC	GC content
1	Genebank: AAB86420.1	VP3-A	0.681	61.0	53.0
2	GeneArt, USA	PR-VP3-HK	0.832	29.3	50.6
3	GeneArt, USA	PR-GFP-VP3-HK	0.815	28.0	49.7
4	GeneArt, USA	PR-Lic-VP3-HK	0.818	27.4	49.8

Non-optimised apoptin sequences showed CAI approximately 0.68 and ENC at 61. However, optimised apoptin sequences showed a higher CAI, which is more than 0.8, and low ENC at approximately 27-29.

3.3.2 Polymerase chain reaction (PCR) amplification and restriction enzyme (RE) digestion profiles of apoptin gene cassettes

Apoptin gene cassettes were generated by using PCR and RE digestion in order to ligate to vectors, pGR-D4, pGR-DN and pGR-D. Apoptin gene cassettes, namely PR-VP3-H, VP3-H, PR-GFP-VP3-H, GFP-VP3-H, PR-Lic-VP3-H and Lic-VP3-H, were amplified by PCR and the amplified PCR products were analysed in 1% gel electrophoresis as shown in Figure 3.2.

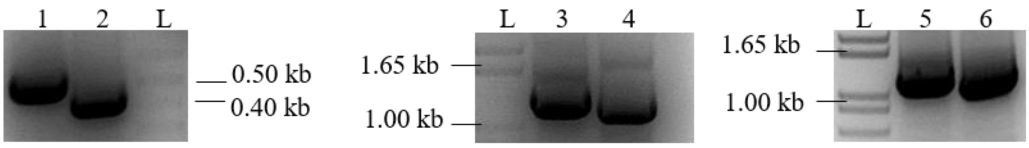

Lane	Gene cassettes	Estimated size
L	1 kb Plus DNA ladder	
1	PR-VP3-H	~ 474 bp
2	VP3-H	~ 384 bp
3	PR-GFP-VP3-H	~ 1203 bp
4	GFP-VP3-H	~ 1116 bp
5	PR-Lic-VP3-H	~1158 bp
6	Lic-VP3-H	~ 1068 bp

Figure 3.2: PCR amplification profiles of apoptin gene cassettes, namely PR-VP3-H, VP3-H, PR-GFP-VP3-H, GFP-VP3-H, PR-Lic-VP3-H and Lic-VP3-H.

Gene cassettes, namely PR-H22-CatAd-VP3-HK, PR-H22-CatAd-VP3-40-121-HK, PR-H22-CatAd-VP3-60-121-HK, PR-H22-CatAd-VP3-80-121-HK, PR-EGF-CatAd-VP3-HK, PR-EGF-CatAd-VP3-40-121-HK, PR-EGF-CatAd-VP3-60-121-HK and PR-EGF-CatAd-VP3-80-121-HK were generated by fusion PCR and PCR amplification profiles of these gene cassettes are shown in Figure 3.3.

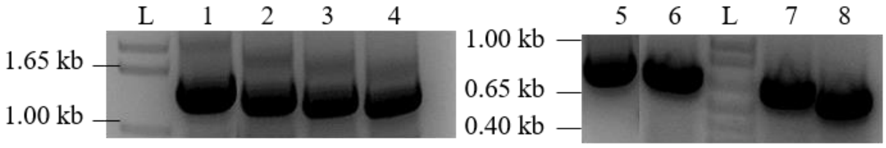

Lane	Gene cassettes	Estimated size
L	1 kb Plus DNA ladder	
1	PR-H22-CatAd-VP3-HK	~ 1338 bp
2	PR-H22-CatAd-VP3-40-121-HK	~ 1299 bp
3	PR-H22-CatAd-VP3-60-121-HK	~ 1279 bp
4	PR-H22-CatAd-VP3-80-121-HK	~ 1259 bp
5	PR-EGF-CatAd-VP3-HK	~ 756 bp
6	PR-EGF-CatAd-VP3-40-121-HK	~ 717 bp
7	PR-EGF-CatAd-VP3-60-121-HK	~ 697 bp
8	PR-EGF-CatAd-VP3-80-121-HK	~ 677 bp

Figure 3.3: PCR amplification profiles of apoptin gene cassettes, namely PR-H22-CatAd-VP3-HK, PR-H22-CatAd-VP3-40-121-HK, PR-H22-CatAd-VP3-60-121-HK, PR-H22-CatAd-VP3-80-121-HK, PR-EGF-CatAd-VP3-HK, PR-EGF-CatAd-VP3-40-121-HK, PR-EGF-CatAd-VP3-60-121-HK and PR-EGF-CatAd-VP3-80-121-HK.

RE digestion profiles of recombinant vectors, pGR-D4:: PR-VP3-HK, pGR-D4:: PR-GFP-VP3-HK and pGR-D4:: PR-EGF-CatAd-VP3-HK are also shown in Figure 3.4. Digested gene cassettes were purified from gel and cloned into pGR-DN vector.

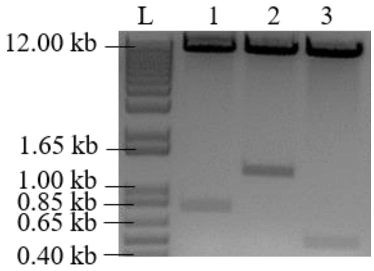

Lane	Vector backbone	Gene cassettes	Estimated size
L		1 kb Plus DNA ladder	
1	pGR-D4	PR-EGF-CatAd-VP3-HK	~ 756 bp
2	pGR-D4	PR-GFP-VP3-HK	~ 1215 bp
3	pGR-D4	PR-VP3-HK	~ 486 bp

Figure 3.4: RE digestion profiles of apoptin gene cassettes, namely PR-VP3-HK, PR-GFP-VP3-HK and PR-EGF-CatAd-VP3-HK.

RE digestion profiles of recombinant vectors, pMAT:: PR-VP3-HK, pMAT:: PR-GFP-VP3-HK, pMAT:: PR-Lic-VP3-HK, pGR-D4:: PR-GFP-VP3-H, pGR-D4:: GFP-VP3-H and pMAT:: mCherryNuc are also shown in Figure 3.5. Digested gene cassettes were purified from gel and cloned into individual vectors, pGR-D4 and pGR-D.

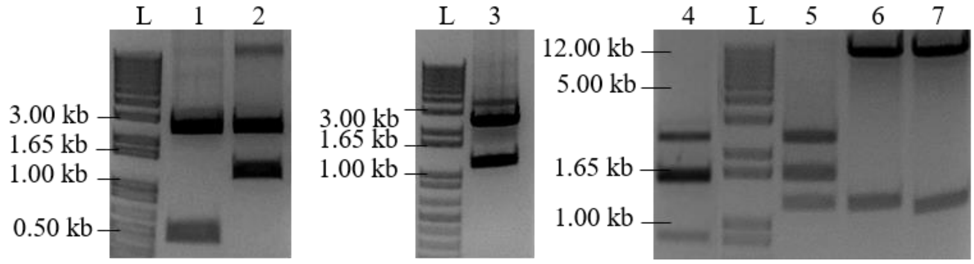

Lane	Vector backbone	Gene cassettes	Estimated size
L		1 kb Plus DNA ladder	
1	pMA-T	PR-VP3-HK	~ 486 bp
2	pMA-T	PR-GFP-VP3-HK	~ 1215 bp
3	pMA-T	PR-Lic-VP3-HK	~ 1184 bp
4	pMA-T	mCherryNuc	~ 780 bp
5	pMA-T	PR-GFP-VP3-HK	~ 1215 bp
6	pGR-D4	PR-GFP-VP3-H	~ 1203 bp
7	pGR-D4	GFP-VP3-H	~ 1116 bp

Figure 3.5: RE digestion profiles of apoptin gene cassettes, namely PR-VP3-HK, PR-GFP-VP3-HK, PR-Lic-VP3-HK, PR-GFP-VP3-H, GFP-VP3-H and mCherryNuc.

3.3.3 Verification of recombinant vectors

All recombinant vectors were analysed via RE digestion before the sequences of samples were further verified via sequencing. The results are shown following the RE digestion by PacI and XhoI for the verification of the recombinant vectors, namely pGR-D4:: PR-VP3-HK, pGR-D4:: PR-VP3-H, pGR-D4:: VP3-H, pGR-D4:: PR-GFP-VP3-HK, pGR-D4:: PR-GFP-VP3-H, pGR-D4:: GFP-VP3-H (Figure 3.6), pGR-D4::PR-Lic-VP3-HK, pGR-D4:: PR-Lic-VP3-H, pGR-D4:: Lic-VP3-H (Figure 3.7), pGR-D4:: PR-H22-CatAd-VP3-HK, pGR-D4:: PR-H22-CatAd-VP3-40-121-HK, pGR-D4:: PR-H22-CatAd-VP3-60-121-HK, pGR-D4:: PR-H22-CatAd-VP3-80-121-HK (Figure 3.8), pGR-D4:: PR-EGF-CatAd-VP3-HK, pGR-D4:: PR-EGF-CatAd-VP3-40-121-HK, pGR-D4:: PR-EGF-CatAd-VP3-60-121-HK, pGR-D4:: PR-EGF-CatAd-VP3-80-121-HK (Figure 3.9).

(a)

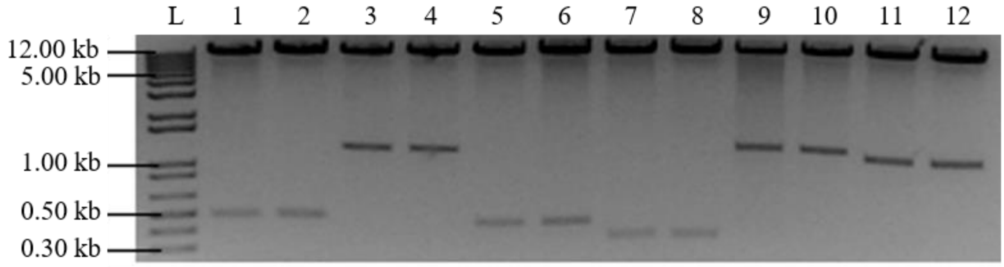

Lane	Recombinant vectors	Gene cassettes released from RE digestion	Estimated size
L	1 kb Plus DNA ladder		
1-2	pGR-D4:: PR-VP3-HK	PR-VP3-HK	~ 486 bp
3-4	pGR-D4:: PR-GFP-VP3-HK	PR-GFP-VP3-HK	~1215 bp
5-6	pGR-D4:: PR-VP3-H	PR-VP3-H	~ 474 bp
7-8	pGR-D4:: VP3-H	VP3-H	~ 384 bp
9-10	pGR-D4:: PR-GFP-VP3-H	PR-GFP-VP3-H	~ 1203 bp
11-12	pGR-D4:: GFP-VP3-H	GFP-VP3-H	~ 1116 bp

(b)

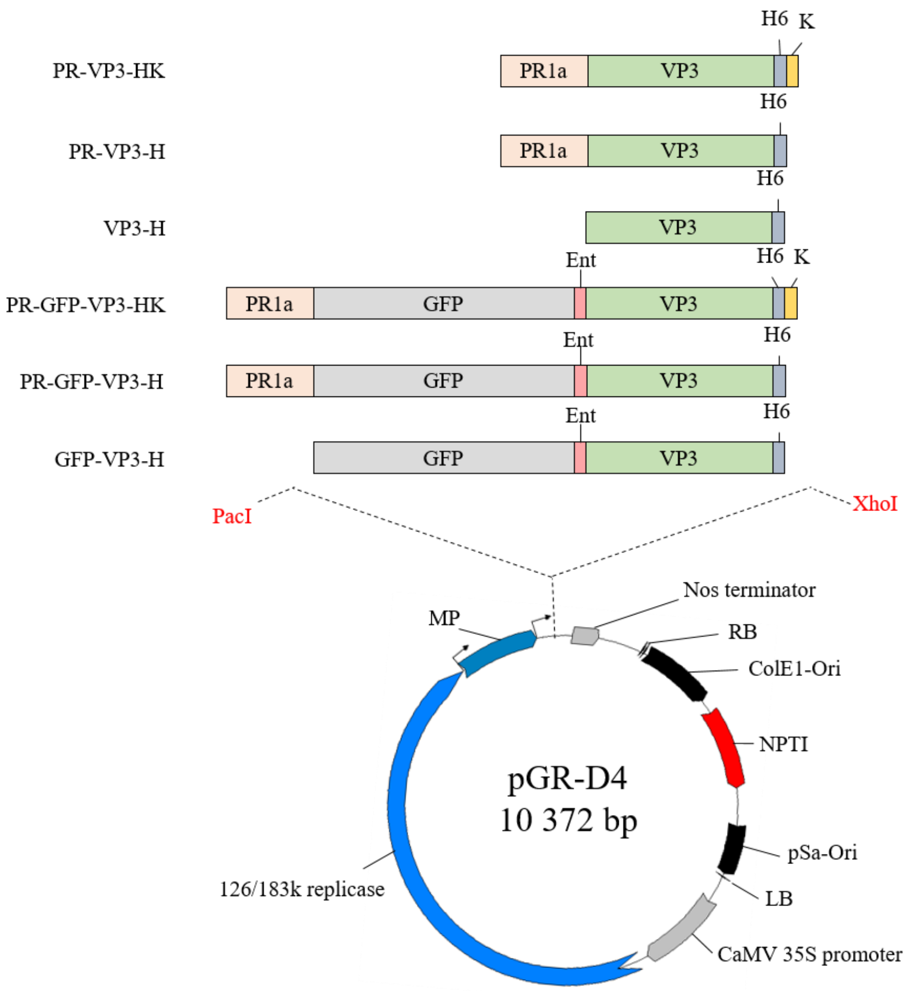

Features	
VP3	: Apoptin gene
GFP	: Green fluorescent protein
PR1a	: Signal peptide
Ent	: Enterokinase site
H6	: Hexahistidine
K	: Endoplasmic reticulum (ER) retention signal
PacI and XhoI	: Restriction enzymes
LB	: Left border
RB	: Right border
CaMV 35S	: Cauliflower mosaic virus 35S promoter
126/183k replicase	: Tobacco mosaic virus (TMV) replicase
MP	: Movement protein
Nos terminator	: Nopaline synthase terminator
NPTI	: Neomycin phosphotransferase
pSa-Ori	: Origin of replication
ColEI	: Origin of replication for high copy number of plasmids in *Escherichia coli*

Figure 3.6: RE verification profiles for recombinant vectors, namely pGR-D4:: PR-VP3-HK, pGR-D4:: PR-VP3-H, pGR-D4:: VP3-H, pGR-D4:: PR-GFP-VP3-HK, pGR-D4:: PR-GFP-VP3-H, pGR-D4:: GFP-VP3-H. (a) RE verification using PacI and XhoI for recombinant vectors; (b) Schematic diagram of the recombinant vector, pGR-D4 with apoptin gene cassettes as inserts.

(a)

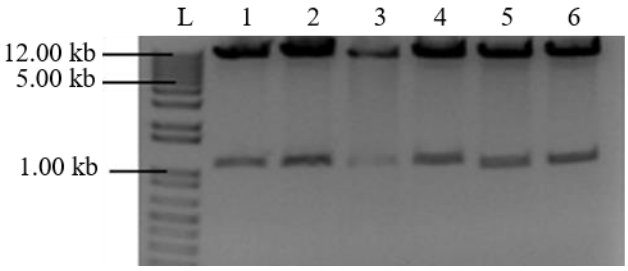

Lane	Recombinant vectors	Gene cassettes released from RE digestion	Estimated size
L	1 kb Plus DNA ladder		
1-2	pGR-D4:: PR-Lic-VP3-HK	PR-Lic-VP3-HK	~ 1170 bp
3-4	pGR-D4:: PR-Lic-VP3-H	PR-Lic-VP3-H	~1158 bp
5-6	pGR-D4:: Lic-VP3-H	Lic-VP3-H	~ 1068 bp

(b)

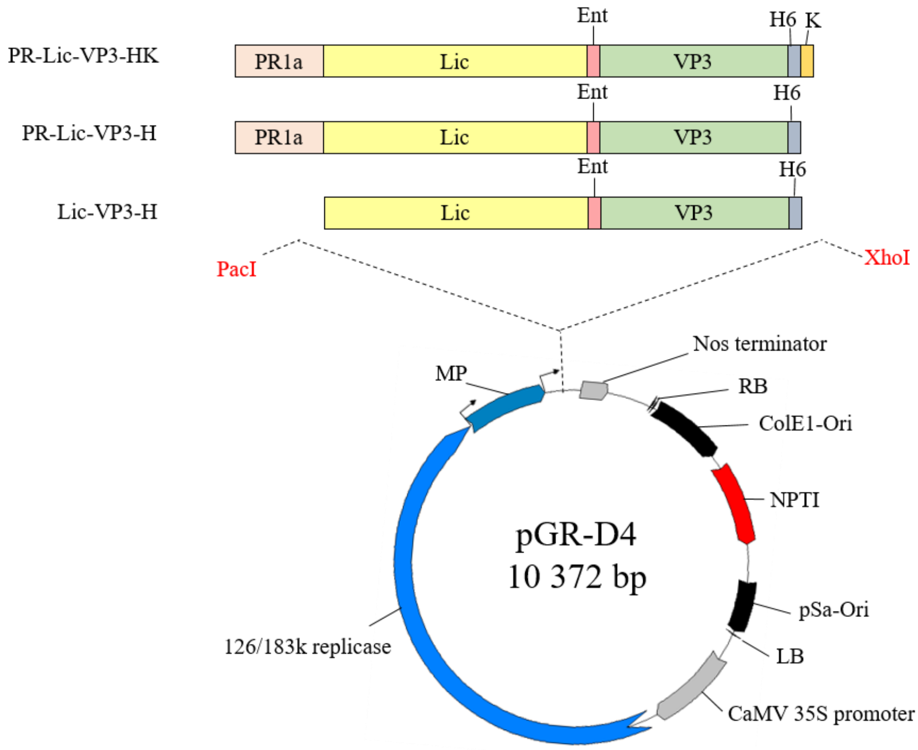

<u>Features</u>

VP3	: Apoptin gene
Lic	: Lichenase
PR1a	: Signal peptide
Ent	: Enterokinase site
H6	: Hexahistidine
K	: Endoplasmic reticulum (ER) retention signal
PacI and XhoI	: Restriction enzymes
LB	: Left border
RB	: Right border
CaMV 35S	: Cauliflower mosaic virus 35S promoter
126/183k replicase	: Tobacco mosaic virus (TMV) replicase
MP	: Movement protein
Nos terminator	: Nopaline synthase terminator
NPTI	: Neomycin phosphotransferase
pSa-Ori	: Origin of replication
ColEI	: Origin of replication for high copy number of plasmids in *Escherichia coli*

Figure 3.7: RE verification profiles for recombinant vectors, namely pGR-D4:: PR-Lic-VP3-HK, pGR-D4:: PR-Lic-VP3-H and pGR-D4:: Lic-VP3-H. (a) RE verification using PacI and XhoI for recombinant vectors; (b) Schematic diagram of the recombinant vector, pGR-D4 with apoptin gene cassettes as inserts.

(a)

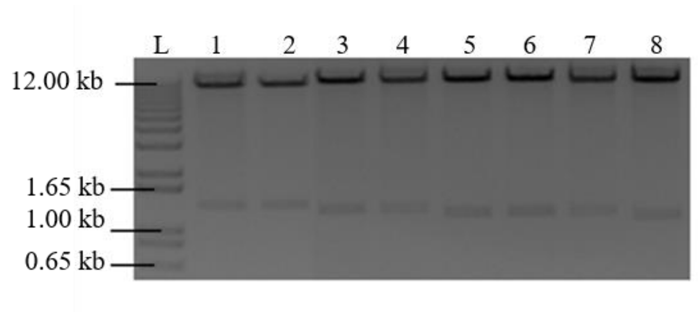

Lane	Recombinant vectors	Gene cassettes released from RE digestion	Estimated size
L	1 kb Plus DNA ladder		
1-2	pGR-D4:: PR-H22-CatAd-VP3-HK	PR-H22-CatAd-VP3-HK	~ 1338 bp
3-4	pGR-D4:: PR-H22-CatAd-VP3-40-121-HK	PR-H22-CatAd-VP3-40-121-HK	~ 1299 bp
5-6	pGR-D4:: PR-H22-CatAd-VP3-60-121-HK	PR-H22-CatAd-VP3-60-121-HK	~ 1279 bp
7-8	pGR-D4:: PR-H22-CatAd-VP3-80-121-HK	PR-H22-CatAd-VP3-80-121-HK	~ 1259 bp

(b)

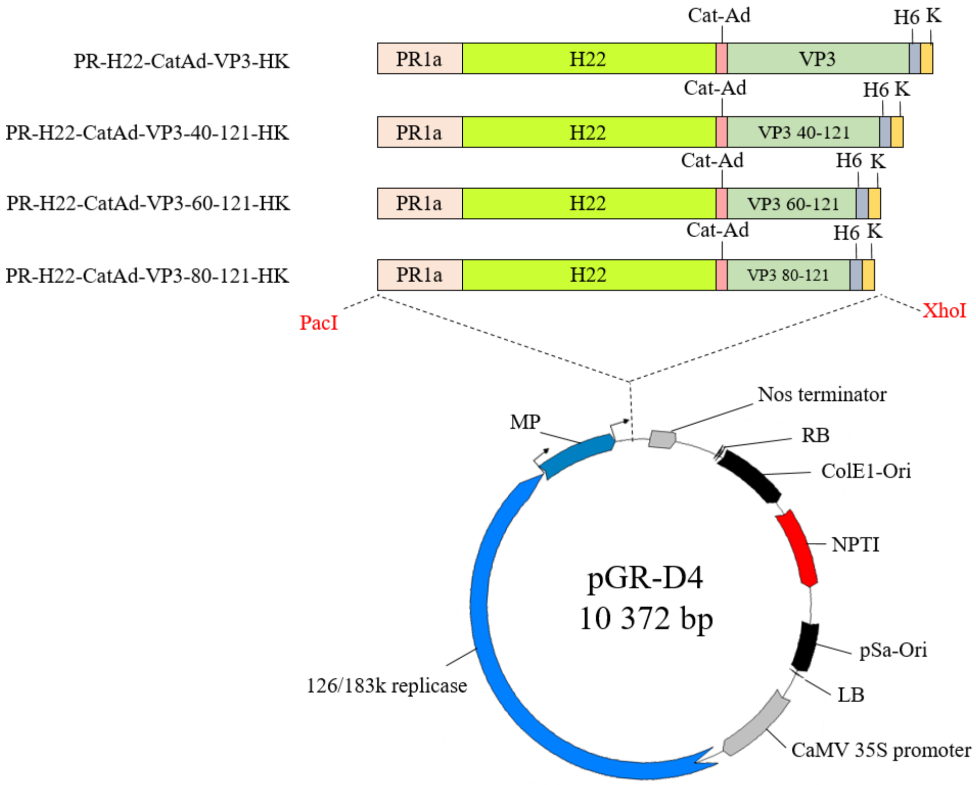

<u>Features</u>

VP3	: Apoptin gene
H22	: H22 single chain antibody
PR1a	: Signal peptide
Cat-Ad	: Molecular adaptor
H6	: Hexahistidine
K	: Endoplasmic reticulum (ER) retention signal
PacI and XhoI	: Restriction enzymes
LB	: Left border
RB	: Right border
CaMV 35S	: Cauliflower mosaic virus 35S promoter
126/183k replicase	: Tobacco mosaic virus (TMV) replicase
MP	: Movement protein
Nos terminator	: Nopaline synthase terminator
NPTI	: Neomycin phosphotransferase
pSa-Ori	: Origin of replication
ColEI	: Origin of replication for high copy number of plasmids in *Escherichia coli*

Figure 3.8: RE verification profiles for recombinant vectors, namely pGR-D4:: PR-H22-CatAd-VP3-HK, pGR-D4:: PR-H22-CatAd-VP3-40-121-HK, pGR-D4:: PR-H22-CatAd-VP3-60-121-HK and pGR-D4:: PR-H22-CatAd-VP3-80-121-HK. (a) RE verification using PacI and XhoI for recombinant vectors; (b) Schematic diagram of the recombinant vector, pGR-D4 with apoptin gene cassettes as inserts.

(a)

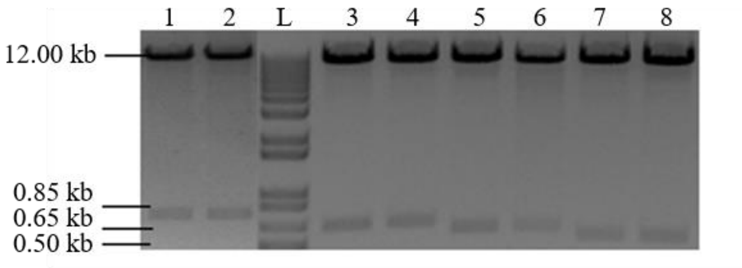

Lane	Recombinant vectors	Gene cassettes released from RE digestion	Estimated size
L	1 kb Plus DNA ladder		
1-2	pGR-D4:: PR-EGF-CatAd-VP3-HK	PR-EGF-CatAd-VP3-HK	~ 756 bp
3-4	pGR-D4:: PR-EGF-CatAd-VP3-40-121-HK	PR-EGF-CatAd-VP3-40-121-HK	~ 717 bp
5-6	pGR-D4:: PR-EGF-CatAd-VP3-60-121-HK	PR-EGF-CatAd-VP3-60-121-HK	~ 697 bp
7-8	pGR-D4:: PR-EGF-CatAd-VP3-80-121-HK	PR-EGF-CatAd-VP3-80-121-HK	~ 677 bp

(b)

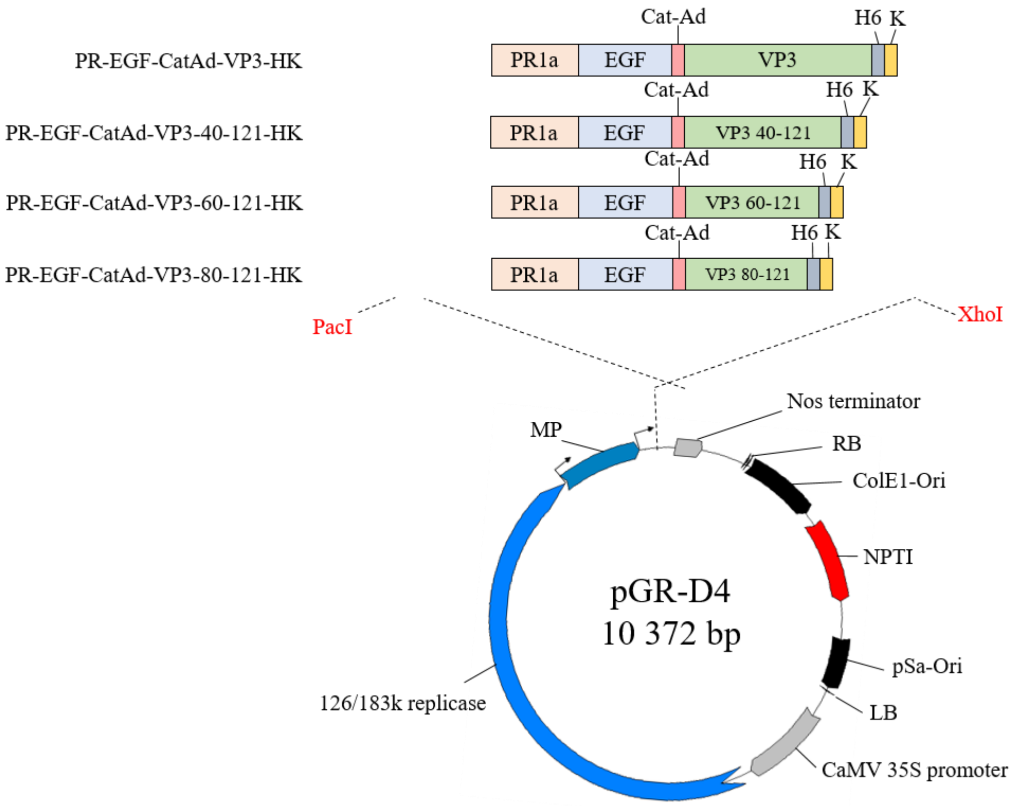

<u>Features</u>

VP3	: Apoptin gene
EGF	: Epidermal growth factor
PR1a	: Signal peptide
Cat-Ad	: Molecular adaptor
H6	: Hexahistidine
K	: Endoplasmic reticulum (ER) retention signal
PacI and XhoI	: Restriction enzymes
LB	: Left border
RB	: Right border
CaMV 35S	: Cauliflower mosaic virus 35S promoter
126/183k replicase	: Tobacco mosaic virus (TMV) replicase
MP	: Movement protein
Nos terminator	: Nopaline synthase terminator
NPTI	: Neomycin phosphotransferase
pSa-Ori	: Origin of replication
ColEI	: Origin of replication for high copy number of plasmids in *Escherichia coli*

Figure 3.9: RE verification profiles for recombinant vectors, namely pGR-D4:: PR-EGF-CatAd-VP3-HK, pGR-D4:: PR-EGF-CatAd-VP3-40-121-HK, pGR-D4:: PR-EGF-CatAd-VP3-60-121-HK and pGR-D4:: PR-EGF-CatAd-VP3-80-121-HK. (a) RE verification using PacI and XhoI for recombinant vectors; (b) Schematic diagram of the recombinant vector, pGR-D4 with apoptin gene cassettes as inserts.

Recombinant vectors, pGR-DN:: PR-VP3-HK__bZIP17, pGR-DN:: PR-VP3-HK__bZIP28, pGR-DN:: PR-VP3-HK__bZIP60, pGR-DN:: PR-GFP-VP3-HK__bZIP17, pGR-DN:: PR-GFP-VP3-HK__bZIP28, pGR-DN:: PR-GFP-VP3-HK__bZIP60, pGR-DN:: PR-EGF-CatAd-VP3-HK__bZIP17, pGR-DN:: PR-EGF-CatAd-VP3-HK__bZIP28 and pGR-DN:: PR-EGF-CatAd-VP3-HK__bZIP60 were verified by released gene cassettes, PR-VP3-HK (Figure 3.10), PR-GFP-VP3-HK (Figure 3.11) and PR-EGF-CatAd-VP3-HK (Figure 3.12) using PacI and XhoI. Besides, recombinant vectors were also digested using BsrGI and NheI to release gene cassettes, bZIP17, bZIP28 and bZIP60. NheI RE site is present on bZIP60 gene sequence (nucleotide 231); hence, bZIP gene released from pGR-DN vector is shorter than expected, which is approximately 670 bp.

(a)

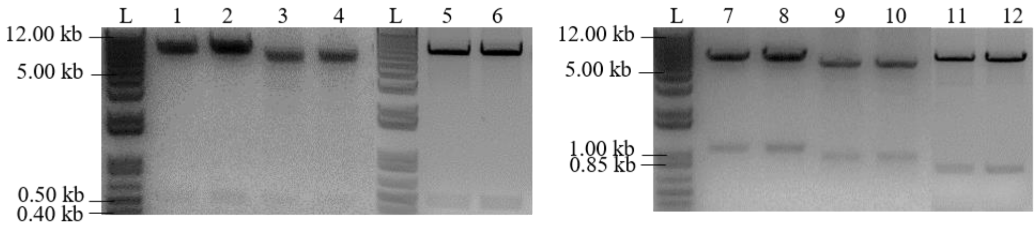

Lane	Recombinant vectors	Gene cassettes released from RE digestion	Estimated size
L	1 kb Plus DNA ladder		
1-2	pGR-DN:: PR-VP3-HK__bZIP17	PR-VP3-HK	~ 520 bp
3-4	pGR-DN:: PR-VP3-HK__bZIP28	PR-VP3-HK	~ 520 bp
5-6	pGR-DN:: PR-VP3-HK__bZIP60	PR-VP3-HK	~ 520 bp
7-8	pGR-DN:: PR-VP3-HK__bZIP17	bZIP17	~ 1092 bp
9-10	pGR-DN:: PR-VP3-HK__bZIP28	bZIP28	~ 960 bp
11-12	pGR-DN:: PR-VP3-HK__bZIP60	bZIP60	~ 900 bp

(b)

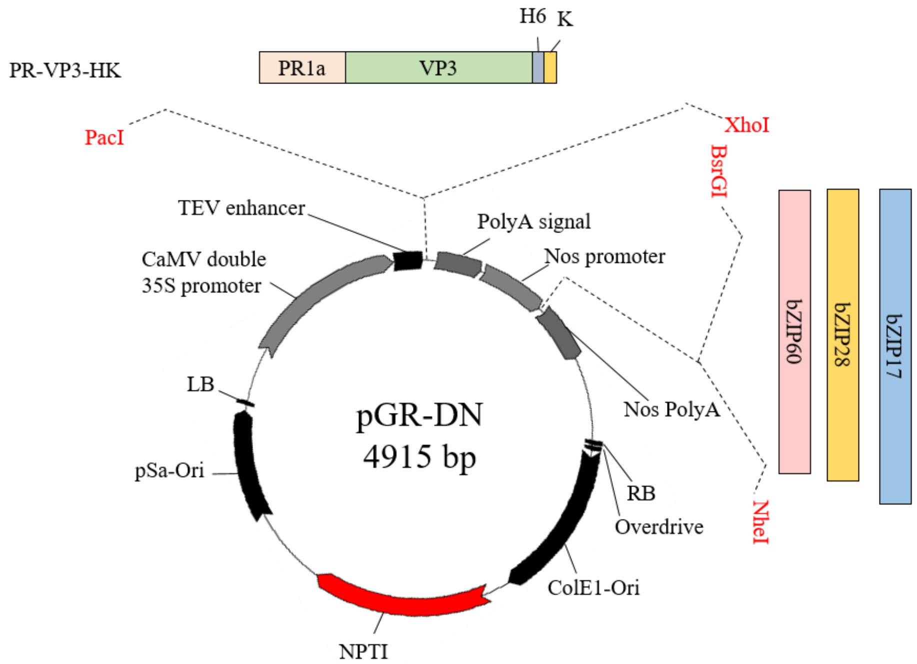

Features

VP3	: Apoptin gene
PR1a	: Signal peptide
H6	: Hexahistidine
K	: Endoplasmic reticulum (ER) retention signal
bZIP17	: bZIP17 transcriptional factor
bZIP28	: bZIP28 transcriptional factor
bZIP60	: bZIP60 transcriptional factor
PacI, XhoI, BsrGI and NheI	: Restriction enzymes
LB	: Left border
RB	: Right border
CaMV 35S	: Cauliflower mosaic virus 35S promoter
TEV enhancer	: Tobacco etch virus enhancer
PolyA signal	: PolyA terminator
Nos promoter	: Nopaline synthase promoter
Nos terminator	: Nopaline synthase terminator
NPTI	: Neomycin phosphotransferase
Overdrive	: Overdrive
pSa-Ori	: Origin of replication
ColEI	: Origin of replication for high copy number of plasmids in *Escherichia coli*

Figure 3.101: RE verification profiles for recombinant vectors, namely pGR-DN:: PR-VP3-HK__bZIP17, pGR-DN:: PR-VP3-HK__bZIP28 and pGR-DN:: PR-VP3-HK__bZIP60. (a) RE verification using PacI and XhoI for recombinant vectors; (b) Schematic diagram of the recombinant vector, pGR-DN with apoptin gene cassettes and bZIP17, bZIP28 and bZIP60 as inserts.

(a)

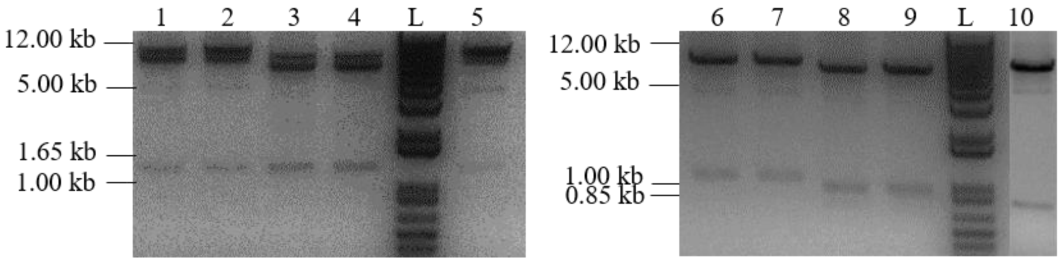

Lane	Recombinant vectors	Gene cassettes released from RE digestion	Estimated size
L	1 kb Plus DNA ladder		
1-2	pGR-DN:: PR-GFP-VP3-HK__bZIP17	PR-GFP-VP3-HK	~ 1249 bp
3-4	pGR-DN:: PR-GFP-VP3-HK __bZIP28	PR-GFP-VP3-HK	~ 1249 bp
5	pGR-DN:: PR-GFP-VP3-HK __bZIP60	PR-GFP-VP3-HK	~ 1249 bp
6-7	pGR-DN:: PR-GFP-VP3-HK__bZIP17	bZIP17	~ 1092 bp
8-9	pGR-DN:: PR-GFP-VP3-HK __bZIP28	bZIP28	~ 960 bp
10	pGR-DN:: PR-GFP-VP3-HK __bZIP60	bZIP60	~ 900 bp

(b)

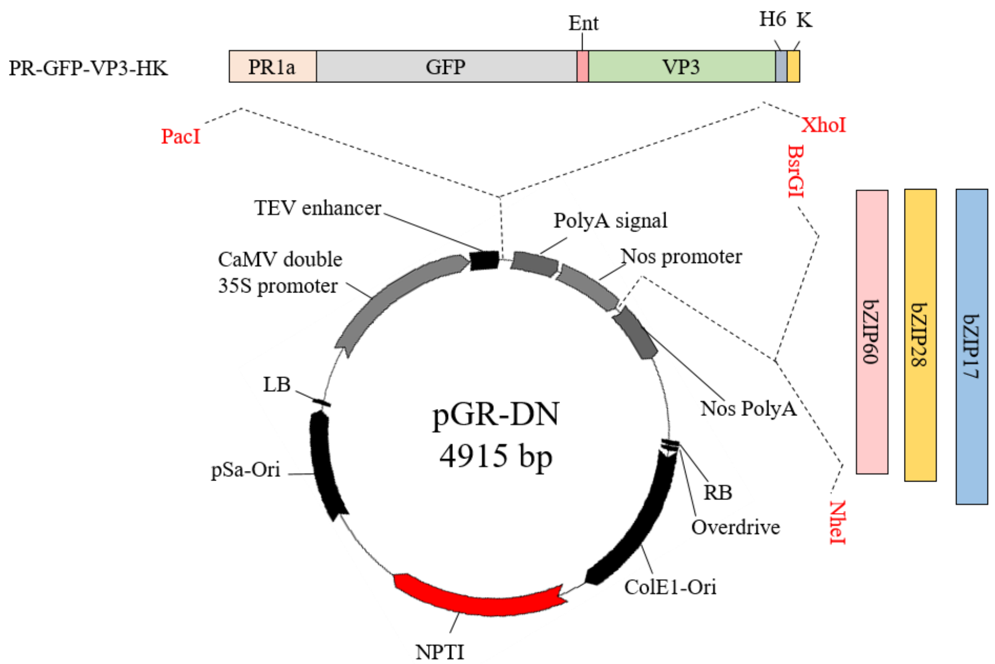

<u>Features</u>

VP3	: Apoptin gene
GFP	: Green fluorescent protein
Ent	: Enterokinase site
PR1a	: Signal peptide
H6	: Hexahistidine
K	: Endoplasmic reticulum (ER) retention signal
bZIP17	: bZIP17 transcriptional factor
bZIP28	: bZIP28 transcriptional factor
bZIP60	: bZIP60 transcriptional factor
PacI, XhoI, BsrGI and NheI	: Restriction enzymes
LB	: Left border
RB	: Right border
CaMV 35S	: Cauliflower mosaic virus 35S promoter
TEV enhancer	: Tobacco etch virus enhancer
PolyA signal	: PolyA terminator
Nos promoter	: Nopaline synthase promoter
Nos terminator	: Nopaline synthase terminator
NPTI	: Neomycin phosphotransferase
Overdrive	: Overdrive
pSa-Ori	: Origin of replication
ColEI	: Origin of replication for high copy number of plasmids in *Escherichia coli*

Figure 3.21: RE verification profiles for recombinant vectors, namely pGR-DN:: PR-GFP-VP3-HK__bZIP17, pGR-DN:: PR-GFP-VP3-HK__bZIP28 and pGR-DN:: PR-GFP-VP3-HK__bZIP60. (a) RE verification using PacI and XhoI for recombinant vectors; (b) Schematic diagram of the recombinant vector, pGR-DN with apoptin gene cassettes and bZIP17, bZIP28 and bZIP60 as inserts.

(a)

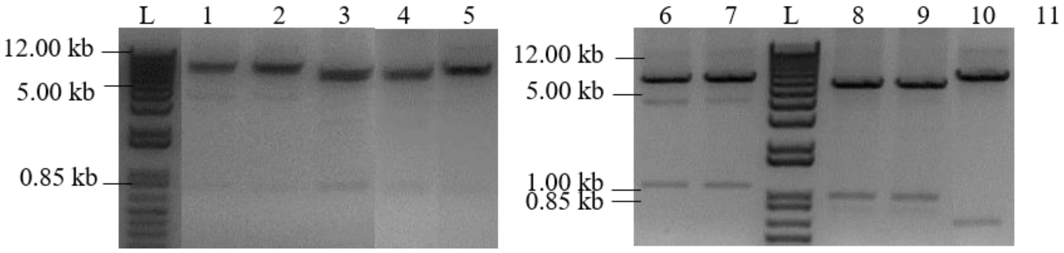

Lane	Recombinant vectors	Gene cassettes released from RE digestion	Estimated size
L	1 kb Plus DNA ladder		
1-2	pGR-DN:: PR-EGF-CatAd-VP3-HK__bZIP17	PR-EGF-CatAd-VP3-HK	~ 790 bp
3-4	pGR-DN:: PR-EGF-CatAd-VP3-HK __bZIP28	PR-EGF-CatAd-VP3-HK	~ 790 bp
5	pGR-DN:: PR-EGF-CatAd-VP3-HK __bZIP60	PR-EGF-CatAd-VP3-HK	~ 790 bp
6-7	pGR-DN:: PR-EGF-CatAd-VP3-HK __bZIP17	bZIP17	~ 1092 bp
8-9	pGR-DN:: PR-EGF-CatAd-VP3-HK __bZIP28	bZIP28	~ 960 bp
10	pGR-DN:: PR-EGF-CatAd-VP3-HK __bZIP60	bZIP60	~ 900 bp

(b)

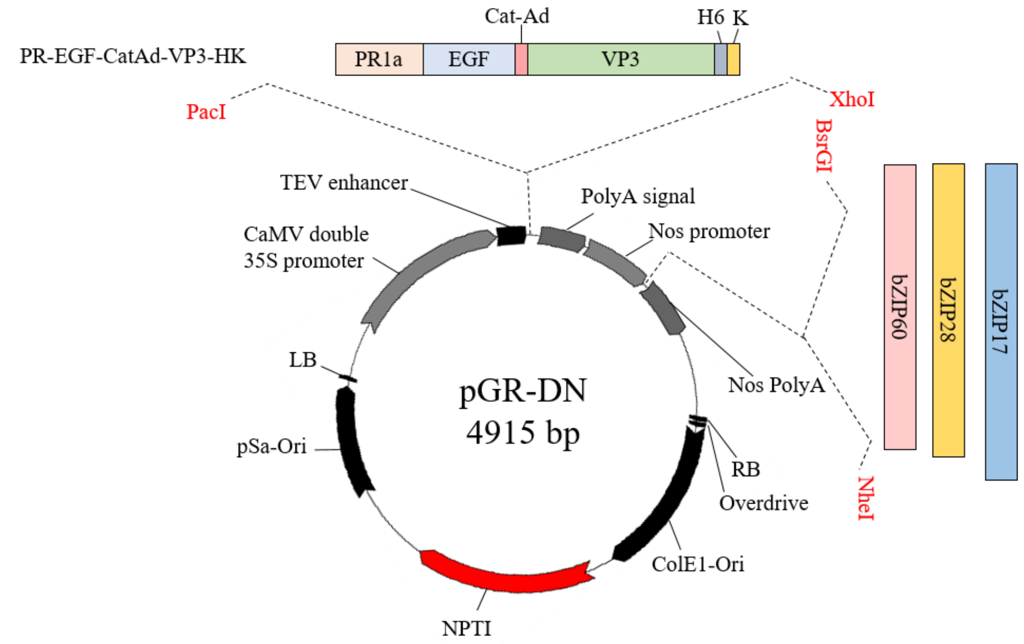

<u>Features</u>

VP3	: Apoptin gene
EGF	: Epidermal growth factor
CatAd	: Molecular adaptor
PR1a	: Signal peptide
H6	: Hexahistidine
K	: Endoplasmic reticulum (ER) retention signal
bZIP17	: bZIP17 transcriptional factor
bZIP28	: bZIP28 transcriptional factor
bZIP60	: bZIP60 transcriptional factor
PacI, XhoI, BsrGI and NheI	: Restriction enzymes
LB	: Left border
RB	: Right border
CaMV 35S	: Cauliflower mosaic virus 35S promoter
TEV enhancer	: Tobacco etch virus enhancer
PolyA signal	: PolyA terminator
Nos promoter	: Nopaline synthase promoter
Nos terminator	: Nopaline synthase terminator
NPTI	: Neomycin phosphotransferase
Overdrive	: Overdrive
pSa-Ori	: Origin of replication
ColEI	: Origin of replication for high copy number of plasmids in *Escherichia coli*

Figure 3.123: RE verification profiles for recombinant vectors, namely pGR-DN:: PR-EGF-CatAd-VP3-HK__bZIP17, pGR-DN:: PR-EGF-CatAd-VP3-HK__bZIP28 and pGR-DN:: PR-EGF-CatAd-VP3-HK__bZIP60. (a) RE verification using PacI and XhoI for recombinant vectors; (b) Schematic diagram of the recombinant vector, pGR-DN with apoptin gene cassettes and bZIP17, bZIP28 and bZIP60 as inserts.

Verification of recombinant vectors, including pGR-D:: PR-GFP-VP3-HK__mCherryNuc, pGR-D:: PR-GFP-VP3-H__mCherryNuc and pGR-D:: GFP-VP3-H__mCherryNuc was performed by PacI and XhoI digestion to release apoptin gene cassettes, namely PR-GFP-VP3-HK, PR-GFP-VP3-H and GFP-VP3-H (Figure 3.13). Besides, recombinant vectors were also RE-digested using BsrGI and NheI to release the gene cassette, mCherryNuc.

(a)

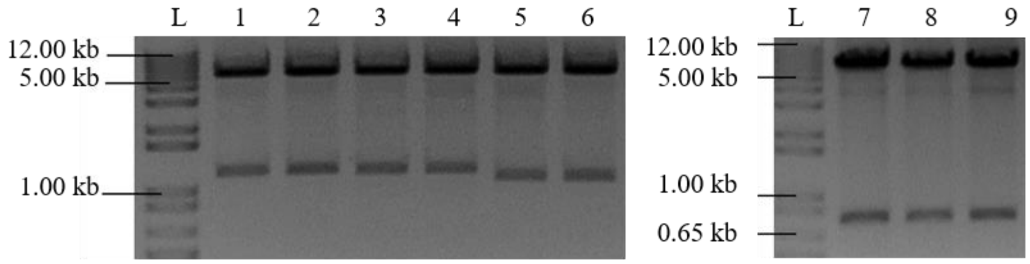

Lane	Recombinant vectors	Gene cassettes released from RE digestion	Estimated size
L	1 kb Plus DNA ladder		
1-2	pGR-D:: PR-GFP-VP3-HK__mCherryNuc	PR-GFP-VP3-HK	~ 1215 bp
3-4	pGR-D:: PR-GFP-VP3-H__mCherryNuc	PR-GFP-VP3-H	~ 1203 bp
5-6	pGR-D:: GFP-VP3-H__mCherryNuc	GFP-VP3-H	~ 1116 bp
7	pGR-D:: PR-GFP-VP3-HK__mCherryNuc	mCherryNuc	~ 783 bp
8	pGR-D:: PR-GFP-VP3-H__mCherryNuc	mCherryNuc	~ 783 bp
9	pGR-D:: GFP-VP3-H__mCherryNuc	mCherryNuc	~ 783 bp

(b)

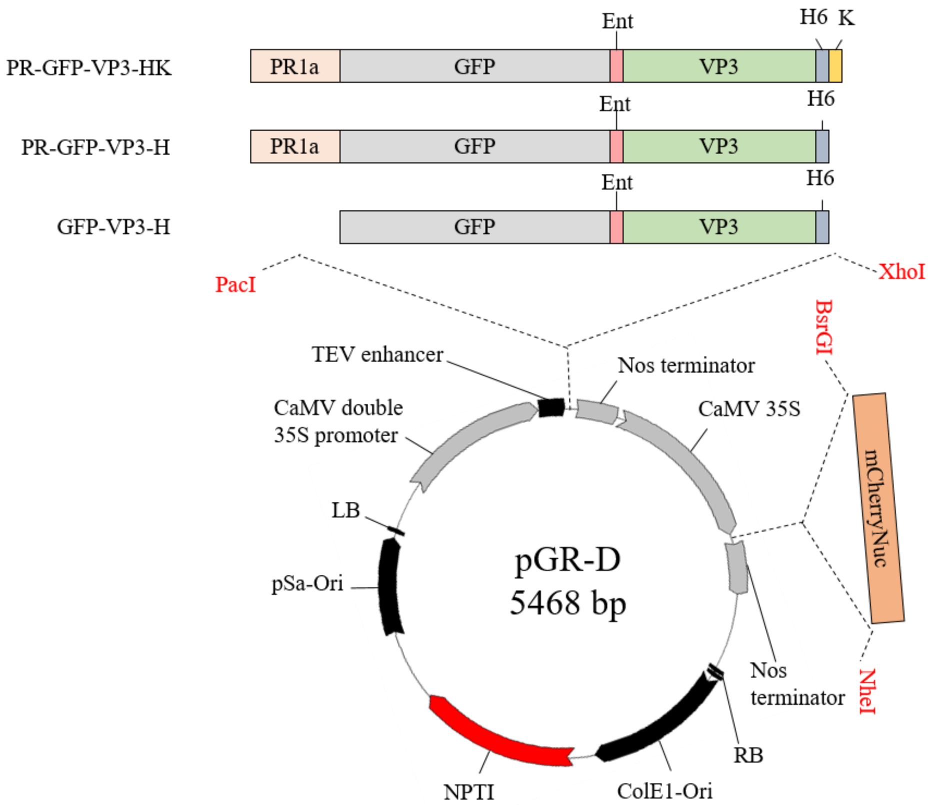

<u>Features</u>

VP3	: Apoptin gene
GFP	: Green fluorescent protein
mCherryNuc	: mCherry fluorescent protein in fusion to N-terminal of nuclear localisation signal
PR1a	: Signal peptide
Ent	: Enterokinase site
H6	: Hexahistidine
K	: Endoplasmic reticulum (ER) retention signal
PacI, XhoI, BsrGI and NheI	: Restriction enzymes
LB	: Left border
RB	: Right border
CaMV 35S	: Cauliflower mosaic virus 35S promoter
TEV enhancer	: Tobacco etch virus enhancer
Nos terminator	: Nopaline synthase terminator
NPTI	: Neomycin phosphotransferase
pSa-Ori	: Origin of replication
ColEI	: Origin of replication for high copy number of plasmids in *Escherichia coli*

Figure 3.13: RE verification profiles for recombinant vectors, namely pGR-D:: PR-GFP-VP3-HK__mCherryNuc, pGR-D:: PR-GFP-VP3-H__mCherryNuc and pGR-D:: GFP-VP3-H__mCherryNuc. (a) RE verification using PacI and XhoI for recombinant vectors; (b) Schematic diagram of the recombinant vector, pGR-D with apoptin gene cassettes and mCherryNuc as inserts.

3.3.4 Sequencing confirmation

Following sequencing analysis, all recombinant vectors used for gene expression were confirmed harbouring the correct nucleotide sequences with no mutation or frameshift occurrence for all gene cassettes.

3.4 Discussion

This chapter describes the upstream procedures for the production of recombinant apoptin in *Nicotiana benthamiana*, focusing on the design of apoptin gene cassettes and construction of recombinant vectors. In this study, apoptin gene cassettes were inserted after movement protein of tobacco mosaic virus (TMV) in pGR-D4 vector and expression of inserted genes were directed by a subgenomic promoter of TMV. Coat protein of this viral vector, responsible for systemic infection, had been removed and delivery of foreign genes to whole plant system was accomplished by agroinfiltration strategy (Roy *et al.*, 2010). Besides, pGR-DN vector was used in this study for co-expression of bZIP proteins with apoptin. For pGR-DN vector, double 35S cauliflower mosaic virus promoter was used to direct the transcription of apoptin gene cassettes; however, a weaker promoter was chosen to control the transcription of bZIP genes (Streatfield, 2007). This design was aimed to have a higher expression of apoptin rather than bZIP proteins.

Codon sequences of apoptin as well as fusion proteins, including green fluorescent protein (GFP), lichenase, H22 single chain antibody and epidermal growth factor (EGF), were optimised and synthesised based on codon usage preference of *N. benthamiana*. Codon bias, which is the preference of using specific type of synonymous codons during process of decoding genetic information into functional polypeptides, is found in diverse organisms as well as different genes within one genome. A favor for specific synonymous codon can cause significant impact on translation efficiency and protein folding (Quax *et al*., 2015) and studies showed that codon bias possesses high correlations with abundance of intracellular tRNA with specific anticodons (Angov, 2011). As high protein expression is directly affected by translation initiation as well as elongation, the presence of preferable codons with abundance of cognate tRNA are the keys for efficient translation. Hence, codon optimisation performed for foreign gene sequences based on preference codon of expression hosts is an important approach applied by researchers to boost up the expression of heterologous protein. Codon adaptation index (CAI), ranging from 0 to 1, is a measurement for codon adaptiveness of a gene sequence towards the favorable codon usage of highly expressed gene in a host species. This measurement was proposed as a way to predict the expression level of a gene (Sharp and Li, 1987). Therefore, higher the CAI value may indicate higher expression level of a protein. In this study, CAI values of synthetic and optimised apoptin gene cassettes showed more than 0.8 and are higher than non-optimised apoptin gene sequences (~ 0.6-0.7).

Thus, a relatively high protein expression level was expected to be obtained with codon optimised apoptin sequence. Instead of CAI value, effective number of codons (ENC), ranging from 20 to 61, was also used to justify the codon bias of a sequences. ENC value of 20 means each amino acid coded by only one kind of codon sequence, hence, the codon sequence for that gene is extremely bias; however, ENC value of 61 means an equally use of all codons for all amino acids and no bias of codon usage is available (Behura and Severson, 2012). In comparison to non-optimised apoptin sequences, codon optimised apoptin gene cassette sequences showed a huge bias of codon usage. Bias of codon usage in optimised sequences could be explained since a preference of usage for one or two codons for each amino acid was observed from codon usage frequency table of *N. benthamiana* (Appendix 3.11).

In this study, recombinant apoptin was aimed to be stored in s specific plant cellular compartment; hence, signal peptide sequences from tobacco pathogenesis related protein 1a (PR1a) was fused to N-terminal of apoptin gene cassettes in order to direct the protein entering into endoplasmic reticulum (ER) lumen (gene cassettes: PR-VP3-H, PR-GFP-VP3-H and PR-Lic-VP3-H). Presence of this signal peptide PR1a on N-terminal of polypeptide is highly important for the entry of recombinant protein into secretory pathway and subsequently passages to extracellular space (Lodish *et al*., 2004). Besides, an investigation was also performed for accumulation of recombinant apoptin in ER by adding signal peptide, PR1a on N-terminal of apoptin gene cassettes with ER retention signal on C-terminal concurrently (gene cassettes: PR-VP3-HK, PR-GFP-VP3-HK, PR-Lic-VP3-HK, PR-H22-CatAd-VP3-HK, PR-H22-CatAd-VP3-40-121-HK, PR-H22-CatAd-VP3-60-121-HK, PR-H22-CatAd-VP3-80-121-HK, PR-EGF-CatAd-VP3-HK, PR-EGF-CatAd-VP3-40-121-HK, PR-EGF-CatAd-VP3-60-121-HK and PR-EGF-CatAd-VP3-80-121-HK). Proteins targeting to ER and apoplast are favorable for subcellular storage compartment chosen by researchers since accumulation of proteins in these cellular compartments always lead to higher yield of recombinant proteins (Komarnytsky *et al*., 2000; Xu *et al*., 2002; Yang *et al*., 2005). Recombinant proteins targeted into secretory pathway obtain proper protein folding and post translational modifications, such as glycosylation, alkylation and carboxylation, which are highly important for the functional activity of proteins.

High amount of recombinant apoptin was expressed as insoluble protein when fused only to hexahistidine tag in *E. coli* expression system (Leliveld[a] *et al*., 2003). Strong denaturants were always used to harvest the protein and followed by a refolding step. This problem had been solved when apoptin was fused to large protein, maltose binding protein (MBP). Besides, a detectable soluble recombinant apoptin was also reported by Lacorte *et al*. (2007) when recombinant apoptin in fusion to GFP was expressed in *N. benthamiana*. In this study, GFP as well as lichenase were fused to N-terminal of apoptin gene (gene cassettes: PR-GFP-VP3-HK, PR-GFP-VP3-H, GFP-VP3-H, PR-Lic-VP3-HK, PR-Lic-VP3-H and Lic-VP3-H) in order to enhance solubility and stability of protein. Signal peptides, PR1a and ER retention signal were also added to the gene cassettes in order to study the best location for subcellular storage of recombinant apoptin. An enterokinase cleavage site was purposely incorporated between GFP and apoptin gene or lichenase and apoptin gene for the removal of fusion proteins after the purification steps since these GFP and lichenase proteins might result unwanted side effects on subsequent cell-based assays. GFP is a common reporter protein and the employment of GFP protein in fusion to apoptin here is to ease detection of recombinant protein during purification process and functionality test of recombinant apoptin in mammalian cells. Lichenase, a thermostable enzyme, b-1,3-1,4-glucanase from *Clostridium thermocellum*, was successfully produced with more than 30 targeted recombinant proteins (Musiychuk *et al*., 2007). Enhancement of recombinant protein expression, stability and incorporation of multiple targets were able to be achieved with the fusion of protein of interest to lichenase (Musiychuk *et al*., 2007).

Cancer treatments always aim to kill cancer cells selectively while confer negligible harm to healthy normal cells; however, common treatments, such as radiation, cytotoxic chemotherapeutic drugs and surgery, cause non-specific harmful effects to healthy neighboring cells or non-effective towards metastasized cancer cells. In order to enhance the effectiveness and specificity of drug towards cancer cells, targeting drug towards cancer cells is achieved via pathophysiological features of cancer cells as well as facilitation of surface receptors or antigens overexpressed on cancer cells (Mohanty *et al*., 2011). In current study, EGF and immunoglobulin G (IgG) receptor (CD64) were chosen as targets for drug delivery to cancer cells overexpressed with both receptors. CD64 is constitutively expressed in myelogenous cells, such as macrophages, monocytes and dendritic cells, and this receptor is upregulated during infection and on cancer cells such as acute myeloid leukemia (AML). CD64 has been chosen as a targeted receptor for the binding of immunotoxins using anti-CD64 single chain antibody H22 for treatment of AML (Hetzel *et al*., 2008; Stahnke *et al*., 2008). Epidermal growth factor receptor (EGFR), also known as ErbB1 receptor in EGF receptor family, is overexpressed especially in breast tissue cancer (Hooper, 2016; Normanno *et al*., 2006). Several kinds of drugs, including non-hormonal cytotoxic drug, suramin and monoclonal antibody, cetuximab, have been developed for cancer treatment via inhibition of signal transduction activities of EGFR (Hooper, 2016). On the other hand, EGF, one of the ligands bound to EGFR, was chosen as ligands in fusion with immunotoxins for targeted therapy (Fuchs *et al*., 2007). EGF and H22 single chain antibody gene sequences were fused to N-terminal of apoptin gene with the addition of N-terminal signal peptide PR1a and C-terminal ER retention signal (PR-H22-CatAd-VP3-HK and PR-EGF-CatAd-VP3-HK). Besides, a peptide transmembrane domain (PTD), CatAd was incorporated between EGF and apoptin gene as well as H22 single chain antibody and apoptin gene in order to enhance the internalization of apoptin into cancer cells. CatAd is a cleavable adaptor developed for the linking between ligands or antibodies and toxin moieties of immunotoxins used for cancer treatment (Keller *et al*., 2001). Incorporation of CadAd between ligands and toxin was reported causing an irreversible detainment of the toxin in the cell cytosol and making a short half-life of toxin, which significantly reduces non-specific toxicity that is always associated with undesirable side effects (Heisler *et al*., 2003).

Instead of full length apoptin, expression of truncated apoptin was also investigated in this research. A bipartite nuclear localisation signals (NLS) are reported on C-terminal of apoptin and this region is believed playing a critical role for apoptosis induction. Hence, several truncated H22-apoptin gene cassettes (PR-H22-CatAd-VP3-40-121-HK, PR-H22-CatAd-VP3-60-121-HK and PR-H22-CatAd-VP3-80-121-HK) and EGF-apoptin gene cassettes (PR-EGF-CatAd-P3-40-121-HK, PR- EGF-CatAd-VP3-60-121-HK and PR- EGF-CatAd-VP3-80-121-HK) were designed by removing N-terminal region as well as reserving the full length and functional C-terminal bipartite NLS. Besides, N-terminal of apoptin was reported containing a leucine rich hydrophobic region that corresponds for the multimerisation of the protein (Leliveld[c] *et al*., 2003). Thus, removal of N-terminal of apoptin in truncated apoptin gene cassettes also aimed to increase the solubility of recombinant apoptin. These designs would like to reduce the potential formation of huge multimers that always lead to instability and insolubility of protein.

In this study, soluble protein level of recombinant apoptin (gene cassettes: PR-VP3-HK, PR-GFP-VP3-HK and PR-EGF-CatAd-VP3-HK) was also tried to be enhanced by co-expression with bZIP proteins (17, 28 and 60), which belong to a group of transcriptional factors involving in elevated level of chaperone proteins. Overexpression of recombinant proteins always results in a huge amount of unfolded proteins, consequently, inducing the unwanted ER stress/unfolded protein response (UPR) (Ruberti *et al*., 2015). bZIP proteins are released during

UPR and play roles as transcriptional factors to enhance transcription of chaperone proteins involving in protein folding activity (Vitale, 2013). Hence, the present study was performed to understand the effect of co-expressions of bZIP17, bZIP28 and bZIP60 with apoptin gene cassettes and the elevated amount of soluble recombinant apoptin was expected and could be harvested via this approach.

In conclusion, all apoptin gene variants were ingeniously designed and cloned into vectors, namely pGR-D4, pGR-DN and pGR-D. Codon optimised apoptin gene sequences were synthesised incorporating with signal peptide PR1a as well as ER retention signal. Apoptin gene cassettes that targeted protein to apoplast and cytoplasm were also generated. Besides, apoptin gene cassettes harbouring apoptin gene in fusion to GFP, lichenase and tumor specific ligands (H22 and EGF) were also designed and cloned into targeted vectors in hope to enhance yield, solubility and stability of recombinant apoptin proteins.

Chapter 4

Protein Expression Profiling on *Nicotiana benthamiana* Receiving Recombinant Apoptin Vector Variants via Agroinfiltration

Table of Contents

4.1 Introduction

Transient expression is conventionally used for rapid assessment of gene functions at the first place. However, this technique has been recently adopted for production of recombinant proteins in plants attributed by its several creditable advantages. High expression yield, short incubation time and absence of adverse effects that are induced by permanent integration of DNA, have made transient expression a robust approach for production of high demanding recombinant proteins (Sainsbury and Lomonossoff, 2014). Among several gene delivery techniques, agroinfiltration is one of the most commonly used techniques by employing *Agrobacterium* as a delivery vector to transfer foreign genes into plants (Chen *et al*., 2013). Infiltrated plants are incubated for 2-8 days for transient expression of foreign genes without requiring any selection activity. Although agroinfiltration is a non-expensive, scalable, rapid and simple gene delivery approach, a requirement for infection of *Agrobacterium* towards specific host range has limited this application.

Conventional *Agrobacterium* transformation protocol allows *Agrobacterium* come into contact with surface or wounding sites of plant samples by incubating plant specimens in *Agrobacterium* suspension. However, agroinfiltration allows bacteria penetrating into deeper and inner layers of infected tissues via infiltration technique, which could be achieved with simple and non-expensive syringes or specialised vacuum system. Using syringe infiltration, diluted bacterial cultures are injected into leaf abaxial side and pressure of injection allows bacteria penetrating into intercellular space of leaf mesophyll rather than leaf surface. Requirements for only small volume of cultures, inexpensive needleless syringes and tolerance with multiple injections using different recombinant vectors on the same leaf have made this approach becoming favourable for researchers working in lab or bench-scale study. However, syringe infiltration approach is no longer feasible for infiltration for large volume of plants in a pilot scale; hence, vacuum infiltration system is essential for efficient infiltration work (Chen *et al*., 2013). Using vacuum infiltration system, plants are firstly submerged into bacterial cultures and subsequently, application of vacuum removes air from plants and cultures. Pressure change causes agrobacterial culture penetrating into intercellular space of leaf mesophyll when vacuum system releases air into the chamber. Currently, this system is used by several biopharmaceutical companies for production of recombinant proteins that are highly valuable for medical purposes, including Medicago Inc (USA), Fraunhofer Center for Molecular Biotechnology (FhCMB, USA), Kentucky Bioprocessing (USA) and Icon Genetics (Germany).

There are always several hurdles encountered in the expression of recombinant proteins in plants in order to recover a satisfied amount of recombinant proteins. First, silencing of transgenes, one of the crucial challenges in this field, occurs at both transcriptional and post-transcriptional levels which is often induced by the presence of multiple copies of transgenes, integration of transgene in highly methylated chromosomal regions and accumulation of high level of aberrant RNA (Stam *et al*., 1997). Second, incompetent transcription and translation of foreign genes also lead to the low recovery of recombinant proteins. Low availability of transcripts restricts subsequent translation process and this is always attributed to the instability of transcripts and inefficient promoters (Streatfield, 2007). In addition, the bias of codon usage and inefficient translation initiation cause low level of expression, while the turnover rate of proteins in plant cells also directly affects the total amount of recombinant proteins yielded. Other than the induction of gene silencing, overexpression and toxicity of recombinant proteins sometimes also induce stress and unwanted early necrosis symptom to the host plants. Hence, an optimised transgene expression cassette is always required in order to achieve a high level of protein expression for subsequent downstream processing.

In current study, recombinant apoptin vector variants were designed as described in Chapter 3 in order to explore the optimised recombinant apoptin vectors leading to a high level of protein expression. To enhance transcription and translation efficiency, apoptin gene sequences were codon-optimised based on codon usage of *Nicotiana benthamiana* and cloned in high expression vectors, i.e. pGR-D4 (TMV-based viral vector) and pGR-DN (binary vector). Signal peptides such as tobacco pathogenesis related protein 1a (PR1a) and endoplasmic reticulum (ER) retention signal (KDEL) were incorporated into recombinant apoptin vector variants in order to target the apoptin to apoplast and ER for accumulation of protein at higher quantity in plant system. In addition, recombinant vector variants harbouring apoptin gene in fusion to C-terminal of fusion proteins including green fluorescent protein (GFP) and lichenase were also designed and constructed in order to increase protein solubility. Whereas, recombinant vector variants harbouring apoptin gene in fusion to C-terminal of H22 single chain antibody, epidermal growth factor (EGF) and molecular adaptor (CatAd) were also constructed for targeting and internalisation of purified recombinant apoptin into specific cancer cells that overexpressed CD64 and EGF receptors. Apoptin gene cassettes were also cloned into pGR-DN vectors that harboured bZIP17, bZIP28 and bZIP60 gene sequences. Co-expression of bZIP proteins and apoptin was aimed to enhance solubility and yield of recombinant apoptin.

In this chapter, recombinant apoptin vector variants were transformed into *Agrobacterium tumefaciens* and delivered into *N. benthamiana* using vacuum infiltration approach. Meanwhile, delivery of *Agrobacterium* harbouring recombinant vectors with pGR-D and pGR-DN backbones were co-infiltrated with gene silencing suppressors. All infiltrated plant leaf samples were harvested from 3 to 8 days post infiltration (dpi) for time course study of accumulation of recombinant proteins. Total protein and total soluble protein extracts from leaf samples were analysed and the results were used as references for subsequent protein purification procedures. Besides, localisation of recombinant apoptin in fusion to green fluorescent protein (GFP) in plant cells was also visualised using confocal microscope.

Therefore, the specific objectives for this chapter were (i) to deliver recombinant apoptin vector variants into *N. benthamiana* via vacuum infiltration, (ii) to compare the yield of total soluble and total protein among recombinant apoptin vector variants expressed in *N. benthamiana*, (iii) to determine the kinetic expression profiles of infiltrated *N. benthamiana* for the peak accumulation of recombinant apoptin and (iv) to examine subcellular localisation of recombinant apoptin in infiltrated *N. benthamiana* leaves.

4.2 Materials and Methods

4.2.1 General materials

4.2.1.1 Plant materials

Four to five weeks old *Nicotiana benthamiana*, serving as a host plant was used for agroinfiltration. *N. benthamiana* was grown in hydroponic system with temperature set at 25±3°C and humidity at ~70% RH receiving 12 hours of light and 12 hours of darkness. Infiltrated plants were also incubated at the similar condition.

4.2.1.2 Bacterial strains and recombinant vectors

Two strains of *Agrobacterium tumefaciens,* GV3101 and AGLI, were used in this study to deliver recombinant vectors into the host plant. Studies reported that delivery of viral vector with pGR-D4 backbone using GV3101 gave higher protein expression; however, delivery of non-viral vector with pGR-D or pGR-DN backbone using AGLI produce higher protein yield. Hence, recombinant vectors, namely pGR-D4:: PR-VP3-HK, pGR-D4:: PR-VP3-H, pGR-D4:: VP3-H, pGR-D4:: PR-GFP-VP3-HK, pGR-D4:: PR-GFP-VP3-H, pGR-D4:: GFP-VP3-H, pGR-D4:: PR-Lic-VP3-HK, pGR-D4:: PR-Lic-VP3-H, pGR-D4:: Lic-VP3-H, pGR-D4:: PR-H22-CatAd-VP3-HK, pGR-D4:: PR-H22-CatAd-VP3-40-121-HK, pGR-D4:: PR-H22-CatAd-VP3-60-121-HK, pGR-D4:: PR-H22-CatAd-VP3-80-121-HK, pGR-D4:: PR-EGF-CatAd-VP3-HK, pGR-D4:: PR-EGF-CatAd-VP3-40-121-HK, pGR-D4:: PR-EGF-CatAd-VP3-60-121-HK and pGR-D4:: PR-EGF-CatAd-VP3-80-121-HK were transformed into agrobacterial strain GV3101. However, pGR-D:: PR-GFP-VP3-HK__mCherryNuc, pGR-D:: PR-GFP-VP3-H__mCherryNuc, pGR-D:: GFP-VP3-H__mCherryNuc, pGR-DN:: PR-VP3-HK__bZIP17, pGR-DN:: PR-VP3-HK__bZIP28, pGR-DN:: PR-VP3-HK__bZIP60, pGR-DN:: PR-GFP-VP3-HK__bZIP17, pGR-DN:: PR-GFP-VP3-HK__bZIP28, pGR-DN:: PR-GFP-VP3-HK__bZIP60, pGR-DN:: PR-EGF-CatAd-VP3-HK__bZIP17, pGR-DN:: PR-EGF-CatAd-VP3-HK__bZIP28 and pGR-DN:: PR-EGF-CatAd-VP3-HK__bZIP60 were transformed into agrobacterial strain AGLI. Meanwhile, pCB:: P19 and pCB:: P1/HC-Pro were transformed into agrobacterial strain GV3101.

4.2.1.3 Reagents

MagicMark™ XP Western Protein Standard, SeeBlue Plus2 Pre-stained Protein Standard, BenchMark™ His-tagged Protein Standard and BenchMark™ Protein Ladder (ThermoFisher Scientific, USA) were protein markers used in protein gel electrophoresis. Besides, HAI standard (FhCMB, USA) and bovine serum albumin (BSA) standard (ThermoFisher Scientific, USA) were also used in protein gel electrophoresis. I-Block™ Protein-Based Blocking Reagent (ThermoFisher Scientific, USA) was used to block membranes prior incubation with antibodies. Tetra·His mouse monoclonal antibody (1: 2 000) (Qiagen, USA), anti-VP3 mouse monoclonal antibody (1: 20 000) (JCU/CAV/1C1) (TropBio Pty Ltd, Australia) and goat anti-mouse antibody (1: 5 000) (Jackson ImmunoResearch Inc, USA) were used to detect the presence of apoptin via Western blotting technique. In addition, SuperSignal West Pico Chemiluminescent Substrate (ThermoFisher Scientific, USA) was used for horseradish peroxidase (HRP) reaction in the Western detection procedure. Coomassie Protein Assay Reagent (ThermoFisher Scientific, USA) was used in this study to stain protein gels.

4.2.1.4 Specialised equipment and accessories

Transformation of *Agrobacterium* via electroporation was performed by using MicroPulser™ Electroporator system (Biorad, USA). Sterile Gene Pulser Electroporation Cuvettes (0.1 cm) (Biorad, USA) were used for each electroporation reaction. Vacuum infiltration system used for infiltration of plant was customised by FhCMB (USA). Protein gel electrophoresis was performed using Mini-PROTEAN Tetra Cell system (Biorad, USA) and protein transfer from gel to (PVDF) membrane was performed using Trans-Blot® Turbo™ (Biorad, USA). In addition, GENE GNOME Chemiluminescence imaging system (Syngene, USA) was used to capture signals and save images of Western blots; HP Scanjet G3110 scanner was used to capture images of protein gels stained by Coomassie blue dye. Besides, Nikon Eclipse Ti Inverted Microscope (Nikon Instruments Inc, USA) and Zeiss 5 Live DUO Highspeed Confocal Microscope (Zeiss, USA) were also used in this study to observe the localisation of apoptin within the plant cells.

4.2.1.5 Analysis tools

Images of Western blots were analysed using GeneSnap and GeneTools (Syngene, USA). Photos taken by Nikon Eclipse Ti Inverted Microscope were analysed using Nikon NIS Elements (Nikon Instruments Inc, USA); on the other hand, photos taken by Zeiss 5 Live DUO Highspeed Confocal Microscope were analysed using Zeiss LSM 5 (Zeiss, USA).

4.2.2 Transformation of *Agrobacterium tumefaciens*

Hundred nanograms of recombinant vectors were incubated with bacterial cells on ice for 5 minutes. Bacterial cell mixtures were subsequently electroporated based on a protocol recommended by manufacturer with voltage at 2.4 kV was applied for 5 milliseconds. Hundred-fifty microlitre of Luria Broth (LB) broth was added to electroporated cells and cell mixtures were subsequently incubated at 28°C as well as shaken horizontally at 220 rpm for at least an hour. Bacterial cells were then plated on LB agar containing 50 mg/L kanamycin and incubated at 28°C for 48 hours.

4.2.3 Agoinfiltration

Overnight bacterial cultures were harvested and diluted to OD_{600} ranging at 0.2 - 1.0 with buffers as described in Table 4.1.

Table 4.1: Dilution of *A. tumefaciens* harbouring recombinant vectors.

No	Recombinant vectors	Agrobacterial strains	OD_{600}	Buffers
1	pGR-D4:: PR-VP3-HK	GV3101	0.5	Distilled water
2	pGR-D4:: PR-VP3-H	GV3101	0.5	Distilled water
3	pGR-D4:: VP3-H	GV3101	0.5	Distilled water
4	pGR-D4:: PR-GFP-VP3-HK	GV3101	0.5	Distilled water
5	pGR-D4:: PR-GFP-VP3-H	GV3101	0.5	Distilled water
6	pGR-D4:: GFP-VP3-H	GV3101	0.5	Distilled water
7	pGR-D4:: PR-Lic-VP3-HK	GV3101	0.5	Distilled water
8	pGR-D4:: PR-Lic-VP3-H	GV3101	0.5	Distilled water
9	pGR-D4:: Lic-VP3-H	GV3101	0.5	Distilled water
10	pGR-D4:: PR-H22-CatAd-VP3-HK	GV3101	0.5	Distilled water
11	pGR-D4:: PR-H22-CatAd-VP3-40-121-HK	GV3101	0.5	Distilled water
12	pGR-D4:: PR-H22-CatAd-VP3-60-121-HK	GV3101	0.5	Distilled water
13	pGR-D4:: PR-H22-CatAd-VP3-80-121-HK	GV3101	0.5	Distilled water
14	pGR-D4:: PR-EGF-CatAd-VP3-HK	GV3101	0.5	Distilled water
15	pGR-D4:: PR-EGF-CatAd-VP3-40-121-HK	GV3101	0.5	Distilled water
16	pGR-D4:: PR-EGF-CatAd-VP3-60-121-HK	GV3101	0.5	Distilled water
17	pGR-D4:: PR-EGF-CatAd-VP3-80-121-HK	GV3101	0.5	Distilled water
18	pGR-D:: PR-GFP-VP3-HK-mCherry__Nuc	AGLI	1.0	MMA
19	pGR-D:: PR-GFP-VP3-H__mCherryNuc	AGLI	1.0	MMA
20	pGR-D:: GFP-VP3-H__mCherryNuc	AGLI	1.0	MMA
21	pGR-DN:: PR-VP3-HK__bZIP17	AGLI	1.0	CMA
22	pGR-DN:: PR-VP3-HK__bZIP28	AGLI	1.0	CMA
23	pGR-DN:: PR-VP3-HK__bZIP60	AGLI	1.0	CMA
24	pGR-DN:: PR-GFP-VP3-HK __bZIP17	AGLI	1.0	CMA
25	pGR-DN:: PR-GFP-VP3-HK __bZIP28	AGLI	1.0	CMA
26	pGR-DN:: PR-GFP-VP3-HK __bZIP60	AGLI	1.0	CMA
27	pGR-DN:: PR-EGF-CatAd-VP3-HK__bZIP17	AGLI	1.0	CMA
28	pGR-DN:: PR-EGF-CatAd-VP3-HK__ bZIP28	AGLI	1.0	CMA
29	pGR-DN:: PR-EGF-CatAd-VP3-HK__bZIP60	AGLI	1.0	CMA
30	pCB:: P1/HC-Pro	GV3101	0.2	MMA
31	pCB:: P19	GV3101	0.2	CMA

Note: MMA= Inifltration buffer composed of 10mM MES, 10 mM $MgCl_2$, 0.15 mM Acetosyringone; CMA= Inifltration buffer composed of 10mM citrate (pH 5.8), 10 mM $MgCl_2$, 0.15 mM Acetosyringone.

Diluted agrobacterial strain AGLI harbouring recombinant vectors, namely pGR-D:: PR-GFP-VP3-HK__mCherryNuc, pGR-D:: PR-GFP-VP3-H__mCherryNuc and pGR-D:: GFP-VP3-H__mCherryNuc were mixed with agrobacterial strain GV3101 harbouring pCB:: P1/HC-Pro. Diluted agrobacterial strain AGLI harbouring recombinant vectors, namely pGR-DN:: PR-VP3-HK__bZIP17, pGR-DN:: PR-VP3-HK__bZIP28, pGR-DN:: PR-VP3-HK__bZIP60, pGR-DN:: PR-GFP-VP3-HK __bZIP17, pGR-DN:: PR-GFP-VP3-HK __bZIP28, pGR-DN:: PR-GFP-VP3-HK __bZIP60, pGR-DN:: PR-EGF-CatAd-VP3-HK__bZIP17, pGR-DN:: PR-EGF-CatAd-VP3-HK__bZIP28 and pGR-DN:: PR-EGF-CatAd-VP3-HK__bZIP60 were also mixed with agrobacterial strain GV3101 harbouring pCB:: P19. All bacterial mixtures were incubated at room temperature for at least 2 hours. On the other hand, agrobacterial strain GV3101 harbouring recombinant vectors, namely pGR-D4:: PR-VP3-HK, pGR-D4:: PR-VP3-H, pGR-D4:: VP3-H, pGR-D4:: PR-GFP-VP3-HK, pGR-D4:: PR-GFP-VP3-H, pGR-D4:: GFP-VP3-H, pGR-D4:: PR-Lic-VP3-HK, pGR-D4:: PR-Lic-VP3-H, pGR-D4:: Lic-VP3-H, pGR-D4:: PR-H22-CatAd-VP3-HK, pGR-D4:: PR-H22-CatAd-VP3-40-121-HK, pGR-D4:: PR-H22-CatAd-VP3-60-121-HK, pGR-D4:: PR-H22-CatAd-VP3-80-121-HK, pGR-D4:: PR-EGF-CatAd-VP3-HK, pGR-D4:: PR-EGF-CatAd-VP3-40-121-HK, pGR-D4:: PR-EGF-CatAd-VP3-60-121-HK and pGR-D4:: PR-EGF-CatAd-VP3-80-121-HK were used immediately after dilution with distilled water for infiltration.

Four to five weeks old *N. benthamiana* leaves were infiltrated with bacterial suspension at 28 inHg for 1 minute and subsequently brief-rinsed with distilled water.

4.2.4 Protein extraction

Plant leaf samples were collected between 3-8 days post infiltration (dpi). Leaf tissues were homogenised with 3 volumes of phosphate-buffered saline (PBS) with 1 mM Dieca. Triton X-100 (0.5% v/v) was added into the lysate to generate soluble protein extract (TSP-T) and 1x sodium dodecyl sulfate (SDS) reducing loading buffer [50mM Tris-Cl (pH 6.8), 2% SDS, 0.1M DTT] was used to generate total protein extract (TP). All cell lysates were pelleted at 16, 000 xg before the supernatant was analysed in 12% polyacrylamide gel electrophoresis.

4.2.5 Western blotting

Electrophoresed gels were transferred onto 0.2 µm PVDF membrane using Trans-Blot Turbo^{TM} blotting system with a preprogrammed protocol at 25 V for 7 minutes.

Blotted membranes were brief-rinsed in PBS before blocking in I-Block buffer for at least half an hour. Membranes were subsequently incubated in either Tetra-His or VP3 monoclonal primary antibody for 1-2 hours. Three-time washing steps with PBS-Tween (PBS-T) buffer at 4-minute intervals were performed before membranes were incubated with secondary antibody for another hour. Membranes were washed again for three times with PBS-T buffer at 4-minute intervals. Then, membranes were incubated in SuperSignal West Pico Chemiluminescent Substrate for 4 minutes before images of membranes were captured and recorded.

Protein bands detected in western blotting was measured using GeneTools and expression of recombinant proteins was quantified in relative to HAI standard (60 ng, 30 ng and 15 ng) loaded on the same gel. Fold change of protein expression was calculated as an approach to compare protein expression between recombinant vectors.

4.2.6 Microscopy

A slice of leaf sample from plants infiltrated with recombinant vectors, pGR-D:: PR-GFP-VP3-HK__mCherryNuc, pGR-D:: PR-GFP-VP3-H__mCherryNuc and pGR-D:: GFP-VP3-H__mCherryNuc on 5 dpi were prepared for observations under Nikon Eclipse Ti Inverted Microscope and Zeiss 5 Live DUO Highspeed Confocal Microscope.

4.3 Results

4.3.1 Protein expression profiles of recombinant apoptin

4.3.1.1 Expression and accumulation of recombinant apoptin alone in subcellular compartments

Time course study for expression of recombinant apoptin was detected between 3 days post infiltration (dpi) and 8 dpi. Expression profile of *Nicotiana benthamiana* infiltrated with recombinant vector without gene insert (mock) confirmed that mock samples were free of recombinant proteins (Appendix 4.1). Expression of recombinant apoptin alone in total soluble protein extract with 0.5% triton (TSP-T) gave low protein yield, which was less than 15% of total protein (TP), in all three recombinant vectors including pGR-D4:: PR-VP3-HK, pGR-D4:: PR-VP3-H and pGR-D4:: VP3-H (Figure 4.1). Hence, most of recombinant apoptin could only be recovered from insoluble plant extract. Plant infiltrated with recombinant vectors, pGR-D4:: PR-VP3-HK (Figure 4.2-a) and pGR-D4:: PR-VP3-H (Figure 4.2-b), by which recombinant proteins were expected accumulating in endoplasmic reticulum (ER) and apoplast, showed necrosis symptom as early as 3-4 dpi. Severe necrosis was subsequently observed on 5 dpi. Interestingly, necrosis was not found on plants infiltrated with recombinant pGR-D4:: VP3-H (Figure 4.2-c).

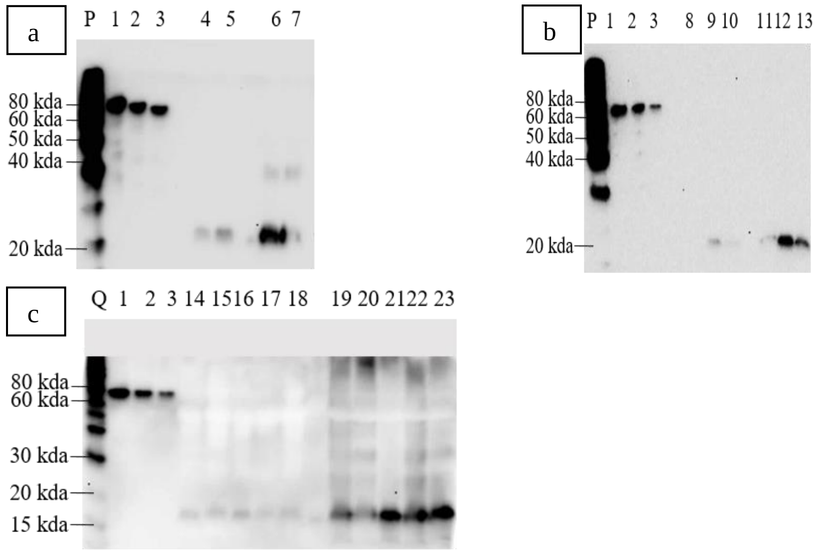

Lane	Sample	Expression vector	Estimated size
P	MagicMark™ XP Western Protein Standard		
Q	BenchMark™ His-tagged Protein Standard		
1-3	60 ng, 30 ng and 15 ng of HAI standard		~ 70 kDa
4-5	TSP-T extract from leaf samples harvested on 4 and 5 dpi	pGR-D4:: PR-VP3-HK	~ 18 kDa
6-7	TP extract from leaf samples harvested on 4 and 5 dpi	pGR-D4:: PR-VP3-HK	~ 18 kDa
8-10	TSP-T extract from leaf samples harvested on 3, 4 and 5 dpi	pGR-D4:: PR-VP3-H	~ 18 kDa
11-13	TP extract from leaf samples harvested on 3, 4 and 5 dpi	pGR-D4:: PR-VP3-H	~ 18 kDa
14-18	TSP-T extract from leaf samples harvested on 4, 5, 6, 7 and 8 dpi	pGR-D4:: VP3-H	~ 18 kDa
19-23	TP extract from leaf samples harvested on 4, 5, 6, 7 and 8 dpi	pGR-D4:: VP3-H	~ 18 kDa

Figure 4.1: Protein expression profiles of recombinant apoptin alone in subcellular compartment of *Nicotiana benthamiana* leaves. Detection was carried out via Western blotting technique which showed recombinant apoptin expressed from recombinant vectors, (a) pGR-D4:: PR-VP3-HK, (b) pGR-D4:: PR-VP3-H and (c) pGR-D4:: VP3-H using Tetra-His mouse monoclonal antibody.

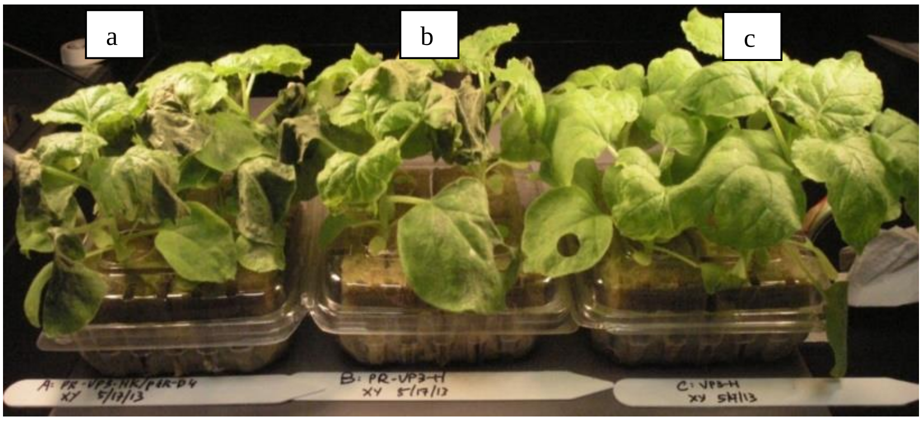

Figure 4.2: Physical appearances of *N. benthamiana* infiltrated with recombinant vectors, pGR-D4:: PR-VP3-HK, pGR-D4:: PR-VP3-H and pGR-D4:: VP3-H on 5 dpi. Plants showed necrosis symptom when infiltrated with recombinant vectors, (a) pGR-D4:: PR-VP3-HK and (b) pGR-D4:: PR-VP3-H as early as 3 dpi. Plants infiltrated with recombinant vector, (c) pGR-D4:: VP3-H did not show necrosis symptom but survived even incubation was extended until 8 dpi.

4.3.1.2 Expression of recombinant apoptin in fusion to C-terminal of green fluorescent protein (GFP)

Recombinant apoptin in fusion to C-terminal of GFP (recombinant vectors: pGR-D4:: PR-GFP-VP3-HK and pGR-D4:: GFP-VP3-H) (Figure 4.3-a and -c) except for recombinant GFP-apoptin (recombinant vector: pGR-D4:: PR-GFP-VP3-H) (Figure 4.3-b) showed an increased TP level to approximately 2-3 folds. Among these three recombinant vectors, recombinant GFP-apoptin (recombinant vector: pGR-D4:: GFP-VP3-H) exhibited the highest expression on both protein (Figure 4.3-c) and fluorescence (Figure 4.4-c) signals but TSP-T extract of this protein was only accounted ~10% of TP level (Figure 4.3-c).

On the other hand, TSP-T extracts of recombinant GFP-apoptin targeted to ER and apoplast (recombinant vectors: pGR-D4:: PR-GFP-VP3-HK and pGR-D4:: PR-GFP-VP3-H) were estimated 10 folds higher than recombinant apoptin expressed alone (recombinant vectors: pGR-D4:: PR-VP3-HK and pGR-D4:: PR-VP3-H) (4.1-a and -b). TSP-T extract of recombinant GFP-apoptin accumulated in ER was ~50% of TP level (4.3-a). However, TSP-T extract of recombinant GFP-apoptin accumulated in apoplast was ~90% of TP level (Figure 4.3-b). TSP-T extract of recombinant GFP-apoptin accumulated in ER was slightly higher than protein accumulated in apoplast but it was ~2.5 folds higher than protein that was not targeted into secretory pathway (recombinant vector: pGR-D4:: GFP-VP3-H).

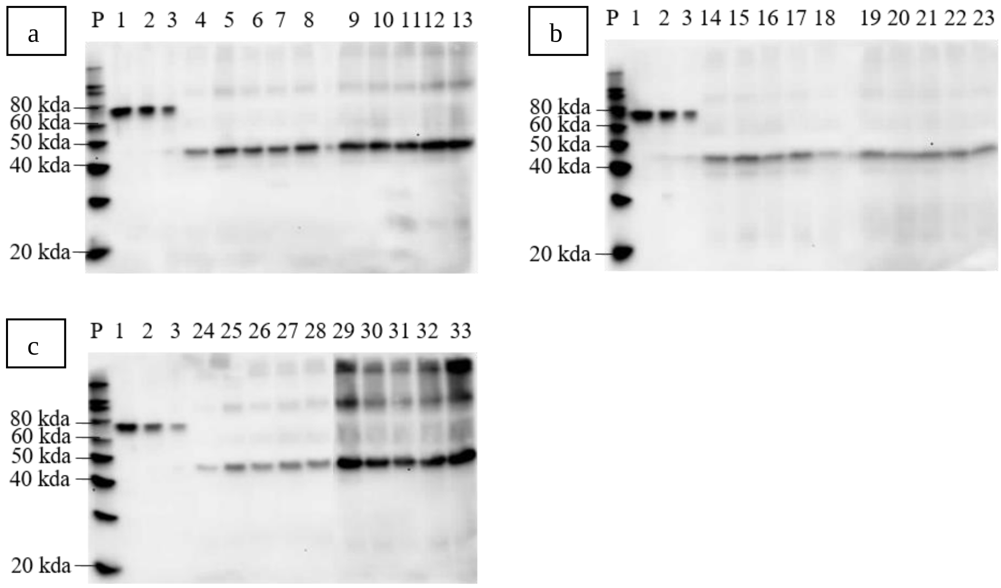

Lane	Sample	Expression vector	Estimated size
P	MagicMark™ XP Western Protein Standard		
1-3	60 ng, 30 ng and 15 ng of HAI standard		~ 70 kDa
4-8	TSP-T extract from leaf samples harvested on 4, 5, 6, 7 and 8 dpi	pGR-D4:: PR-GFP-VP3-HK	~ 42 kDa
9-13	TP extract from leaf samples harvested on 4, 5, 6, 7 and 8 dpi	pGR-D4:: PR-GFP-VP3-HK	~ 42 kDa
14-18	TSP-T extract from leaf samples harvested on 4, 5, 6, 7 and 8 dpi	pGR-D4:: PR-GFP-VP3-H	~ 42 kDa
19-23	TP extract from leaf samples harvested on 4, 5, 6, 7 and 8 dpi	pGR-D4:: PR-GFP-VP3-H	~ 42 kDa
24-28	TSP-T extract from leaf samples harvested on 4, 5, 6, 7 and 8 dpi	pGR-D4:: GFP-VP3-H	~ 42 kDa
29-33	TP extract from leaf samples harvested on 4, 5, 6, 7 and 8 dpi	pGR-D4:: GFP-VP3-H	~ 42 kDa

Figure 4.3 : Protein expression profiles of recombinant apoptin in fusion to C-terminal of GFP. Detection was carried out via Western blotting technique which showed recombinant GFP-apoptin expressed from recombinant vectors, (a) pGR-D4:: PR-GFP-VP3-HK, (b) pGR-D4:: PR-GFP-VP3-H and (c) pGR-D4:: GFP-VP3-H using Tetra-His mouse monoclonal antibody.

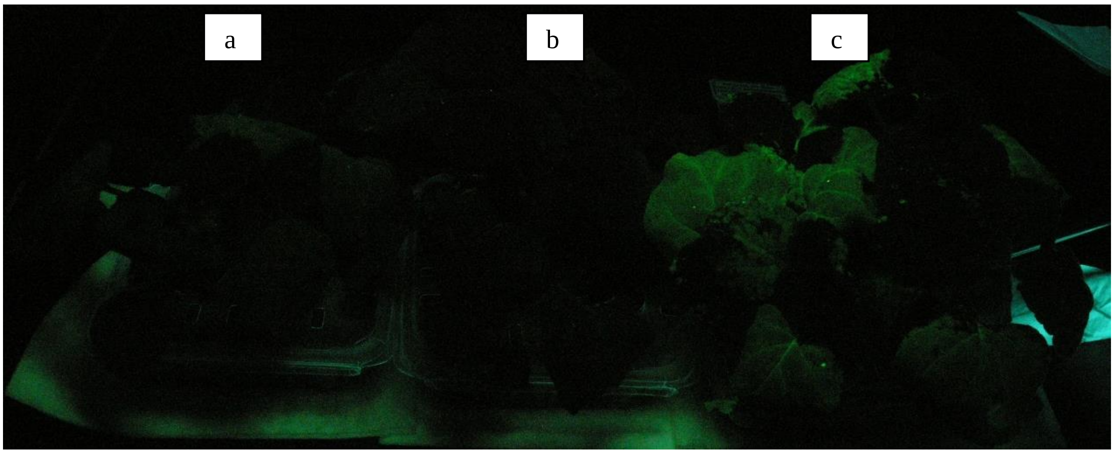

Figure 4.4: GFP fluorescent signals detected using UV lamp of plants infiltrated with recombinant vectors, (a) pGR-D4:: PR-GFP-VP3-HK, (b) pGR-D4:: PR-GFP-VP3-H and (c) pGR-D4:: GFP-VP3-H. Recombinant pGR-D4:: GFP-VP3-H exhibited the highest GFP signal.

Under microscopic observation, recombinant GFP-apoptin (recombinant vector: pGR-D:: GFP-VP3-H__mCherryNuc) (Green) expressed in cytoplasm, was relocalised and accumulated in plant cell nucleus. This argument is in concordance with the expectation of the same localisation pattern as mCherry (Red) protein pre-incorporated with a nuclear localisation signal, was redirected into the nucleus (Figure 4.5-c). However, relocalisation of protein into nucleus was not observed when recombinant GFP-apoptin targeted to ER and apoplast (recombinant vectors: pGR-D:: PR-GFP-VP3-HK__mCherryNuc and pGR-D:: PR-GFP-VP3-H__mCherryNuc) (Figure 2-a and -b).

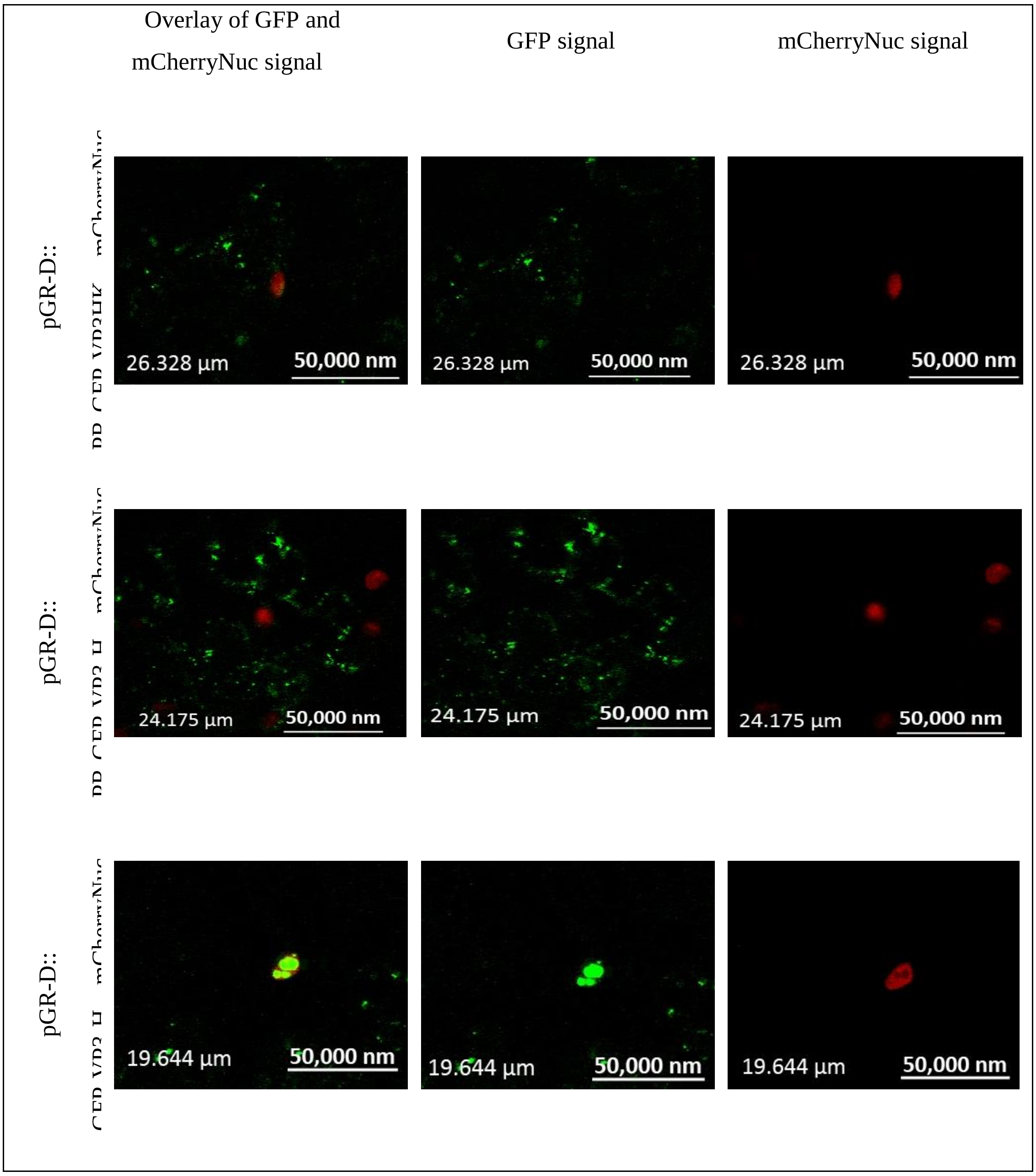

Figure 4.5: Microscopic observation of co-expression of recombinant GFP-VP3 (Green) and mCherryNuc (Red) in *N. benthamiana* cells. mCherry protein containing nuclear localisation signal on C-terminal end is expected to be relocated into plant cell nucleus as evidenced in previous study. Images above show the redistribution of protein in cells instead of directing into cell nucleus for (a) and (b) occurred with the addition of signal peptides to VP3 protein. Expression of (c) GFP-VP3 showed the protein accumulation within the nucleus of plant cells since mCherry and GFP signals were co-localised at the same position.

4.3.1.3 Expression of recombinant apoptin in fusion to C-terminal of lichenase

Expression of recombinant lichenase-apoptin showed similar expression profiles as recombinant apoptin alone (Figure 4.6). Necrosis symptom was observed when recombinant lichenase-apoptin targeted to ER (recombinant vector: pGR-D4:: PR-Lic-VP3-HK) (Figure 4.7-a) and apoplast (recombinant vector: pGR-D4:: PR-Lic-VP3-H) (Figure 4.7-b) but not for recombinant vector pGR-D4:: Lic-VP3-H (Figure 4.7-c). Low TSP-T level was detected for all three recombinant proteins. However, 2-3 folds higher level of insoluble protein (TP) was able to be collected from recombinant lichenase-apoptin (recombinant vector: pGR-D4:: Lic-VP3-H) (Figure 4.6-c) than recombinant apoptin alone (recombinant vector: pGR-D4:: VP3-H) (Figure 4.1-c) and recombinant GFP-apoptin (recombinant vector: pGR-D4:: GFP-VP3-H) (Figure 4.3-c).

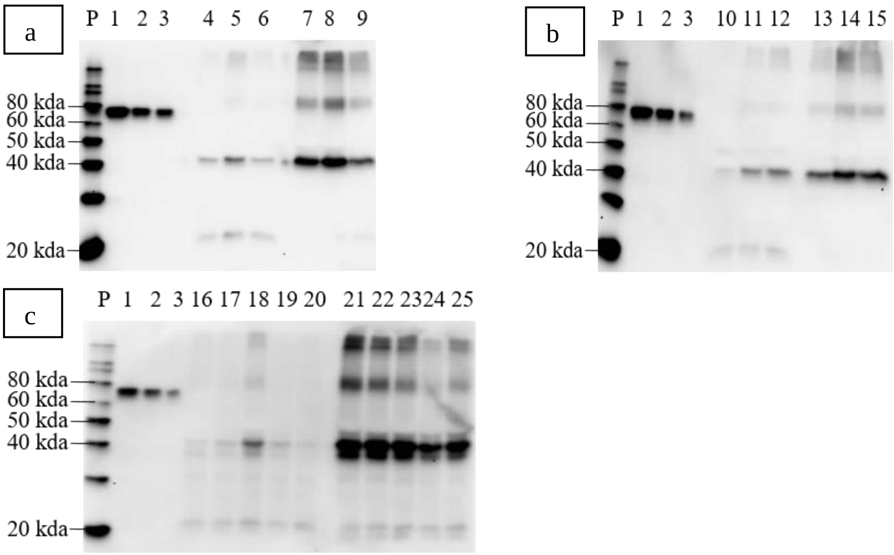

Lane	Sample	Expression vector	Estimated size
P	MagicMark™ XP Western Protein Standard		
1-3	60 ng, 30 ng and 15 ng of HAI standard		~ 70 kDa
4-6	TSP-T extract from leaf samples harvested on 3, 4 and 5 dpi	pGR-D4:: PR-Lic-VP3-HK	~ 40 kDa
7-9	TP extract from leaf samples harvested on 3, 4 and 5 dpi	pGR-D4:: PR-Lic-VP3-HK	~ 40 kDa
10-12	TSP-T extract from leaf samples harvested on 3, 4 and 5 dpi	pGR-D4:: PR- Lic-VP3-H	~ 40 kDa
13-15	TP extract from leaf samples harvested on 3, 4 and 5 dpi	pGR-D4:: PR- Lic-VP3-H	~ 40 kDa
16-20	TSP-T extract from leaf samples harvested on 4, 5, 6, 7 and 8 dpi	pGR-D4:: Lic-VP3-H	~ 40 kDa
21-25	TP extract from leaf samples harvested on 4, 5, 6, 7 and 8 dpi	pGR-D4:: Lic-VP3-H	~ 40 kDa

Figure 4.6: Protein expression profiles of recombinant apoptin in fusion to C-terminal of lichenase. Detection was carried out via Western blotting technique which showed recombinant lichenase-apoptin expressed from recombinant vector, (a) pGR-D4:: PR-Lic-VP3-HK, (b) pGR-D4:: PR-Lic-VP3-H and (c) pGR-D4:: Lic-VP3-H using Tetra-His mouse monoclonal antibody.

Figure 4.7: Physical appearances of *N. benthamiana* infiltrated with recombinant vectors, pGR-D4:: PR-Lic-VP3-HK, pGR-D4:: PR-Lic-VP3-H and pGR-D4:: Lic-VP3-H on 5 dpi. Plants showed necrosis symptom when infiltrated with recombinant vectors, (a) pGR-D4:: PR-Lic-VP3-HK and (b) pGR-D4:: PR-Lic-VP3-H as early as 3 dpi. Plants infiltrated with recombinant vector, (c) pGR-D4:: Lic-VP3-H did not show necrosis symptom but were viable even incubation was extended until 8 dpi.

4.3.1.4 Expression of full length and truncated recombinant apoptin in fusion to C-terminal of H22 single chain antibody and CatAd molecular adaptor

All four recombinant H22-CatAd-apoptin showed low expression level (Figure 4.8). Instead of full size protein, degradation was observed in all four recombinant protein expression profiles. Presence of 2-3 lower molecular weight protein bands was observed instead of the expected full size proteins. For example, full size protein for recombinant H22-CatAd-apoptin (recombinant vector: pGR-D4:: PR-H22-CatAd-VP3-HK) was expected to be 43 kDa but smaller molecular weight protein band was detected at sizes between 30 and 40 kDa (Figure 4.8-a). Similar observation could be detected in expression profiles of recombinant vectors, pGR-D4:: PR-H22-CatAd-40-121-VP3-HK (Figure 4.8-b), pGR-D4:: PR-H22-CatAd-60-121-VP3-HK (Figure 4.8-c) and pGR-D4:: PR-H22-CatAd-80-121-VP3-HK (Figure 4.8-d).

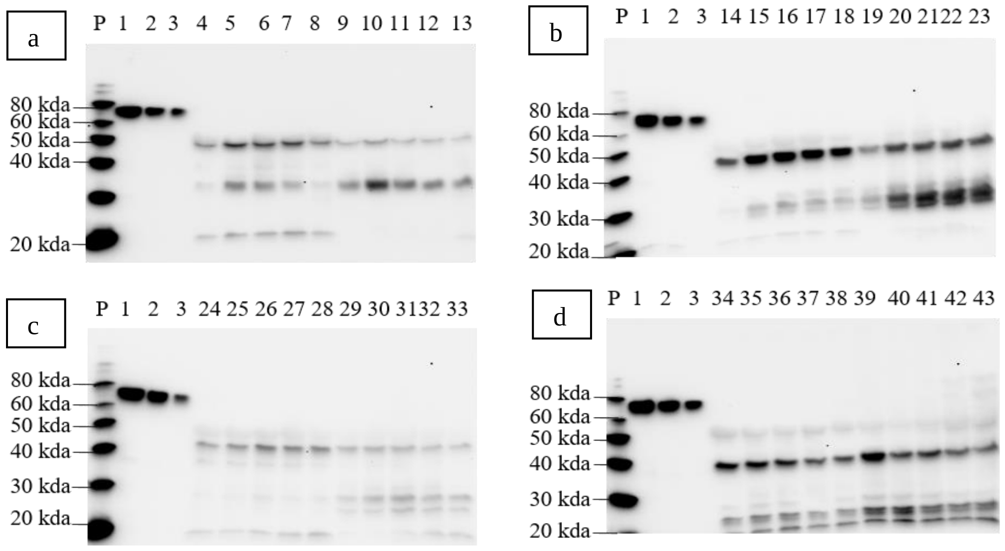

Lane	Sample	Expression vector	Estimated size
P	MagicMark™ XP Western Protein Standard		
1-3	60 ng, 30 ng and 15 ng of HAI standard		~ 70 kDa
4-8	TSP-T extract from leaf samples harvested on 4, 5, 6, 7 and 8 dpi	pGR-D4:: PR-H22-CatAd-VP3-HK	~ 43 kDa
9-13	TP extract from leaf samples harvested on 4, 5, 6, 7 and 8 dpi	pGR-D4:: PR-H22-CatAd-VP3-HK	~ 43 kDa
14-18	TSP-T extract from leaf samples harvested on 4, 5, 6, 7 and 8 dpi	pGR-D4:: PR-H22-CatAd-40-121-VP3-HK	~ 40 kDa
19-23	TP extract from leaf samples harvested on 4, 5, 6, 7 and 8 dpi	pGR-D4:: PR-H22-CatAd-40-121-VP3-HK	~ 40 kDa
24-28	TSP-T extract from leaf samples harvested on 4, 5, 6, 7 and 8 dpi	pGR-D4:: PR-H22-CatAd-60-121-VP3-HK	~ 37 kDa
29-33	TP extract from leaf samples harvested on 4, 5, 6, 7 and 8 dpi	pGR-D4:: PR-H22-CatAd-60-121-VP3-HK	~ 37 kDa
34-38	TSP-T extract from leaf samples harvested on 4, 5, 6, 7 and 8 dpi	pGR-D4:: PR-H22-CatAd-80-121-VP3-HK	~ 35 kDa
39-43	TP extract from leaf samples harvested on 4, 5, 6, 7 and 8 dpi	pGR-D4:: PR-H22-CatAd-80-121-VP3-HK	~ 35 kDa

Figure 4.8: Protein expression profiles of recombinant apoptin in fusion to C-terminal of H22 single chain antibody and CatAd molecular adaptor. Detection was performed via Western blotting technique using Tetra-His mouse monoclonal antibody which showed recombinant H22-CatAd-apoptin expressed from recombinant vectors, (a) pGR-D4:: PR-H22-CatAd-VP3-HK, (b) pGR-D4:: PR-H22-CatAd-40-121-VP3-HK, (c) pGR-D4:: PR-H22-CatAd-60-121-VP3-HK and (d) pGR-D4:: PR-H22-CatAd-80-121-VP3-HK.

4.3.1.5 Expression of full length and truncated recombinant apoptin in fusion to C-terminal of epidermal growth factor (EGF) and CatAd molecular adaptor

Detectable levels of TP and TSP-T for recombinant EGF-CatAd-apoptin were observed in expression profiles of recombinant vector, pGR-D4:: PR-EGF-CatAd-VP3-HK (Figure 4.9-a). In addition, approximately 2-3 folds higher level was observed in expression profiles of recombinant vectors, pGR-D4:: PR-EGF-CatAd-VP3-40-121-HK (Figure 4.9-b) and pGR-D4:: PR-EGF-CatAd-VP3-80-121-HK (Figure 4.9-d) but severe early necrosis symptom appeared on recombinant pGR-D4:: PR-EGF-CatAd-VP3-80-121-HK (Figure 4.10-d) only. Low expression of recombinant vector, pGR-D4:: PR-EGF-CatAd-VP3-60-121-HK (Figure 4.9-c) was detected in both TP and TSP-T extracts as compared to three other recombinant vectors. No significant degradation band was observed in expression of recombinant EGF-CatAd-apoptin.

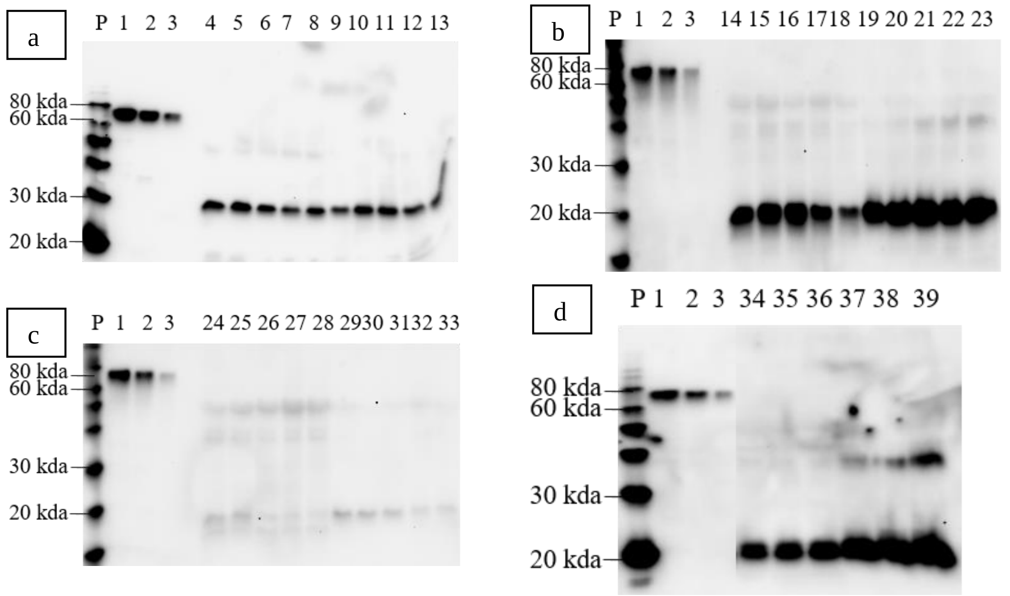

Lane	Sample	Expression vector	Estimated size
P	MagicMark™ XP Western Protein Standard		
1-3	60 ng, 30 ng and 15 ng of HAI standard		~ 70 kDa
4-8	TSP-T extract from leaf samples harvested on 4, 5, 6, 7 and 8 dpi	pGR-D4:: PR-EGF-CatAd-VP3-HK	~ 30 kDa
9-13	TP extract from leaf samples harvested on 4, 5, 6, 7 and 8 dpi	pGR-D4:: PR- EGF-CatAd-VP3-HK	~ 30 kDa
14-18	TSP-T extract from leaf samples harvested on 4, 5, 6, 7 and 8 dpi	pGR-D4:: PR- EGF-CatAd-40-121-VP3-HK	~ 25 kDa
19-23	TP extract from leaf samples harvested on 4, 5, 6, 7 and 8 dpi	pGR-D4:: PR- EGF-CatAd-40-121-VP3-HK	~ 25 kDa
24-28	TSP-T extract from leaf samples harvested on 4, 5, 6, 7 and 8 dpi	pGR-D4:: PR- EGF-CatAd-60-121-VP3-HK	~ 22 kDa
29-33	TP extract from leaf samples harvested on 4, 5, 6, 7 and 8 dpi	pGR-D4:: PR- EGF-CatAd-60-121-VP3-HK	~ 22 kDa
34-36	TSP-T extract from leaf samples harvested on 3, 4 and 5 dpi	pGR-D4:: PR- EGF-CatAd-80-121-VP3-HK	~ 20 kDa
37-39	TP extract from leaf samples harvested on 3, 4 and 5 dpi	pGR-D4:: PR- EGF-CatAd-80-121-VP3-HK	~ 20 kDa

Figure 4.9: Protein expression profiles of recombinant apoptin in fusion to C-terminal of EGF and CatAd molecular adaptor. Detection was performed via Western blotting technique using Tetra-His mouse monoclonal antibody which showed recombinant EGF-CatAd-apoptin expressed from recombinant vectors, (a) pGR-D4:: PR-EGF-CatAd-VP3-HK, (b) pGR-D4:: PR-EGF-CatAd-40-121-VP3-HK, (c) pGR-D4:: PR-EGF-CatAd-60-121-VP3-HK and (d) pGR-D4:: PR-EGF-CatAd-80-121-VP3-HK.

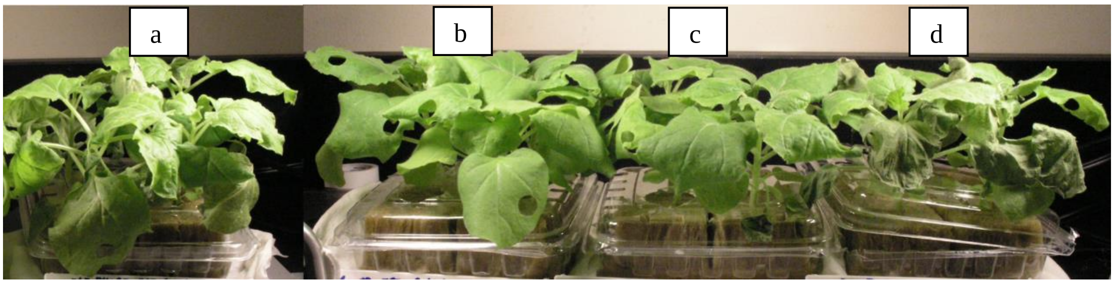

Figure 4.10: Physical appearances of *N. benthamiana* infiltrated with recombinant vectors, pGR-D4:: PR-EGF-CatAd-VP3-HK, pGR-D4:: PR-EGF-CatAd-40-121-VP3-HK, pGR-D4:: PR-EGF-CatAd-60-121-VP3-HK and pGR-D4:: PR-EGF-CatAd-80-121-VP3-HK on 5 dpi. Plants showed early necrosis symptom when infiltrated with recombinant vectors, (d) pGR-D4:: PR-EGF-CatAd-80-121-VP3-HK as early as 3 dpi. Mild necrosis symptom was also observed on plants infiltrated with recombinant vector, (a) pGR-D4:: PR-EGF-CatAd-VP3-HK on 7 dpi. However, recombinant vectors, (b) pGR-D4:: PR-EGF-CatAd-40-121-VP3-HK and (c) pGR-D4:: PR-EGF-CatAd-60-121-VP3-HK did not show any necrosis symptom where plants were viable even until 8 dpi.

4.3.1.6 Co-expression of recombinant apoptin alone, recombinant GFP-apoptin and recombinant EGF-CatAd-VP3 with ER stress proteins, bZIP17, bZIP28 and bZIP60

Expression of recombinant apoptin alone was low in recombinant vector, pGR-D4:: PR-VP3-HK (Figure 4.1-a); however, expression of recombinant apoptin alone was increased when co-expressed with ER stress proteins (Figure 4.11). In comparison to pGR-D4:: PR-VP3-HK, expression of recombinant apoptin alone was ~6 folds higher in TP and TSP-T extracts when co-expressed with bZIP17 (recombinant vector: pGR-DN:: PR-VP3-HK__bZIP17) (Figure 4.11-a). Meanwhile, it was ~10 folds higher in TP and TSP-T extracts when protein was co-expressed with bZIP60 (recombinant vector: pGR-DN:: PR-VP3-HK__bZIP60) (Figure 4.11-c). For recombinant apoptin co-expressed with bZIP28 (Figure 4.11-b), ~5 folds higher level of TP was able to be harvested but not significantly increased as observed in TSP-T extract compared with that of expression of recombinant vector, pGR-D4:: PR-VP3-HK. Plants infiltrated with recombinant vectors, pGR-DN:: PR-VP3-HK__bZIP17 (Figure 4.12-a) and pGR-DN:: PR-VP3-HK__bZIP28 (Figure 4.12-b) showed early necrosis symptom similar to plants infiltrated with recombinant vector, pGR-D4:: PR-VP3-HK (Figure 4.2-a). However, mild necrosis symptom was also observed in plants infiltrated with recombinant vector, pGR-DN:: PR-VP3-HK__bZIP60 (Figure 4.12-c).

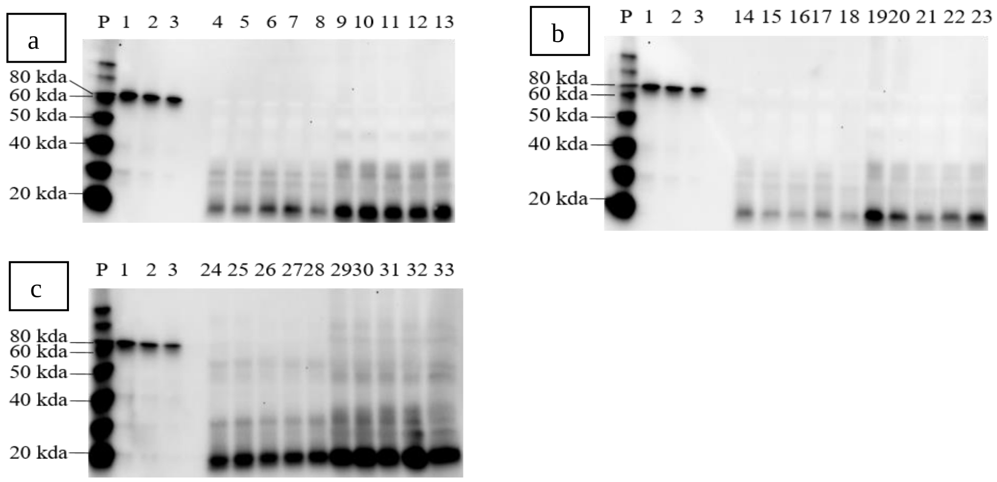

Lane	Sample	Expression vector	Estimated size
P	MagicMark™ XP Western Protein Standard		
1-3	60 ng, 30 ng and 15 ng of HAI standard		~ 70 kDa
4-8	TSP-T extract from leaf samples harvested on 4, 5, 6, 7 and 8 dpi	pGR-DN:: PR-VP3-HK__bZIP17	~ 18 kDa
9-13	TP extract from leaf samples harvested on 4, 5, 6, 7 and 8 dpi	pGR-DN:: PR-VP3-HK__bZIP17	~ 18 kDa
14-18	TSP-T extract from leaf samples harvested on 3, 4, 5, 6 and 7 dpi	pGR-DN:: PR-VP3-HK__bZIP28	~ 18 kDa
19-23	TP extract from leaf samples harvested on 3, 4, 5, 6 and 7 dpi	pGR-DN:: PR-VP3-HK__bZIP28	~ 18 kDa
24-28	TSP-T extract from leaf samples harvested on 3, 4, 5, 6 and 7 dpi	pGR-DN:: PR-VP3-HK__bZIP60	~ 18 kDa
29-33	TP extract from leaf samples harvested on 3, 4, 5, 6 and 7 dpi	pGR-DN:: PR-VP3-HK__bZIP60	~ 18 kDa

Figure 4.11: Protein expression profiles of recombinant apoptin alone co-expressed with ER stress proteins in *N. benthamiana* leaves. Detection was conducted via Western blotting technique which showed expressions of (a) recombinant apoptin alone that co-expressed with bZIP17 (recombinant vector: pGR-DN:: PR-VP3-HK__bZIP17), (b) recombinant apoptin alone that co-expressed with bZIP28 (recombinant vector: pGR-DN:: PR-VP3-HK__bZIP28) and (c) recombinant apoptin alone that co-expressed with bZIP60 (recombinant vector: pGR-DN:: PR-VP3-HK__bZIP60) reacted with Tetra-His mouse monoclonal antibody.

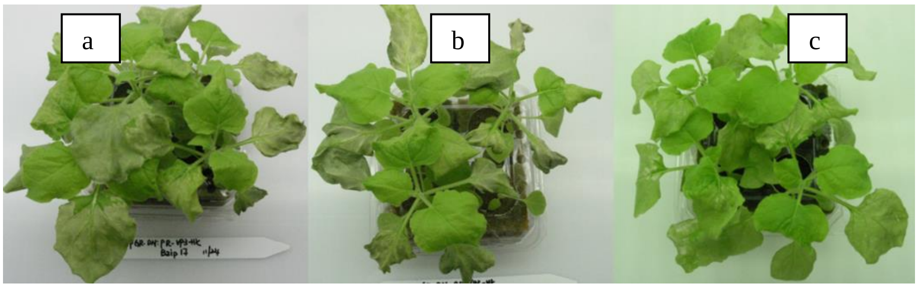

Figure 4.12: Physical appearances of *N. benthamiana* infiltrated with recombinant vectors, pGR-DN:: PR-VP3-HK__bZIP17, pGR-DN:: PR-VP3-HK__bZIP28 and pGR-DN:: PR-VP3-HK__bZIP60 on 5 dpi. Plants showed early necrosis symptom when infiltrated with recombinant vectors, (a) pGR-DN:: PR-VP3-HK__bZIP17 and (b) pGR-DN:: PR-VP3-HK__bZIP28 as early as 3-4 dpi. Plants infiltrated with recombinant vector, (c) pGR-DN:: PR-VP3-HK__bZIP60 showed milder necrosis symptom on 5 dpi.

Approximately 2-fold increment on TSP-T expression levels for recombinant vectors, pGR-DN:: PR-GFP-VP3-HK__bZIP17 (Figure 4.13-a) and pGR-DN:: PR-GFP-VP3-HK__bZIP60 (Figure 4.13-c) were observed when compared to expression of recombinant vector, pGR-D4:: PR-GFP-VP3-HK (Figure 4.3-a). However, expression of TSP-T level for recombinant GFP-apoptin that co-expressed with bZIP28 (pGR-DN:: PR-GFP-VP3-HK__bZIP28) (Figure 4.13-b) did not show significant difference from expression of recombinant vector, pGR-D4:: PR-GFP-VP3-HK. Nevertheless, ~2-4 folds of increment in TP levels of recombinant GFP-apoptin that co-expressed with all three ER stress proteins (bZIP17, bZIP28 and bZIP60) were noticed.

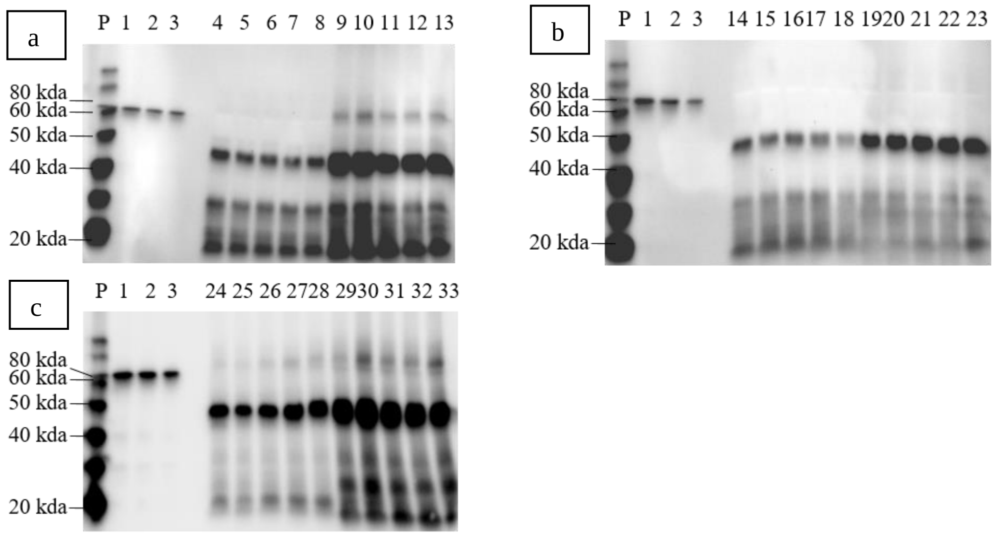

Lane	Sample	Expression vector	Estimated size
P	MagicMark™ XP Western Protein Standard		
1-3	60 ng, 30 ng and 15 ng of HAI standard		~ 70 kDa
4-8	TSP-T extract from leaf samples harvested on 4, 5, 6, 7 and 8 dpi	pGR-DN:: PR-GFP-VP3-HK__bZIP17	~ 42 kDa
9-13	TP extract from leaf samples harvested on 4, 5, 6, 7 and 8 dpi	pGR-DN:: PR-GFP-VP3-HK__bZIP17	~ 42 kDa
14-18	TSP-T extract from leaf samples harvested on 4, 5, 6, 7 and 8 dpi	pGR-DN:: PR-GFP-VP3-HK__bZIP28	~ 42 kDa
19-23	TP extract from leaf samples harvested on 4, 5, 6, 7 and 8 dpi	pGR-DN:: PR-GFP-VP3-HK__bZIP28	~ 42 kDa
24-28	TSP-T extract from leaf samples harvested on 4, 5, 6, 7 and 8 dpi	pGR-DN:: PR-GFP-VP3-HK__bZIP60	~ 42 kDa
29-33	TP extract from leaf samples harvested on 4, 5, 6, 7 and 8 dpi	pGR-DN:: PR-GFP-VP3-HK__bZIP60	~ 42 kDa

Figure 4.13: Protein expression profiles of recombinant GFP-apoptin co-expressed with ER stress proteins. Detection was carried out via Western blotting analysis using Tetra-His mouse monoclonal antibody which showed expressions of (a) recombinant GFP-apoptin that co-expressed with bZIP17 (recombinant vector: pGR-DN:: PR-GFP-VP3-HK__bZIP17), (b) recombinant GFP-apoptin that co-expressed with bZIP28 (recombinant vector: pGR-DN:: PR-GFP-VP3-HK__bZIP28) and (c) recombinant GFP-apoptin that co-expressed with bZIP60 (recombinant vector: pGR-DN:: PR-GFP-VP3-HK__bZIP60).

In comparison to recombinant vector pGR-D4:: PR-EGF-CatAd-VP3-HK (Figure 4.9-a), expression of recombinant EGF-CatAd-apoptin increased in 2-4 folds when co-expressed with ER stress proteins. Especially, recombinant vector, pGR-DN:: PR-EGF-CatAd-VP3-HK__bZIP28 (Figure 4.14-d) gave the highest yield of TSP-T among three recombinant vectors, which was ~4 folds of protein higher than that expressed by recombinant vector, pGR-D4:: PR-EGF-CatAd-VP3-HK. Mild necrosis symptom was observed on plants infiltrated with recombinant vector, pGR-DN:: PR-EGF-CatAd-VP3-HK__bZIP28 (Figure 4.15-b).

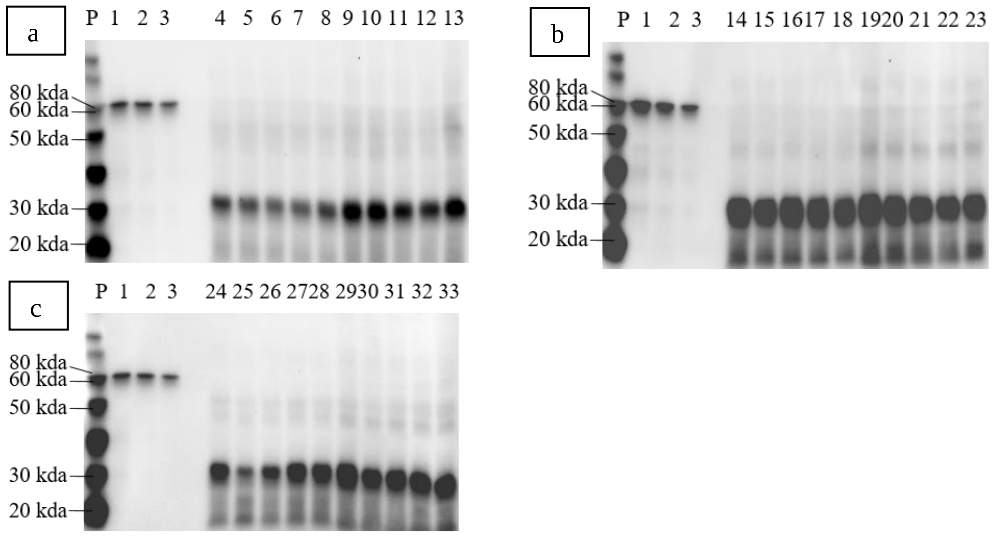

Lane	Sample	Expression vector	Estimated size
P	MagicMark™ XP Western Protein Standard		
1-3	60 ng, 30 ng and 15 ng of HAI standard		~ 70 kDa
4-8	TSP-T extract from leaf samples harvested on 4, 5, 6, 7 and 8 dpi	pGR-DN:: PR-EGF-CatAd-VP3-HK__bZIP17	~ 30 kDa
9-13	TP extract from leaf samples harvested on 4, 5, 6, 7 and 8 dpi	pGR-DN:: PR-EGF-CatAd-VP3-HK__bZIP17	~ 30 kDa
14-18	TSP-T extract from leaf samples harvested on 4, 5, 6, 7 and 8 dpi	pGR-DN:: PR-EGF-CatAd-VP3-HK__bZIP28	~ 30 kDa
19-23	TP extract from leaf samples harvested on 4, 5, 6, 7 and 8 dpi	pGR-DN:: PR-EGF-CatAd-VP3-HK__bZIP28	~ 30 kDa
24-28	TSP-T extract from leaf samples harvested on 4, 5, 6, 7 and 8 dpi	pGR-DN:: PR-EGF-CatAd-VP3-HK__bZIP60	~ 30 kDa
29-33	TP extract from leaf samples harvested on 4, 5, 6, 7 and 8 dpi	pGR-DN:: PR-EGF-CatAd-VP3-HK__bZIP60	~ 30 kDa

Figure 4.14: Protein expression profiles of recombinant EGF-CatAd-apoptin co-expressed with ER stress proteins. Detection was performed by Western blotting analysis which showed expressions of (a) recombinant EGF-CatAd-apoptin that co-expressed with bZIP17 (pGR-DN:: PR-EGF-CatAd-VP3-HK__bZIP17), (b) recombinant EGF-CatAd-apoptin that co-expressed with bZIP28 (pGR-DN:: PR-EGF-CatAd-VP3-HK__bZIP28) and (c) recombinant EGF-CatAd-apoptin that co-expressed with bZIP60 (pGR-DN:: PR-EGF-CatAd-VP3-HK__bZIP60) reacted with Tetra-His mouse monoclonal antibody.

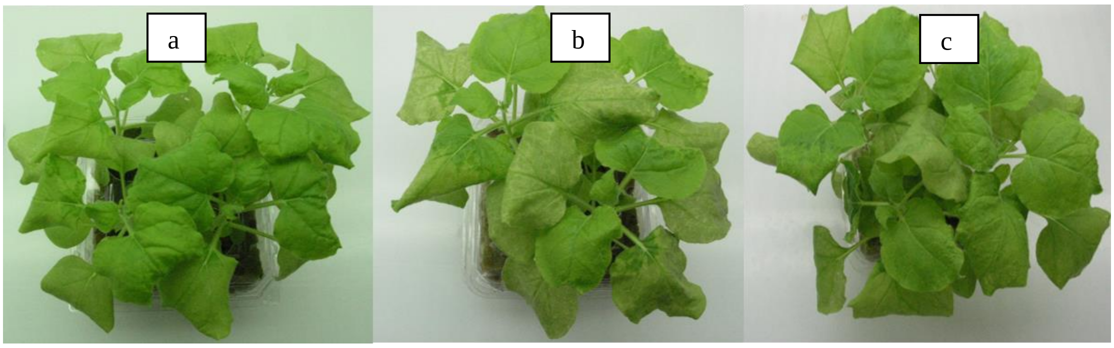

Figure 4.15: Physical appearances of *N. benthamiana* infiltrated with recombinant vectors, pGR-DN:: PR-EGF-CatAd-VP3-HK__bZIP17, pGR-DN:: PR-EGF-CatAd-VP3-HK__bZIP28 and pGR-DN:: PR-EGF-CatAd-VP3-HK__bZIP60 on 5 dpi. Plants infiltrated with recombinant vectors, (a) pGR-DN:: PR-EGF-CatAd-VP3-HK__bZIP17 and (b) pGR-DN:: PR-EGF-CatAd-VP3-HK__bZIP28 were healthy throughout until the last harvest date on 8 dpi. Plants showed mild necrosis symptom when infiltrated with recombinant vector, (c) pGR-DN:: PR-EGF-CatAd-VP3-HK__bZIP60 on 5 dpi.

4.4 Discussion

This chapter illustrates the delivery of recombinant apoptin vector variants into *Nicotiana benthamiana* via agroinfiltration and expression profiling on the production of recombinant apoptin proteins in order to seek for the most ideal recombinant cassettes that could offer high yield and stable proteins for subsequent downstream purification study. This study fully hired vacuum infiltration as a delivery approach for *Agrobacterium* to get into *N. benthamiana.* A standard infiltration protocol was applied for all infiltration works, hence, the delivery efficiency of *Agrobacterium* to plants is expected to be the same for all recombinant vectors. As described above, vacuum infiltration is an efficient way to infiltrate large batches of plants in a short period of time. Thus, time spent for infiltration works was reduced in this study especially when large quantities of leaf materials were required for downstream purification work (Chen *et al*., 2013). Besides, adverse injuries of infiltrated plants that always occur during syringe infiltration could also be eliminated when vacuum infiltration system was applied. Therefore, the necrosis symptoms observed in this study was believed to be solely induced by the expression of recombinant apoptin.

Other than the importance of optimised design for expression cassettes, the uses of agrobacterial concentration for infiltration and gene silencing suppressors are also the two factors that affect expression yield of recombinant proteins. An optimised concentration of *Agrobacterium* required for infiltration is always studied when a specific and optimised expression cassette is obtained. It was reported that high concentration of bacteria always induces hypersensitive response of plants and undoubtedly, an insufficient amount of bacteria also cause a lower level of protein expression (Leuzinger *et al.*, 2013). Concentration of *Agrobacterium* cultures for agroinfiltration was adjusted to OD_{600} = 0.5-1.0 in current study, fitting well into the recommended range for agroinfiltration by previous studies (Lindbo, 2007; Wroblewski *et al.*, 2005).

Gene silencing suppressors, P19 and P1/HC-Pro (Proteinase1/Helper component-proteinase), were used together with the recombinant vectors, pGR-D and pGR-DN (binary vectors) in this study in order to enhance protein expression level. Occurrence of gene silencing in plants suppresses expression of genes and hence resulting low protein expression levels. Especially, post transcriptional gene silencing (PTGS) in plants is induced by the presence of double stranded RNA (dsRNA), which is possibly caused by the transcription of antisense genes, overexpression of mRNA and virus infection (Escobar and Dandekar, 2000-2013). To confront the silencing effect of infected plants, viral gene silencing suppressors are always found during viral infection. For example, P19 and P1/ HC-Pro are the commonly found gene silencing suppressors in virus, which are believed playing a role in interrupting the assembly of RNA-induced silencing complex (RISC) and preventing translation inhibition caused by RISC (Burgyan and Havelda, 2011). Therefore, gene silencing suppressors were employed to co-infiltrate with transgenes to prevent inhibitory effect of host plants on foreign protein expression (Feller *et al.*, 2013; Garabagi *et al.*, 2012; Shah *et al.*, 2013). Instead of using external gene silencing suppressors, it was reported that 126k protein of tobacco mosaic virus (TMV) was believed involving in gene silencing suppression activities leading to the accumulation of sufficient short RNA (sRNA) (Vogler *et al.*, 2007). Hence, there was no gene silencing suppressor used when infiltration was performed using a TMV-based vector, pGR-D4 since an internal gene silencing suppressor had already been included.

In this study, accumulation of recombinant apoptin was compared when protein was targeted to cytoplasm, ER and apoplast. Recombinant apoptin was targeted to ER using tobacco pathogenesis related protein 1a (PR1a) signal peptide and ER retention signal (KDEL) (gene cassettes: PR-VP3-HK, PR-GFP-VP3-HK and PR-Lic-VP3-HK). Meanwhile, recombinant apoptin was targeted into secretory pathway by incorporating PR1a signal peptide only which resulted protein accumulation in apoplast of plant cells (gene cassettes: PR-VP3-H, PR-GFP-VP3-H and PR-Lic-VP3-H). Recombinant apoptin without signal peptide and ER retention signal (gene cassettes: VP3-H, GFP-VP3-H and Lic-VP3-H) was expected to accumulate in cell cytoplasm; however, recombinant GFP-apoptin (gene cassette: GFP-VP3-H) was observed relocalising into cell nucleus rather than staying in cytoplasm (Figure 4.5) as observed under the microscope. Similar observation was reported by Lacorte and his colleagues (2007) when they expressed Chicken Anemia Virus (CAV) Viral Protein 1 (VP1), VP2 and VP3 in *N. benthamiana.* Localisation of apoptin in cell nucleus was initially identified in chicken lymphoblastoid T-cell line, MDCC-MSBI and subsequently in mammalian cancerous cell lines (Noteborn *et al*., 1994; Noteborn *et al*., 1998). It was believed that the localisation activity of apoptin was directed by the bipartite nuclear localisation signal (NLS) residing on C-terminal of protein (amino acids 82-88 and 111-121) (Danen-Van Oorschot *et al*., 2003; Poon *et al*., 2005). Nevertheless, the authentic activities of apoptin in plant cells are remained to be determined.

Focusing on the accumulation of recombinant apoptin in three cellular compartments, it is interesting to find out that recombinant apoptin always showed the highest protein expression (at least 2-3 folds higher) when it is accumulated in nucleus in comparison to protein accumulated in ER and apoplast in this study. However, most of the expressed proteins were in the insoluble fraction. These proteins could only be harvested by using strong denaturants, such as sodium dodecyl sulfate (SDS) which was present in SDS reducing loading buffer (in section 4.2.4) or guanidium hypochlorite (GuHCl) (to be described in Chapter 5). Insoluble fraction of recombinant apoptin might be caused by the formation of large multimers that are hardly solubilised in the buffer without strong denaturants due to the huge size of protein. Formation of protein aggregates by apoptin was first observed in CAV-VP3 transfected lymphoblastoid T-cell line, MDCC-MSBI (Noteborn *et al*., 1994). Furthermore, formation of large multimers were also discovered when recombinant apoptin in fusion with maltose binding protein (MBP) was expressed in *Escherichia coli* as well as in mammalian cell Saos-2 (Leliveld[a] *et al.*, 2003). Ectopically expressed MBP-apoptin in Saos-2 cells formed dense protein aggregates, which could be pelleted at 10, 000 – 30, 000 xg centrifugation speed. Besides, Leliveld[a] and his colleagues (2003) also reported that the multimerised recombinant MBP-apoptin harvested from *E. coli* remained active when protein was microinjected into mammalian cells.

On the other hand, detectable level of soluble recombinant apoptin was observed but extremely low when protein was targeted to apoplast and ER (gene cassettes: PR-GFP-VP3-HK, PR-GFP-VP3-H, PR-Lic-VP3-HK and PR-Lic-VP3-H) as compared to accumulation that occurred in nucleus. Targeting recombinant protein into secretory pathway always results a higher yield of soluble protein and this most likely due to the presence of higher quantity of chaperones that involve in the protein folding process. In the study of Streatfield and his colleagues (2003), they showed that more than 100 folds of recombinant receptor binding (B) subunit of the heat-labile toxin (Lt-B) protein of enterotoxigenic *E. coli* was recovered when protein was accumulated in vacuole, cell surface and ER rather than cytoplasm of transgenic corn. Besides, spider silk-elastin was also successfully produced at 80 mg per kg of transgenic tobacco leaf materials when protein was targeted into ER (Scheller *et al.*, 2004).

Early necrosis symptom (observed from 3 dpi) was detected on plants infiltrated with recombinant apoptin vector variants especially those gene cassettes that targeted protein accumulation in ER and apoplast (gene cassettes: PR-VP3-HK, PR-VP3-H, PR-Lic-VP3-HK and PR-Lic-VP3-H). It is believed that the plant death might be co-related to the ER stress response/unfolded protein response (UPR) induced by the overexpression of recombinant protein. When protein translation exceeds the capacity of protein processing in ER lumen, efficiency of protein folding is questionable and this always leads to accumulation of unfolded or misfolded proteins (Kopito, 2000). As the amount of unfolded proteins accumulated over a threshold, UPR would be triggered to resolve the ER stress condition. This includes restraining protein biosynthesis, preventing protein loading into ER lumens, up-regulation of UPR genes especially those encode chaperone proteins and ER associated degradation of unfolded protein via ubiquitin-proteosome pathway in cytoplasm (Duwi Fanata *et al.*, 2013). ER stress-induced apoptosis would also be triggered that causes an irreversibly lethal effect if the stress condition is not resolved. Risk of unfolded protein is not only present in plants, similar issues are also observed in other system. For example, ‘inclusion body’ is always formed as a result of aggregation of unfolded protein induced by overexpression of recombinant proteins in *E. coli* expression system (Kopito, 2000). In human, misfolded proteins also form protein aggregates leading to several lethal diseases, such as type II diabetes, Alzheimer, Parkinson and Huntington diseases (Ashraf *et al.*, 2014).

In plant expression system, there are several fusion proteins used to increase solubility and stability of recombinant proteins, for examples, Zera, Elastin like protein (ELP), ubiquitin, b-glucuronidase, cholera toxin B (CTB), viral coat protein (CP) and human immunoglobulin A (IgA). In this study, solubility of recombinant protein was increased especially when apoptin was in fusion to green fluorescent protein (GFP) and epidermal growth factor (EGF). Soluble protein expression of recombinant GFP-apoptin (gene cassette: PR-GFP-VP3-HK) and recombinant EGF-apoptin (gene cassette: PR-EGF-CAtAd-VP3-HK) was approximately 5 folds over that of recombinant apoptin alone (gene cassette: PR-VP3-HK). In the study of Leliveld[a] and his co-workers (2003), as much as 100 mg per liter of recombinant apoptin was also obtained from *E. coli* when large fusion tag, maltose binding protein (MBP) was incorporated in the cassette; however, only 40 mg per liter of recombinant apoptin was able to be harvested from bacterial inclusion bodies. Although mechanisms of fusion protein partners increasing solubility of recombinant proteins are still unclear, there are several suggested explanations such as formation of fusion proteins in micelle-like structure, high propensity of fusion partners on attraction of chaperone proteins, presence of intrinsic chaperone-like activity and preventing formation of protein aggregates by electrostatic repulsion (Costa *et al.*, 2014). In addition to enhance expression of recombinant proteins, fusion proteins are also used for purification purpose which include short peptides, such as polyhistidine-tag (His-tag), FLAG-tag and c-myc, as well as large polypeptides, including MBP and Glutathione S-transferase (Terpe, 2003). In current study, hexa-histidine tag was fused to C-terminal of all recombinant apoptin. Fusion of tag is important for subsequent protein purification step since immobilized affinity chromatography (IMAC) was chosen as the approach used in the capturing step (to be described in Chapter 5). Yet, instead of increasing yield and solubility of recombinant protein, fusion proteins sometimes also cause unexpected side effects on recombinant proteins, including changes of protein conformation, loss of bioactivity of recombinant proteins and induction of unwanted immunogenic reaction (Chelur *et al.*, 2008). Severe protein degradation was noticed in this study when recombinant apoptin was in fusion to H22 single chain antibody (gene cassettes: PR-H22-CatAd-VP3-HK, PR-H22-CatAd-40-121-VP3-HK, PR-H22-CatAd-60-121-VP3-HK and pGR-D4:: PR-H22-CatAd-80-121-VP3-HK). Hence, careful selection of a suitable fusion protein candidate for the targeted proteins and methods for removal of fusion proteins during purification must be considered.

Other than fusion protein, truncated version of recombinant apoptin was also studied to enhance solubility of protein. Amino acid 29-69 of recombinant MBP-apoptin was reported as multimerisation domain by Leliveld[b] and his colleagues (2003); in addition, amino acids 80-121 and 1-69 on C-terminal of recombinant apoptin in fusion to GFP retained ~50% and 17% of apoptotic activity as induced by the full length GFP-VP3 (Danen-Van Oorschot *et al.*, 2003). Hence, truncated apoptin was generated in this study by removal of short peptide from N-terminal of apoptin. For recombinant EGF-apoptin, it was noted that higher soluble protein was detected when amino acids 1-40 and 1-80 of apoptin were removed but not the removal of amino acid 1-60. Although the inhibition of amino acids 60-80 on the expression of truncated recombinant EGF-apoptin is unclear, presence of unexpected secondary structure might be one of the possible considerations that prevent expression of proteins.

Plant death symptom observed in infiltrated plants was suspected to be related to ER stress. Hence, recombinant apoptin was co-expressed with transcriptional factors, namely bZIP17, bZIP28, and bZIP60, which are always incorporated in stimulating expression of UPR related genes. Up regulation of UPR related genes always leads to increased availability of chaperone proteins (Duwi *et al*., 2013; Vitale, 2013); therefore, more folded and soluble recombinant proteins are expected to be harvested. In current study, co-expression of bZIP60 with apoptin alone (PR-VP3-HK) resulted several folds of higher protein expression and early plant death symptom also did not appear on infiltrated plants. Nevertheless, this did not apply to co-expression of recombinant apoptin with transcriptional factors, bZIP17 and bZIP28. Effect of bZIP proteins towards the expression of recombinant GFP-VP3 and EGF-VP3 proteins also did not contribute any huge changes. Therefore, a combination use of bZIP proteins could be tried in future instead of using a single kind of bZIP protein, which scarcely paved a significant impact to the expression of recombinant apoptin.

Expression profiles of recombinant apoptin variants had shown several suitable candidates used for downstream purification study. For recombinant apoptin expressed alone, recombinant vector, pGR-D4:: VP3-H gave high insoluble protein expression on 7 dpi while recombinant pGR-DN:: PR-VP3-HK yielded high soluble protein from 3-7 dpi (infiltrated plants on 4 dpi were harvested for purification). In addition, recombinant vectors, pGR-D4:: PR-GFP-VP3-HK (7 dpi) and pGR-D4:: GFP-VP3-H (7 dpi) yielded the highest soluble and insoluble recombinant GFP-apoptin, respectively. On the other hand, recombinant vector, pGR-D4:: Lic-VP3-H (7 dpi) yielded the highest insoluble recombinant lichenase-apoptin and recombinant vector, pGR-D4:: PR-EGF-VP3-HK also gave the highest soluble recombinant EGF-apoptin on 5 dpi. All these recombinant vectors generating high expression yield were chosen for subsequent purification study. Expression profiling study in this chapter was carried out for only once for each expression vector; hence, a relative quantification was indicated to compare expression profiles between vectors. Expression yield for selected recombinant apoptin variants was evaluated in protein purification analysis (with 2-3 replicates) and illustrated in Chapter 5.

In conclusion, recombinant apoptin variants have been successfully expressed in *N. benthamiana* via vacuum infiltration of transformed *Agrobacterium* that harboured recombinant vectors into plant cells. Expression profiles and incubation time for accumulation of recombinant apoptin were assessed and several recombinant vectors (Chapter 5) were chosen rationally based on the screening results as discussed above for downstream purification works. Besides, it is noteworthy to mention that apoptin expressed in *N. benthamiana* also retains the intrinsic nuclear localisation activity of protein in plants which might generate an interest for further study in future focusing on the plant death or apoptotic effects of apoptin in plant system.

Chapter 5

Protein Purification of Recombinant Apoptin Extracted from *Nicotiana benthamiana*

Table of Contents

5.1 Introduction

Protein purification is essential for the recovery of recombinant proteins through a series of fractionation procedures by segregating targeted proteins from host cell proteins (HCP). Purification work could not be omitted, unless recombinant proteins were produced in edible hosts or as by-products of expression hosts. For instance, productions of edible vaccine in potato tubers against dengue virus 2 (Kim *et al.,* 2016), oral vaccine in probiotic strain *Lactobacillus* against *Streptococcus pyogenes* M6 antigen (Mansour and Abdelaziz, 2016) and recombinant cytokine (hG-CSF) in milk of goat (Batista *et al*., 2014), are free from purification works and direct consumption is feasible. It is not surprised that protein purification can account for more than 80% of total production cost (Barh, 2013). Hence, a cost-effective purification approach is always required. In fact, it is sometimes more preferably for manufacturers to invest in optimising the upstream process of production in order to enhance protein expression yield when a satisfactory protein purification efficiency has not been achieved. To date, common steps in protein purification include extraction, clarification and fractionation.

The secreted proteins produced in plant expression system could proceed directly to centrifugation and fractionation steps without a pre-requisite extraction work. This approach is highly attractive when high amount of recombinant proteins are secreted with good stability in culture medium of stably transformed plant cell lines or hydroponic plant (Borisjuk *et al*., 1999; James *et al*., 2000; Lee *et al*., 2002). However, extraction or homogenisation is always the first step for the recovery of non-secreted recombinant proteins from host plants. Leaf is the most widely chosen tissue for expression of recombinant proteins, especially the tobacco plant leaf which gives a large volume of biomass. The most common leaf protein extraction method involves mechanical disruption of cells. This could be achieved using pestle and mortar at a laboratory scale or homogeniser at a pilot scale. Alternatively, solid-liquid separation (Wilken and Nikolov, 2012), vacuum infiltration (Kingsbury and McDonald, 2014) and enzyme digestion (Fischer *et al*., 1999) approaches are also applied to isolate recombinant proteins. During the extraction process, huge amounts of unspecific plant products are released including the plant proteins (such as proteases), secondary metabolites, nucleotides, plant viruses and *Agrobacterium*. Hence, a proper formulation of extraction buffer containing appropriate pH, salt concentration, detergents and additives is important to obtain a high recovery of recombinant proteins from plant tissues during the extraction process (Buyel *et al*., 2015).

In order to separate large particulates and precipitates from crude protein extracts, clarification is always performed using high-speed centrifugation and ultrafiltration technique before the protein extracts are subjected for subsequent chromatography based purification procedures (Scopes, 1994). Generally, protein fractionation includes capturing, intermediate and polishing. Various kinds of chromatography or non-chromatography based methods could be combined and applied in these three steps in order to achieve a final product with higher purity. Using chromatography based protein fractionation method; targeted protein could be separated from total protein based on specific protein properties including affinity, charge, hydrophobicity and size of protein (Berg *et al*., 2002). In affinity chromatography, antibody and fusion tag proteins such as FLAG-tag, maltose binding protein (MBP), glutathione S-transferase (GST), polyHis tag, are the most widely used affinity purification tools (GE Healthcare[1], 2016). Affinity chromatography isolates specific protein from total protein pool based on specific interaction between regions on protein and affinity media. This approach is suitable to be used in capturing step of protein purification process and the selective purification allows purity of eluted protein to increase from hundred to thousand folds in majority of cases just within a single step (Urh *et al*., 2009). Owing to the presence of specific net surface charge of a protein in a specific pH range, ion exchange chromatography (IEX) performs a group separation of protein sample by encouraging a reversible binding of charged protein to opposite-charged media. In addition to pH, interaction of protein to media is affected by the ionic strength of buffers since the presence of high concentration of ions is a competitor of bound proteins (GE Healthcare[2], 2016). However, protein binding is enhanced when high concentration of salt is present in the buffer of hydrophobic interaction chromatography (HIC). Protein binding to HIC media is attributed by the suitable hydrophobic interaction; the reverse phase chromatography (RPC) also applies similar principle in the purification process. However, protein is eluted in non-polar organic solvent and usually in denaturing condition since protein is strongly bound to higher concentration of hydrophobic ligands in RPC (GE Healthcare[3], 2016). Application of IEX, HIC and RPC is suitable for group separation of proteins; hence, they are mostly used in capturing step when affinity chromatography is not applicable or used in intermediate step to remove the unwanted contaminants. Size exclusion chromatography (SEC) is always the recommended tool for polishing step in protein purification. Purified protein samples could be easily separated from a small amount of unspecific host protein contaminants based on size difference. On the other hand, non-chromatography based method has been developed rapidly since the costly chromatography based purification is always a huge challenge in the production process of recombinant proteins. Particularly, cross flow filtration, two aqueous phase separation and sucrose gradient purification have successfully developed to recover a large variety of recombinant proteins (Azevedo *et al*., 2009; Biemelt *et al*., 2003; Forman *et al*., 1990).

Expressions of recombinant apoptin alone, green fluorescent protein (GFP)-apoptin, lichenase (Lic)-apoptin and epidermal growth factor (EGF)-apoptin have been analysed and illustrated in details in Chapter 3. In this chapter, protein purification works were carried out on plant leaves infiltrated with recombinant vectors, pGR-D4:: VP3-H, pGR-D4:: PR-GFP-VP3-HK, pGR-D4:: GFP-VP3-H, pGR-D4:: Lic-VP3-H and pGR-D4:: PR-EGF-CatAd-VP3-HK that yielded relatively higher amount of recombinant protein (> 20 mg/kg of total protein). Hexa-histidine sequence was present in all C-terminal of recombinant apoptin; hence, immobilised metal affinity chromatography (IMAC) was chosen as the major capturing tool for the purification works to isolate the recombinant apoptin from total plant proteins. Besides, IEX and HIC were used to remove plant protein contaminants and SEC was performed to elucidate the molecular weight of the purified recombinant apoptin in this study. Hence, the specific objectives for this chapter were (i) to illustrates the purification of recombinant apoptin, GFP-apoptin and EGF-apoptin using IMAC in native and denaturing conditions, (ii) to remove host cell protein from recombinant GFP-apoptin and EGF-apoptin using IEX (HiTap SP) and HIC (Phenyl Sepharose 6TM FF (high sub), HiTrap Butyl Sepharose HP and HiTrap Octyl Sepharose FF) and (iii) to characterise size of recombinant GFP-apoptin using size exclusion chromatography (SEC).

5.2 Materials and Methods

5.2.1 General materials

5.2.1.1 Plant materials

All plant materials used for purification were prepared as described in Chapter 3. Plants infiltrated with recombinant vectors, namely pGR-D4:: VP3-H, pGR-D4:: PR-GFP-VP3-HK, pGR-D4:: GFP-VP3-H and pGR-D4:: Lic-VP3-H were harvested on 7 days post infiltration (dpi), when the infiltrated plants gave the highest protein expression; however, plants infiltrated with recombinant vector, pGR-D4:: PR-EGF-CatAd-VP3-HK were harvested on 5 dpi when the infiltrated plants produced the highest protein yield as discussed in Chapter 4. Approximately 10-100 g of leaf material was used for each purification experiment.

5.2.1.2 Columns and kits

HisTrap HP 1ml and 5 ml columns were used for immobilised metal affinity chromatography (IMAC) (GE Healthcare, USA). HiTrap SP HP 1ml column was used for ion exchange chromatopgraphy (IEX) (GE Healthcare, USA). HiTrap Butyl Sepharose HP 1ml, HiTrap Octyl Sepharose FF 1 ml and Phenyl Sepharose 6^{TM} FF (high sub) columns were used for hydrophobic interaction chromatography (HIC) (GE Healthcare, USA). Analytical Superdex 200 10/300GL column (GE Healthcare, USA) and Sepax SRT SEC 1000 (Sepax Technologies, Inc) column were used for size exclusion chromatography (SEC). Quickfold^{TM} Protein Refolding Kit (Athena Environmental Sciences, Inc) was used to refold recombinant protein. Slide-A-Lyzer™ Dialysis Cassettes (ThermoScientific, USA) were used for buffer exchange and protein refolding activities. Besides, PD-10 desalting columns (GE Healthcare, USA) were also used for buffer exchange of protein sample prior loading into HIC or IEX column. Amicon Ultra-4 and 15 Centrifugal Filter Units were used for concentrating purified protein.

5.2.1.3 Buffers

All buffers components used for protein purification are listed as in Table 5.1.

Table 5.1: Components of buffers.

No	Buffers	Components
1	IMAC Extraction Buffer A	50 mM sodium phosphate, 500 mM sodium chloride, 20 mM imidazole, 1 mM Dieca, pH 8.0, 4°C
2	IMAC Extraction Buffer B	50 mM sodium phosphate, 500 mM sodium chloride, 20 mM imidazole, 0.5% Triton, 1 mM Dieca, pH 8.0, 4°C
3	IMAC Extraction Buffer C	6 M Guanidine hypochlorite, 50 mM sodium phosphate, 500 mM sodium chloride, 20 mM imidazole, pH 8.0, 4°C
4	IMAC Extraction Buffer D	6 M Guanidine hypochlorite, 50 mM sodium phosphate, 500 mM sodium chloride, 20 mM imidazole, 0.5% Triton, pH 8.0, 4°C
5	IMAC Extraction Buffer E	6 M Guanidine hypochlorite, 50 mM sodium phosphate, 500 mM sodium chloride, 2.5 mM imidazole, 20 mM Glycine, 2 mM GSH, pH 7.4, 4°C
6	IMAC Wash Buffer A	50 mM sodium phosphate, 500 mM sodium chloride, 20 mM imidazole, pH 7.5, 4°C
7	IMAC Wash Buffer B	6 M Guanidine hypochlorite, 50 mM sodium phosphate, 500 mM sodium chloride, 20 mM imidazole, pH 7.5, 4°C
8	IMAC Wash Buffer C	50 mM sodium phosphate, 500 mM sodium chloride, 20 mM imidazole, 0.5% Triton, pH 7.5, 4°C
9	IMAC Wash Buffer D	6 M Guanidine hypochlorite, 50 mM sodium phosphate, 500 mM sodium chloride, 20 mM imidazole, 2 mM GSH, pH 7.4, 4°C
10	IMAC Wash Buffer E	50 mM sodium phosphate, 400 mM sodium chloride, 5 mM imidazole, 2 mM GSH, 2 mM $MgCl_2$, pH 6.5, 4°C
11	IMAC Elution Buffer A	50 mM sodium phosphate, 500 mM sodium chloride, 500 mM imidazole, pH 7.5, 4°C
12	IMAC Elution Buffer B	6 M Guanidine hypochlorite, 50 mM sodium phosphate, 500 mM sodium chloride, 500 mM imidazole, pH 7.5, 4°C
13	IMAC Elution Buffer C	50 mM sodium phosphate, 400 mM sodium chloride, 500 mM imidazole, 2 mM GSH, 2 mM $MgCl_2$, pH 6.5, 4°C
14	Storage Buffer A	50mM sodium phosphate, 100mM NaCl, pH 7.5, 4°C
15	Customised Buffer 11	50 mM Tris-Cl, 9.6 mM NaCl, 0.4 mM KCl, 1 mM EDTA, 1 mM DTT, 0.5 % Triton, pH 8.5
16	Customised Buffer 13	50 mM Tris-Cl, 240 mM NaCl, 10 mM KCl, 1 mM EDTA, 1 mM DTT, 500 mM Arginine, 750 mM GuHCl, 0.5 % Triton, pH 8.5
17	HIC Starting Buffer A	50mM sodium phosphate, 0.7 M NaCl, pH 7.5, 4°C
18	HIC Starting Buffer B	50mM sodium phosphate, 1.0 M NaCl, pH 7.5, 4°C
19	HIC Elution Buffer	50mM sodium phosphate, pH 7.5, 4°C
20	IEX Starting Buffer A	50mM sodium phosphate, pH 6.7, 4°C

21	IEX Starting Buffer B	50mM Bicine, pH 9.0, 4°C
22	IEX Starting Buffer C	50mM Bicine, pH 8.5, 4°C
23	IEX Starting Buffer D	50mM sodium phosphate, pH 7.7, 4°C
24	IEX Starting Buffer E	50mM sodium phosphate, pH 8.0, 4°C
25	IEX Starting Buffer F	50mM sodium phosphate, 0.2 M NaCl, pH 8.0, 4°C
26	IEX Elution Buffer A	50mM sodium phosphate, 1M NaCl, pH 6.7, 4°C
27	IEX Elution Buffer B	50mM Bicine, 1M NaCl, pH 9.0, 4°C
28	IEX Elution Buffer C	50mM Bicine, 1M NaCl, pH8.5, 4°C
29	IEX Elution Buffer D	50mM sodium phosphate, 1 M NaCl, pH 7.7, 4°C
30	IEX Elution Buffer E	50mM sodium phosphate, 1 M NaCl, pH 8.0, 4°C

5.2.1.4 Specialised equipment

Akta Purifier (GE Healthcare, USA) was used to perform all protein purification activities. Besides, peristaltic pump (EP-1 Econo Pump) (Biorad, USA) was also used for small scale work. Size exclusion chromatography (SEC) of protein samples were analysed using Agilent 1260 system (Agilent Technologies, USA) and multi-angle light scattering (MALS) was performed using Wyatt HELEOS (Wyatt Technology, USA).

5.2.1.5 Analysis software

Purification performed using Akta Purifier was analysed using Unicorn^{TM} 5.11 (GE Healthcare, USA).

5.2.2 Overview of protein purification study for recombinant apoptin variants

Recombinant GFP-apoptin, namely GFP-VP3-HK (expressed from recombinant vector, pGR-D4:: PR-GFP-VP3-HK), and recombinant EGF-apoptin, namely EGF-VP3-HK (expressed from recombinant vector, pGR-D4:: PR-EGF-CatAd-VP3-HK), yielded ~ 50% of soluble protein. Hence, capturing of recombinant GFP-VP3-HK and EGF-VP3-HK from total plant protein extract was carried out using IMAC (HisTrap HP column) in native condition with or without presence of detergent (such as triton). Size of purified recombinant GFP-VP3-HK was subsequently analysed using Analytical Superdex 200 10/300GL column and SRT SEC-1000 column. However, partial purified recombinant EGF-VP3-HK was further purified using HiTrap SP, HiTrap Butyl Sepharose HP 1ml, HiTrap Octyl Sepharose FF 1 ml and Phenyl Sepharose 6TM FF (high sub) columns.

High amount of recombinant apoptin VP3-H (expressed from vector pGR-D4:: VP3-H), recombinant GFP-apoptin GFP-VP3-H (expressed from vector pGR-D4:: GFP-VP3-H) and recombinant Licchenase-apoptin Lic-VP3-H (expressed from vector pGR-D4:: Lic-VP3-H) were detected in insoluble fraction of plant extracts (Chapter 3). Hence, recombinant VP3-H, GFP-VP3-H and Lic-VP3-H were captured and recovered from total insoluble protein of plant extract using IMAC in denaturing condition. Purified recombinant GFP-VP3-H and Lic-VP3-H were subsequently refolded with phosphate buffer. Protein purification of recombinant apoptin variants was summarized as shown in Table 5.2.

Table 5.2: Protein purification of recombinant apoptin variants.

No	Recombinant vector	Recombinant protein	Protein purification strategy	Purification condition	Purification procedure
1	pGR-D4:: VP3-H	VP3-H	IMAC	Denaturing	5.2.3.2
2	pGR-D4:: PR-GFP-VP3-HK	GFP-VP3-HK	IMAC; SEC	Native	5.2.3.1 and 5.2.8
3	pGR-D4:: GFP-VP3-H	GFP-VP3-H	IMAC	Denaturing	5.2.3.3
4	pGR-D4:: Lic-VP3-H	Lic-VP3-H	IMAC	Denaturing	5.2.3.2
5	pGR-D4:: PR-EGF-CatAd-VP3-HK	EGF-VP3-HK	IMAC; HIC; IEX	Native	5.2.3.1, 5.2.6 and 5.2.7

5.2.3 General immobilised metal affinity chromatography (IMAC) procedures

5.2.3.1 Native condition

Three volumes of Extraction Buffer A (v/w) were added into frozen leaf tissues (~50-100 g) and homogenised. The homogenised leaf extract was mixed by stirring and incubated for 20 minutes at 4°C; subsequently, the extract was pelleted at 16, 000 xg for 30 minutes at 4°C. Supernatant was filtered using miracloth and 0.2 µm polyethersulfone (PES) filter before loaded into column. HisTrap HP column was equilibrated using 5 column volume (CV) of Wash Buffer A, 5 CV of Elution Buffer A and followed by 5 CV of Wash Buffer A. Extract was loaded into column at 5 ml/min for 5 ml column and 1 ml/min for 1 ml column. Subsequently, column was washed with 5 CV of Wash Buffer A and protein was eluted from column in stepwise gradient using 4% (40 mM imidazole), 9% (60 mM imidazole), 60% (300 mM imidazole) and 100% (500 mM imidazole) of Elution Buffer A. Protein samples from each fraction were collected for Western blotting analysis (which was similarly described in Chapter 4, section 4.2.5).

5.2.3.2 Denaturing condition (Protocol 1)

Three volumes of Extraction Buffer B (v/w) were used to homogenise the frozen leaf tissues (~50-100 g). The homogenised leaf extract was stirred and incubated for 20 minutes at 4°C; subsequently, the extract was pelleted at 16, 000 xg for 30 minutes at 4°C. Extraction with Extraction Buffer A was repeated for additional 3 times before pellet was resuspended with 1.5 V of Extraction Buffer C. Protein extract was incubated at 4°C for 20 minutes, subsequently, extract was sonicated (amplitude: 70%) for 4 minutes (20 seconds on and 20 seconds off) before extract was pelleted at 16, 000 xg for 30 minutes at 4°C. Supernatant was filtered using miracloth and 0.2 µm PES filter before loaded into column. HisTrap HP column was equilibrated using 5 CV of Wash Buffer B, 5 CV of Elution Buffer B and followed by 5 CV of Wash Buffer B. Extract was loaded into columns at 5 ml/min and 1 ml/min for 5 ml and 1 ml columns, respectively. Then, column was washed with 5 CV of Wash Buffer B and protein was eluted from column in stepwise gradient using 4% (40 mM imidazole), 9% (60 mM imidazole), 60% (300 mM imidazole) and 100% (500 mM imidazole) of Elution Buffer B. Protein samples collected from each fraction were subjected to Western blotting analysis.

5.2.3.3 Denaturing condition (Protocol 2)

Similar preparation steps of leaf samples were conducted as described in section 5.2.2.2 (Protocol 1) until the soluble protein extract was pelleted. Extraction with Extraction Buffer B was repeated for additional 3 times before extract pellet was resuspended with 1.5 V of Extraction Buffer D. Protein extract was incubated at 4°C for 20 minutes, subsequently, extract was sonicated (amplitude: 70%) for 4 minutes (20 seconds on and 20 seconds off) before extract was pelleted again at 16, 000 xg for 30 minutes at 4°C. Supernatant was filtered using miracloth and 0.2 µm PES filter before the filtrate was diluted at 20X in Extraction Buffer B. Diluent was mixed at 4°C for 20 minutes and followed by filtration using 0.2 µm PES filter. HisTrap HP column was equilibrated using 5 CV of Wash Buffer C, 5 CV of Elution Buffer A and followed by 5 CV of Wash Buffer C. Extract was loaded into 5 ml HisTrap HP overnight. Subsequently, the column was washed with 5-10 CV of Wash Buffer C and 5-10 CV of Wash Buffer A. Protein was eluted from column in stepwise gradient using 4% (40 mM imidazole), 9% (60 mM imidazole), 60% (300 mM imidazole) and 100% (500 mM imidazole) of Elution Buffer A. Protein samples were ready for Western blotting analysis.

5.2.4 Buffer exchange

Purified protein was transferred into Slide-A-Lyzer™ Dialysis Cassettes before incubated in ~100 volumes of storage buffer A or phosphate buffer saline (PBS) (v/v) for at least 4 hours. Incubation was repeated with fresh buffer before protein samples were analysed.

Protein refolding using Quickfold™ Protein Refolding Kit was performed as recommended by manufacturer. Approximately 50 µg of protein was added into 950 µl of buffers (buffers 1-15). Mixtures were vortexed and mixed before incubated at 4°C overnight. Mixtures were centrifuged at 16, 000 xg for 15 minutes and supernatant was analysed using Western blotting.

Buffer of recombinant protein eluted from IMAC was exchanged to starting buffer of hydrophobic interaction chromatography (HIC) or ion exchange chromatography (IEX) before sample was loaded into the HIC or IEX column. Buffer exchange was carried out using PD10 column and gravity flow protocol. PD10 column was initially equilibrated using 25 ml of starting buffer before 2.5 ml of protein sample was added to the column. Flow through from PD10 column was discarded and protein was subsequently eluted using 3.5 ml of starting buffer.

5.2.5 Concentrating protein

Protein was concentrated using Amicon Ultra-4 and 15 Centrifugal Filter Units. Protein sample was centrifuged at 3 000 – 6 000 rpm until a desired volume was remained in the filter unit.

5.2.6 Hydrophobic interaction chromatography (HIC)

HiTrap™ Butyl Sepharose HP 1ml, HiTrap™ Octyl Sepharose FF 1 ml and Phenyl Sepharose 6™ FF (high sub) columns were equilibrated using 5 CV of starting buffer, 5 CV of elution buffer following by 5 CV of starting buffer. Protein sample was loaded into column at 1 ml/min. Subsequently, column was washed and eluted using ~ 3 CV of elution buffer and deionised buffer.

5.2.7 Ion exchange chromatography (IEX)

HiTrap™ SP HP 1ml column was equilibrated using 5 CV of starting buffer, 5 CV of elution buffer followed by 5 CV of starting buffer. Protein sample was loaded into column at 1 ml/min. Subsequently, column was washed and eluted in stepwise gradient using 20%-100% (containing 200 mM NaCl – 1M NaCl) of elution buffer.

5.2.8 Size exclusion chromatography (SEC) and multi-angle light scattering (MALS)

SEC analysis of recombinant GFP-apoptin (GFP-VP3-H) was performed and analysed by Dr Mark Jone and Ms April Horsey (Fraunhofer CMB, USA). Purified protein samples were analysed using SEC SRT-1000 column at flow speed ~1 ml/minute and separated proteins were subsequently analysed using MALS Wyatt HELEOS. SEC-MALS analysis was performed using Storage Buffer A.

5.3 Results

5.3.1 Protein purification of recombinant apoptin using immobilised metal chromatography (IMAC)

5.3.1.1 Purification of recombinant apoptin alone VP3-H

Recombinant apoptin VP3-H expressed alone (without fusion) in plants infiltrated with pGR-D4:: VP3-H (Chapter 4) gave very low amount of soluble protein but with high level of insoluble protein detected. Hence, this recombinant VP3-H was attempted to be purified from insoluble protein extract (IMAC purification in denaturing condition, protocol 1). Total protein (TP) harvested from leaf material yielded ~ 31 mg/kg (Figure 5.1-a: Lane *4*); however, amount of total soluble protein with 0.5% triton (TSP-T) *(*Figure 5.1-a: Lane 5*)* was lower than the detectable range. Extraction of recombinant protein using Extraction buffer C containing high concentration of denaturant (GuHCl) was able to harvest ~ 4 mg/kg (Figure 5.1-a: Lane 6) of protein and only ~ 1.2 mg/kg (30% of recovery) of recombinant apoptin (~ 18 kDa) was able to be recovered from IMAC eluent containing 300 mM imidazole (Figure 5.1-a: Lane 1*1*). Since purified protein was in low amount, no detectable protein was observed on gel stained with coomassie blue (Figure 5.1-b: Lane 16).

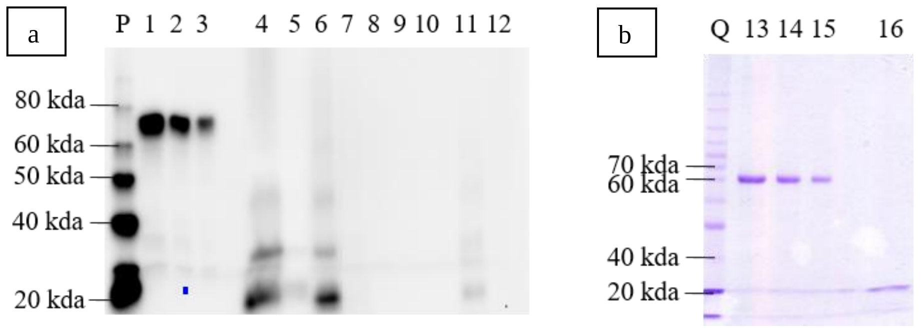

Lane	Sample	Estimated size
P	MagicMark™ XP Western Protein Standard	
Q	Benchmark™ Protein Ladder	
1-3	60 ng, 30 ng and 15 ng of HAI standard	~ 70 kDa
4	TP extract from leaf sample	~ 18 kDa for recombinant VP3-H
5	TSP-T extract from leaf sample	~ 18 kDa for recombinant VP3-H
6	Insoluble protein extract from leaf sample	~ 18 kDa for recombinant VP3-H
7	Flow through fraction from IMAC	~ 18 kDa for recombinant VP3-H
8-12	IMAC eluent containing 20, 40, 60, 300 and 500 mM imidazole	~ 18 kDa for recombinant VP3-H
13-15	0.9, 0.6 and 0.3 mg of BSA protein standard	~ 67 kDa
16	IMAC eluent containing 300 mM imidazole	~ 18 kDa for recombinant VP3-H

Figure 5.1: IMAC protein purification profiles of recombinant apoptin alone VP3-H. (a) Western profiles showed the detection of recombinant apoptin at a molecular size of ~ 18 kDa reacted with Tetra-His mouse monoclonal antibody in each step of IMAC. All sample volume was adjusted to the volume of starting material and subsequently loaded into gel at the same volume for all fractions. (b) SDS-PAGE profiles of coomassie blue-stained protein samples recovered from IMAC eluent containing 300 mM imidazole. No expected protein band (~ 18 kDa) was identified from the gel.

5.3.1.2 Purification of recombinant green fluorescent protein (GFP)-apoptin

Plants infiltrated with recombinant vector, pGR-D4:: PR-GFP-VP3-HK yielded higher soluble protein level in relative to those of recombinant vectors, pGR-D4:: PR-GFP-VP3-H and pGR-D4:: GFP-VP3-H (Chapter 4). Therefore, IMAC was carried out using soluble protein extract from leaves infiltrated with pGR-D4:: PR-GFP-VP3-HK. The TP extract from this GFP-VP3-HK protein was ~ 20 mg/kg (Figure 5.2-a: Lane 4), while total soluble protein (TSP) yielded ~ 9 mg/kg (~ 50% of total protein) (Figure 5.2-a: Lane 5). Approximately 7 mg/kg (~ 80% recovery) of recombinant GFP-VP3-HK was recovered from IMAC eluent containing 300 mM imidazole (Figure 5.2-a: Lane 10 and Figure 5.2-c: Lane 19). Nevertheless, ~ 50 kDa plant protein contaminant was also present in purified recombinant GFP-VP3-HK eluted from IMAC eluent containing 300 mM imidazole (Figure 5.2-c: Lane 19). Hence, an additional step was required to remove the plant protein contaminant.

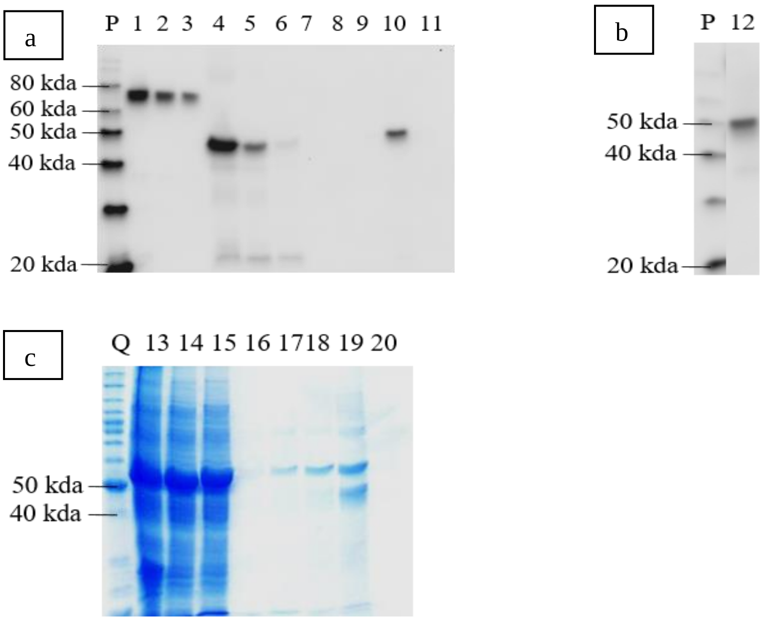

Lane	Sample	Estimated size
P	MagicMark™ XP Western Protein Standard	
Q	Benchmark™ Protein Ladder	
1-3	60 ng, 30 ng and 15 ng of HAI standard	~ 70 kDa
4 and 13	TP extract from leaf sample	~ 45 kDa for recombinant GFP-VP3-HK
5 and 14	TSP extract from leaf sample	~ 45 kDa for recombinant GFP-VP3-HK
6 and 15	Flow through fraction from IMAC	~ 45 kDa for recombinant GFP-VP3-HK
7-11 and 16-20	IMAC eluent containing 20, 40, 60, 300 and 500 mM imidazole	~ 45 kDa for recombinant GFP-VP3-HK
12	IMAC eluent containing 300 mM imidazole	~ 45 kDa for recombinant GFP-VP3-HK

Figure 5.2: IMAC protein purification profiles of recombinant GFP-apoptin (GFP-VP3-HK) in native condition. (a) Western profiles showed the detection of recombinant GFP-apoptin at a molecular size of ~ 45 kDa reacted with Tetra-His mouse monoclonal antibody in each step of IMAC. All sample volume was adjusted to the volume of starting material and subsequently loaded into gel at the same volume for all fractions. (b) Western profiles showed the detection of recombinant GFP-VP3-HK eluted from IMAC eluent containing 300

mM imidazole at a molecular size of ~ 45 kDa reacted with anti-VP3 mouse monoclonal antibody. (c) SDS-PAGE profiles of coomassie blue-stained protein extracts and samples recovered from IMAC fractions. A 50 kDa plant protein was eluted with recombinant GFP-VP3-HK from IMAC eluent containing 300 mM imidazole.

In addition, IMAC of recombinant GFP-VP3-HK was also performed using TSP-T plant extract (9 mg/kg). Low amount of this recombinant protein (~ 13% recovery) was eluted from column if triton was removed during the purification process (Figure 5.3-a). However, higher amount of protein was eluted from column when column was washed and eluted with 0.031% (~ 95% recovery) (Figure 5.3-b) and 0.015% (~ 74% recovery) (Figure 5.3-c) of triton containing elution buffer. However, a high amount of plant protein contaminants was still found in the eluent of recombinant GFP-VP3-HK especially the ~ 50 kDa proteins (Figure 5.3-d).

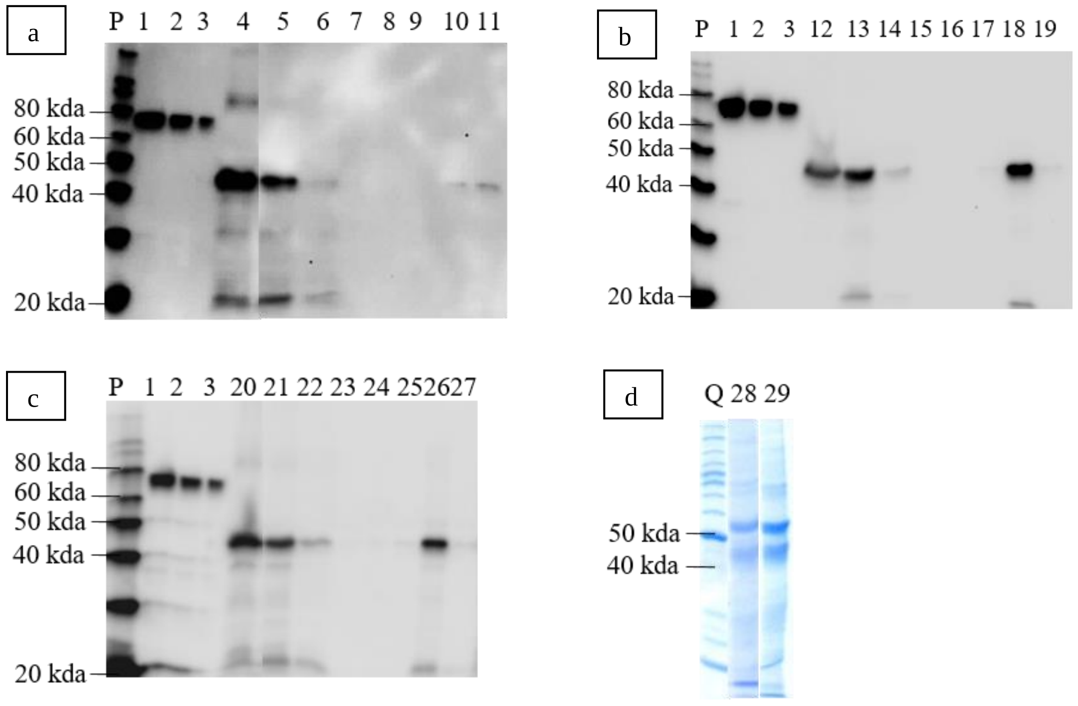

Lane	Sample	Estimated size
P	MagicMark™ XP Western Protein Standard	
Q	Benchmark™ Protein Ladder	
1-3	60 ng, 30 ng and 15 ng of HAI standard	~ 70 kDa
4, 12 and 20	TP extract from leaf sample	~ 45 kDa for recombinant GFP-VP3-HK
5, 13 and 21	TSP-T extract from leaf sample	~ 45 kDa for recombinant GFP-VP3-HK
6, 14 and 22	Flow through fraction from IMAC	~ 45 kDa for recombinant GFP-VP3-HK
7-11	IMAC eluent containing 20, 40, 60, 300 and 500 mM imidazole without triton	~ 45 kDa for recombinant GFP-VP3-HK
15-19	IMAC eluent containing 20, 40, 60, 300 and 500 mM imidazole with 0.031% of triton	~ 45 kDa for recombinant GFP-VP3-HK
23-27	IMAC eluent containing 20, 40, 60, 300 and 500 mM imidazole with 0.015% of triton	~ 45 kDa for recombinant GFP-VP3-HK
28 and 29	IMAC eluent containing 300 mM imidazole with 0.031% and 0.015% of triton	~ 45 kDa for recombinant GFP-VP3-HK

Figure 5.3: IMAC protein purification profiles of recombinant GFP-apoptin (GFP-VP3-HK) in TSP-T extract. All sample volume was adjusted to the volume of starting material and subsequently loaded into gel at the same volume for all fractions tested by using Western blotting. Western profiles showed the detection of recombinant GFP-VP3-HK at a molecular size of ~ 45 kDa reacted with Tetra-His mouse monoclonal antibody in each step of IMAC. (a) Triton was removed from washing and elution buffer. (b) Protein bound in IMAC column was washed and eluted using buffer containing 0.031% of triton. (c) Protein bound in IMAC column was washed and eluted using buffer containing 0.015% of triton. (d) SDS-PAGE profiles of coomassie blue-stained protein samples recovered from IMAC eluent containing 300 mM imidazole with 0.031% and 0.015% of triton. A 50 kDa plant protein was eluted with recombinant GFP-VP3-HK from IMAC eluent.

Instead of purifying recombinant GFP-apoptin in native condition, recombinant GFP-apoptin (GFP-VP3-H) showing high protein expression in insoluble protein fraction was also purified in denaturing condition (protocol 2) using leaf materials infiltrated with recombinant vector, pGR-D4:: GFP-VP3-H (Chapter 4). Insoluble protein extract of GFP-VP3-H was estimated at more than 25 mg/kg (Figure 5.4-a: Lane 2) and ~ 21 mg/kg (> 70% recovery) of recombinant GFP-apoptin was able to be eluted from IMAC eluent containing 500mM imidazole (Figure 5.4-a: Lane 10). Purified recombinant GFP-VP3-H was relatively clean since no major plant protein contaminant band was detected in IMAC eluent (Figure 5.4-c: Lane 18). Purified recombinant GFP-VP3-H was buffer exchanged and concentrated (Figure 5.4-c: Lane 19) and subsequently used for microinjection procedure as described in Chapter 6.

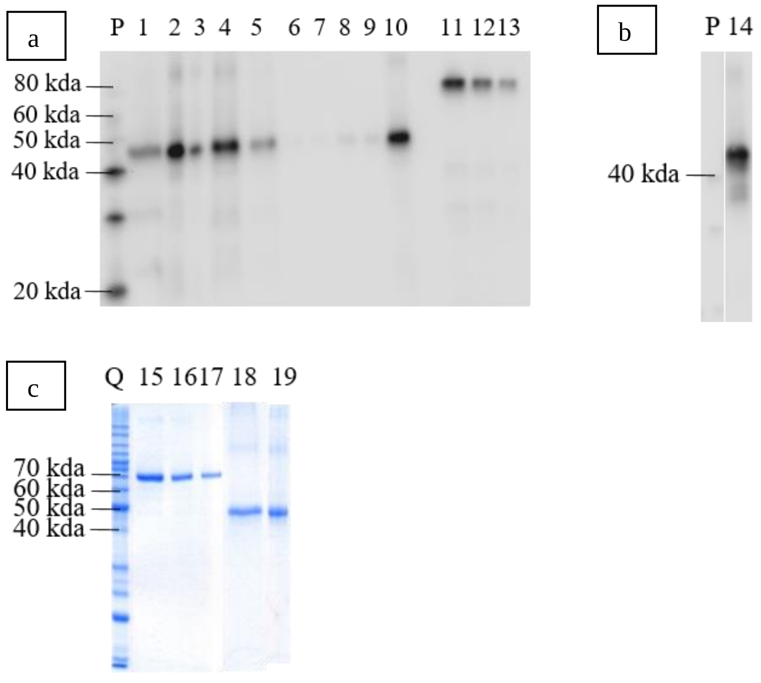

Lane	Sample	Estimated size
P	MagicMark™ XP Western Protein Standard	
Q	Benchmark™ Protein Ladder	
1	TP extract from leaf sample	~ 45 kDa for recombinant GFP-VP3-H
2	Insoluble protein extract from leaf sample using IMAC Extraction Buffer D	~ 45 kDa for recombinant GFP-VP3-H
3	Pellet of leaf sample after insoluble protein extraction	~ 45 kDa for recombinant GFP-VP3-H
4	20X dilution of insoluble protein with IMAC Extraction Buffer B	~ 45 kDa for recombinant GFP-VP3-H
5	Flow through fraction from IMAC	~ 45 kDa for recombinant GFP-VP3-H
6	IMAC column washed using IMAC Wash Buffer C	~ 45 kDa for recombinant GFP-VP3-H
7-10	IMAC eluent containing 20, 40, 60 and 500 mM imidazole using IMAC Elution Buffer A	~ 45 kDa for recombinant GFP-VP3-H
11-13	60 ng, 30 ng and 15 ng of HAI standard	~ 70 kDa
14 and 18	IMAC eluent containing 500 mM imidazole	~ 45 kDa for recombinant GFP-VP3-H

15-17	0.9, 0.6 and 0.3 mg of BSA protein standard	~ 67 kDa
19	Buffer exchanged recombinant GFP-apoptin in storage buffer A	~ 45 kDa for recombinant GFP-VP3-H

Figure 5.4: IMAC protein purification profiles of recombinant GFP-apoptin (GFP-VP3-H) in denaturing condition. (a) Western profiles showed the detection of recombinant GFP-VP3-H at a molecular size of ~ 45 kDa reacted with Tetra-His mouse monoclonal antibody in each step of IMAC. All sample volume was adjusted to the volume of starting material and subsequently loaded into gel at the same volume for all fractions. (b) Western profiles showed the recombinant GFP-VP3-H eluted in IMAC eluent containing 300 mM imidazole was detected at a molecular size of ~ 45 kDa by using anti-VP3 mouse monoclonal antibody. (c) SDS-PAGE profiles of coomassie blue-stained protein samples recovered from IMAC eluent containing 300 mM imidazole and buffer exchanged. No major plant protein contaminant band was detected in IMAC eluent.

5.3.1.3 Purification of recombinant lichenase (Lic)-apoptin

IMAC was performed in denaturing condition (protocol 1) using leaves infiltrated with recombinant vector, pGR-D4:: Lic-VP3-H since high expression level of insoluble protein (~ 40 mg/kg) (Figure 5.5-a and b: Lane 6 and 17) was detected (Chapter 4). Approximately 20 mg/kg of recombinant Lic-apoptin (Lic-VP3-H) (Figure 5.5-a and b: Lane 11 and 22) was recovered from IMAC column with 50% of protein did not bind to column which resembled ~50% recovery (Figure 5.5-a and b: Lane 7 and 18). A clear band of recombinant Lic-VP3-H was identified in gel stained using coomasssie blue and no major plant protein contaminant band was detected in IMAC eluent (Figure 5.5-b: Lane 22). Protein was precipitated when IMAC eluent was buffer exchanged with PBS buffer (Figure 5.5-a and b: Lane 13, 14, 24 and 25). Using refolding kit, recombinant Lic-VP3-H did not precipitate in buffer 11 and 13 (Figure 5.5-c: Lane 27 and 28); however, removal of triton from buffer 11 and 13 caused a protein precipitation (Figure 5.5-c: Lane 31 and 32).

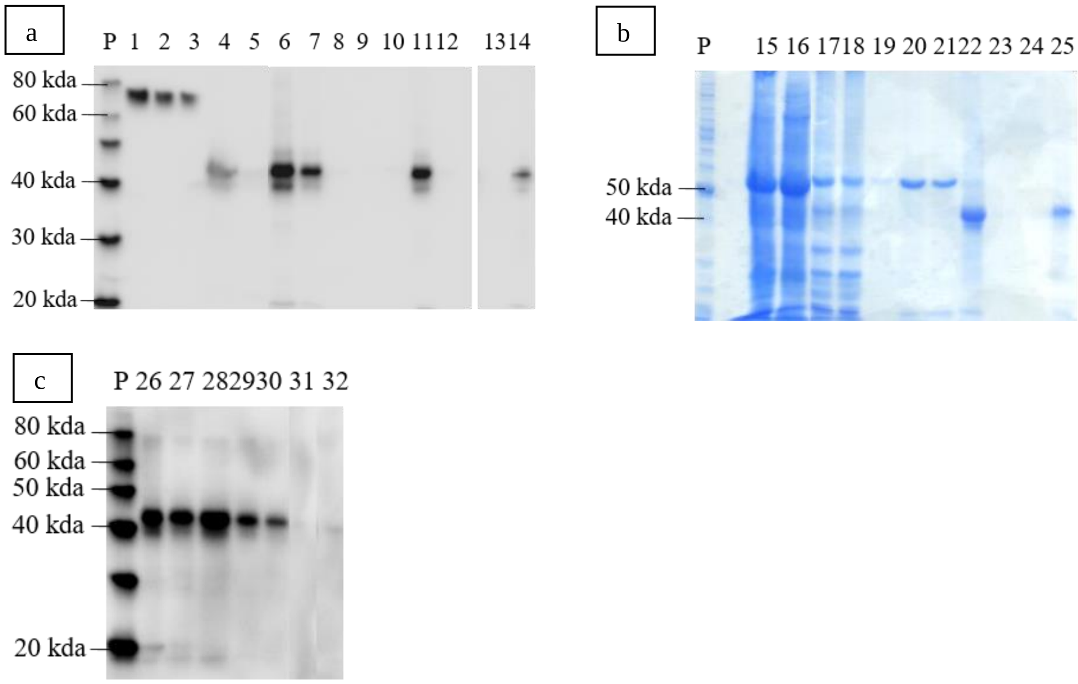

Lane	Sample	Estimated size
P	MagicMark™ XP Western Protein Standard	
Q	Benchmark™ Protein Ladder	
1-3	60 ng, 30 ng and 15 ng of HAI standard	~ 70 kDa
4 and 15	TP extract from leaf sample	~ 40 kDa for recombinant Lic-VP3-H
5 and 16	TSP-T extract from leaf sample	~ 40 kDa for recombinant Lic-VP3-H
6 and 17	Insoluble protein extract from leaf sample	~ 40 kDa for recombinant Lic-VP3-H
7 and 18	Flow through fraction from IMAC	~ 40 kDa for recombinant Lic-VP3-H
8-12 and 19-23	IMAC eluent containing 20, 40, 60, 300 and 500 mM imidazole	~ 40 kDa for recombinant Lic-VP3-H
13 and 24	Dialysis against PBS (Supernatant)	~ 40 kDa for recombinant Lic-VP3-H
14 and 25	Dialysis against PBS (Pellet)	~ 40 kDa for recombinant Lic-

		VP3-H
26	IMAC Eluent containing 300 mM imidazole	~ 40 kDa for recombinant Lic-VP3-H
27	Refolded protein using Quickfold Buffer 11	~ 40 kDa for recombinant Lic-VP3-H
28	Refolded protein using Quickfold Buffer 13	~ 40 kDa for recombinant Lic-VP3-H
29	Refolded protein using customised Buffer 11	~ 40 kDa for recombinant Lic-VP3-H
30	Refolded protein using customised Buffer 13	~ 40 kDa for recombinant Lic-VP3-H
31	Refolded protein using customised Buffer 11 without triton	~ 40 kDa for recombinant Lic-VP3-H
32	Refolded protein using customised Buffer 13 without triton	~ 40 kDa for recombinant Lic-VP3-H

Figure 5.5: IMAC protein purification profiles of recombinant Lic-apoptin (Lic-VP3-H) in denaturing condition. (a) Western profiles showed the detection of recombinant Lic-VP3-H at a molecular size of ~ 40 kDa reacted with Tetra-His mouse monoclonal antibody in each step of IMAC. All sample volume was adjusted to the volume of starting material and subsequently loaded into gel at the same volume for all fractions. (b) SDS-PAGE profiles of coomassie blue-stained protein samples recovered from each step of IMAC. No major plant protein contaminant band was detected in IMAC eluent. (c) Western profiles of recombinant Lic-VP3-H refolding from IMAC eluent containing 300 mM imidazole using Quickfold refolding kit and customised buffers. Bands of ~ 40 kDa Lic-VP3-H reacted with Tetra-His mouse monoclonal antibody were detected.

Other than performing buffer exchange after IMAC, high concentration of denaturant was also removed when protein was binding in IMAC column using IMAC Wash Buffer D and IMAC Wash Buffer E. In comparison to the purification in complete denaturing condition, only 16% of Lic-VP3-H (Figure 5.6-a: Lane 10 and 11) was able to be recovered in IMAC using this method.

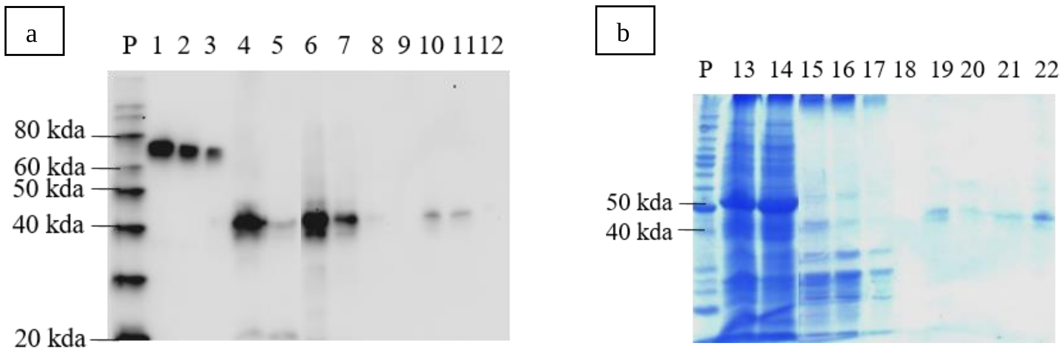

Lane	Sample	Estimated size
P	MagicMark™ XP Western Protein Standard	
Q	Benchmark™ Protein Ladder	
1-3	60 ng, 30 ng and 15 ng of HAI standard	~ 70 kDa
4 and 13	TP extract from leaf sample	~ 40 kDa for recombinant Lic-VP3-H
5 and 14	TSP-T extract from leaf sample	~ 40 kDa for recombinant Lic-VP3-H
6 and 15	Insoluble protein extract from leaf sample using IMAC Extraction Buffer E	~ 40 kDa for recombinant Lic-VP3-H
7 and 16	Flow through fraction from IMAC using	~ 40 kDa for recombinant Lic-VP3-H
8 and 17	IMAC column washed using IMAC Wash Buffer D	~ 40 kDa for recombinant Lic-VP3-H
9 and 18	IMAC column washed using IMAC Wash Buffer E	~ 40 kDa for recombinant Lic-VP3-H
10-11 and 19-20	IMAC eluent containing 500 mM imidazole	~ 40 kDa for recombinant Lic-VP3-H
12 and 21	Dialysis supernatant	~ 40 kDa for recombinant Lic-VP3-H
22	Dialysis (pellet)	~ 40 kDa for recombinant Lic-VP3-H

Figure 5.6: IMAC protein purification profiles of recombinant Lic-VP3-H in denaturing condition. (a) Western profiles showed the detection of recombinant Lic-VP3-H at a molecular size of ~ 40 kDa reacted with Tetra-His mouse monoclonal antibody in each step of IMAC. All sample volume was adjusted to the volume of starting material and subsequently loaded into gel at the same volume for all fractions. (b) SDS-PAGE profiles of coomassie blue-stained protein samples recovered from each step of IMAC. No major plant protein contaminant band was detected in IMAC eluent.

5.3.1.4 Purification of recombinant epidermal growth factor (EGF)-apoptin

TP extract of recombinant EGF-apoptin (EGF-VP3-HK) from leaves infiltrated with pGR-D4:: PR-EGF-CatAd-VP3-HK was ~ 29 mg.kg (Figure 5.7-a: Lane 4) and ~ 8-11 mg/kg of TSP was detected (Figure 5.7-a: Lane 5). However, only ~ 3-4 mg/kg of recombinant EGF-VP3-HK was detected in IMAC eluent (Figure 5.7-a: Lane 10 and 12) and huge amount of plant protein contaminant (especially 50 kDa plant protein) was detected in the IMAC eluent (Figure 5.7-b: Lane 16).

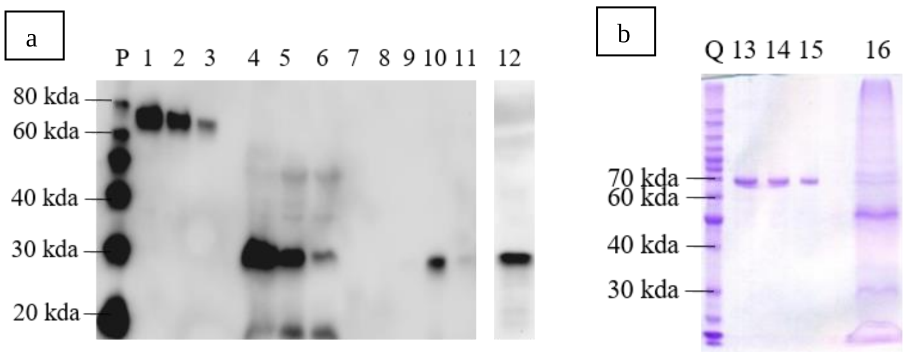

Lane	Sample	Estimated size
P	MagicMark™ XP Western Protein Standard	
Q	Benchmark™ Protein Ladder	
1-3	60 ng, 30 ng and 15 ng of HAI standard	~ 70 kDa
4	TP extract from leaf sample	~ 30 kDa for recombinant EGF-VP3-H
5	TSP extract from leaf sample	~ 30 kDa for recombinant EGF-VP3-H
6	Flow through fraction from IMAC column	~ 30 kDa for recombinant EGF-VP3-H
7-11	IMAC eluent containing 20, 40, 60, 300 and 500 mM imidazole	~ 30 kDa for recombinant EGF-VP3-H
12 and 16	IMAC eluent containing 300 mM imidazole	~ 30 kDa for recombinant EGF-VP3-H
13-15	0.9, 0.6 and 0.3 mg of BSA protein standard	~ 67 kDa

Figure 5.7: IMAC protein purification profiles of recombinant EGF-apoptin (EGF-VP3-HK) in native condition. (a) Western profiles showed the detection of recombinant EGF-VP3-HK at a molecular size of ~ 30 kDa reacted with Tetra-His (Lane 1-11) and anti-VP3 (Lane 12) mouse monoclonal antibodies in each step of IMAC. All sample volume was adjusted to the volume of starting material and subsequently loaded into gel at the same volume for all fractions. (b) SDS-PAGE profiles of coomassie blue-stained protein samples recovered from IMAC eluent containing 300 mM imidazole. A 50 kDa plant protein was eluted with recombinant EGF-VP3-HK from IMAC eluent.

Purified recombinant EGF-VP3-HK in IMAC eluent containing 300 mM imidazole was eluted with huge amount of ~ 50 kDa plant protein contaminant. Hence, IMAC was performed again on IMAC eluent in order to remove the impurities. It was noticed that additional IMAC purification step did not improve the purity of recombinant EGF-apoptin and only 37% of protein was able to be recovered from samples loaded into the IMAC column (Figure 5.8-a and -b: Lane 9 and 18).

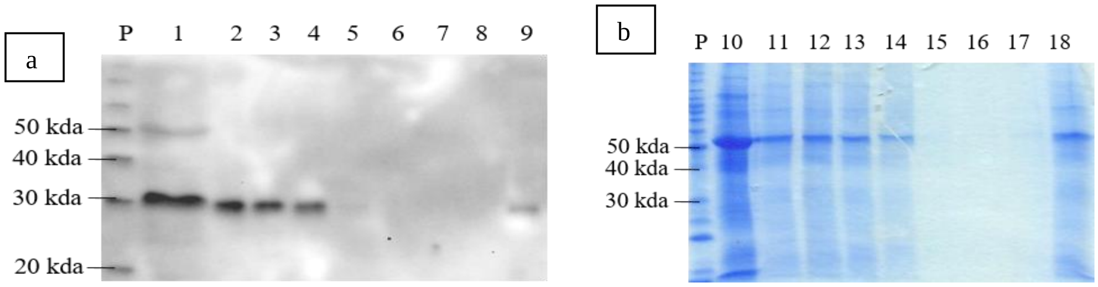

Lane	Sample	Estimated size
P	MagicMark™ XP Western Protein Standard	
Q	Benchmark™ Protein Ladder	
1 and 10	TSP extract from leaf sample	~ 30 kDa for recombinant EGF-VP3-H
2 and 11	IMAC eluent containing 300 mM imidazole	~ 30 kDa for recombinant EGF-VP3-H
3 and 12	Supernatant of IMAC eluent after centrifuged at 40, 000 xg	~ 30 kDa for recombinant EGF-VP3-H
4 and 13	Buffer exchange of IMAC eluent buffer containing 300 mM imidazole to IMAC Extraction Buffer A	~ 30 kDa for recombinant EGF-VP3-H
5 and 14	Flow through fraction from IMAC	~ 30 kDa for recombinant EGF-VP3-H
6-9 and 15-18	IMAC eluent containing 20, 40, 60 and 500 mM imidazole	~ 30 kDa for recombinant EGF-VP3-H

Figure 5.8: IMAC protein purification profiles of recombinant EGF-apoptin (EGF-VP3-HK) in native condition. (a) Western profiles showed the detection of recombinant EGF-VP3-HK at a molecular size of ~ 30 kDa reacted with anti-VP3 mouse monoclonal antibody in each step of IMAC. All sample volume was adjusted to the volume of starting material and subsequently loaded into gel at the same volume for all fractions. (b) SDS-PAGE profiles of coomassie blue-stained protein samples recovered from each step of IMAC. A plant protein

(50 kDa) was the major plant protein contaminant eluted with recombinant EGF-VP3-HK from IMAC eluent.

5.3.2 Improvement for protein purity

5.3.2.1 Hydrophobic interaction chromatography (HIC)

In addition to IMAC, partial purified recombinant EGF-apoptin (EGF-VP3-HK) was further separated from plant protein impurities using HIC and IEX. Using HIC, EGF-VP3-HK bound tightly to HIC mediums, including Phenyl Sepharose 6^{TM} FF (high sub), HiTrap^{TM} Butyl Sepharose HP and HiTrap^{TM} Octyl Sepharose FF, and protein was not able to be recovered from mediums (Figure 5.9-a, -b and -c: Lane 6, 11 and 17).

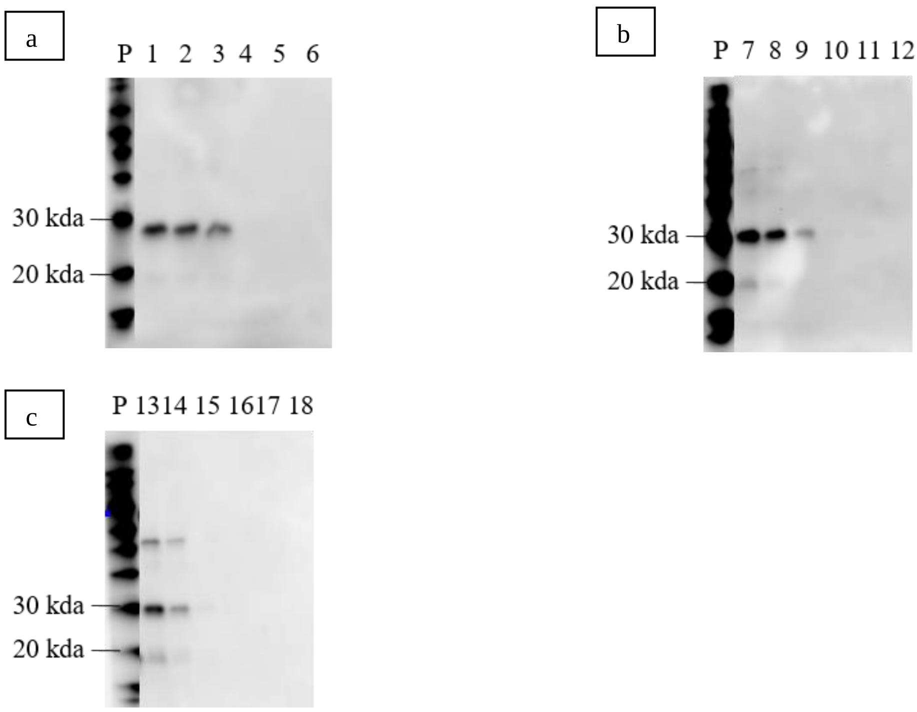

Lane	Sample	Estimated size
P	MagicMark™ XP Western Protein Standard	
Q	Benchmark^{TM} Protein Ladder	
1, 7 and 13	IMAC eluent containing 300 mM imidazole	~ 30 kDa for recombinant EGF-VP3-H
2	Supernatant of IMAC eluent after centrifuged at 40, 000 xg	~ 30 kDa for recombinant EGF-VP3-H
3	Buffer exchange IMAC eluent to HIC Starting Buffer A	~ 30 kDa for recombinant EGF-VP3-H
4	Flow through fraction from Phenyl Sepharose 6^{TM} FF (high sub)	~ 30 kDa for recombinant EGF-VP3-H
5	Phenyl Sepharose 6^{TM} FF (high sub) medium washed using HIC Starting Buffer A	~ 30 kDa for recombinant EGF-VP3-H
6	Phenyl Sepharose 6^{TM} FF (high sub) medium eluted using HIC Elution Buffer	~ 30 kDa for recombinant EGF-VP3-H

8 and 14	Buffer exchange IMAC eluent to HIC Starting Buffer B	~ 30 kDa for recombinant EGF-VP3-H
9	Flow through fraction from HiTrap Butyl Sepharose HP column	~ 30 kDa for recombinant EGF-VP3-H
10	HiTrap Butyl Sepharose HP column washed using HIC Starting Buffer B	~ 30 kDa for recombinant EGF-VP3-H
11	HiTrap Butyl Sepharose HP column eluted using HIC Elution Buffer	~ 30 kDa for recombinant EGF-VP3-H
12	HiTrap Butyl Sepharose HP column eluted using deionised water	~ 30 kDa for recombinant EGF-VP3-H
15	Flow through fraction from HiTrap Octyl Sepharose FF column	~ 30 kDa for recombinant EGF-VP3-H
16	HiTrap Octyl Sepharose FF column washed using HIC Starting Buffer B	~ 30 kDa for recombinant EGF-VP3-H
17	HiTrap Octyl Sepharose FF column eluted using HIC Elution Buffer	~ 30 kDa for recombinant EGF-VP3-H
18	HiTrap Octyl Sepharose FF column eluted using deionised water	~ 30 kDa for recombinant EGF-VP3-H

Figure 5.9: HIC protein purification profiles of recombinant EGF-apoptin (EGF-VP3-HK) in native condition. All sample volume was adjusted to the volume of starting material and subsequently loaded into gel at the same volume for all fractions. Western profiles showed the detection of recombinant EGF-apoptin at a molecular size of ~ 30 kDa reacted with anti-VP3 mouse monoclonal antibody in each step of HIC using (a) Phenyl Sepharose 6TM FF (high sub) column, (b) HiTrap Butyl Sepharose HP column and (c) HiTrap Octyl Sepharose FF column. No protein was successfully eluted from these columns using respective elution buffers.

5.3.2.2 Ion exchange chromatography (IEX)

Isoelectric point of recombinant EGF-apoptin (EGF-VP3-HK) was estimated as ~ pH 7.7. Using cationic exchanger HiTrap SP column, positively charged recombinant EGF-VP3-HK bound column tightly and protein was not able to be eluted from column (Figure 5.10-a: Lane 5-9) when chromatography was performed at pH 6.7. In contrast, when IEX was performed at pH 9.0, most of the protein was able to be eluted from column (Figure 5.10-b: Lane 18) and small amount of protein was detected in the flow through fraction (Figure 5.10-b: Lane 16). When IEX was performed at pH 8.5, approximately 35% of loaded recombinant EGF-

VP3-HK was eluted in fraction using buffer containing 0.4 M of sodium chloride (Figure 5.10-c: Lane 25). However, this approach did not successfully remove plant protein contaminants from the partial purified products (Figure 5.10-c: Lane 28).

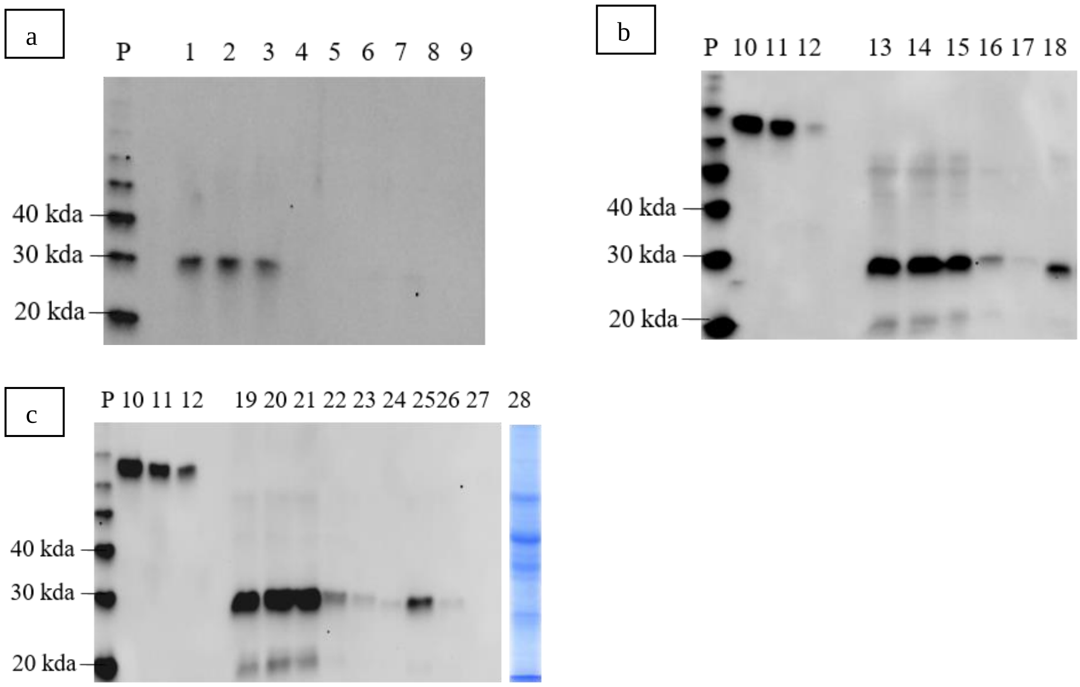

Lane	Sample	Estimated size
P	MagicMark™ XP Western Protein Standard	
1, 13 and 19	IMAC eluent containing 300 mM imidazole	~ 30 kDa for recombinant EGF-VP3-H
2, 14 and 20	Supernatant of IMAC eluent after centrifuged at 40, 000 xg	~ 30 kDa for recombinant EGF-VP3-H
3	Buffer exchange of IMAC eluent containing 300 mM imidazole to IEX Starting Buffer A	~ 30 kDa for recombinant EGF-VP3-H
4	Flow through fraction from HiTrap SP column	~ 30 kDa for recombinant EGF-VP3-H
5-9	Eluent containing 0.2, 0.4, 0.6, 0.8 and 1 M NaCl from HiTrap SP column using IEX Elution Buffer A	~ 30 kDa for recombinant EGF-VP3-H
10-12	60 ng, 30 ng and 15 ng of HAI standard	~ 70 kDa
15	Buffer exchange of IMAC eluent containing 300 mM imidazole sample to IEX Starting Buffer B	~ 30 kDa for recombinant EGF-VP3-H

16	Flow through fraction from HiTrap SP column	~ 30 kDa for recombinant EGF-VP3-H
17	HiTrap SP column washed using IEX Starting Buffer B	~ 30 kDa for recombinant EGF-VP3-H
18	HiTrap SP column eluted using IEX Starting Buffer B	~ 30 kDa for recombinant EGF-VP3-H
21	Buffer exchange of IMAC Eluent containing 300 mM imidazole sample to IEX Starting Buffer C	~ 30 kDa for recombinant EGF-VP3-H
22	Flow through fraction from HiTrap SP column	~ 30 kDa for recombinant EGF-VP3-H
23	HiTrap SP column washed using IEX Starting Buffer C	~ 30 kDa for recombinant EGF-VP3-H
24-27	Eluent containing 0.2, 0.4, 0.6 and 0.8 M NaCl from HiTrap SP column using IEX Elution Buffer C	~ 30 kDa for recombinant EGF-VP3-H
28	Eluent containing 0.4 M NaCl	~ 30 kDa for recombinant EGF-VP3-H

Figure 5.10: IEX protein purification profiles of recombinant EGF-apoptin (EGF-VP3-HK) in native condition using 1 ml HiTrap^{TM} SP column. All sample volume was adjusted to the volume of starting material and subsequently loaded in the same volume for all fractions. (a) Western profiles showed the detection of recombinant EGF-apoptin at a molecular size of ~ 30 kDa reacted with anti-VP3 mouse monoclonal antibody (Lane 1-9) in each step of IEX performed at pH 6.7. Western profiles showed the detection of recombinant EGF-VP3-HK at a molecular size of ~ 30 kDa reacted with Tetra-His mouse monoclonal antibody in each step of IEX performed at (b) pH 9.0 and (c) pH 8.5.

5.3.3 Characterisation of recombinant GFP-apoptin

In gel filtration analysis, recombinant GFP-apoptin (GFP-VP3-H), always separated as ~ 45 kDa protein molecule in reduced SDS page (Figure 5.4), did not migrate as monomer when analysed using SRT SEC1000 column in Storage Buffer A. In SEC analysis, GFP-VP3-H (~ 0.75 mg/ml) migrated as a single peak at 10 ml with a small shoulder ~ 10.7 ml (Figure 5.11-a). Majority of these protein molecules showed a similar molecular mass, which was ~ 944.3 kDa (size estimation based on normalisation of BSA from Zenix C 300 column) (Figure 5.11-b).

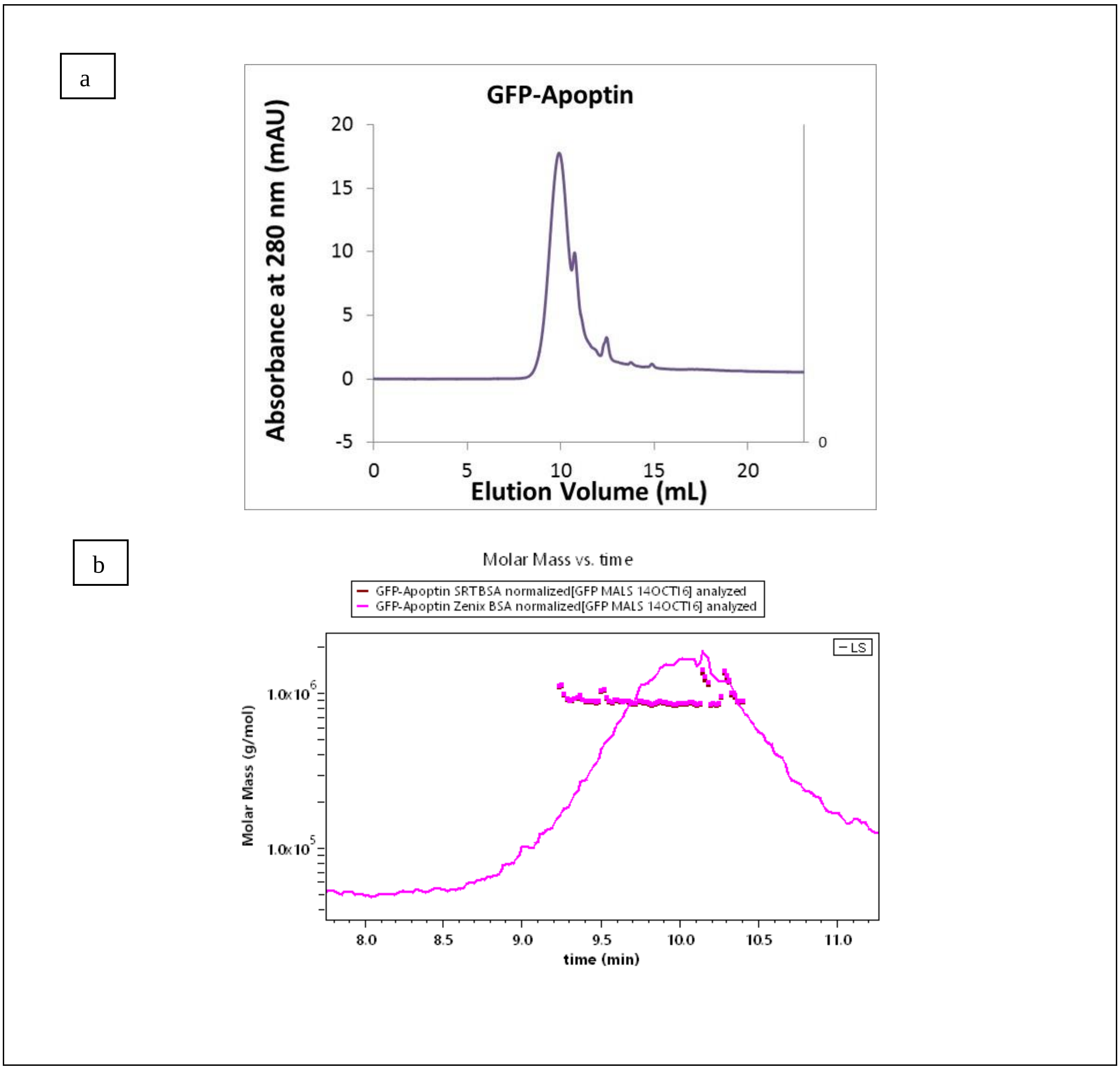

Figure 5.11: SEC-MALS analysis of recombinant GFP-apoptin. (a) SEC of recombinant GFP-VP3-H using SRT SEC1000 column in Storage Buffer A yielded a single peak at 10 ml and a shoulder at 10.7 ml. (b) MALS analysis of recombinant GFP-VP3-H immediately after SEC. Majority of the proteins showed a similar molecular mass of ~ 944. 3 kDa (size estimation based on normalisation of BSA from Zenix C 300 column).

5.4 Discussion

In this chapter, a detailed description was provided on the study of downstream processing of recombinant apoptin alone (without fusion, VP3-H), GFP-apoptin (GFP-VP3-HK and GFP-VP3-H), Lichenase-apoptin (Lic-VP3-H) as well as EGF-apoptin (EGF-VP3-HK). The purified recombinant proteins obtained from this study would be used for subsequent cell-based assays. At the beginning, hexa-histidine sequence was added to C-terminal end of all recombinant apoptin which aimed to employ immobilised affinity chromatography (IMAC) as the major purification approach. Owing to the selective binding of IMAC resin to histidine tags which are present on the protein surface, IMAC is widely used in capturing step of purification process to recover the targeted proteins as well as eliminate majority of unspecific host proteins. IMAC was performed in both denaturing and native conditions in this study based on the solubility of the recombinant proteins.

Expression of recombinant apoptin alone (VP3-H) procured the highest protein yield as compared to those leaves infiltrated with recombinant vectors, i.e. pGR-D4:: PR-VP3-HK and pGR-D4:: PR-VP3-H. Protein purification was however performed in denaturing condition using high concentration of denaturants, guanidine hypochloride (GuHCl) because majority of protein was found in insoluble state. In fact, insoluble recombinant apoptin alone was not extracted efficiently from leaf materials even with the use of high concentration of denaturants. Therefore, alternative buffering systems or additional additives might be necessary to enhance the recovery of protein during extraction process, such as sugars, salt, reducing agents, detergents and chaotropic agents (Leibly *et al.*, 2012). According to the IMAC, only 30% recombinant apoptin was able to be recovered and this resulted low amount of purified protein (~ 1.2 mg/kg) harvested (section 5.3.1). Based on protein expression profiles in Chapter 4, soluble recombinant apoptin was detected in higher quantity (~ 4 mg/kg) when leaf was infiltrated with pGR-DN:: PR-VP3-HK__bZIP60 compared to pGR-DN:: PR-VP3-HK__bZIP17, pGR-DN:: PR-VP3-HK__bZIP28, pGR-D4:: PR-VP3-HK, pGR-D4:: PR-VP3-H and pGR-D4:: VP3-H. However, IMAC purification performed using 50 g leaf materials infiltrated with recombinant vector, pGR-DN:: PR-VP3-HK__bZIP60 yielded low amount of purified protein (< 1 mg/kg) (Appendix 5.1). Purification of recombinant apoptin alone has been reported by Leliveld[a] and his colleague (2003) from *Escherichia coli* expression system. High amount (~ 40 mg/L of culture) of recombinant apoptin in fusion to hexa-histidine tag was recovered using two-step chromatographic process, i.e. cation exchange chromatography following by Ni^{2+}-NTA-agarose in denaturing condition. It was reported that only 50% of protein refolded efficiently and protein migrated as single species at 400 ± 50 kDa on Superose 6 HR 10/30. Although small amount (2 mg/L of culture) of soluble recombinant apoptin alone was obtained in the previous study of Nogueira-Dantas *et al.* (2007), majority of the recombinant apoptin was remained in the bacterial inclusion body which could only be recovered using high-concentration denaturant containing buffer or in bacterial pellet. In relative to *E. coli* system, expression yield of recombinant apoptin was low in plant system obtained in this study. Nevertheless, recombinant apoptin alone was found accumulating in insoluble protein fraction either in *E. coli* or *Nicotiana benthamiana* expression system.

In contrast to recombinant apoptin alone, expression of soluble recombinant apoptin was detected upon fusion to green fluorescent protein (GFP), especially GFP-VP3-HK which yielded 50% soluble protein (~ 9-10 mg/kg). IMAC recovered 80% of GFP-apoptin from total soluble protein extract (Figure 5.2). However, a ~ 50 kDa plant protein, which might be Rubisco was detected in purified recombinant GFP-apoptin eluent. Removal of host cell proteins from tobacco extract (especially Rubisco protein) has always been a major issue encountered in downstream processing of recombinant proteins (Buyel *et al.*, 2015). In order to remove host cell protein, chromatography (Kittur *et al.*, 2015) and acidic precipitation methods (adjusting protein extract to ~ pH 5) are the commonly used method. Application of polishing step using ion exchange chromatography (IEX) HiTrap SP column was not efficient to remove the unspecific plant proteins (Appendix 5.2). It is noted that most plant host cell proteins always have low pI value (Azzoni *et al.*, 2002). Therefore, as long as the targeted recombinant proteins are stable in acidic condition, a lower pH nearing pI of host cell proteins could be adjusted in order to precipitate these unspecific contaminating proteins. However, the recombinant GFP-apoptin was found precipitated at acidic condition (Appendix 5.4) as well. Therefore, using either cationic exchange chromatography HiTrap SP column or low pH precipitation method was not ideal to remove these unwanted host cell proteins. When triton was added to extraction buffer, yield of soluble protein of recombinant GFP-apoptin was not increased. Triton (MW= 625 Da) is a kind of non-ionic surfactant used for disruption of cell membrane during extraction process. However, huge micelle size (MW= 90 kDa) of triton disabled the surfactant to be removed via dialysis approach from the final purified product. Hence, it is always encouraged to remove triton during the purification process. However, it was also observed that removal of triton during purification caused protein precipitation in the column and a minimum of ~ 0.015% triton was required to avoid the precipitation occurrence (Figure 5.3). Instead of solely purifying recombinant GFP-apoptin from soluble protein fraction, the insoluble fraction of GFP-VP3-H protein harvested was also purified using IMAC. Insoluble recombinant GFP-apoptin was isolated using extraction buffer containing strong denaturant (GuHCl) and triton. The denatured recombinant protein could be refolded and diluted for 20 times in buffer without denaturants but in the presence of triton prior loading into IMAC column (section 5.2.3.3 – Denaturing protocol 2) (Figure 5.4). Recombinant GFP-VP3-H purified using this strategy showed a higher recovery yield and lower amount of unspecific plant protein contaminants. In addition, refolding efficiency of protein via this method was believed to be higher than that of protein purified under denaturing condition with subsequent refolding process (section 5.2.3.2 – Denaturing protocol 1) (Appendix 5.3). This could be explained as protein was concentrated after purification process and low refolding efficiency always obtained at high protein concentration. Aggregation usually arose due to hydrogen bond formation between protein chains of partially folded intermediate that close to each other in high protein concentration (Gupta *et al*., 1998). So far, no membrane penetrating domain was detected on either apoptin or GFP. Therefore, external delivery tools would be required to transfer the protein into intracellular space of mammalian cells in order to examine for the bioactivity of purified protein. In this circumstance, the presence of surfactants (such as triton) or chemicals (such as GuHCl) used for protein purification would threaten the viability of mammalian cells. Hence, all these chemicals were removed from the final product before the protein sample was used for cell-based assay as illustrated in Chapter 6.

Refolded GFP-apoptin (GFP-VP3H) analysed using SEC-MALS showed the protein owed a multimeric structure (~ 944.3 kDa) instead of presence as a monomer (~ 45 kDa). Majority of GFP-VP3-H proteins were from a single population composed of approximately 20 units of monomer. Multimerisation of recombinant apoptin was also shown in the study of Leliveld[a] *et al.* (2003) for purified recombinant MBP-apoptin and refolded apoptin from *E. coli* expression system. Results showed that ~ 30-40 monomers of recombinant MBP-apoptin (monomer: 56 kDa) assembled into multimeric form as 2.5 ± 0.3 MDa in size (Leliveld[b] *et al*., 2003); while ~ 27 monomers of refolded apoptin (monomer: 14.5 kDa) assembled into 400 ± 50 kDa mutimers. In addition, MBP-apoptin was presented as globular particles with a radius of ± 40 nm under scanning electron microscope in a uniform population. Recombinant

MBP-apoptin and apoptin protein molecules could be broken down into monomer with SDS (similar as recombinant GFP-apoptin); therefore, interaction of apoptin molecules is believed to be non-covalently linked.

Purification of recombinant Lic-apoptin (Lic-VP3-H) was performed under denaturing condition and refolding of protein required the presence of triton (Figure 5.5). Besides, refolding of recombinant protein in IMAC column showed poor protein yield in IMAC eluent (Figure 5.6). Although IMAC purified recombinant Lic-apoptin showed high purity in this study, refolding process of protein did not work as expected. On the other hand, IMAC purification of recombinant EGF-apoptin (EGF-VP3-HK) in native condition showed poor yield (~3-4 mg/kg) and low purity. Besides, polishing chromatography using IMAC, HIC, IEX and acidic precipitation method (Appendix 5.4) also did not improve the situation. Recombinant EGF-apoptin yielded ~ 50 % of soluble protein, so, by starting purification from insoluble protein fraction would loss half of the protein amount. Hence, IMAC purification from denaturing condition had been performed from total protein of recombinant EGF-apoptin extract (Appendix 5.5). Unfortunately, the contaminating host cell proteins (especially ~ 50 kDa) were detected in IMAC eluent (Appendix 5.5).

Based on the current observations, recombinant apoptin purified in native condition (recombinant GFP-VP3-HK and EGF-VP3-HK) was always encountered with challenges of having host protein contaminants in the final purified products. The low ratio of recombinant apoptin to total protein pool with the initial attribution of low expression level is suspected to be one of the reasons that affect the selectivity of IMAC resin. Currently, IMAC was performed using nickel ion and other immobilized metal ions, such as copper, zinc and cobalt, could also be used to recover recombinant apoptin in future study. IMAC performed in denaturing condition (recombinant GFP-VP3-H and Lic-VP3-H) always required several washing steps with soluble protein extraction buffer (such as IMAC Extraction Buffer A) in the presence of triton before the recombinant apoptin was extracted from pellet using insoluble protein extraction buffer containing high concentration of strong denaturants. These washing steps are imperative to remove huge amount of soluble host cell proteins in addition to increase the ratio of recombinant apoptin to protein pool in the protein extract. Thus, a higher purity of recombinant apoptin could be detected in IMAC eluent. Instead of using IMAC, other affinity chromatography methods could be considered in the future.

It is known from previous studies that fusion of recombinant apoptin to other large protein would increase its solubility, stability as well as expression yield. Hence, large fusion tag proteins, such as maltose binding proten (MBP) and glutathione S-transferase (GST), are the favorable choices. In the study of Lee *et al*. (2012), recombinant GST-TAT-apoptin was 10-fold higher in expression quantity in relation to recombinant Histidine-TAT-apoptin. Besides, Lee *et al*. (2003) also showed soluble recombinant MBP-apoptin was 2.5-fold higher expression level in relation to the recombinant apoptin-histidine that was present in inclusion body. Fusion of either MBP or GST to recombinant EGF-apoptin would be one of the solutions in order to recover this protein more efficiently. Numerous approaches are available for downstream processing and yet, a suitable purification protocol can be found only after attempting various combinations of purification strategies.

In conclusion, a few protein purification protocols of recombinant apoptin extracted from tobacco leaf materials were attempted and further study might be required to enhance purification efficiency in future. Based on current findings, recombinant apoptin alone (VP3-H), GFP-apoptin (GFP-VP3-HK) and Lichenase apoptin (Lic-VP3-H) did not yield good purity or promising amount of purified proteins. On the other way, good purity of refolded GFP-apoptin (GFP-VP3-H) was collected at ~ 2 mg/ml. Although purification of recombinant EGF-apoptin (EGF-VP3-HK) did not yield high purity in the final product, this purified protein was still tested in subsequent cell-based study. Recombinant EGF-apoptin was expected to be selectively internalised into EGF overexpressed cell via endocytosis after the binding of recombinant protein to EGF receptors and passed through plasma membrane via the CatAd molecular adaptor. Hence, refolded GFP-apoptin and IMAC purified EGF-apoptin were used for cell-based study to determine the bioactivity of both plant expressed apoptin in mammalian cells.

Chapter 6

Evaluation of bioactivity of recombinant apoptin in human lung cancer cells

Table of Contents

6.1 Introduction

Viral protein 3 (VP3) from Chicken Anemia Virus (CAV) is responsible for the destruction of lymphocytes during viral infection by induction of apoptosis; hence, the protein was named “apoptin” (Los *et al*., 2009). Apoptin is a 14 kDa non-structural protein. There is a leucine rich region, resides between amino acids 33-46, and a bipartite nuclear localization signal (NLS), resides between amino acids 82-88 and 111-121. Apoptin showed selective killing activity towards ~ 70 cancer or transformed cell lines including breast cancer, osteosarcoma, lung carcinoma, hepatoma, SV-40 transformed fibroblast and adenovirus-5-transformed embryonal retinoblasts (Noteborn *et al*., 2008). However, apoptosis was usually not induced by apoptin in normal and non-transformed cells such as human umbilical cord vascular endothelial cells (HUVEC), smooth muscle (HSM), primary T cells and rat embryo fibroblasts (REF) (Danen-van Oorschot *et al*., 1997; Noteborn *et al*., 2008). Apoptin-induced apoptosis is independent of p53 (Zhuang *et al*., 1995) and involves mitochondria-mediated apoptotic pathway by loss of mitochondrial membrane potential (MMP), releasing of cytochrome *c* and activation of caspase 3 (Danen-van Oorschot *et al*., 2000). Currently, cell killing ability of apoptin was tested in various cancer cell lines as well as in mice using various kinds of delivery method including viral vectors, bacteria (*Salmonella typhimurium*), intratumoral injection, electroporation and cell penetrating peptides (such as trans-activator protein (TAT) from human immunodeficiency virus (HIV) or protein transduction domain 4 (PTD4)) (Rollano Peñaloza *et al*., 2014).

Apoptosis, also named as programmed cell death, is one of the cell death mechanisms that plays role in various kinds of cellular activities such as cell number controlling (Hall *et al*., 1994), elimination of self-reactive lymphocytes (Parijs *et al*., 1998) and cellular stresses (induced by irradiation or drugs) leading to cellular DNA damage (Enoch and Norbury, 1995) as well as senescence. Regulated apoptosis is crucial since excess activity of apoptosis caused atrophy and defective in apoptosis results the progression of cancer. Round in shape, shrink, smaller in size and losing contact with neighbouring cells, chromatin condensation, DNA fragmentation and formation of apoptotic bodies are the several features observed during apoptosis (Walker *et al*., 1994). Apoptosis is induced through extrinsic (cell death receptor) or intrinsic (mitochondria) pathway. Apoptosis induced by extrinsic pathway involves activation of receptors located on plasma membrane such as TNF-R (tumour necrosis factor receptor) and Fas receptor (Ashkenazi, 2008). On the other hand, intrinsic pathway is induced by the loss of mitochondrial membrane potential, releasing of cytochrome *c* and formation of apoptosome (Elmore, 2007). Triggering of apoptotic pathway eventually leads to the activation of caspases that are important for the degradation of cellular proteins in apoptotic cells, activation of other cellular proteins involved in apoptosis and DNA fragmentation (McIlwain *et al.*, 2013).

The lipophilic feature of plasma membrane restrains the direct transport of biomolecules, hence, macromolecules (such as DNA, RNA and proteins) and micromolecules (such as ions and organic molecules) could not freely pass through the membrane without involving a specific transport mechanism. In order to determine bioactivity of pharmacological drugs, delivery of these compounds into intracellular space or specific cellular compartment is always a challenge with low risk of damage or toxic effect towards the tested cell lines or animals. Currently, there are two major categories of delivery methods including invasive approach (such as microinjection and electroporation) and non-invasive approach (such as liposomes, nanoparticles and cell penetrating peptides). Microinjection is a precise delivery method for single cell transduction with high transduction efficiency. Microinjection has lower cytotoxicity in relative to chemical transfection and it is feasible for the transduction of cells with difficulty in transfection (Zhang and Yu, 2008). However, microinjection requires specialised equipment as well as involves sophisticated and laborious techniques to deliver exogenous biomolecules into the cells. Currently, this technique is always used for developmental biology, neurobiology, cell biology, and signal transduction (Carroll, 2009). Cell penetrating peptides (CPPs) or peptide transfer domains (PTD) are short peptides that facilitate entry of macromolecules or drugs (such as DNA, RNA or proteins) through the plasma membrane into intracellular space. Mechanisms of internalisation for these CPPs include endocytosis, direct translocation, inverted micelle formation and pore formation (Bechara and Sagan, 2013). Most of these CPPs are low toxicity and less immunogenic and these peptides have been used for intestinal delivery of insulin, cell immunity, cancer therapy and enzyme replacement (Dinca *et al.*, 2016). A molecular adaptor, catAd, was a cell penetrating peptide composes of membrane transfer sequence (MTS), cytosolic cleavable unit (CCU) and endosomal cleavable unit (ECU). Cell specific ligands or antibodies were linked to adaptor to increase the selectiveness of the drugs binding to targeted cells. Drug molecules (toxins or proteins) bound to the adaptor were endocytosed into cells and subsequently transferred through plasma membrane via the MTS sequence from the adaptor. Drug molecules were then released into cell cytosol by the cleavage of CCU. This adaptor was used for the delivery of immunotoxins, such as diphtheria toxin (Keller *et al*., 2001), saporin (Fuchs *et al*., 2007; Heisler *et al*., 2003) and human angiogenin (Hetzel *et al*., 2008).

In this chapter, bioactivity of purified recombinant GFP-apoptin (GFP-VP3-H) and recombinant EGF-apoptin (EGF-VP3-HK) was tested in human lung carcinoma A549. In the absence of cell penetrating peptides on recombinant GFP-VP3-H, the purified protein was delivered into A549 cells using microinjection approach. Viability of cells injected with recombinant GFP-VP3-H was determined by checking the morphology of cell nucleus. However, recombinant EGF-VP3-HK was directly added into culture medium since this protein contained molecular adaptor harbouring a membrane transfer peptide. Translational fusion of apoptin with EGF (EGF-VP3-HK) was expected to target the recombinant protein towards EGF receptors (EGFR) that are overexpressed at lung cancer cell surface. Therefore, the binding activity of recombinant EGF-VP3-HK to EGFR was determined using enzyme-linked immunosorbent assay (ELISA). Viability of cells treated with recombinant EGF-VP3-HK was quantified by checking the cleavage of tetrazolium salt WST-1 to formazan by mitochondrial dehydrogenases which are present in viable cells. Besides, loss of mitochondrial membrane potential and activation of caspase 3/7 which are among the hallmarks of apoptosis were determined in cells receiving individual treatments of recombinant apoptin (GFP-VP3-H and EGF-VP3-HK).

Therefore, the specific objectives of this chapter were: (i) to examine the interactions between the respective recombinant apoptin (GFP-VP3-H and EGF-VP3-HK) and A549 cells as well as EGF receptors; (ii) to deliver recombinant GFP and GFP-VP3-H into A549 cells via microinjection; (iii) to investigate the cellular activities including cell killing, nuclear localisation and apoptosis potential of recombinant GFP-VP3-H in A549 cells; (iv) to examine the internalisation of recombinant EGF-VP3-HK into A549 cells; and (v) to evaluate cell killing efficiency and apoptosis potential of recombinant EGF-VP3-HK in A549 cells.

6.2 Materials and Methods

6.2.1 General materials

6.2.1.1 Cells and cell culture reagents

Human lung adenocarcinoma epithelial cell A549 (ATCC® CCL-185™) (American Type Cell Collection –ATCC) was used for the assessment of bioactivity of recombinant apoptin purified using method as described in Chapter 5. A549 cell line was maintained in F-12 Ham medium without phenol red (Sigma Aldrich, USA), supplemented with 10% fetal bovine serum (FBS), 0.29 mg/ml L-glutamine, 1.5 mg/L sodium bicarbonate and antibiotic solutions (100 IU penicillin and 100 µg/ml streptomycin) (Corning, USA).

6.2.1.2 Protein samples

Recombinant GFP-apoptin (GFP-VP3-H) was prepared as described in Chapter 5 (section 5.3.1.2) and recombinant EGF-apoptin (EGF-VP3-HK) was prepared as described in Chapter 5 (section 5.3.1.4). Recombinant GFP-apoptin was buffer exchanged to Storage buffer A (50 mM sodium phosphate, 100 mM NaCl, pH 7.5, 4°C) and concentrated to 2.4 mg/ml. Small aliquots of protein was prepared and stored at -80°C. Recombinant GFP (19 mg/ml) was prepared using immobilised affinity chromatography (IMAC) by Dr Konstantin Musiychuk (Fraunhofer CMB, USA). Recombinant GFP was diluted to 2.5 mg/ml using Storage buffer A and small aliquots were stored at -80°C.

6.2.1.3 Reagents and injection consumables

For microinjection, femtotips II (Eppendorf, USA), microloader tips (Eppendorf, USA), 35 mm collagen coated glass bottom dish (No. 1.5 Coverslip, 14 mm Glass Diameter) (Matek Corporation, USA), dextran conjugated fluorescein (70 000 MW) Anionic (Thermo scientific, USA) and lysine fixable dextran conjugated texas red (10 000 MW) (Thermo Scientific, USA) were used in this study. Propidium iodide (PI) with RNase (ThermoScientific, USA), SYB Green I for nuclei acid stain and ready to used 200 µg/ml hoechst 33342 (Immunochemistry Technologies LLC, USA) were used for staining of cell nucleus. Mouse monoclonal VP3 antibody (JCU/CAV/1C1) (1: 200) (TropBio Pty Ltd, Australia), rabbit polyclonal anti-GFP antibody (1: 250) (Invitrogen), rhodamine (TRITC) affiniPure goat anti-mouse IgG (H+L) (1:100) (Jackson Immunoresearch Laboratories Inc, USA) and anti-rabbit conjugated FITC (1:100) were used for immunofluorescence (IF) assay. Human EGFR/HER1/ErbB1 protein (His tag) (100001-H08H, Sino Biological Inc, China), rabbit monoclonal antibody to human EGFR/ErbB/HER1 (10001-R021, Sino Biological Inc, China), Epidermal growth factor (EGF) recombinant protein (RP-10914, ThermoScientific, USA), human EGF Monoclonal antibody (M806, ThermoScientific, USA), Peroxidase AffiniPure Goat Anti-Mouse IgG (H+L) (Jackson Immunoresearch Laboratories Inc, USA), peroxidase affiniPure Goat Anti-Rabbit IgG (H+L) (Jackson Immunoresearch Laboratories Inc, USA) and sigma Fast OPD (Sigma-Aldrich, USA) were used for enzyme-linked immunosorbent assay (ELISA). slowFade® diamond antifade mountant (ThermoScientific, USA) was used to mount cell samples used for microscopic examination. Cell proliferation reagent WST-1 (Roche Applied Science, USA) was used to measure viability of cultures. MitoPT TMRM assay kit (Immunochemistry Technologies, USA) and magic red caspase 3 & 7 assay kit were used to analyse depolarization of mitochondrial membrane potential and caspase activity of apoptin-treated cell samples.

6.2.1.4 Specialised equipment

Nikon Instruments Eclipse Ti-E inverted microscope and Zeiss Observer Z1 microscope and Zeiss LSM 510 META highspeed confocal microscope were used for microscopic imaging of cell samples. FemtoJet pressure unit (Eppendorf, USA), three-axis coarse positioning micromanipulator MMN-1 (Narishige, USA) and three-axis joystick type oil hydraulic fine micromanipulator MMO-202ND (Narishige, USA) were the microinjection system used to deliver recombinant GFP and GFP-apoptin into mammalian A549 cells. Inverted microscope Axiovert 40°C (Zeiss) was used for visualising cells during microinjection. Molecular Devices MPR-100 SpectraMax M2 was used to collect absorbance for ELISA and cell viability assay.

6.2.1.5 Bioinformatics and statistical analysis

Photos taken by Nikon Eclipse Ti Inverted Microscope were analysed using Nikon NIS Elements (Nikon Instruments Inc, USA); while, photos taken by Zeiss 5 Live DUO Highspeed Confocal Microscope were analysed using Zeiss LSM 5 (Zeiss, USA). Data collected from cell viability assay and enzyme-linked immunosorbent assay (ELISA) were plotted using four parameter fitting model from Microsoft Excel.

6.2.2 Enzyme-linked immunosorbent assay (ELISA)

A549 cells were seeded at 0.8 X 10^4 cells/ well on 96-wells plate and incubated at 37°C overnight. ELISA plates were also coated with 2.5 mg/ml of human EGFR/HER1/ErbB1 protein at 4ºC for 24 hours. A549 cells were fixed with 1% formaldehyde for 10 minutes, methanol for 5 minutes and 80% acetone for 2 minutes (Zhang *et al.*, 2003). Fixed cells as well as coated ELISA plates were blocked using 0.5% I-block buffer (dissolved in PBST-T) for at least an hour. Recombinant EGF-apoptin (EGF-VP3-HK), GFP-apoptin (GFP-VP3-H) and recombinant GFP were incubated with fixed A549 cells or pre-coated ELISA plates at room temperature for at least an hour. Samples were then washed for 6 times with 1 X PBS buffer. Primary antibodies (Table 6.1) were added to samples and incubated for another hour. Samples were washed for 6 times with 1 X PBS buffer and followed by incubation with secondary antibodies (Figure 6.1) for an hour. Again, samples were washed similarly as abovementioned. Subsequently, 90 µl of Sigma Fast OPD was added to each well of samples and incubated at room temperature in dark for 20-30 minutes. Reactions were then stopped by adding 10 µl 5 M of sulphuric acid (H_2SO_4) and absorbance was taken at 492 nm. Absorbance for each sample was normalised with negative control to eliminate unspecific binding caused by rabbit polyclonal anti-GFP antibody or mouse monoclonal VP3 antibody.

Table 6.1: List of antibodies used in ELISA.

No	Protein samples	Incubation with primary antibodies and amount used in ELISA	Incubation with secondary antibodies and amount used in ELISA
1	Recombinant GFP	Rabbit polyclonal anti-GFP antibody (1 µg/ml)	Peroxidase AffiniPure Goat Anti-Rabbit IgG (H+L) (1: 25 000)
2	Recombinant GFP-VP3-H	Rabbit polyclonal anti-GFP antibody (1 µg/ml)	Peroxidase AffiniPure Goat Anti-Rabbit IgG (H+L) (1: 25 000)
3	Recombinant GFP-VP3-H	Mouse monoclonal VP3 antibody (1: 10 000)	Peroxidase AffiniPure Goat Anti-Mouse IgG (H+L) (1: 7 500)
4	Recombinant EGF-VP3-HK	Mouse monoclonal VP3 antibody (1: 10 000)	Peroxidase AffiniPure Goat Anti-Mouse IgG (H+L) (1: 7 500)

6.2.3 Microinjection procedures

A549 cells were seeded on coverslip at 40-50% confluency a day (preferable incubation for at least 24 hours) before microinjection. Protein samples (2.5 mg/ml recombinant GFP or ~ 0.8-1.0 mg/ml GFP-VP3-H) were prepared as described in section 6.2.1.2. Ideally, protein concentration ~ 3 mg/ml was recommended for microinjection work; however, concentration of recombinant GFP-VP3-H (~ 0.8-1.0 mg/ml) is the maximum protein concentration could be obtained in current study. For the identification of injected cells, protein samples were prepared with 2 mg/ml of dextran conjugated fluorescein (70 000 MW) Anionic or lysine fixable dextran conjugated texas red (10 000 MW). Injection mixtures were centrifuged at 15 000 xg for 20 minutes immediately before microinjection to eliminate precipitates that might clog the opening of microinjection capillary. Approximately 3.5 μl of mixtures were transferred to microloader tips in order to load samples into femtotips II. Femtotips II loaded with protein mixture was then incubated vertically at room temperature for 1-2 minutes for capillary reaction to fill the tip with protein sample. Air bubbles trapped in the liquid sample within the capillary should be removed with a gentle tap before pushing sample out from the capillary into a fresh PBS buffer using a pre-set <clean> function of microinjector at maximum pressure. Culture was replaced with fresh medium prior microinjection. Microinjection parameters were optimised by observing the condition of the cells which were microinjected with recombinant GFP. Thereafter, both recombinant GFP and GFP-VP3-H were delivered into cells by using microinjection pressure at 100 hPa and injection time for 1s. Approximately 50-100 cells were injected for each sample. Culture was replaced with fresh medium again immediately after the microinjection procedure.

6.2.4 Indirect immunofluorescence (IF) assay

The A549 cells receiving microinjection (GFP-VP3-H) and recombinant EGF-VP3-HK were washed for 3 times with 1X PBS buffer before cells were fixed with 1% formaldehyde for 10 minutes, methanol for 5 minutes and 80% acetone for 2 minutes (Zhang *et al.*, 2003). Fixed cell samples were blocked using 0.5% I-block buffer (dissolved in PBST-T) for at least an hour before samples were incubated with primary antibody (Table 6.2) for another hour. Subsequently, cells were washed for 3 times with 1X PBS-T buffer (5 minutes interval). Cells were then incubated with secondary antibody (Table 6.2) for an hour following by the same 3-time washing step with 1X PBS-T buffer. Eventually, cell nucleus was stained using nuclear staining dye (Hoechst, PI or SYB Green). Nuclei of detected cells were stained using PI (for cells microinjected with recombinant GFP) and SYB Green (for cells microinjected with recombinant GFP-VP3-H). The mounted samples were viewed and images were captured. For cells microinjected with recombinant GFP and GFP-VP3-H, all detected cells were counted to quantify for the detection and survival rate of cells.

Table 6.2: List of antibodies used in IF.

No	Cell samples	Incubation with primary antibodies and amount used in IF	Incubation with secondary antibodies and amount used in IF
1	Cells microinjected with recombinant GFP-VP3-H	Mouse monoclonal VP3 antibody (1: 250)	Rhodamine (TRITC) affiniPure Goat Anti-Mouse IgG (H+L) (1:100)
2	Cells incubated with recombinant EGF-VP3-HK	Mouse monoclonal VP3 antibody (1: 250)	Rhodamine (TRITC) affiniPure Goat Anti-Mouse IgG (H+L) (1:100)
3	Cells incubated with recombinant EGF-VP3-HK	Rabbit monoclonal antibody to human EGFR/ErbB/HER1 (10 µg/ml)	Anti-rabbit conjugated FITC (1:100)

6.2.5 Cell Proliferation Reagent WST-1 assay

A549 cells were seeded at 0.8 x 10^4 cells/ well (96-well plates) in 100 µl of culture medium a day before the experiment. Recombinant EGF-VP3-HK (330-3000 nM) and recombinant EGF (0.15-15 000 nM) were incubated separately with A549 cells (3 replicates for each samples) for 72 hours before 10 µl of cell proliferation reagent WST-1 was added into each well of cell samples. Cell and reagent mixtures were incubated for ~ 1.5-2 hours. Samples were gently shaken before absorbance was measured at 420 nm. Cell viability of cells incubated with recombinant EGF-VP3-HK and recombinant EGF was calculated in relative to untreated cells (reflected as 100% of viable cells). Cell viability of recombinant EGF-VP3-HK and recombinant EGF was then plotted using four parameter fitting model from Microsoft Excel.

6.2.6 Mitochondrial membrane potential assay (MMP)

Mitochondrial membrane is polarised when it is intact. Polarised mitochondrial membrane is negative charged within mitochondria and positive charged at the outer region. Loss of mitochondrial membrane potential is always caused by the depolarisation of charges or damage of mitochondrial membrane, which can occur in cells that are undergoing stress or apoptosis. Cell permeant, positively charged and lipophilic TMRM dye accumulates in mitochondria of normal cells and hence red fluorescence will be observed. However, red fluorescence is diminished as the membrane of mitochondria becomes permeable or depolarised in apoptotic or stressed cells. The charged reagent does not accumulate in mitochondria but disperses in the cytoplasm. The redistribution of this reagents causes the significant drop of signal; thus, red fluorescent signal will no longer be observed.

In order to assess the MMP, microinjection was performed on every cells located within a grid. On the other hand, MMP test was performed on recombinant EGF-VP3-HK treated A549 cells using 3030 nM of recombinant protein. Cells microinjected with recombinant GFP and GFP-VP3-H as well as cells incubated with recombinant EGF and recombinant EGF-VP3-HK were washed for 3 times with PBS buffer before samples were incubated with 200 nM of MitoPT assay TMRM reagent for 15-20 minutes at 37°C in dark. Cell samples were washed for 3 times with PBS buffer before image of samples were captured using Nikon Eclipse Ti inverted microscope.

6.2.7 Caspase 3/7 assay

Activation of caspase is also a hallmark for apoptosis. Evaluation for activity of caspase could be assessed by examining cleaving activity of caspases (such as caspase 3) towards targeted amino acid aspartate-glutamate-valine-aspartate, $(z\text{-DEVD})_2$ peptide. Cell permeant magicred caspase-3/7 reagent is DEVD-based caspase substrate coupled with cresyl violet fluorophore. Upon the cleavage of DEVD targeted sequence by caspase, the active fluorophores will be released and more intense fluorescent signal is observed after the cleavage. Hence, elevated amount of caspases in cells could be assessed by the elevation of the fluorescent signal.

In order to assess the caspases activity, microinjection was performed on every cells located within a grid. On the other hand, caspases activity was performed on recombinant EGF-VP3-HK treated A549 cells using 3030 nM of recombinant protein. Cells microinjected with recombinant GFP and GFP-VP3-H as well as cells incubated with recombinant EGF and recombinant EGF-VP3-HK were washed for 3 times with PBS buffer before samples were incubated with magicred caspase-3/7 reagent (1:150) for 60 minutes at 37°C. Then, cell samples were rinsed twice with PBS buffer (1 minute per rinse) before images were captured using Nikon Eclipse Ti inverted microscope.

6.3 Results

6.3.1 Evaluation for the interaction of recombinant apoptin (GFP-VP3-H and EGF-VP3-HK), A549 cells and EGF receptors

Epidermal growth factor receptors (EGFR) were overexpressed on cell surface of A549 cells; hence, A549 cells and recombinant EGF receptors were used to determine the specific binding efficiency of recombinant apoptin (GFP-VP3-H and EGF-VP3-HK). Serving as a control, recombinant GFP did not bind to EGF receptors (dark green line) but it bound to A549 cells (light green line) at very low efficiency (Figure 6.1). Recombinant GFP-VP3-H bound to Human EGF receptors (red lines) as well as A549 cells (purple lines) (Figure 6.1). Binding of recombinant GFP-VP3-H to A549 cells was steadily higher than that of Human EGF receptors as reacted with both antibodies. Besides, detection levels of recombinant GFP-VP3-H using rabbit polyclonal anti-GFP antibody (dark purple and dark red) were shown higher than those of mouse monoclonal VP3 antibody (blue and pink).

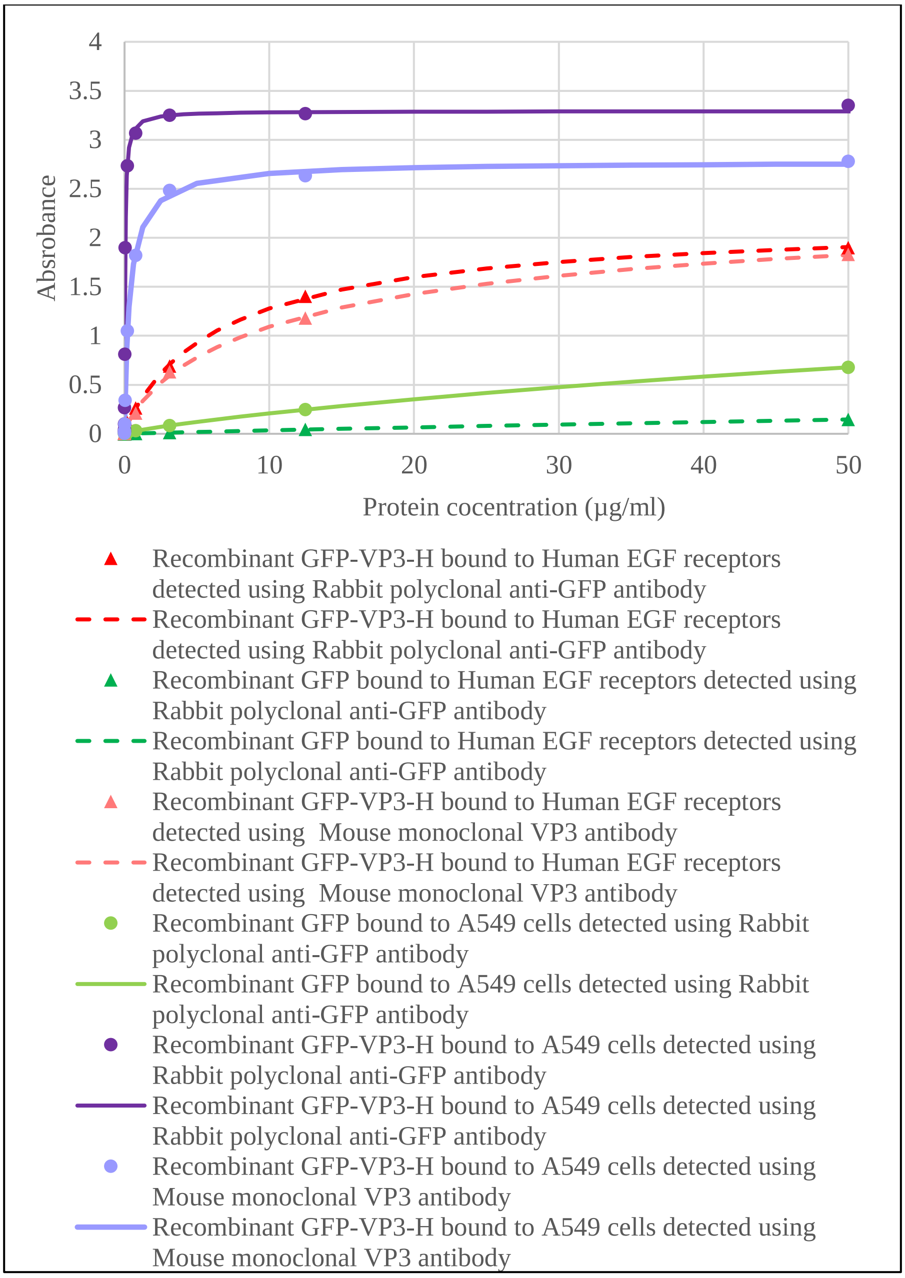

Figure 6.1: Binding activities of recombinant GFP (green lines) and GFP-VP3-H (red and purple lines) towards A549 cells and Human EGF receptors as tested by ELISA. Absorbance for each sample was normalised with negative control to eliminate unspecific binding caused by rabbit polyclonal anti-GFP and mouse monoclonal VP3 antibodies. Collected data was plotted using four parameter fitting model from Microsoft Excel. In contrast to recombinant GFP control (green lines), recombinant GFP-VP3-H (purple and red lines) bound strongly to A549 cells and Human EGF receptors but with a higher level towards A549 cells.

Recombinant EGF-VP3-HK bound to A549 cells as well as human EGF receptors (Figure 6.2). Binding of recombinant EGF-VP3-HK to human EGF receptors (dark blue) was slightly stronger than that of A549 cells (light blue).

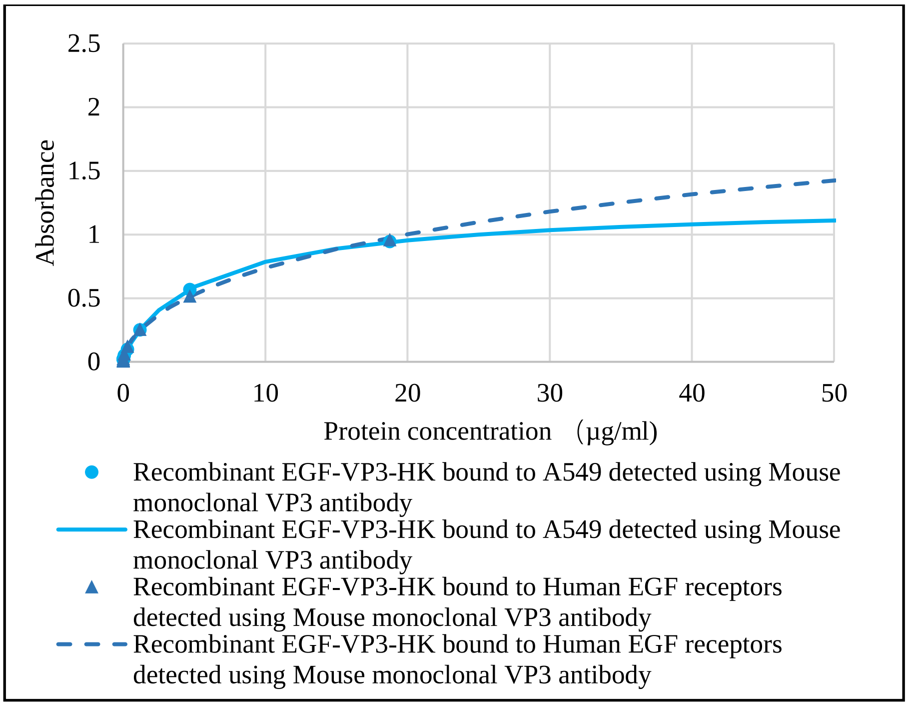

Figure 6.2: Binding activities of recombinant EGF-VP3-HK towards A549 cells (light blue) and Human EGF receptors (dark blue) as tested by ELISA. Absorbance for each sample was normalised with negative control to eliminate unspecific binding caused by rabbit polyclonal anti-GFP and mouse monoclonal VP3 antibodies. Collected data was plotted using four parameter fitting model from Microsoft Excel. Recombinant EGF-VP3-HK bound to A549 cells as well as EGF receptors with the latter shown a higher level.

6.3.2 Bioactivity of recombinant GFP-apoptin (GFP-VP3-H) in A549 cells delivered via microinjection

6.3.2.1 Standardisation of microinjection procedure

Microinjection was performed for ~ 100-150 cells per sample. Intrinsic signal of recombinant GFP protein was detected in microinjected cells from 2 to 24 hours (Figure 6.3). It was estimated that ~ 60% of cells microinjected with recombinant GFP protein was detected and remained healthy until 24 hours post microinjection. However, signal of the GFP protein was gradually faded over time with the lowest level was observed from microinjected samples incubated for 24 hours (Figure 6.3 -e).

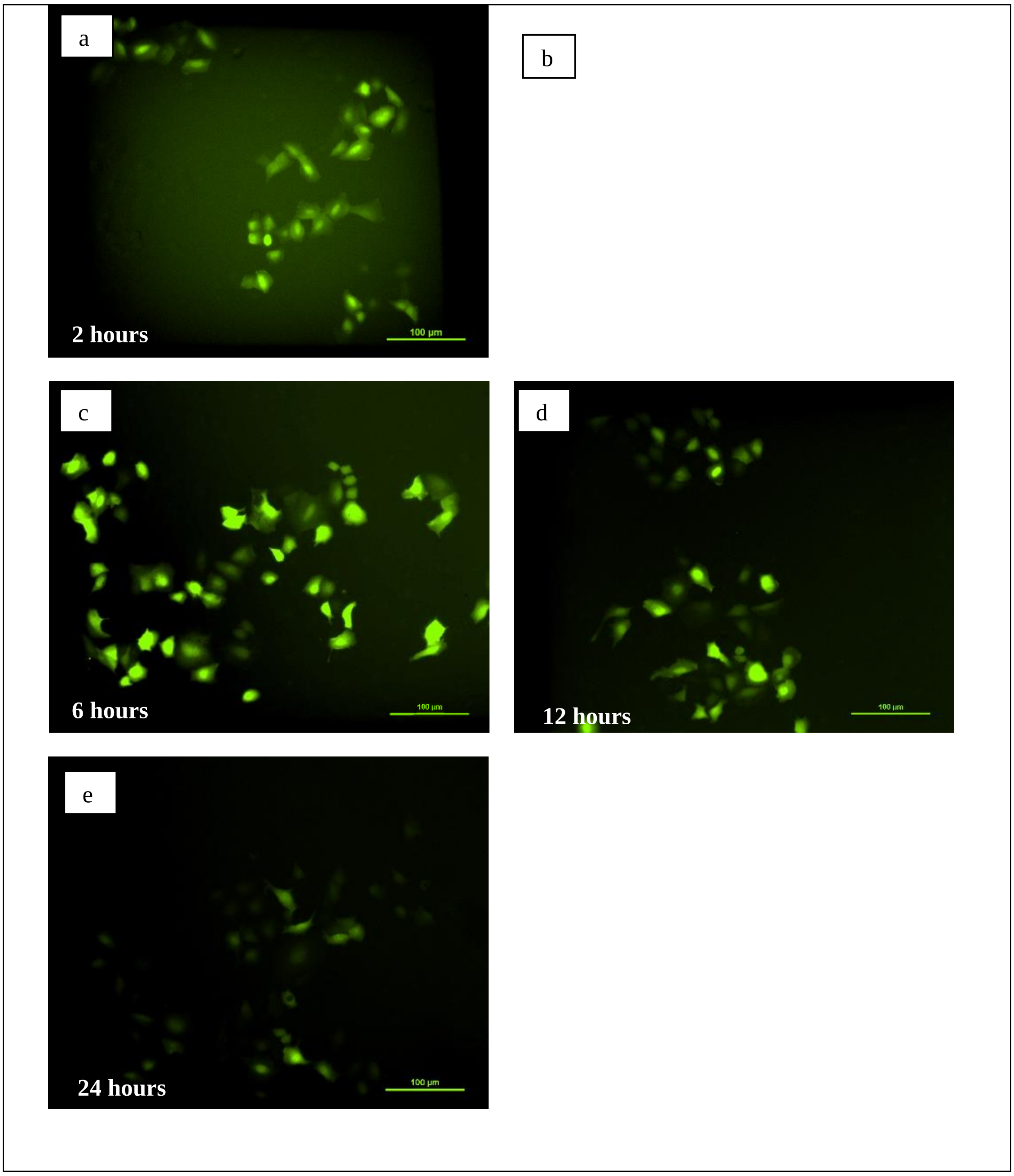

Figure 6.3: Fluorescence microscopic observation of A549 cells microinjected with recombinant GFP protein. Images of microinjected A549 cells were captured at (a) 2 hours, (b) 4 hours, (c) 6 hours, (d) 12 hours and (e) 24 hours post microinjection. Recombinant GFP was microinjected at 2.4 mg/ml and intrinsic signal of recombinant GFP was detected in microinjected cells using Nikon Instruments Eclipse Ti-E inverted microscope. Intrinsic GFP signal of recombinant GFP faded when cells were incubated for a longer period, especially at 24 hours post microinjection.

6.3.2.2 Immunofluorescence detection of A549 cells microinjected with recombinant GFP-VP3-H

Since concentration of recombinant GFP-VP3-H was low (~ 0.8 – 1.0 mg/ml), intrinsic signal of GFP was difficult to be detected in microinjected cells. Therefore, detection of cells microinjected with recombinant GFP-VP3-H was performed using indirect immunofluorescence assay (IF) using mouse monoclonal VP3 antibody and Rhodamine (TRITC) AffiniPure Goat Anti-Mouse IgG (H+L). Cells were successfully microinjected with recombinant GFP-VP3-H would fluorescent in red (Figure 6.4) after IF was performed. Nuclei of detected cells were stained using PI (for cells microinjected with recombinant GFP) and SYB Green (for cells microinjected with recombinant GFP-VP3-H). Viability of cells (50-100 cells) was scored based on the morphology of cell nucleus (Figure 6.5). Figure 6.5 shows only viability of cells generated from a single experiment. Cell viability for microinjection of recombinant GFP remained above 50% when samples were incubated from 2 to 12 hours; however, cell viability was dropped to ~ 35% when samples incubated for 24 hours (Figure 6.5). For microinjection of recombinant GFP-VP3-H, chromatin condensation was observed (Figure 6.6) and viable cells were found as low as 20-35 % at 2-4 hours post microinjection. This conformed to the number of cells microinjected with recombinant GFP-VP3-H with red fluorescent signal decreased over time and almost diminished at 24 hours post microinjection (Figure 6.4 -e). Hence, limited viable cells was considered since very low red fluorescent signal was detected.

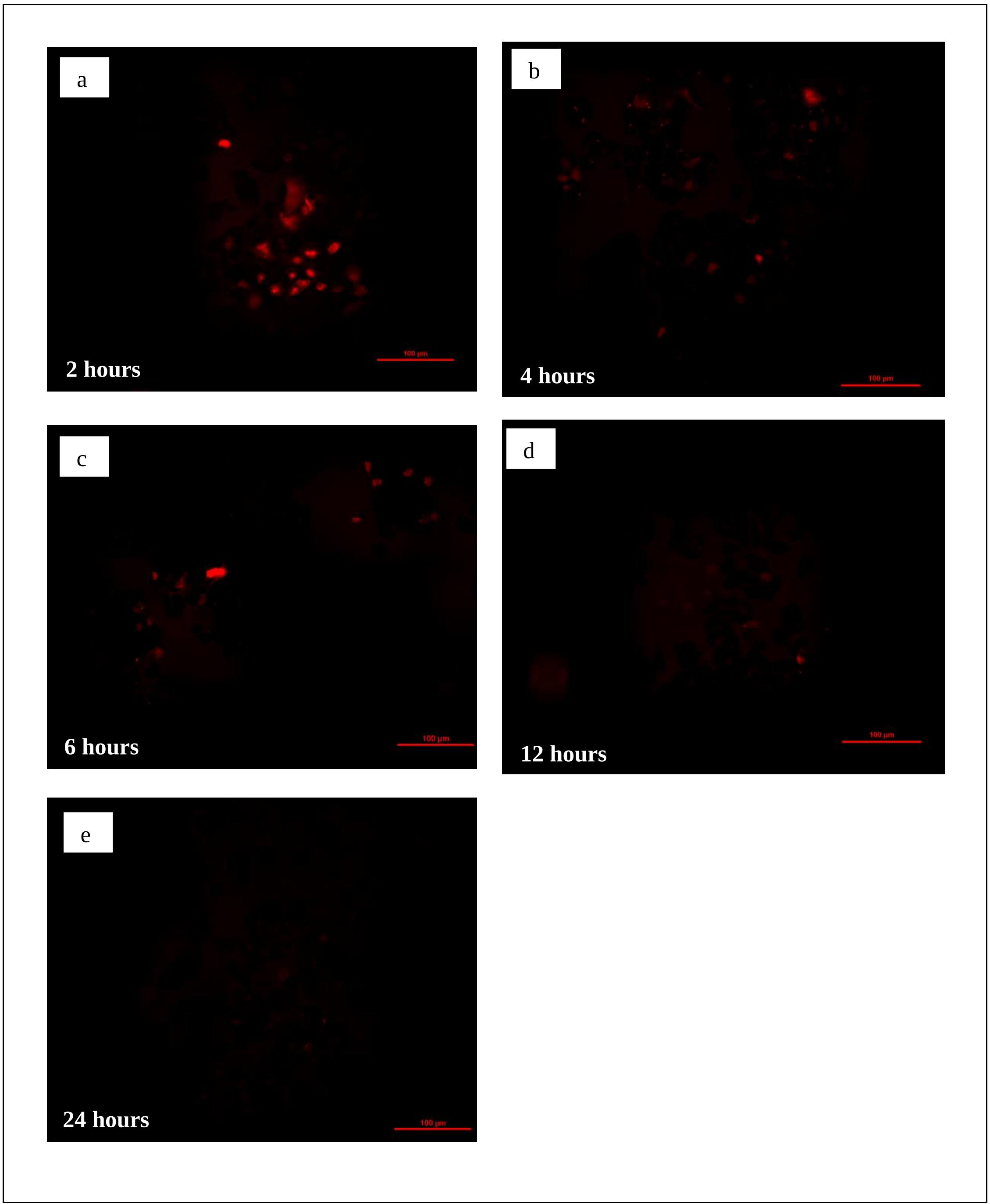

Figure 6.4: Fluorescence microscopic observation of A549 cells microinjected with recombinant GFP-VP3-H protein under IF using mouse monoclonal VP3 antibody and Rhodamine (TRITC) AffiniPure Goat Anti-Mouse IgG (H+L). Images of microinjected A549 cells were captured at (a) 2 hours, (b) 4 hours, (c) 6 hours, (d) 12 hours and (e) 24 hours post microinjection. Recombinant GFP-VP3-H was microinjected at ~0.8-1.0 mg/ml. Detected signal of recombinant GFP-VP3-H (red fluorescence) faded when cells were incubated for a longer period.

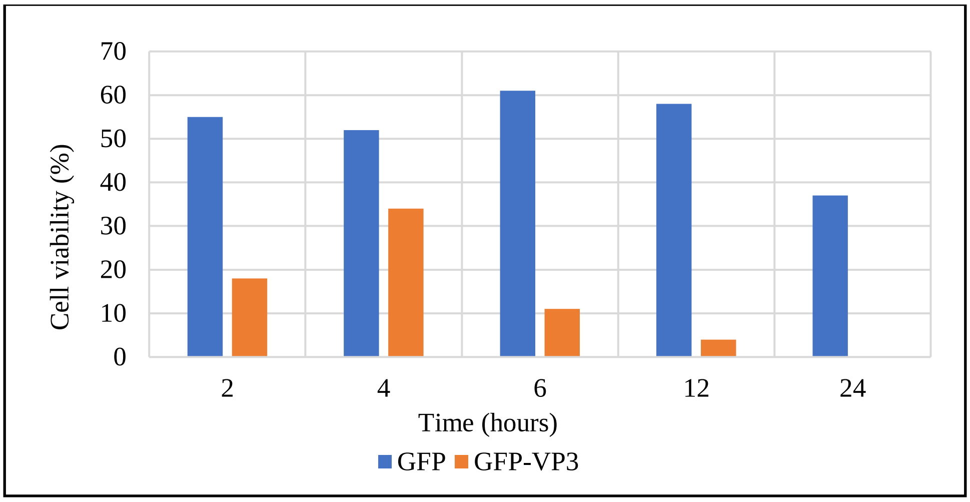

Figure 6.5: Viability of cells microinjected with recombinant GFP and GFP-VP3-H calculated based on total cell numbers receiving microinjection. Cells microinjected with recombinant GFP was determined based on intrinsic signal of the protein; however, cells microinjected with recombinant GFP-VP3-H was identified based on IF using mouse monoclonal VP3 antibody and Rhodamine (TRITC) AffiniPure Goat Anti-Mouse IgG (H+L). Nuclei of detected cells were stained using PI (for cells microinjected with recombinant GFP) and SYB Green (for cells microinjected with recombinant GFP-VP3-H). Viability of cells (50-100 cells) was scored based on the morphology of cell nucleus. The data were represented only viability of cells obtained from a single experiment. Complete scoring data for detected cells as well as viability of cells are shown in Appendix 6.3. For microinjection of recombinant GFP-VP3-H, viability of cells was lower than that of cells microinjected with recombinant GFP. In general, decrements of detected as well as viable cell numbers were observed in cells microinjected with recombinant GFP-VP3-H.

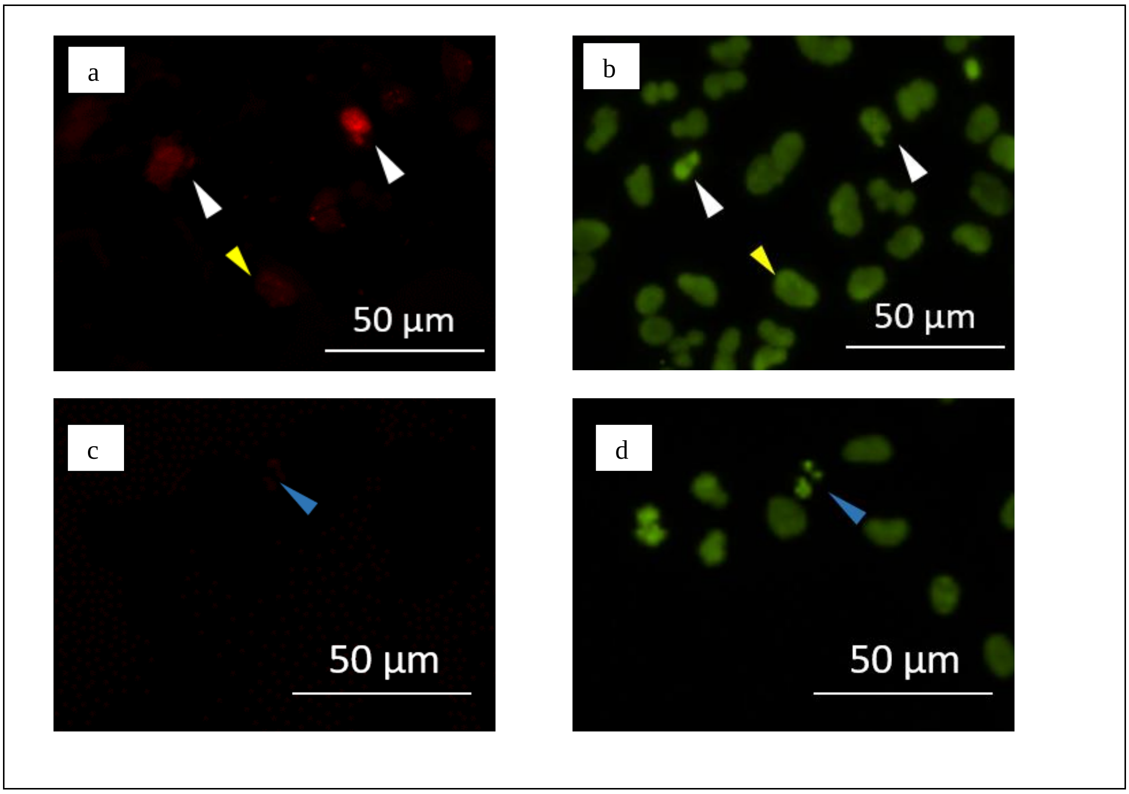

Figure 6.6: Immunofluorescence microscopic observation of cells microinjected with recombinant GFP-VP3-H its stained nuclei. Photos in this section were representative data for microinjected cells showing morphological changes at 6 and 24 hours. Nevertheless, similar morphological changes could also been observed on other time points. (a) A549 cells microinjected with recombinant GFP-VP3-H at pressure 100 hPa at 6 hours post microinjection under IF using mouse monoclonal VP3 antibody and Rhodamine (TRITC) AffiniPure Goat Anti-Mouse IgG (H+L). Red colours indicated the location of recombinant GFP-VP3-H in A549 cells. (b) Nuclear staining of A549 cells microinjected with recombinant GFP-VP3-H at pressure 100 hPa at 6 hours post microinjection using SYB Green. Chromatin condensation (white arrowheads) was observed in some A549 cells microinjected with recombinant GFP-VP3-H in contrast to normal and healthy nuclei (yellow arrowheads). (c) A549 cells microinjected with recombinant GFP-VP3-H at pressure 50 hPa at 24 hours post microinjection under IF using mouse monoclonal VP3 antibody and Rhodamine (TRITC) AffiniPure Goat Anti-Mouse IgG (H+L). Red colours indicated the location of recombinant GFP-VP3-H in A549 cells. (blue arrowheads). (d) Nuclear staining of A549 cells microinjected with recombinant GFP-VP3-H at

pressure 50 hPa using SYB Green. Chromatin fragmentation (blue arrowheads) was observed in some A549 cells microinjected with recombinant GFP-VP3-H in contrast to normal and healthy nuclei.

6.3.2.3 Nuclear localisation characteristics of recombinant GFP-VP3-H microinjected into A549 cells

Recombinant GFP and GFP-VP3-H were microinjected into cytoplasm of A549 cells. Microinjected recombinant GFP distributed equally in A549 cells (Figure 6.7 -a(i)); however, majority of recombinant GFP-VP3-H was localised to cell nucleus (Figure 6.7 -b and c(ii)). Nuclear localisation activity of recombinant GFP-VP3-H was confirmed by the staining of cell nucleus using Hoechst dye. IF signal detected for recombinant GFP-VP3-H (red) was co-localised with Hoechst dye (blue). Nuclear localisation activity of recombinant GFP-VP3-H was detected as early as 2 hours post microinjection.

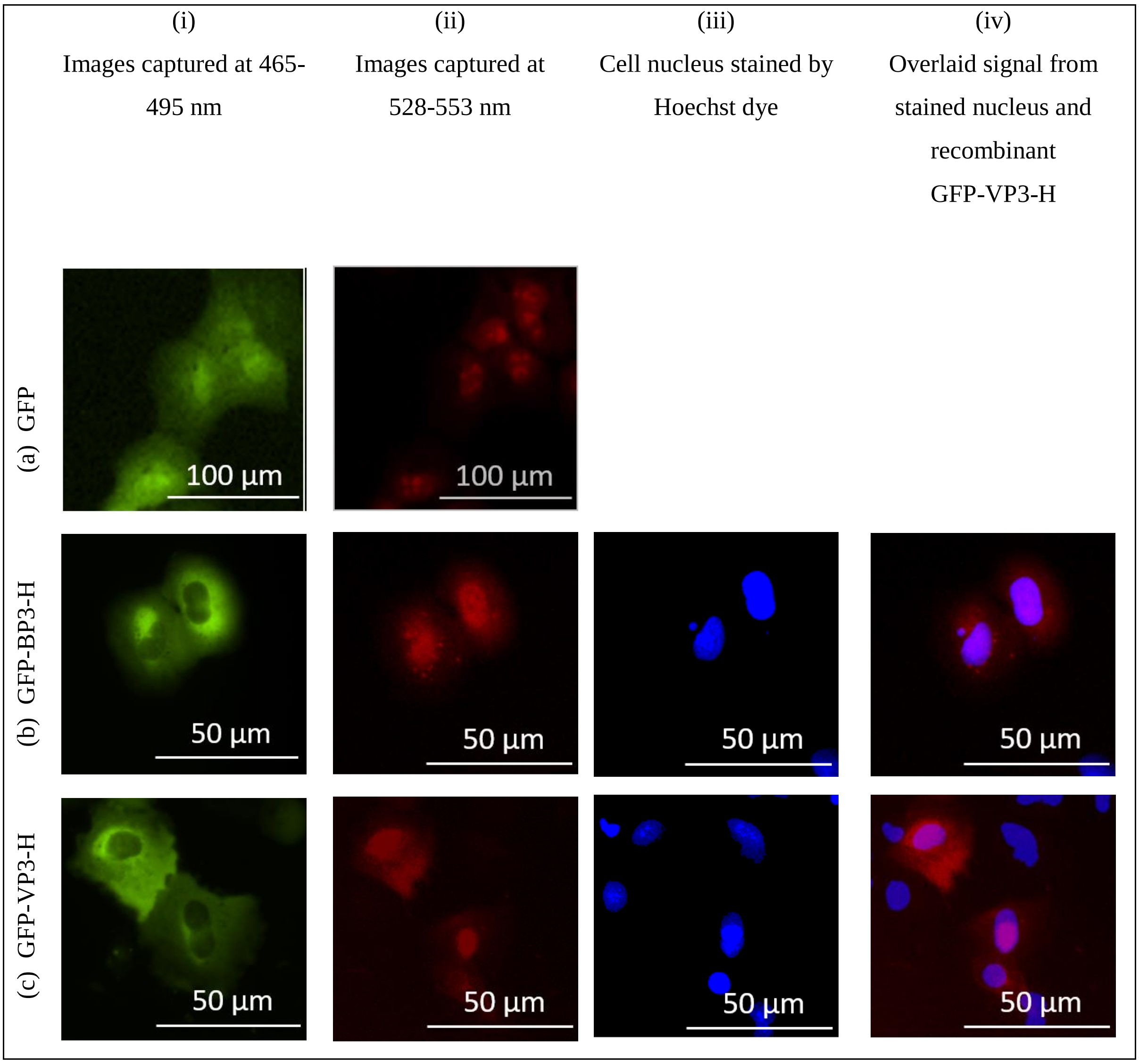

Figure 6.7: Immunofluorescence microscopic observation of A549 cells microinjected with recombinant GFP and GFP-VP3-H proteins at 2 hours post microinjection. Photos in this section were representative data for microinjected cells showing morphological changes at 6 and 24 hours. Nevertheless, similar morphologhical changes could also been observed on other time points. (a) Microinjected A549 cells with recombinant GFP. Microinjected recombinant GFP was distributed evenly in A549 cells. (a-i) Image captured at 465-495 nm was intrinsic signal of recombinant GFP in microinjected A549 cells. (a-ii) Image captured at 528-553 nm was nuclei

of cells microinjected with recombinant GFP stained with PI. (b and c) Representative images of microinjected A549 cells with recombinant GFP-VP3-H. (b-i and c-i) Images captured at 465-495 nm were fluorescent signal detected from cells microinjected with recombinant GFP-VP3-H and Dextran conjugated Fluorescein (70 000 MW). (b-ii and c-ii) Images captured at 528-553 nm were IF assay of microinjected cell samples using mouse monoclonal VP3 antibody (JCU/CAV/1C1). (b-iii and c-iii) Nuclei of microinjected cells were stained by Hoechst dye. (b-iv and c-iv) Overlaid images of stained nuclei and fluorescent signal detected upon IF for recombinant GFP-VP3-H protein in A549 cells.

6.3.2.4 Evaluation of depolarization of mitochondrial membrane potential (MMP) for cells microinjected with recombinant GFP-VP3-H

MMP was evaluated for cells microinjected with recombinant GFP-VP3-H. Since loss of MMP is an early event of apoptosis, MMP assay was performed for 2 hours and 6 hours post microinjection. Red fluorescent signal due to the accumulation of MitoPT TMRM reagent in mitochondria was observed in normal and untreated A549 cells (Figure 6.8 -a and c). Loss of fluorescent signal should be observed if the MMP has been disturbed (refer to Appendix 6.4 using a positive control). However, no apparent difference of fluorescent signal was observed between untreated cells and cells microinjected with recombinant GFP-VP3-H (Figure 6.8 -b and d).

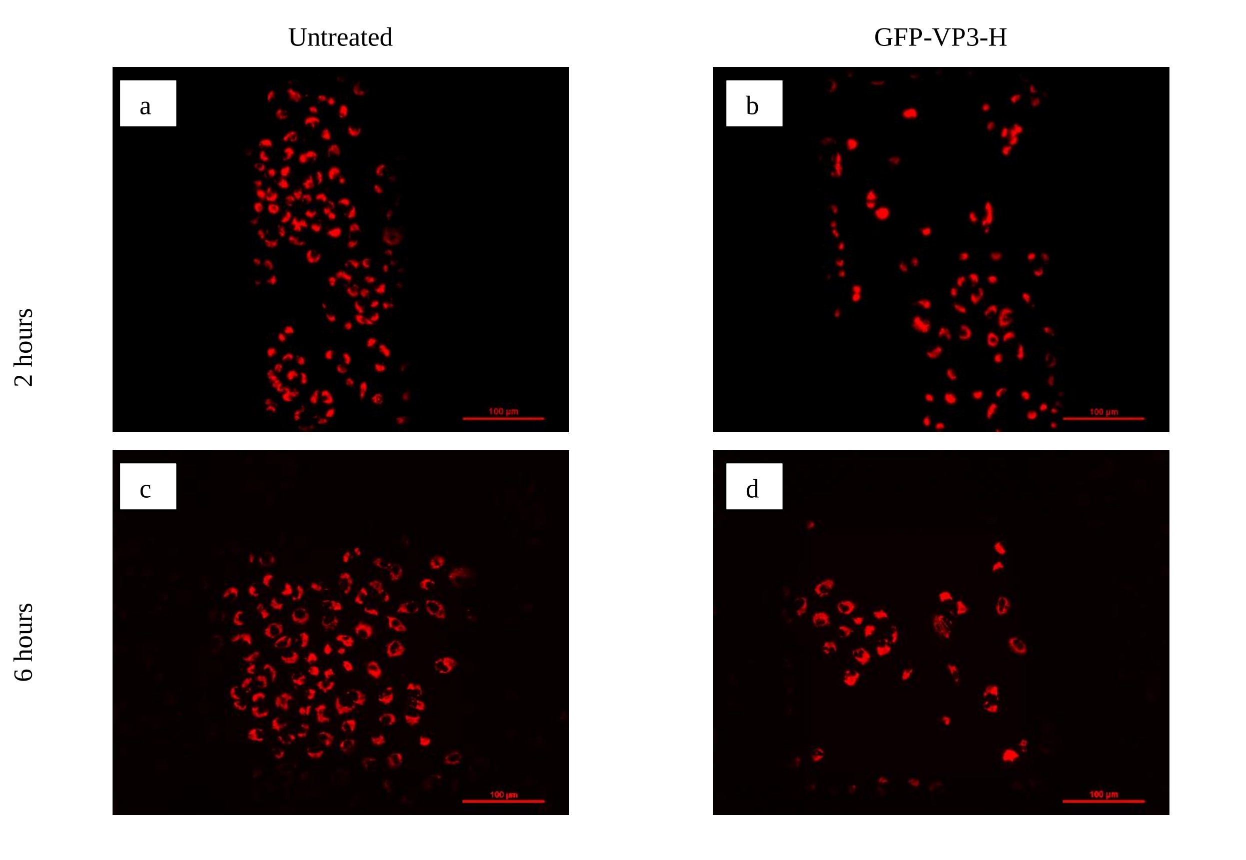

Figure 6.8: Immunofluorescence microscopic observation of A549 cells microinjected with recombinant GFP-VP3-H under MMP assay. MMP assay was performed on untreated control at (a) 2 hours and (c) 6 hours post microinjection as well as on cells microinjected with recombinant GFP-VP3-H at (b) 2 hours and (d) 6 hours post microinjection. No difference was observed between fluorescent signal from untreated samples and cells microinjected with recombinant GFP-VP3-H. Most mitochondrial membranes of cells microinjected with recombinant GFP-VP3-H were still intact.

6.3.2.5 Assessment of Caspase 3/7 activity for cells microinjected with recombinant GFP-VP3-H

Activation of caspases is an event happens at a later stage of apoptosis; hence, caspase 3/7 assay was performed started at 6 hours to 48 hours. The presence of activated capase 3 and 7 in apoptotic cells causes the accumulation of red fluorescent signal in cells, which could be observed from the result using a positive control as shown in Appendix 6.5. However, no fluorescent signal was observed in untreated A549 cells (Figure 6.9 -a, c and e) and cells microinjected with recombinant GFP-VP3-H (Figure 6.9 -b, d and f).

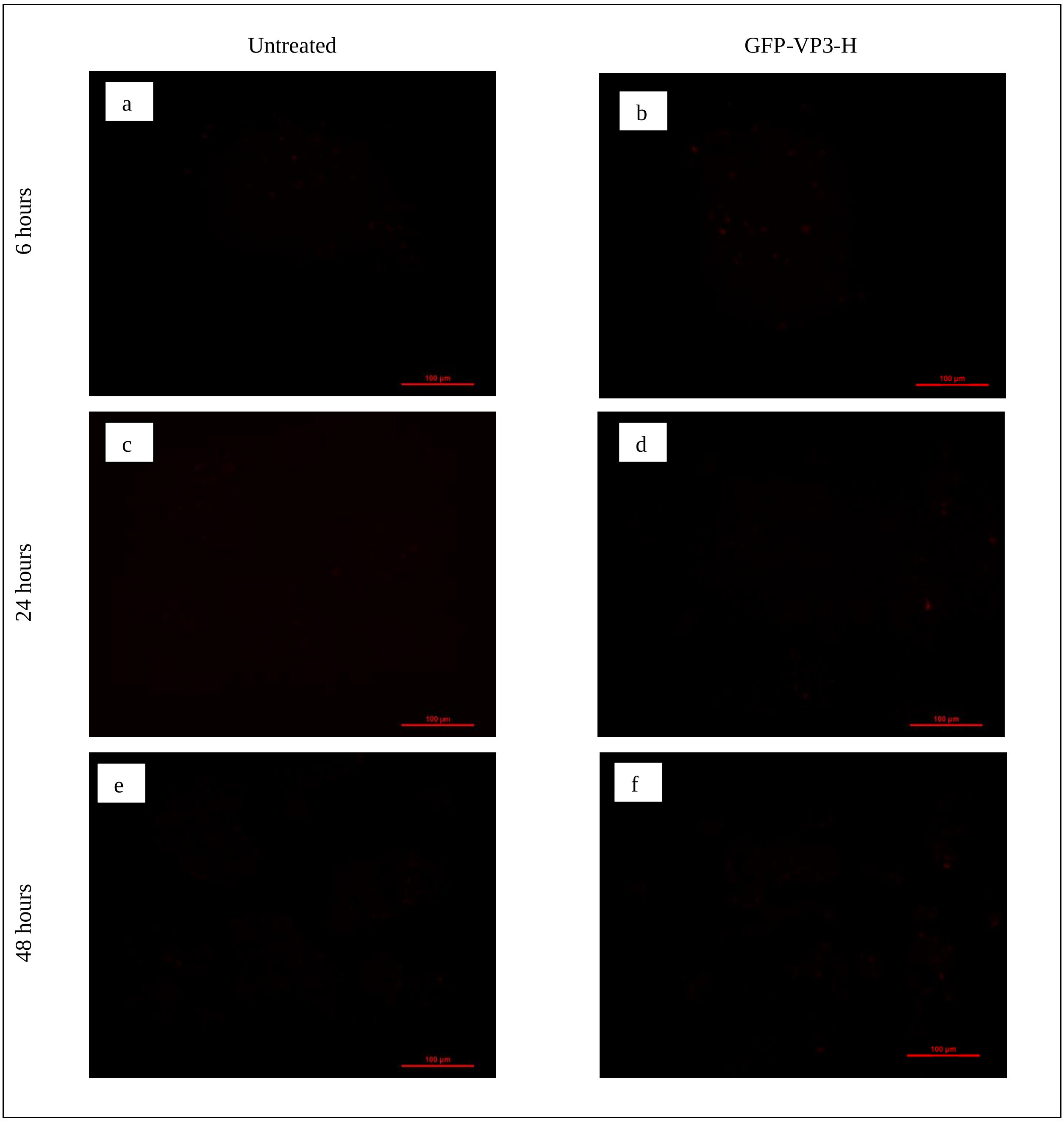

Figure 6.9: Immunofluorescence microscopic observation for caspase 3/7 assay performed for microinjected recombinant GFP-VP3-H. Caspase 3/7 assay performed on untreated control at (a) 6 hours (c) 24 hours and (e) 48 hours post microinjection. Besides, caspase 3/7 assay performed on cells microinjected with recombinant GFP-VP3-H at (b) 6 hours, (d) 24 hours and (f) 48 hours post microinjection. No fluorescent signal was observed from untreated samples as well as cells microinjected with recombinant GFP-VP3 proteins. Hence, caspase 3 and 7 might not be activated.

6.3.3 Bioactivity of recombinant EGF-apoptin (EGF-VP3-HK) in A549 cells

6.3.3.1 Immunofluorescence detection of recombinant EGF-VP3-HK in A549 cells incubated with recombinant EGF-VP3-HK

Recombinant EGF-apoptin (EGF-VP3-HK) is expected to bind to EGF receptors located on the cell surface of A549 cells and internalised into cells via catAd molecular adaptor; hence, no physical or chemical delivery tool was required to transfer the protein into intracellular space. At 18 hours post treatment, IF results showed that recombinant EGF-VP3-HK was randomly distributed on cells at either cell surface or cytoplasm (Figure 6.10) without any apparent nuclear localisation signal as contrasted to which was found in ectopically expressed apoptin in A549 cells (Appendix 6.1) and cells microinjected with recombinant GFP-VP3-H.

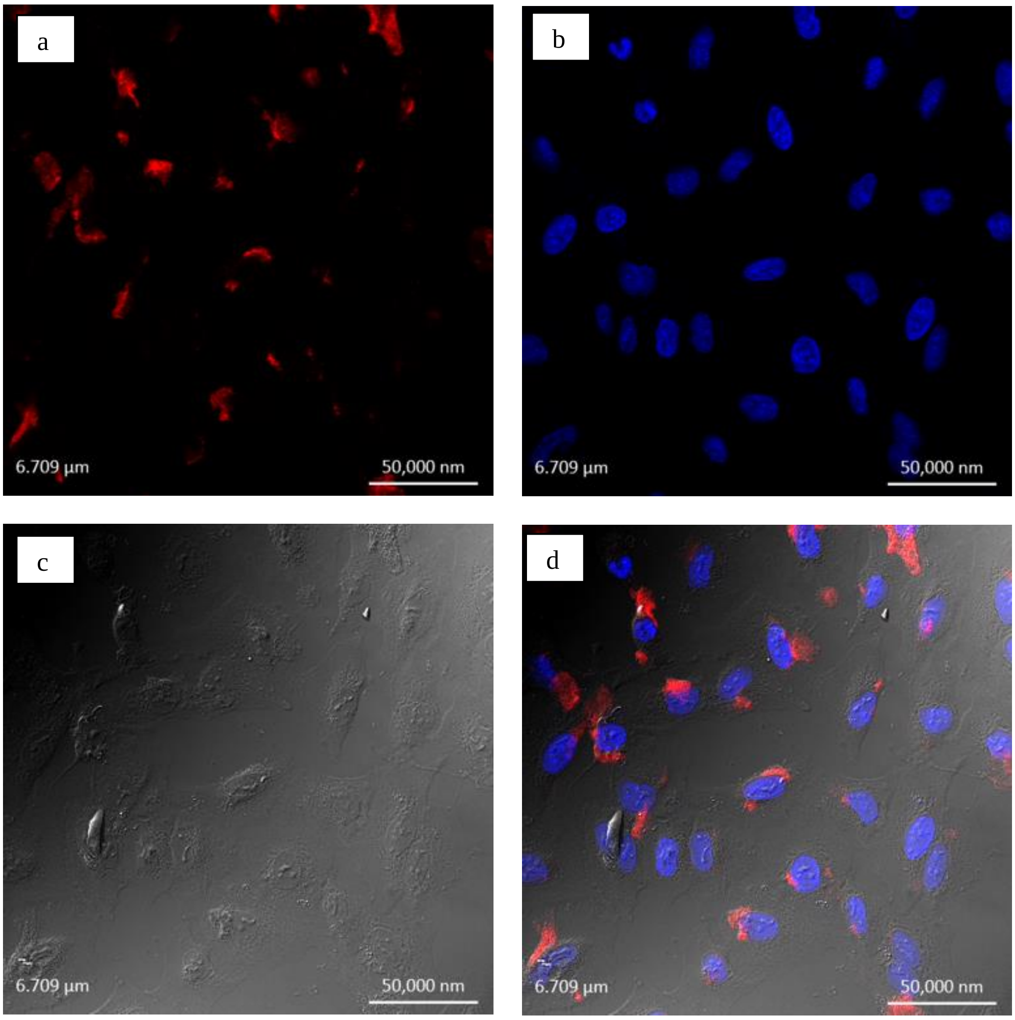

Figure 6.10: Immunofluorescence microscopic observation of recombinant EGF-VP3-HK treated A549 cells on ~ 18 hours post incubation using mouse monoclonal VP3 antibody. Images were captured using Zeiss LSM 510 META highspeed confocal microscope. (a) Detection of recombinant EGF-VP3-HK on treated A549 cell samples under IF using mouse monoclonal VP3 antibody and Rhodamine (TRITC) AffiniPure Goat Anti-Mouse IgG (H+L). (b) Cell nuclei of treated cell samples were stained using Hoechst dye. (c) Images of differential interference contrast (DIC) of treated cell samples. (d) Overlaid image of (a), (b) and (c). Recombinant EGF-VP3-HK was still able to be detected 1 day post incubation of recombinant protein in A549 cells; however, distribution of protein was randomly located on either cell surface or cytoplasm.

In order to identify the internalisation of recombinant EGF-VP3-HK protein into intracellular space of cells, EGF receptors on A549 cells were detected using monoclonal antibody raised against Human EGFR/ErbB/HER1to determine the location of plasma membrane of cells (Figure 6.11 and Figure 6.12). In untreated A549 cells, EGF receptors were distributed evenly on plasma membrane of the cells, which could be observed in Figure 6.11 (b-ii) and Figure 6.12 (a). Inclusion of a negative control confirmed the signal (Figure 6.11 -c) detected was due to specific binding of Rabbit Monoclonal antibody to Human EGFR/ErbB/HER1 to EGF receptor located on A549 cells and not the unspecific binding of anti-rabbit conjugated FITC to A549 cells. From Figure 6.12 (a), Z-stack images of untreated A549 cells clearly showed that EGF receptors formed a layer of Green, which was expected to be the plasma membrane of A549 cells, locating out of nucleus region (blue fluorescent signal as a result of staining by Hoechst dye). However, signal of EGF receptors (Green) obtained from recombinant EGF-VP3-HK treated A549 cells (Figure 6.11-a-ii) did not show the normal distribution of EGF receptors (Figure 6.11-b-ii) but the signal was found sharing similar distribution as that of recombinant EGF-VP3-HK (red) (Figure 6.11-a-iii). Since plasma membrane of recombinant EGF-VP3-HK treated A549 cells could not be indicated by the presence of EGF receptors, which supposed to be arranged on the cell surface, hence, the localisation of recombinant EGF-VP3-HK in either intracellular or extracellular could not be confirmed.

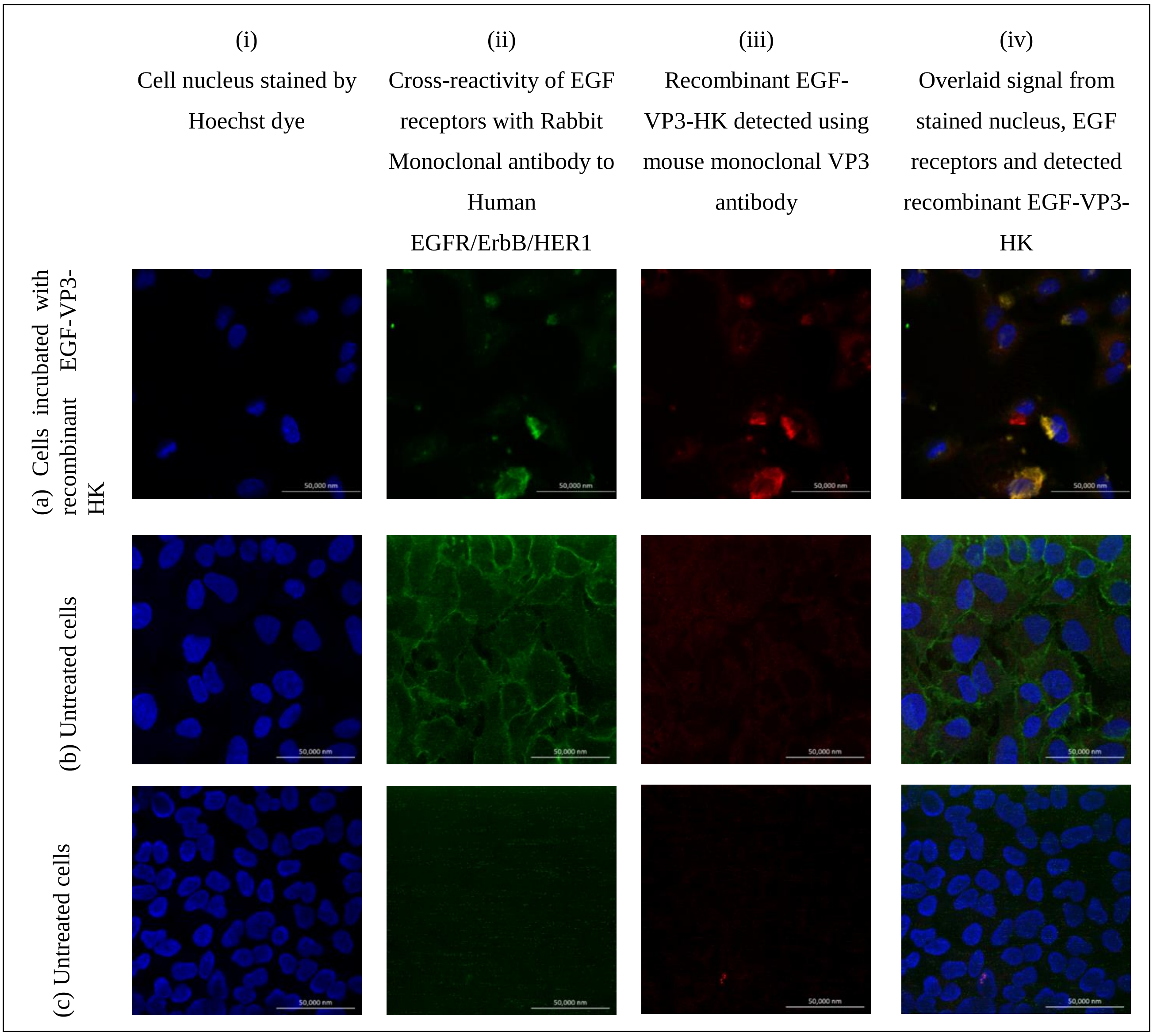

Figure 6.11: Immunofluorescence microscopic observation of recombinant EGF-VP3-HK treated and untreated A549 cells on ~ 18 hours post incubation using Rabbit Monoclonal antibody to Human EGFR/ErbB/HER1 and mouse monoclonal VP3 antibody. Images were captured using Zeiss LSM 510 META highspeed confocal microscope. (a) Detection of recombinant EGF-VP3-HK in treated A549 cells. Signal of recombinant EGF-VP3-HK showed similar location as signal detected from EGF receptors. (b) Detection of EGF receptors in untreated A549 cells. EGF receptors were distributed evenly on plasma membrane of A549 cells. (c) Detection of untreated A549 cells serving as a negative control for IF assay. Images of nuclei were shown for (a-i) A549 cells incubated with recombinant EGF-VP3-HK, (b-i) and (c-i) untreated A549 cells

stained with Hoechst dye. Besides, detection of EGF receptors was conducted by using Rabbit Monoclonal antibody to Human EGFR/ErbB/HER1 and anti-rabbit conjugated FITC for (a-ii) A549 cells incubated with recombinant EGF-VP3-HK and (b-i) untreated A549 cells. (c-ii) Image of untreated A549 cells incubated with anti-rabbit conjugated FITC without Rabbit Monoclonal antibody to Human EGFR/ErbB/HER1. In addition, images for detection of recombinant EGF-VP3-HK using mouse monoclonal VP3 antibody and Rhodamine (TRITC) AffiniPure Goat Anti-Mouse IgG (H+L) were also shown for recombinant EGF-VP3-HK treated A549 cells (a-iii) as well as untreated A549 cells (b-iii and c-iii). (a-iv), (b-iv) and (c-iv) Overlaid signal from stained nuclei, EGF receptors and detected recombinant EGF-VP3-HK.

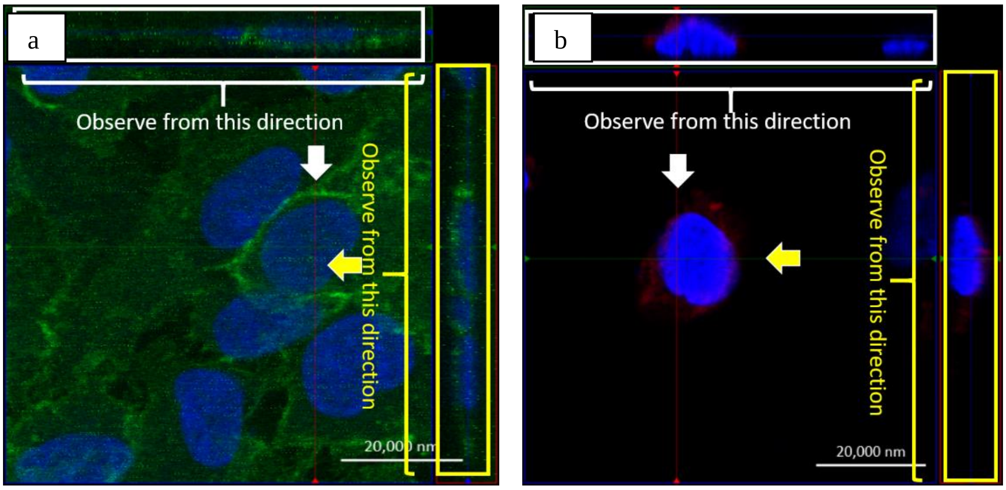

Figure 6.12: Immunofluorescence microscopic examination at higher resolution of recombinant EGF-apoptin (EGF-VP3-HK) treated and untreated A549 cells on ~ 18 hours post incubation. The Z-stack images were captured using Zeiss LSM 510 META highspeed confocal microscope. (a) Z-stack images of untreated A549 cells detected using mouse monoclonal VP3 antibody, Rhodamine (TRITC) AffiniPure Goat Anti-Mouse IgG (H+L), Rabbit Monoclonal antibody to Human EGFR/ErbB/HER1 and anti-rabbit conjugated FITC. EGF receptors which represented as a green layer, was expected to be the plasma membrane, located outside of cell nucleus. (b) Z-stack images of recombinant EGF-VP3-HK treated A549 cells detected using mouse monoclonal VP3 antibody and Rhodamine (TRITC) AffiniPure Goat Anti-Mouse IgG (H+L). Recombinant EGF-VP3-HK could not be confirmed to localise inside the cell nucleus.

6.3.3.2 Cell viability assessment for A549 cells incubated with recombinant EGF-VP3-HK

Viability of recombinant EGF-VP3-HK treated A549 cells were assessed using Cell Proliferation Reagent WST-1 at 72 hours post incubation (Figure 6.13). Measurement for viability of treatment was represented by the ratio between recombinant EGF as well as recombinant EGF-VP3-HK treated A549 cell samples to untreated A549 smaples. Recombinant EGF did not show any cell toxicity but promoted cell proliferation even at high concentration (~ 1500 nM). Recombinant EGF-VP3-HK also showed similar cell growth induction activty but a dose-dependent growth inhibitory was observed when cell was treated at high concentration of recombinant protein (~ 3000 nM).

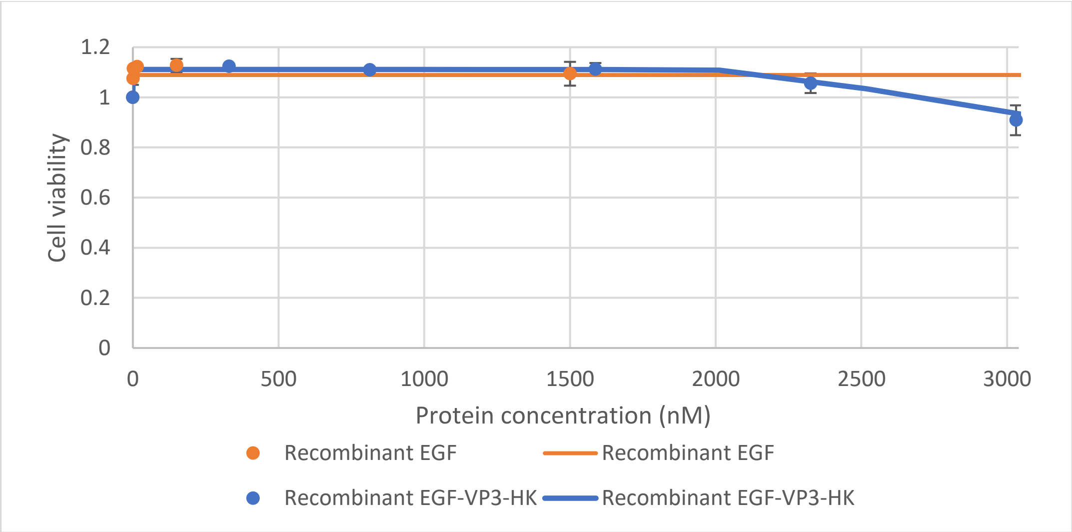

Figure 6.13: Cell viability of A549 cells treated with recombinant EGF-VP3-HK as tested by using Cell Proliferation Reagent WST-1 at 72 hours post incubation. Recombinant EGF promoted cell growth even at high centration at ~1500 nM. A similar effect was seeen in recombinant EGF-VP3-HK treated A549 cells. Cell growth was noticed to have dose-dependent inihibitory effect at high concentration (~ 3000 nM). Measurement for viability of treatment was represented by the ratio between recombinant EGF as well as recombinant EGF-VP3-HK treated A549 cell samples to untreated A549 smaples. Data was plotted using four parameter fitting model from Microsoft Excel to fit all data on the best line.

6.3.3.3 Evaluation of depolarization of mitochondrial membrane potential (MMP) for A549 cells treated with recombinant EGF-VP3-HK

MitoPT TMRM assay kit was also used to check depolarization of mitochondrial membrane of recombinant EGF-VP3-HK treated A549 cells. Results showed that the accumulation of MitoPT TMRM reagent in untreated and recombinant EGF treated A549 cells (Figure 6.14 -a and b) since strong red fluorescent signal was observed. However, red fluorescent signal in recombinant EGF-VP3-HK treated cells (Figure 6.14-c) were lost. Loss of the fluorescent signal indicated that mitochondrial membrane of cells might become permeable or membrane potential had been lost.

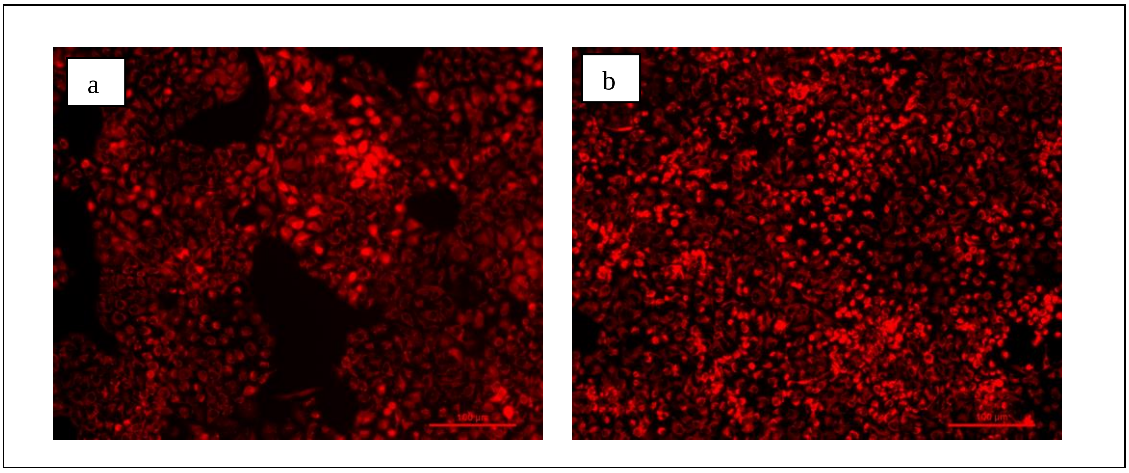

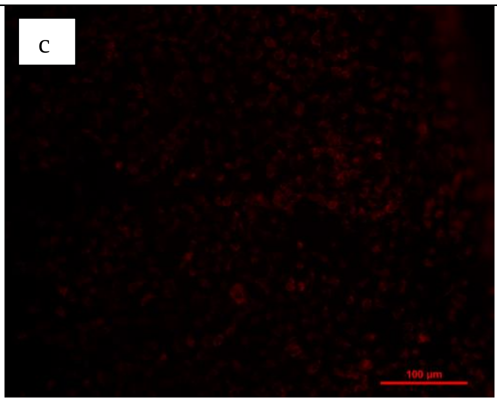

Figure 6.14: Fluorescence microscopic observation of recombinant EGF-VP3-HK treated A549 cells for the evaluation of MMP. Accumulation of MitoPT TMRM reagents (red) was observed in (a) untreated and (b) recombinant EGF treated A549 cells. Accumulation of MitoPT TMRM reagents indicated that mitochondrial membrane of the cells was intact without losing membrane potential. Red fluorescent signal diminished as A549 cells were incubated with (c) 3030 nM of recombinant EGF-VP3-HK for 72 hours. This showed that treatment of recombinant EGF-VP3-HK caused the loss of mitochondrial membrane potential or the increase of permeability of A549 cells.

6.3.3.4 Assessment of caspase 3/7 activity in A549 cells treated with recombinant EGF-VP3-HK

Results showed that limited red signal was detected on both untreated (Figure 6.15 -a) as well as recombinant EGF (Figure 6.15-b) treated A549 cells. The faint signal might be caused by the background signal from MagicRed Caspase-3/7 substrate. No red fluorescent signal was observed in A549 cell samples treated with recombinant EGF-VP3-HK; therefore, caspase 3 or 7 might not be activated in A549 cells treated with recombinant EGF-VP3-HK.

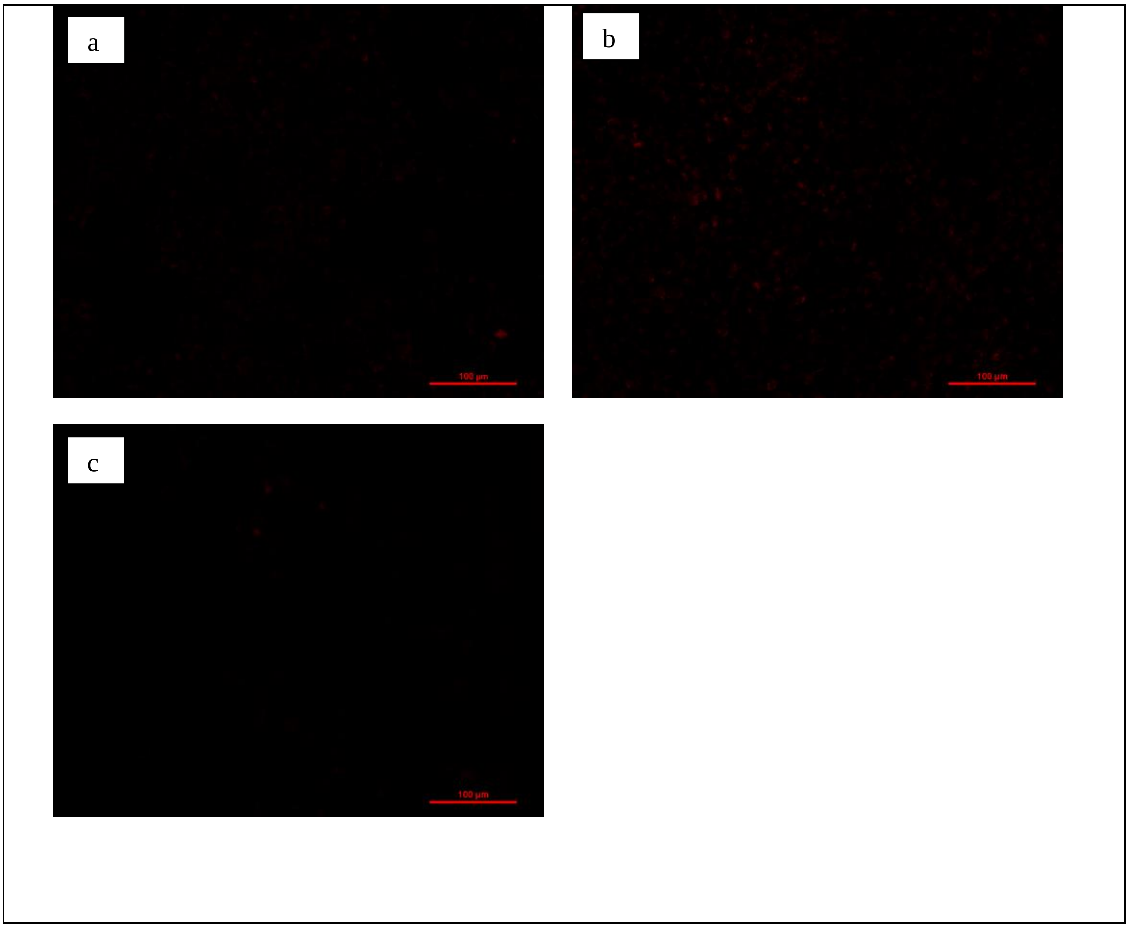

Figure 6.15: Fluorescence microscopic observation of A549 cells treated with recombinant EGF and EGF-VP3-HK for the assessment of Caspase 3/7 activity. Limited fluorescent signal was observed from (a) untreated and (b) recombinant EGF treated A549 cells. The faint signal might be caused by the background signal from MagicRed Caspase-3/7 substrate. However, no fluorescent signal was observed from (c) recombinant EGF-VP3-HK treated A549 cells. Hence, caspase 3/7 might not be activated in A549 cells treated with 3030 nM recombinant EGF-VP3-HK for 72 hours.

6.4 Discussion

This chapter discusses the cell-based study of recombinant apoptin. More than 20 years, apoptin had shown effective cell killing ability in more than 70 cancer cell lines including breast cancer (MCF-7), osteosarcoma (Saos-2 and U2OS), lung carcinoma (SLCC-1 and SLCC-2), hepatoma (HepG2 and Hep3B), SV-40 transformed fibroblast (Pre) and adenovirus-5-transformed embryonal retinoblasts (911) (Noteborn *et al*., 2008). Apoptin-induced apoptosis was reported that it triggers apoptosis via intrinsic (mitochondria-mediated) apoptosis pathway (Los *et al.*, 2009) and most of the studies reported that apoptosis induced by apoptin is independent of extrinsic pathway. Mitochondria-mediated apoptosis pathway was determined by several apoptotic events including loss of mitochondrial membrane potential, releasing of cytochrome *c*, formation of apoptosome and subsequently activation of caspases (especially caspases 3 and 9). In the study of Danen-van Oorschot *et al*. (2000), apoptin-induced apoptosis involved loss of mitochondrial membrane potential, releasing of cytochrome *c* and activation of caspase 3 in human osteosarcoma cell line Saos-2. In addition, apoptin-induced apoptosis is also independent on the presence of p53 and regulated by anti-apoptotic Bcl-2 in several tumour cell lines (Los *et al.*, 2009).

In this study, lung carcinoma (A549) was chosen to investigate for the recombinant apoptin due to the overexpression of epidermal growth factor receptors (EGFR) on the cell surface (Qian *et al*., 2014) (Figure 6.11-b) which is important to determine the activity of the plant-made recombinant EGF-apoptin (EGF-VP3-HK). Based on previous study, A549 cells were susceptible to apoptin when recombinant Newcastle disease virus was employed as delivery tool (Olijslagers *et al*., 2006). Activity of ectopically expressed apoptin had also been evidenced in A549 cells (Appendix 6.1). Significant cell death was observed from cells expressing apoptin alone, GFP-apoptin and EGF-apoptin on 4, 5 and 6 days post transfection. Besides, cell shrinkage, chromatin condensation and fragmentation of cell nucleus, which are the hallmarks of apoptosis, were observed from cells that expressing apoptin (Appendix 6.1- Figure A6.4). A549 cells was confirmed to be susceptible to apoptin-induced apoptosis and hence this cell line was used to evaluate for the bioactivity of both recombinant GFP-apoptin (GFP-VP3-H) and EGF-apoptin (EGF-VP3-HK).

Since A549 cell line was chosen for evaluating the bioactivity of the recombinant apoptin, interaction between apoptin and A549 cells was also studied by using enzyme-linked immunosorbent assay (ELISA). Apoptin was found interacting with A549 cells as well as EGFR in this ELISA binding assay. Instead of the expected binding activity from recombinant EGF-VP3-HK, recombinant GFP-VP3-H was also noticed interacting with EGFR (Figure 6.1). For the detection, rabbit polyclonal anti-GFP antibody and mouse monoclonal VP3 antibody were both employed for the detection of recombinant GFP-VP3-H and EGF-VP3-HK. Higher detection was observed by using rabbit polyclonal anti-GFP antibody and this most likely due to the presence of small amount of degraded protein (Figure 5.4) as well as differences in binding efficiency for both kinds of antibodies. Up to date, there is no study of interaction between apoptin and EGFR. Besides, there is also no homology sequence found between apoptin and ligands of EGFR, including EGF, amphiregulin, Heparin-binding EGF-like growth factor and Betacellulin. A leucine rich regions (LRS) of apoptin, located on amino acids 33-46, was a region responsible for the multimerisation activity of protein (Leliveld[b] *et al*., 2004). Apoptin monomers interact via hydrophobic interaction into huge multimers via this LRS region. Leucine rich regions were also found in EGFRs separately on L1 and L2 extracellular domains (Ward and Garrett, 2001). Besides, small leucine-rich proteoglycan decorins was also found interacting with EGFRs via leucine rich region on both decorins and EGFRs (Santra *et al.*, 2002). Hence, it is speculated that apoptin might interact with EGFRs via this LRS region located on both apoptin and EGFRs. Anyway, specific region results the interaction between apoptin and EGFRs should be studied and point mutation would be one of suitable option for study the region responsible for protein interaction in future.

In this study, recombinant GFP-apoptin did not have cell penetrating peptides; therefore, delivery tool was required to assist the penetration of protein into intracellular space of A549 cells. PULSin® protein delivery reagent had been employed to deliver the protein into A549 cells; however, huge protein aggregates and clumps were found on A549 cells when IF was performed on transfected cells using mouse monoclonal VP3 antibody (Appendix 6.2). One of the possible reasons to form protein aggregates on transfected cells was the changes of environmental buffer and temperature, which were non-favorable for the stability of recombinant GFP-apoptin (Ciechanover, 2005). Besides, apoptin was found that it might interact with A549 cells or EGF receptors, which were also overexpressed on surface of A549 cells. Aggregation of EGF receptors occurs upon the binding of ligands. Hence, protein aggregates on A549 cells after protein transfection procedure may be also caused by the aggregation of apoptin-EGF receptor complexes. Recombinant apoptin may clump into huge aggregates via the interaction of apoptin protein via the LRS region. The huge size of protein aggregates was the key research challenge for internalisation of the protein into A549 cells. For this instance, protein transfection as delivery tool was not successful.

Hence, microinjection, an alternative delivery tool, was used for the delivery of recombinant GFP-apoptin (GFP-VP3-H) into cytoplasm of A549 cells. Microinjection, a direct and precise delivery approach, is usually performed at 50-120 hPa to deliver high concentration of protein (~ 3mg/ml) into mammalian cells (Li *et al.*, 1997; Lim *et al*., 2011). In this study, GFP was microinjected into A549 cells as negative control since GFP is of low toxicity to mammalian cells (Appendix 6.3) and it was a fusion protein for the recombinant apoptin (GFP-VP3-H). Based on a thorough observation for several attempts, cells microinjected with recombinant GFP was always detected at ~ 50-60% after the procedure and the remaining microinjected cells were suspected killed by the mechanical injury during injection process. Although microinjection can deliver protein precisely to cells and even to specific cellular compartment, minimising the mechanical injury induced during microinjection process is a huge challenge for this approach. Especially, microinjection in this study was performed manually, which may directly increase the risk of mechanical damage to microinjected cells. Besides, concentration of recombinant GFP-VP3-H was low (~ 0.8 mg/ml); hence, injection pressure was set at 100 hPa with injection time of ~ 1s. With this parameter set for microinjection, cells microinjected with recombinant GFP was still detected at ~ 50-60% and survived cells also maintained above 50%.

In order to safeguard the bioactivity of recombinant apoptin using microinjection, assessment of the protein was performed within 24 hours (Lim *et al*., 2011; Zhang *et al*., 2003). In the study of Zhang *et al*. (2003), apoptin-induced apoptosis in osteosarcoma cells (Saos-2) was observed starting from 2 hours post microinjection and almost 80% of microinjected cells was dead at 24 hours post microinjection. In this study, cells microinjected with recombinant GFP-VP3-H could not be identified based on the intrinsic signal of GFP from the protein since the green fluorescent signal was not detectable. Failure for the detection of intrinsic GFP signal from the recombinant

GFP-VP3-H after microinjection might be due the low amount of microinjected protein since the initial concentration of the protein was low. Besides, it might also due to the denaturation of protein after microinjected into the cells with a non-favorable environment for protein stability. In order to detect cells microinjected with recombinant GFP-VP3-H, indirect immunofluorescent (IF) assay was carried out using mouse monoclonal VP3 antibody. Based on the IF results, it was noticed that number of detected cells microinjected with recombinant GFP-VP3-H decreased rapidly when cell samples were incubated at 2-24 hours post microinjection (Figure 6.4). The most possible reason contributing to the reduced cell numbers from 2-24 hours post microinjection might due to the presence of intracellular proteolysis. Degradation of microinjected protein is probable as the decrease of intrinsic GFP signal of recombinant GFP in microinjected cells occurred when cells were incubated for a longer period (12-24 hours) (Figure 6.3 and Table A6.1). The major challenge using proteins as therapeutic drugs is the stability of proteins after delivering into mammalian cells or animals. Intracellular stability of foreign proteins is always challenged by physiological pH, temperatures, salts and endogenous proteases (Torchilin, 2008). Denaturation or changes of folding state of proteins in the non-favourable cellular environment always lead to the loss of function and eventually to be degraded by proteolytic system such as ubiquitin-based proteolysis (Ciechanover, 2005). In this study, IF signal from cells injected with recombinant GFP-VP3-H was also 3-5 times lower than that of ectopically expressed cells undergoing apoptosis (Appendix 6.1). This might be due to the low concentration of protein stock used in microinjection. With the low amount of recombinant protein, the presence of intracellular proteolysis would further reduce the availability of protein in the cell, which might directly affect the activity of apoptin-induced apoptosis.

The decrease of cell number may also be caused by the putative cell killing effect of recombinant GFP-VP3-H. Detected number of cells injected with recombinant GFP-VP3-H decreased faster than the number of cells injected with recombinant GFP (Appendix 6.3); hence, the decrease of detected cell number might not be attributed by the mechanical injury induced by the microinjection. To investigate the cell killing effect of recombinant GFP-VP3-H, protein localisation, nucleus morphology, depolarization of mitochondrial membrane potential (MMP) and activation of caspase 3/7 of microinjected cells were examined. Nuclear localisation of recombinant GFP-apoptin was observed in majority of injected cells (~ 70% of cells) and the localization activity of the protein was detected as early as 2 hours post microinjection (Figure

6.7). Nuclear localisation of apoptin was observed in various types of cancer cells (Noteborn *et al*., 1998) as well as in our study when apoptin was expressed ectopically in A549 cells (Appendix 6.1). Besides, apoptin was also found that it interacted with DNA and colocalised with heterochromatin (Danen-Van Oorschot[2] *et al*., 2003; Leliveld[c] *et al*., 2004). Hence, the DNA binding ability of apoptin was believed playing a role in regulating expression of gene involving in apoptosis. On the other hand, chromatin condensation was observed in nuclei of some cells microinjected with recombinant GFP-VP3-H (Figure 6.6). However, it was found that cells injected with recombinant GFP-VP3-H did not show detectable positive result in the tests of depolarization of mitochondrial membrane potential (MMP) and activation of caspases 3/7. Increasing permeability of mitochondrial membrane or loss of mitochondrial membrane potential was an early event occurred in mitochondria-mediated apoptosis pathway. The release of cytochrome *c* always due to the permeable mitochondrial membrane leads to the formation of apoptosome, which is crucial to activate caspase 9. Active caspase 9 cleaves caspases 3, 6 and 7 that involve in cellular protein degradation. Previous study of Maddika *et al.* (2005) confirmed that apoptin-induced apoptosis involves the loss of mitochondrial membrane potential and release of cytochrome *c* in Jurkat cells. Activation of caspase 3 was also confirmed in apoptin-induced apoptosis in Jurkat as well as MCF-7 cells (Maddika *et al.*, 2005; Burek *et al*., 2006). Nevertheless, increment in permeability of MMP and activation of caspase 3/7 were not convincingly detectable in cells microinjected with recombinant GFP-VP3-H. One of the reasons might be due to the low concentration of recombinant protein microinjected into cells, which is unable to trigger an apparent apoptosis in these two assays. Nevertheless, the probable induction of apoptosis cannot be absolutely ruled out as nuclear localization activity and some features of apoptosis (chromatin condensation and fragmentation as shown in Figure 6.6) were evidenced in the microinjected cells. Yet, more investigations on apoptotic activity induced by apoptin in current study are necessitated for a concrete confirmation.

Based on the results of ELISA, binding of recombinant EGF-VP3-HK to EGF receptors was confirmed which might be due to the interaction between EGF and/or apoptin to EGF receptors. Upon the binding, recombinant EGF-VP3-HK is expected to be internalised into A549 cells without requiring any delivery tool. In this study, EGF linked molecular adaptor, containing membrane transfer sequence (MTS) and cytosolic cleavable unit (CCU), was employed to deliver the apoptin into A549 cells that overexpressed with the EGF receptors. In theory, EGF from recombinant EGF-apoptin would bind to EGF receptors of A549 cells that subsequently internalised the apoptin into the cells via clathrin-mediated endocytosis. MTS could assist the penetration of apoptin through endosomal membrane and cleavage at cytosolic cleavable unit (CCU) could release apoptin into cytosol. Currently, the data as shown in section 6.3.3 could not confirm the exact location that the recombinant EGF-VP3-HK bound which could be either inside or outside the cells. This is owing to the location of EGF receptors, which supposed to be an indicator for the location of plasma membrane of recombinant EGF-VP3-HK treated A549 cells was unlikely redistributed. Signal of EGF receptors was found at area exactly where signal of recombinant EGF-VP3-HK was detected in IF assay (Figure 6.11-a). Besides, EGF receptors were found aggregated into patches in contrast to the even distribution on plasma membrane, which is the case for the untreated A549 cells (Figure 6.11-b). Aggregation of EGF receptors into patches was reported by Schlessinger *et al* (1978) upon the binding of EGF ligands before the ligand-receptors complexes were internalized via endocytosis. Hence, it is believed that the EGF receptor patches observed from the recombinant EGF-VP3-HK treated cultures might be induced by the binding of recombinant EGF from the protein. Besides, microscopic images showed that recombinant EGF-VP3-HK precipitated into huge size and distributed randomly in recombinant EGF-VP3-HK treated A549 culture (Figure 6.10). This protein did not localise to cell nucleus, which was contrarily observed in ectopically expressed apoptin (Appendix 6.1). To date, the reason for the precipitation of protein is still unknown. Hence, it is crucial to investigate whether aggregation of protein is induced before or after internalisation since the aggregation of protein might hamper the internalisation of protein into cytoplasm as well as localisation into nucleus. For future study, application of fluorescence scanning electron microscope (FL-SEM) and fluorescence integrated transmission electron microscope will be necessary to examine for the internalisation of protein by using fluorescence based protocols.

From the current findings, the growth of A549 cells was not inhibited at ~ 500 -1500 nM of recombinant EGF-VP3-HK. However, treated A549 cells with recombinant EGF-VP3-HK induced proliferation of cells, which could also be observed from the cells treated with recombinant EGF (Figure 6.13). This result could be explained since binding of EGF to EGFR could lead to numerous kinds of cellular activities, including an enhancement of cell proliferation, differentiation and cancer development (Hyder *et al*., 2012). However, a dose-dependent growth inhibitory effect was observed when cells were incubated with recombinant EGF-VP3-HK at a higher concentration (~ 3000 nM) though with an only ~20% reduced viability. Unlikely, due to limited protein, further concentrations could not be continued in the assay. Activation of caspase 3/7 was not observed in this study but result showed that cells had a loss of MMP after incubation with recombinant EGF-VP3-HK at 3000 nM which concentration was coincided with the evidence of reduced cell viability. Considering the fact that the loss of MMP requiring a constant threshold stimulus of pro-apoptotic proteins, such as Bax; owing to the limited concentrations of EGF-VP3-HK tested, it may be speculated that the insufficient stimulus of Bax may halt the subsequent release of cytochrome *c* and thereby diminishing the probable formation of executioner caspase cascades including the caspase 3/7 activation which could not be detected currently in the study. In contrarily, one of the possible reasons leading to the growth inhibitory effect and undetectable caspase 3/7 activation at this high concentration of recombinant EGF-VP3-HK may be due to the overloaded cultures with considerable amount of impure proteins. Purification of recombinant EGF-VP3-HK did not yield a good purity of protein as observed in Chapter 5 and huge amount of plant protein contaminants were detected in final eluted protein sample. Increasing MMP is an early event of apoptosis but it can also occur when cells undergoing a stress condition. Therefore, the recombinant EGF-VP3-HK treated A549 cells may be in stress condition rather than in the process of apoptosis. Further tests on the cellular Bax level and cytochrome *c* release as well as plant protein contaminant effect on cells should be conducted in order to verify for the actual reason and address the shortfall in the interpretations of apoptotic activity induced by the recombinant apoptin.

In shorts, ectopically expressed apoptin using DNA transfection approach confirmed that A549 cell line was susceptible to apoptin. Via ELISA binding assay, recombinant GFP-VP3-H and EGF-VP3-HK interacted with A549 cells as well as EGF receptors. However, the reasons for the interaction between recombinant apoptin and EGF receptors are yet to be made known. In this study, recombinant GFP-VP3-H was confirmed to be delivered into A549 cells using microinjection. Cells microinjected with recombinant GFP-VP3-H decreased rapidly when the cultures were incubated for a longer period. Although apoptotic features were observed in some cells, the decrease of microinjected cells still could not be concluded to be caused by the apoptosis induced by apoptin. Nevertheless, confirmation of nuclear localisation activity of recombinant GFP-VP3-H confirms the nuclear localisation domains of apoptin is active. In current stage of study, recombinant EGF-VP3-HK was found binding to EGF receptors located on A549 cells due to the detected clumps of EGF receptors upon treatment. However, internalisation of recombinant EGF-VP3-HK is yet to be confirmed. Recombinant EGF-VP3-HK stimulated cell proliferation but a dose-dependent growth inhibitory effect was observed when cells were incubated with recombinant protein at a higher concentration. In addition, apoptin-induced apoptosis still could not be verified by current study for A549 cells treated with recombinant EGF-VP3-HK. In order to make apoptin becoming a great anticancer candidate in the future, an efficient delivery of the protein must be developed and understanding on the mechanisms of apoptin-induced apoptosis is also critical in order to correctly target apoptin to cancer cells.

Chapter 7

General Discussion

Apoptin, the smallest 14 kDa non-structural Viral Protein (VP3) of Chicken Anemia Virus (CAV), is responsible for the destruction of lymphocytes via induction of apoptosis (Noteborn *et al*., 1994). Due to the apoptosis-inducing feature of the protein, VP3 was called as "apoptin" by Noteborn and Koch (1995). Other than inducing apoptosis in chicken lymphoblastoid T and myeloid cells that are susceptible to CAV infection, apoptin-induced apoptosis was also found in tumourigenic and transformed mammalian cells (Zhuang *et al*., 1995). More than 70 cancer cells were reported sensitive to apoptin and underwent apoptosis eventually (Los *et al*., 2009.). Up to date, normal or non-transformed cells, including chicken fibroblast that lacks susceptibility to CAV infection are not sensitive to apoptin. Apoptin contains 121 amino acids coding for a leucine rich region (LRR), locating at amino acids 33-16, and a bipartite nuclear localisation signal NLS1 and NLS2, locating at amino acids 82-88 and 111-121. Although exact mechanisms of apoptin-induced apoptosis are yet to be elucidated, the intrinsic pathway involvement had been evidenced and a huge variety of apoptosis-related proteins were found interacting with apoptin (Los *et al*., 2009.). Study of apoptin was achieved in mice as well as mammalian cell lines via liposome-based DNA transfection, nanoparticles, viral vectors, recombinant proteins and intratumoural injection (Rollano Penaloza *et al*., 2014). Up to date, recombinant apoptin had been successfully expressed in bacteria (*E. coli*), plants (*Nicotiana benthamiana*) and mammalian cells (HUVEC) (Zhang *et al*., 2003; Lacorte *et al*., 2007; Ma *et al*., 2012). The apoptotic induction activity in tumor cells was obtained from recombinant apoptin recovered from bacterial and mammalian cells. However, bioactivity of plant-made apoptin has not been assessed in mammalian cell lines. Besides, several issues have been encountered during the research of apoptin, including uneven delivery of apoptin gene into cancer cells using DNA transfection method, risk of potential infection when mammalian viral vectors are used, cytotoxic effect from transfection reagents as well as huge amount of recombinant apoptin harvested from insoluble protein fraction (Anson, 2004; Backendorf *et al*., 2008). Hence, this study would like to evaluate the feasibility of plant expression system for the production of recombinant apoptin. Besides, some preliminary studies were also performed to explore the apoptosis-inducing potential of plant-made apoptin.

Flexibility for up-scaling, high expression level as well as lack of potential infectious or pathogenic microbes are the attractive benefits of using plant-based system. In this study, tobacco, *N. benthamiana*, was used for the expression of recombinant apoptin since *N. benthamiana* is a non-crop, model plant as well as a huge amount of biomass could be harvested from its leaf tissue (Tremblay *et al*., 2010.). Agroinfiltration, a scalable, non-expensive, rapid and simple gene delivery tool, was employed in this study to deliver recombinant DNA vectors into leaves of *N. benthamiana*. Instead of using syringe, vacuum infiltration, a more efficient and productive way, was used to infiltrate large batches of plants in order to generate a huge amount of plant materials in a short period of times for downstream bioprocessing procedures. With the similar delivery efficiency for each batch of plants, data generated for protein expression-associated morphological changes as well as comparative expression profiles of recombinant vectors were more reliable.

In order to obtain an optimal protein expression and ease for purification, several gene cassettes were designed. Recombinant apoptin was inserted into vectors as apoptin gene alone (gene cassettes: PR-VP3-HK, PR-VP3-H and VP3-H), apoptin gene in fusion to C-terminal of green fluorescent protein (GFP) (gene cassettes: PR-GFP-VP3-HK, PR-GFP-VP3-H and GFP-VP3-H) and apoptin gene in fusion to C-terminal of lichenase (gene cassettes: PR-Lic-VP3-HK, PR-Lic-VP3-H and Lic-VP3-H). Signal peptide (PR1a), hexa-histidine tag as well as endoplasmic reticulum (ER)(KDEL) retention signal were separately fused to apoptin gene cassettes in order to target recombinant proteins to ER, apoplast or cytoplasm. Besides, apoptin gene was also designed in fusion to H22 single chain antibody (gene cassettes: PR-H22-CatAd-VP3-HK, PR-H22-CatAd-VP3-40-121-HK, PR-H22-CatAd-VP3-60-121-HK and PR-H22-CatAd-VP3-80-121-HK) and epidermal growth factor (EGF) (gene cassettes: PR-EGF-CatAd-VP3-HK, PR-EGF-CatAd-VP3-40-121-HK, PR-EGF-CatAd-VP3-60-121-HK and PR-EGF-CatAd-VP3-80-121-HK). The design of fusion to H22 single chain antibody and EGF was to target the protein to specific cancer cells that overexpressed immunoglobulin G (IgG)(CD64) and EGF receptors. Truncated apoptin versions in fusion to H22 single chain antibody as well as EGF were also attempted. Protein expression profiles of all gene cassettes were compared and the most ideal recombinant vectors with promising protein yield were selected for the use in the downstream purification steps.

In order to obtain high protein yield for recombinant apoptin from plant-based expression system, several improvement strategies were applied at transcriptional and translational levels which could be achieved by using recombinant vectors enabling high expression of protein, co-expression with gene silencing suppressors as well as codon optimisation for gene of interest. In this study, tobacco mosaic viral (TMV) based vector pGR-D4 as well as binary vector pGR-DN were used for the expression of recombinant apoptin. Expression of recombinant proteins using viral vectors always yields several folds higher of proteins. High expression of proteins is normally induced by the strong promoters and untranslated regions located on viral genome (Kanoria and Burma, 2012). Recombinant apoptin was also expressed using binary vector, pGR-DN, that harbours a strong promoter (CaMV double 35S promoter) and tobacco etch virus (TEV) enhancer. Infiltration of transformants bearing the recombinant vector, pGR-DN requires the co-infiltration with gene silencing suppressors (P19 and P1/HC-Pro). Employment of gene silencing suppressors is crucial for inhibiting gene silencing events from host plants that suppress transcription as well as translation programme of foreign proteins (Feller *et al.*, 2013). Gene silencing suppressor is not used with TMV-based vector since 126k protein of TMV is believed involving in gene silencing suppression activities. Codon optimisation is also commonly performed to increase preferable codons used by the host plants in order to increase transcription and translation efficiency (Quax *et al.*, 2015). In this study, codon optimisation was performed on sequences of recombinant apoptin and fusion proteins, including green fluorescent protein (GFP), lichenase, H22 single chain antibody and epidermal growth factor (EGF), to increase the percentage of *N. benthamiana* preferable codon and remove mRNA secondary structure that might hamper the translation process. Codon adaptation index (CAI), a measurement for codon adaptiveness of a gene sequence towards the favorable codon usage of highly expressed gene in a host species, of optimised gene sequences increased from 0.6-0.7 to 0.8 (Chapter3). In addition, effective number of codon (ENC) value of optimised gene sequences was also reduced showing a bias of codon towards the preference codons used by *N. benthamiana*.

Besides, several approaches were applied to increase the yield of recombinant apoptin at post translational level. Recombinant apoptin was in fusion to large protein, targeted to specific cellular compartment, co-expressed with endoplasmic reticulum (ER) stress proteins as well as expressed in truncated peptides in order to stabilise the protein and escape from proteolytic degradation. Fusion of recombinant apoptin to large proteins, especially GFP (recombinant pGR-D4:: PR-GFP-VP3-HK) and lichenase (recombinant pGR-D4:: PR-Lic-VP3-HK), was observed with several folds of protein yield increase as compared to apoptin expressed alone (recombinant pGR-D4:: PR-VP3-HK) (Chapter 4). The fusion to large proteins might promote stability and consequently increase solubility of the targeted protein via formation of fusion proteins in micelle-like structure, high propensity of fusion partners in the attraction of chaperone proteins, presence of intrinsic chaperone-like activity and preventing the formation of protein aggregates by electrostatic repulsion (Costa *et al.*, 2014). However, not all fusion proteins might result a positive impact for the expression of recombinant apoptin. In this study, fusion of apoptin to H22 single chain antibody yielded a huge amount of degraded bands instead of full length recombinant H22-apoptin. Besides, recombinant apoptin was also stored at specific plant cellular compartments in order to rescue proteins from degradation by a high amount of cytosolic active proteases as well as receive a proper folding (Streatfield, 2007.). It was noticed that apoptin gene cassettes without signal peptide and ER retention signal were expected to be accumulated in cytoplasm. However, the protein was in fact accumulated in nucleus (gene cassette: GFP-VP3-H) and this might be due to the nuclear localisation activity caused by the bipartite nuclear localisation signal (NLS) located at the C-terminal end of apoptin. Accumulation of soluble fraction of recombinant apoptin showed a higher amount in ER than in nucleus and apoplast. In particular, recombinant GFP-apoptin (recombinant pGR-D4:: PR-GFP-VP3-HK) yielded ~ 2 folds of soluble protein when was accumulated in ER rather than in apoplast (recombinant pGR-D4:: PR-GFP-VP3-H) and nucleus (recombinant pGR-D4:: GFP-VP3-H). However, it was noticed that recombinant apoptin, including apoptin alone, GFP-apoptin and lichenase-apoptin, targeted to nucleus produced the highest amount of proteins in relative to ER and apoplast. Hence, a higher solubility of protein could be obtained when the protein was targeted and retained in ER compartment. This is most probably due to the presence of a huge variety of chaperones that always facilitates protein folding (Streatfield, 2007). Overexpression of recombinant gene always leads to ER stress response as a result of loss of balance for protein processing in ER lumen (Kopito, 2000). ER stress response causes the accumulation of insoluble protein as well as early plant death in infiltrated plants. Early plant death was observed in plants infiltrated with recombinant pGR-D4:: PR-VP3-HK, pGR-D4:: PR-VP3-H, pGR-D4:: PR-Lic-VP3-HK and pGR-D4:: PR-Lic-VP3-H. ER stress proteins, such as bZIP17, bZIP28 and bZIP60, are transcriptional factors inducing expression of unfolded protein response (UPR) related genes. Up-regulation of UPR genes would lead to an elevated level of chaperones (Duwi Fanata *et al*., 2013). In this study, co-expression of bZIP60 with apoptin alone (recombinant pGR-DN:: PR-VP3-HK_bZIP60) had resolved early plant death symptom as observed when apoptin was expressed alone. On the other hand, co-expression of recombinant apoptin alone with ER stress proteins bZIP60 also caused increasing protein expression in soluble fraction as well as total protein. However, co-expression of recombinant bZIP 28 and bZIP17 did not cause any significant changes for the plants as well as protein expression. Besides, co-expression of ER stress proteins also did not improve expression of recombinant GFP-apoptin (gene cassette: PR-GFP-VP3-HK) and EGF-apoptin (gene cassette: PR-EGF-VP3-HK). In the other hand, expression of truncated domains of recombinant apoptin was also studied. Since the N-terminal region of apoptin was responsible for the aggregation activity (Leliveld[c] *et al*., 2003), truncated versions of apoptin (VP3-40-121, VP3-60-121 and VP3-80-121) in fusion to EGF and H22 single chain antibody were generated by removing the N-terminal region of the protein. Higher amount of recombinant apoptin was obtained in soluble fraction from recombinant EGF-apoptin reserving amino acid 40-121 and 80-121. However, lower amount of recombinant EGF-apoptin was recovered when amino acids 1-60 were removed. Fusion of truncated apoptin to H22 single chain antibody produced degraded protein fragments showing a similar result as full length apoptin in fusion to H22 single chain antibody. Indeed, not all approaches were suitable applied for the expression of recombinant apoptin in *N. benthamiana*. Combination of approaches might be required to further investigate a better method for enhancing the protein expression yield of recombinant apoptin in *N. benthamiana*. Nevertheless, recombinant vectors were selected from each group of recombinant apoptin, including apoptin alone, GFP-apoptin, lichenase-apoptin and EGF-apoptin, for downstream protein purification works. These included the recombinant vectors, pGR-D4:: VP3-H, pGR-DN:: PR-VP3-HK_bZIP60, pGR-D4:: PR-GFP-VP3-HK, pGR-D4:: GFP-VP3-H, pGR-D4:: Lic-VP3-H and pGR-D4:: EGF-CatAd-VP3-H by which the infiltrated plants were harvested, extracted and purified in various defined processes.

Hexa-histidine tag was fused to the C-terminal of all proteins; hence, immobilised metal affinity chromatography (IMAC) was employed in the capturing step to purify the recombinant apoptin. Recombinant proteins were isolated from total protein pool based on a specific interaction between hexa-histidine regions and divalent metal nickel (Ni^{2+}). In this study, IMAC was performed in both non-denaturing and denaturing conditions as the recombinant apoptin was present in both soluble and insoluble fractions. For IMAC purification performed in non-denaturing condition, recombinant apoptin alone (recombinant vector pGR-DN:: PR-VP3-HK) was recovered at a low amount of purified protein (< 1 mg/kg). However, ~7 mg/kg of recombinant GFP-apoptin (recombinant vector pGR-D4:: PR-GFP-VP3-HK) was recovered and ~3-4 mg/kg of EGF-apoptin (pGR-D4:: PR-EGF-CatAd-VP3-HK) was also recovered from IMAC in non-denaturing condition. A large amount of host cell proteins (HCPs) was always detected in the final eluted recombinant apoptin, including apoptin alone, GFP-apoptin as well as EGF-apoptin, in non-denaturing condition of IMAC. In fact, removal of HCPs contamination with acidic precipitation as well as second chromatography, using hydrophobic interaction (HIC) columns (including Phenyl Sepharose 6TM FF (high sub), HiTrap Butyl Sepharose HP and HiTrap Octyl Sepharose FF) and cation exchange chromatography (IEX) column (HiTrap SP), did not give a positive feedback for the trials. Instead of purifying protein from soluble protein fraction, recombinant apoptin expressed in insoluble protein fraction was also performed using IMAC in denaturing condition. Recombinant apoptin alone (from recombinant vector pGR-D4:: VP3-H) did not solubilise completely in extraction buffer by using high concentration of guanidium hypochlorite (GuHCl); hence, a low amount of protein (~ 1 mg/kg) was recovered from IMAC. On the other hand, recombinant GFP-apoptin (from recombinant vector pGR-D4:: GFP-VP3-H) and lichenase-apoptin (from recombinant vector pGR-D4:: Lic-VP3-H) yielded a high amount of protein with good purity from IMAC in denaturing condition. Recombinant GFP-apoptin (GFP-VP3-H) was recovered at 21 mg/kg and purified protein was refolded without the requirement of other additives; ~ 20 mg/kg of recombinant lichenase-apoptin (Lic-VP3-H) was harvested from IMAC in denaturing condition but refolding of recombinant Lic-VP3-H required the addition of triton in order to stabilise the protein in the buffer. Characterisation of protein multimerisation was also performed for refolded recombinant GFP-VP3-H using size exclusion chromatography coupled with multi-angle light scattering (SEC-MALS). Recombinant GFP-VP3-H was migrated as a single peak at 10 ml with a small shoulder at ~ 10.7 ml in SRT SEC1000 column and MALS analysis showed that majority of these protein molecules shared a similar molecular mass, which was ~ 944.3 kDa. This data showed that refolded GFP-VP3-H was existed in a multimerised state with ~ 20 monomers per protein molecules. A similar result was also reported by Leliveld[a] *et al.* (2003). Since refolded GFP-VP3-H was recovered at a high amount with good purity and partial purified recombinant EGF-VP3-HK was able to be internalised directly into targeted cancer cells; hence, both proteins were subjected to subsequent cell-based experiments in order to collect some preliminary understanding regarding bioactivity of plant-made apoptin in mammalian cells.

Human lung adenocarcinoma epithelial cell A549 cell line was chosen for evaluating the bioactivity of recombinant GFP-VP3-H and EGF-VP3-HK. The key reason of using A549 cells is due the overexpression of EGF receptors was present on the cell surface as this is crucial for evaluation of bioactivity of recombinant EGF-VP3-HK. In addition, ectopically expression of apoptin via DNA transfection also confirmed that A549 cell line was susceptible to apoptin. Interaction between recombinant apoptin and A549 cells was also studied using enzyme-linked immunosorbent assay (ELISA) binding assay. Based on the ELISA result, recombinant apoptin (GFP-VP3-H and EGF-VP3-HK) interacted with EGF receptors as well as A549 cells, which overexpressed with EGF receptors. Up to date, there is no report about the interactions between apoptin and EGF receptors as well as apoptin and cell surface of cancers. The interaction between apoptin and EGF receptors might be due to the presence of leucine rich region (LRR), a region that is responsible for the multimerization of apoptin, on both apoptin and EGF receptors. Nevertheless, the underlying mechanism for the interaction between apoptin and EGF receptors requires more investigations.

Although recombinant GFP-apoptin (GFP-VP3-H) could bind to EGF receptors and A549 cells, this protein did not have cell penetrating peptides and a delivery tool was required to transfer protein into the intracellular space of A549 cells. Presence of protein aggregates on A549 cells was observed when recombinant GFP-apoptin (GFP-VP3-HK) was delivered into A549 cells using PULSin® protein delivery reagent. The changes of buffer condition and temperature may cause the incidence of protein aggregates. Besides, clumping of recombinant apoptin-EGF receptor complexes may also be the reason causing the protein aggregates. Since the size of protein precipitates was huge, the internalisation of protein was a challenge. Instead of using transfection reagent, microinjection, a precise delivery method, was used to deliver recombinant GFP-apoptin (GFP-VP3-H) into A549 cells. By using microinjection, recombinant GFP-VP3-H was directly introduced into cytoplasm of cells and huge protein aggregates were no longer observed. In microinjection, number of cells microinjected with recombinant GFP-VP3-H reduced rapidly in relative to those cells microinjected with recombinant GFP when the cell samples were incubated from 2-24 hours post microinjection. The most possible reason contributing to the decrease of cell numbers might be due to the intracellular degradation activity since reducing signal of recombinant GFP in microinjected cells was also observed. It is not surprised to find that intracellular bioavailability of recombinant proteins is always challenged by the changes of physiological pH, temperature, salt as well as the presence of proteases (Torchilin, 2008). Besides, cell killing activity of recombinant apoptin might also contribute for the decrease of cells since changes of nuclear morphology was observed in small amount of microinjected cells. Besides, microinjected recombinant GFP-VP3-H was also localised into cell nucleus of A549 cells which is crucial for apoptosis induction. However, it could not be concluded at this stage that the decreased cell number was absolutely due to apoptotic activity induced by the recombinant apoptin since no convincingly positive result was collected from the tests for depolarization of mitochondrial membrane potential (MMP) and activation of caspase 3/7, which are both significant hallmarks for an apoptosis event.

On the other hand, recombinant EGF-VP3-HK is expected to bind specifically to EGF receptors located on cell surface of A549 cells and the protein will then be internalised into cell via endocytosis. Subsequently, apoptin would be transferred and released into cytoplasm via the activity of membrane transfer unit (MTU) as well as cytosolic cleavable unit (CCU) from CatAd adaptor linked between EGF and apoptin. Based on current indirect immunofluorescent (IF) assay, internalisation of recombinant EGF-VP3-HK could not be confirmed after it was applied on the culture. This is because the identification of plasma membrane by detecting the EGF receptors was interrupted by the redistribution of EGF receptors. The redistribution of EGF receptors was believed due to the binding of recombinant EGF. Hence, a future study on the protein internalisation is required by using other plasma membrane staining markers. The recombinant EGF-VP3-HK induced cell proliferation of A549 cells at a lower concentration, which was also observed in the cells incubated with recombinant EGF. However, a dose-dependent growth inhibitory effect was observed when cells were incubated at a higher concentration of recombinant proteins. In current study, no activation for caspase 3/7 activity was observed in cells incubated with recombinant EGF-VP3-HK; however, loss of mitochondrial membrane potential (MMP) was observed. Since a loss of mitochondrial membrane potential occurs in both cells undergoing apoptosis as well as stress, activation of apoptin-induced apoptosis is probable, however, the loss of MMP caused by the cells under a stress condition could not be ruled out too. Apoptin protein concentration is a limiting factor in the study. Therefore, the protein may provide inadequate stimulus for cellular pro-apoptotic proteins involving in the upstream event of apoptosis, such as Bax and Bak. Increasing level of these cellular proteins may lead to the loss of MMP; however, inadequate stimulus may render the activation of caspase 3, which is the executor caspase actived at later stage in apoptosis pathway. Evaluation for activation of pro-apoptotic proteins, which is upstream event for apoptosis before loss of mitochondria, could be performed to investigate this assumption. Besides, activation for cellular proteins (such as caspase 9, cytochrome c and apaf-1) involving in apoptosis, which activated after loss of MMP and before activation for caspase 3, could also be measured to examine this hypothesis.

Limitations of the Current Study and Future Recommendations

Some limitations of the current study are found and prospective research of apoptin is highlighted herein. The main objective of this study was to evaluate the potential of using a plant-based system, i.e. agroinfiltration approach for the production of recombinant apoptin. By using plant as a biofactory, it was found that only a low amount of recombinant apoptin in soluble protein fraction was able to be recovered and fusion of apoptin to a large protein had increased the yield of soluble protein. In the current study, GFP, lichenase as well as EGF were adopted in fusion to apoptin and yields of soluble protein varied among these fusion proteins (~ 10-20 mg/kg). In comparison to *E. coli* expression, plant-derived apoptin alone and apoptin in fusion with the abovementioned proteins have not resulted a more satisfactorily soluble protein yield. In fact, other large proteins could be considered to be fused to apoptin in future in order to enhance the solubility and stability of recombinant apoptin. For examples, maltose binding protein (MBP), glutathione S-transferase (GST) and elastin like protein (ELP) are the commonly used large proteins for fusion purpose. In the study of Leliveld[a] *et al.* (2003), MBP-apoptin fusion had been proven to significantly increase the soluble recombinant protein production with a level up to ~ 40 mg/L in *E. coli* system. Besides, the employment of MBP or GST as a fusion protein to recombinant apoptin could also be an alternative protein purification option over IMAC, which might improve the overall purity of recombinant apoptin, better than that of generated by IMAC in this study. Removal of fusion protein after purification is also a concern for the production of recombinant protein since fusion protein might induce an unwanted response in the animal experiment. In the current study, an enterokinase site was incorporated between apoptin and fusion proteins making the apoptin can be purified as a single pure protein. However, cleavage of fusion protein and evaluation for the stability of apoptin after cleavage have yet to be carried out for current study.

Besides, protein targeting was also one of the strategies used in the current study to increase stability of recombinant protein. Among three cellular compartments, recombinant apoptin showed a high soluble protein level when protein was accumulated in ER. However, protein was accumulated in nucleus at the highest amount but in an insoluble state. Accumulation of recombinant apoptin in ER at lower quantity might be due to the activation of proteolysis machinery for unfolded or improper folded proteins produced rapidly in a short period of time. Instead of using a strong promoter, a weak promoter like nopaline synthase can be attempted in future to reduce the rate of protein synthesis, which might in turn lead to a higher amount of soluble protein to be harvested. Besides, recombinant protein could also be targeted to chloroplast, which is an alternative protein accumulation site within plant cells. In addition to protein fusion, several parameters, including agrobacterium strain, infiltration bacterial OD, vectors, gene silencing suppressors and storage of protein in specific cellular compartments, could also be optimised in order to enhance protein expression.

In the protein purification process, IMAC dependent on the interaction between hexa-histidine and metal ion, was the major tool used for capturing recombinant protein from total protein pool in this study. Other purification approaches, such as ion exchange chromatography (IEX), glutathione-S-transferase GST-based affinity chromatography and MBP-based chromatography, could be examined for purification of recombinant apoptin in the future. Besides, multimerisation of apoptin is interesting but the mechanism has yet been understood. The multimerisation characteristics of recombinant protein had been analysed in this study using SEC and MALS to evaluate the molecular weight of the recombinant protein. For future investigations, hydrodynamic radius of recombinant apoptin could be measured by using dynamic light scattering (DLS) and size of protein could be further validated using electron microscopy (EM). A lack of elucidation of the protein structure of recombinant apoptin is one of the major missing parts in this study. Protein structure could be analysed using circular dichroism to characterise for the secondary structure of protein. Up to date, no crystallography of apoptin has been reported. The protein structure captured after crystallisation might have a great impact in the current apoptin research in order to understand the three-dimensional structure of apoptin macromolecules at an atomic resolution. Understanding on the proper protein folding and structure could give a guidance for the design of gene cassettes and probably help to explain the mechanism of apoptin-induced apoptosis.

Protein stability is also required for future study. Instability of recombinant apoptin was noticed during protein purification process; however, recruitment of suitable stabilising agents, such as sucrose and glycerol, has yet to be conducted. Difficulty for studying protein function in subsequent cell-based or animal experiments has been encountered in current study since the protein precipitation occurred upon storage. Hence, investigation for improving the stability of recombinant protein is important in future to overcome this research bottleneck.

Lung adenocarcinoma was chosen as the cell lines tested for activity of recombinant apoptin in the current study. However, apoptin is actively against various kinds of cancer cells. Hence, it is also suggested to test recombinant apoptin in other cancer cell lines. Besides, low protein concentration is also a critical limiting factor in this study. Significant apoptosis activity might be able to be detected when apoptin is tested in other cells since efficient cell killing dosage of therapeutic proteins might not be the same for different cell lines. In the other hand, an unexpected interaction between apoptin and EGF receptors was noticed in this study. However, there is no study reported regarding this sort of interaction between apoptin and EGF receptors or cancer cells. Truncated or point mutation study on recombinant GFP-apoptin sequences could be performed in future for elucidating the region which is responsible for the interaction. More studies on protein interaction and domain binding between apoptin and EGFR are important for determining the suitability of EGFR as a site for recombinant protein binding and successful internalisation.

Besides, recombinant GFP- apoptin could not pass through plasma membrane directly and employment of microinjection technique was required for the delivery of recombinant protein into the cells. Microinjection is not a favourable delivery tool for long term study of recombinant protein since the technique is of high cost, laborious and not feasible when protein is tested *in vivo*. Therefore, the use of cell-penetrating peptides (CPPs) may resolve these research problems as identified. Up to date, researches have employed Tat protein from HIV and PTD4 to deliver apoptin into animal cells and significant cell death was observed in treated tumour cells (Sun *et al*., 2009: Lee *et al*., 2012). In this study, cell specific ligands, such as EGF and H22 single chain antibody, were used in addition to CPPs. However, H22-apoptin did not yield a good amount of proteins and recombinant EGF-apoptin requires more studies in order to elucidate the protein internalisation activity. EM would be a direct method to check for the localisation of protein inside A549 cells. Besides, internalisation of protein could also be quantified using MALDI-TOF MS in addition to fluorescence-based protocol (Benchara, 2012). Hence, in addition to the study of internalisation of recombinant EGF-apoptin, other cell specific ligands could also be exploited, such as RGD tri-peptide, Bombesin (BBN) peptide, somatostatin and follicle-stimulating hormone analogs, which could increase the targeting efficiency for cancer cells (Raha *et al*., 2011). In addition, evaluation on the cleavage of apoptin from EGF fusion protein after internalisation will also be one of the important parameters to study the delivery strategy. Cytosolic cleavage site located between apoptin and EGF harbours cellular enzyme cleavage sites, such as Caspase-1 and Caspase-3 cleavage sites.

Hence, cleavage efficiency of apoptin from EGF fusion protein could be determined by incubating the protein with cellular cytoplasmic extract that containing high amount of enzymes. Cleavage of apoptin from EGF fusion protein is important to release apoptin from vesicle and allow apoptin to be relocalised to nucleus, where the protein expected to trigger apoptosis pathway.

Upon several attempts, the results in the current study were not conclusive enough to validate the apoptosis activity. One of the major factors that contributes to this research outcome is the low concentration of recombinant protein, especially for the recombinant GFP-apoptin used in microinjection procedure. Hence, stability of recombinant apoptin is the main challenge for next investigations in order to evaluate for the functionality of recombinant protein in mammalian cell lines and animal model. Instead of checking the activity of caspase 3/7 and MMP, other cellular proteins activated during apoptosis could also be determined, such as Bax, Bak, cytochrome c, Nur77, caspase 9 and Apoptotic protease activating factor 1 (Apaf-1).

Conclusions

It is of no doubt that the recombinant apoptin alone, GFP-apoptin, Lic-apoptin, EGF-apoptin as well as H22-apoptin had been successfully expressed in *N. benthamiana*. In current study, recombinant apoptin, GFP-apoptin as well as EGF-apoptin could not be purified from soluble protein fraction efficiently since eluted proteins were always contaminated with a huge amount of HCPs. Alternatively, purification using denaturing condition yielded the protein at higher purity, especially recombinant GFP-apoptin (GFP-VP3-H) and lichenase-apoptin (Lic-VP3-H). In preliminary cell-based experiments, apoptin-induced apoptosis was not able to be confirmed in cells microinjected with recombinant GFP-VP3-H; however, majority of injected protein was found localising to cell nucleus. On the other hand, a dose-dependent growth inhibitory was observed when recombinant EGF-VP3-HK at high concentration was incubated with A549 cells. Internalisation of recombinant EGF-VP3-HK could not be confirmed in this study and more studies might be necessary to clarify for the internalisation activity of the protein. Although current cell-based experiment could not provide convincing data for the bioctivity of plant-made apoptin, there was some important findings that suggested future research orientation.

Chapter 8

References

Adair, B. M. 2000. Immunopathogenesis of chicken anemia virus infection. *Development and Comparative Immunology*. 24(2-3): 247-255.

American Cancer Society. Lung cancer (Non-small cell). 2016.

Angov, E. 2011. Codon usage: Nature's roadmap to expression and folding of proteins. *Biotechnology Journal*. 6: 650–659.

Anson, D. S. 2004. The use of retroviral vectors for gene therapy-what are the risks? A review of retroviral pathogenesis and its relevance to retroviral vector-mediated gene delivery. *Genetic Vaccines and Therapy*. 2: 9.

Artimo, P., Jonnalagedda, M., Arnold, K., Baratin, D., Csardi, G., De Castro, E., Duvaud, S., Flegel, V., Fortier, A., Gasteiger, E., Grosdidier, A,, Hernandez, C., Ioannidis, V., Kuznetsov, D., Liechti, R., Moretti, S., Mostaguir, K., Redaschi, N,, Rossier, G., Xenarios, I., and Stockinger, H. ExPASy: SIB bioinformatics resource portal, Nucleic Acids Res, 40(W1):W597-W603, 2012. URL: http://viralzone.expasy.org/all_by_species/117.html. Accessed date: 1th March 2013.

Ashkenazi, A. 2008. Targeting the extrinsic apoptosis pathway in cancer. *Cytokine & Growth Factor Reviews*. 19(3–4): 325–331.

Ashraf, G.M., Greig, N.H., Khan, T.A., Hassan, I., Tabrez, S., Shakil, S., Sheikh, I.A., Zaidi, S.K., Akram, M., Jabir, N.R., Firoz, C.K., Naeem, A., Alhazza, I.M., Damanhouri, G.A., Kamal, M.A. 2014. Protein misfolding and aggregation in Alzheimer's disease and type 2 diabetes mellitus. *CNS & Neurological Disorders - Drug Targets*. 13(7):1280-93.

Azevedo, A.M., Rosa, P.A., Ferreira, I.F. and Aires-Barros, M.R. 2009. Chromatography-free recovery of biopharmaceuticals through aqueous two-phase processing. *Trends in biotechnology*. 27(4):240-7.

Azzoni, A.R., Kusnadi, A.R., Miranda, E.A. and Nikolov, Z.L. 2002. Recombinant aprotinin produced in transgenic corn seed: extraction and purification studies. *Biotechnology and Bioengineering*. 80(3):268-76.

Backendorf, C., Visser, A. E., de Boer, A. G., Zimmerman, R., Visser, M., Voskamp, P., Zhang, Y. H., Noteborn, M. 2008. Apoptin: therapeutic potential of an early sensor of carcinogenic transformation. *The Annual Review of Pharmacology and Toxicology*. 48:143-69.

Backendorf, C., Visser, A. E., de Boer, A. G., Zimmerman, R., Visser, M., Voskamp, P., Zhang, Y. H., Noteborn, M. 2008. Apoptin: therapeutic potential of an early sensor of carcinogenic transformation. *The Annual Review of Pharmacology and Toxicology*. 48:143-69.

Bae Y1, Green ES2, Kim GY3, Song SJ4, Mun JY5, Lee S6, Park JI7, Park JS8, Ko KS9, Han J10, Choi JS11. 2016. Dipeptide-functionalized polyamidoamine dendrimer-mediated apoptin gene delivery facilitates apoptosis of human primary glioma cells. *International Journal of Pharmaceutics.* 515(1-2):186-200.

Barh, D. 2013. Molecular farming in the decades of omics. OMICS Applications in Crop Science. Pg: 583.

Batista, R. I. T. P., Teixeira, D. I. A., Melo, L. M., Bhat, M. H., Andreeva , L. E., Serova, I. A., Serov, O. L., Freitas, V. J. F. 2014. Phenotypic characteristics of F1 generation of transgenic goats producing hG-CSF in milk. *Biotechnology Letter*. 36:2155–2162.

Bechara, C. and Sagan, S. 2013. Cell-penetrating peptides: 20 years later, where do we stand? *FEBS Letters*. 587(12):1693-702.

Behura, S. K. and Severson, D. W. 2012. Comparative analysis of codon usage bias and codon context patterns between dipteran and hymenopteran sequenced genomes. *Public Library of Science PLOS ONE*. 7(8): e43111.

Bellamy, C. O. C. 1997. p53 and apoptosis. *British Medical Bulletin*. 53(3): 522-538.

Berg, J.M., Tymoczko, J.L., Stryer, L. 2002. Section 4.1, The Purification of Proteins Is an Essential First Step in Understanding Their Function. Biochemistry- 5th edition. Available from: http://www.ncbi.nlm.nih.gov/books/NBK22410/.

Biemelt, S., Sonnewald, U., Galmbacher, P., Willmitzer, L. and Müller, M. 2003. Production of human papillomavirus type 16 virus-like particles in transgenic plants. *Journal of virology*. 77(17):9211-20.

Borisjuk, N.V., Borisjuk, L.G., Logendra, S., Petersen, F., Gleba, Y. and Raskin, I. 1999. Production of recombinant proteins in plant root exudates. *Nature biotechnology*. 17(5):466-9.

Burek, M., Maddika, S., Burek, C. J., Daniel, P. T., Schulze-Osthoff, K. and Los, M. 2006. Apoptin-induced cell death is modulated by Bcl-2 family members and is Apaf-1 dependent. *Oncogene*. 25(15): 2213-2222.

Burgyan, J. and Havelda, Z. 2011. Viral suppressors of RNA silencing. *Trends in Plant Sciences*. 16(5):265-72.

Buyel, J.F., Twyman, R.M. and Fischer, R. 2015. Extraction and downstream processing of plant-derived recombinant proteins. *Biotechnology advances*. 33(6 Pt 1):902-13.

Calle, E. E. and Kaaks, R. 2004. Overweight, obesity and cancer: epidemiological evidence and proposed mechanisms. *Nature Reviews Cancer*. 4: 579-591.

Calle, E. E. and Thun, M. J. 2004. Obesity and cancer. *Oncogene*. 23: 6365–6378.

Cancer Research UK. Lung cancer survival statistics. Accessed on 26th December 2016. http://www.cancerresearchuk.org/health-professional/cancer-statistics/statistics-by-cancer-type/lung-cancer/survival#heading-Zero.

Cancer Research UK. URL: http://www.cancerresearchuk.org/home/. Accessed date: 4th May 2013.

Carmeliet, P. and Jain, R. K. 2000. Angiogenesis in cancer and other disease. *Nature*. 407: 249-257.

Carroll, D. J. 2009. Microinjection: methods and applications. pg:v.

Chelur, D., Strickler, J., Unal, O. and Scholtyssek, M. 2008. Fusion tags can improve the yield and solubility of many recombinant proteins. Of course, no single tag or cleavage method will answer every need. Fusion Tags for Protein Expression and Purification. Available from: http://www.biopharminternational.com/fusion-tags-protein-expression-and-purification?id=&pageID=1&sk=&date= (Date of accessed: 25 June 2016).

Chen, C. J., Chen, C. W., Wu, M. M. and Kuo, T. L. 1992. Cancer potential in liver, lung, bladder and kidney due to ingested inorganic arsenic in drinking water. *British Journal of Cancer*. 66(5): 888-892.

Chen, Q., Lai, H., Hurtado, J., Stahnke, J., Leuzinger, K. and Dent, M. 2013. Agroinfiltration as an effective and scalable strategy of gene delivery for production of pharmaceutical proteins. *Advanced Techniques in Biology & Medicine*. 1: 103.

Cheng, C. M., Huang, S. P., Chang, Y. F., Chung, W. Y. and You, C. Y. 2003. The viral death protein Apoptin interacts with Hippi, the protein interactor of Huntingtin-interacting protein 1. *Biochemical and Biophysical Research Communication*. 305(2): 359-3564.

Ciechanover, A. 2005. Proteolysis: from the lysosome to ubiquitin and the proteasome. *Nature Reviews Molecular Cell Biology*. 6: 79-87.

Cipriano, L.E., Romanus, D., Earle, C.C, Neville, B.A., Halpern, E. F. Gazelle, G.S. and McMahon, P.M. 2011. Lung cancer treatment costs, including patient responsibility, by stage of disease and treatment modality, 1992–2003. *Value Health*. 14(1): 41–52.

Costa, S., Almeida, A., Castro, A., & Domingues, L. 2014. Fusion tags for protein solubility, purification and immunogenicity in Escherichia coli: the novel Fh8 system. *Frontiers in Microbiology*. 5: 63.

Cotman, C. W. and Anderson, A. J. 1995. A potential role for apoptosis in neurodegeneration and Alzheimer's disease. *Molecular Neurobiology*. 10(1): 19-45.

Coultas, L. and Strasser, A. 2003. The role of the Bcl-2 protein family in cancer. *Seminars in Cancer Biology*. 13(2): 115-123.

Crowther, R.A., Berriman, J.A., Curran, W.L., Allan, G.M. and Todd, D. 2003. Comparison of the Structures of Three Circoviruses: Chicken Anemia Virus, Porcine Circovirus Type 2, and Beak and Feather Disease Virus. *Journal of Virology*. 77(24): 13036–13041.

Danen-van Oorschot, A. A. A. M., Fischer, D.F., Grimbergen, J. M., Zhuang, S. M., Falkenburr, J. H. F., Backendorf, C., Quax, P. H. A., Van der Eb, A. J. and Noteborn, M. H. M. 1997. Apoptin induces apoptosis in human transformed and malignant cells but not in normal cells. *Proceeding National Academy of Science USA*. 94: 5843–5847.

Danen-van Oorschot, A. A. A. M., Zhang, Y. H., Leliveld, S. R., Rohn, J. L., Seelen, M. C. M. J., Bolk, M. W., Van Zon, A., Erkeland, S. J., Abrahams, J. P., Mumberg, D. and Noteborn, M. H. M. 2003. Importance of Nuclear Localisation of Apoptin for Tumour-specific Induction of Apoptosis. *The Journal of Biological Chemistry*. 278 (30): 27729-27736.

Danen-van Oorschot, A. A., Voskamp, P., Seelen, M. C., van Miltenburg, M. H., Bolk, M. W., Tait, S. W., Boesen-de Cock, J. G., Rohn, J. L., Borst, J. and Noteborn, M. H. 2004. Human death effector domain-associated factor interacts with the viral apoptosis agonist Apoptin and exerts tumour-preferential cell killing. *Cell Death and Differentiation*. 11(5): 564-73.

Danen-van Oorschot2, A. A. A. M., Van der Eb, A. J. and Noteborn, M. H. M. 2000. The Chicken Anemia Virus-Derived Protein Apoptin Requires Activation of Caspases for Induction of Apoptosis in Human Tumor Cells. *Journal of virology*. 74(15): 7072-7078.

Danen-Van Oorschot2, A.A., Zhang, Y.H., Leliveld, S.R., Rohn, J.L., Seelen, M.C., Bolk, M.W., Van Zon, A., Erkeland, S.J., Abrahams, J.P., Mumberg, D., Noteborn, M.H. 2003. Importance of nuclear localization of apoptin for tumor-specific induction of apoptosis. *The Journal of Biological Chemistry*. 278(30):27729-36.

Dara, L., Aisner, M.D., Carrie, B., and Marshall, M.D. 2012. Molecular Pathology of Non–Small Cell Lung CancerA Practical Guide. *American Journal of Clinical Pathology*. 138(3):332-46.

Das, M. and Wakelee, H. 2014. Angiogenesis and lung cancer: ramucirumab prolongs survival in 2nd-line metastatic NSCLC. *Translational Lung Cancer Research*. 3(6): 397–399.

Daugas, E., Susin, S. A., Zamzami, N., Ferri, K. F., Irinopoulou, T., Larochette, N., Prevost, M. C., Leber, B., Andrews, D., Penninger, J. and Kroemer, G. 2000. Mitochondrio-nuclear translocation of AIF in apoptosis and necrosis. *The Journal of the Federation of American Societies for Experimental Biology*. 14(5): 729-739.

Davidson, E., Bryan, C., Fong, R. H., Barnes, T., Pfaff, J. M., Mabila, M., Rucker, J. B. and Doranz, B. J. 2015. Mechanism of Binding to Ebola Virus Glycoprotein by the ZMapp, ZMAb, and MB-003 Cocktail Antibodies. *Nature*. 89(21): 10982-10992.

De-la Monte, S. M., Sohn, T. K. and Wands, J. R. 1997. Correlates of p53- and Fas (CD95)-mediated apoptosis in Alzheimer's disease. *Journal of Neurological Sciences*. 152(1): 73-83.

Dinca, A., Chien, W.M. and Chin, M. T. 2016. Intracellular Delivery of Proteins with Cell-Penetrating Peptides for Therapeutic Uses in Human Disease. *International Journal of Molecular Sciences*.17(2): 263.

Dix, D. and Cohen, P. 1980. On The Role of Aging in Cancer Incidence. *Journal of Theoretical Biology*. 83(1): 163–173.

Duwi Fanata, W.I., Lee, S.Y., Lee, K.O. 2013. The unfolded protein response in plants: a fundamental adaptive cellular response to internal and external stresses. *Journal of Proteomics*. 93:356-68.

Elmore, S. 2007. Apoptosis: A review of programmed cell death. *Toxicologic Pathology*. 35(4):495-516

Enoch, T. and Norbury, C. 1995. Cellular responses to DNA damage: cell-cycle checkpoints, apoptosis and the roles of p53 and ATM. *Trends in Biochemical Sciences*. 20(10): 426-430.

Escobar, C., Hernández, L.E., Jiménez, A., Creissen, G., Ruiz, M.T. and Mullineaux, P.M. 2003. Transient expression of Arabidopsis thaliana ascorbate peroxidase 3 in *Nicotiana benthamiana* plants infected with recombinant potato virus X. *Plant cell report*. 21(7):699-704.

Escobar, M.A. and Dandekar A. M. 2000-2013. Post-Transcriptional Gene Silencing in Plants. In: Madame Curie Bioscience Database [Internet]. Austin (TX): Landes Bioscience. Available from: http://www.ncbi.nlm.nih.gov/books/NBK6037/ = (Date of accessed: 25 June 2016).

Feller, T., Thom, P., Koch, N., Spiegel, H., Addai-Mensah, O., Fischer, R., Reimann, A., Pradel, G., Fendel, R., Schillberg, S., Scheuermayer, M. and Schinkel, H. 2013. Plant-based production of recombinant Plasmodium surface protein pf38 and evaluation of its potential as a vaccine candidate. *Public Library of Science*. 8(11): e79920.

Ye, F., Zhong, B., Dan, G.R., Jiang, F., Sai,Y., Zhao, J.Q., Sun,H.Q. and Zou, Z.M. 2013. Therapeutic anti-tumor effect of exogenous apoptin driven by human survivin gene promoter in a lentiviral construct. *Archives of Medical Science.* 9(3): 561–568.

Fischer, R., Emans, N., Schuster, F., Hellwig, S. and Drossard, J. 1999. Towards molecular farming in the future: using plant-cell-suspension cultures as bioreactors. *Biotechnology and Applied Biochemistry*. 30(2): 109–112.

Fischer, R., Liao, Y.C. and Drossard, J. 1999. Affinity-purification of a TMV-specific recombinant full-size antibody from a transgenic tobacco suspension culture. *Journal of immunological methods.* 226(1-2):1-10.

Fischer, R., Stoger, E., Schillberg, S., Christou, P. and Twyman, R. M. 2004. Plant-based production of biopharmaceuticals. Current Opinion in Plant Biology. 7(2): 152–158.

Folkman, J. and Shing, Y. 1992. Angiogenesis. *Journal of Biology and Chemistry*. 267: 10931-10934.

Forman, S.M., DeBernardez, E.R., Feldberg, R.S. and Swartz, R.W. 1990. Crossflow filtration for the separation of inclusion bodies from soluble proteins in recombinant Escherichia coli cell lysate. 48(2–3): 263-279.

Fuchs, H., Bachran, C., Li, T., Heisler, I., Dürkop, H. and Sutherland, M. 2007. A cleavable molecular adapter reduces side effects and concomitantly enhances efficacy in tumor treatment by targeted toxins in mice. *Journal of Control Release*. 117(3):342-50.

Garabagi, F., Gilbert, E., Loos, A., McLean, M.D., Hall, J.C. 2012. Utility of the P19 suppressor of gene-silencing protein for production of therapeutic antibodies in Nicotiana expression hosts. *Plant Biotechnology Journal*. 10(9):1118-28.

Gazdar, A.F. 2009. Activating and resistance mutations of EGFR in non-small-cell lung cancer: role in clinical response to EGFR tyrosine kinase inhibitors. *Oncogene*. 28(Suppl 1): S24–S31.

GE Healthcare1. 2016. Affinity chromatography volume 2: Tagged proteins.

GE Healthcare2. 2016. Ion exchange chromatography: Principles and methods.

GE Healthcare3. 2016. Hydrophobic Interaction and Reversed Phase Chromatography Principles and Methods.

Gelvin, S. B. 2003. Agrobacterium-Mediated Plant Transformation: the Biology behind the “Gene-Jockeying” Tool. *Microbiology and Molecular Biology Reviews*. 67(1): 16–37.

Generic and Biosimilars Initiative. 2013. Biosimilar trastuzumab made in tobacco plants. URL: http://www.gabionline.net/Biosimilars/News/Biosimilar-trastuzumab-made-in-tobacco-plants. Accessed on: 25th December 2016.

Gleba, Y., Klimyuk, V. and Marillonnet, S. 2005. Magnifection—a new platform for expressing recombinant vaccines in plants. *Vaccine*. 23(17–18): 2042–2048.

Gleba, Y., Klimyuk, V. and Marillonnet, S. 2007. Viral vectors for the expression of proteins in plants. *Current Opinion in Biotechnology*. 18: 134-141.

GLOBOCAN. 2012. Fact sheets. Accessed on 25/12/2016. URL: http://globocan.iarc.fr/Pages/fact_sheets_cancer.aspx

Golan, D. E., Tashjiran, Jr. A. H., Armstrong, E. J. and Armstrong, A. W. 2005. Chapter 31: Principles of chemotherapy. In: Principles of pharmacology: The pathophysiologic basis of drug therapy. 2nd edition. Lippincott Williams & Wilkins. USA. Pg: 565-732.

Greenblatt, M. S., Bennett, W. P., Hollstein, M. and Harris, C. C. 1994. Mutations in the p53 Tumor Suppressor Gene: Clues to Cancer Etiology and Molecular Pathogenesis. *Cancer Research*. 54: 4855-4878.

Gross, A., McDonnell, J. M. and Korsmeyer, S. J. 1999. BCL-2 family members and the mitochondria in apoptosis. *Genes and Development*. 13: 1899-1911.

Gruijl, F. R. D. 1999. Skin Cancer and solar UV radiation. *European Journal of Cancer*. 35(14): 2003-2009.

Gruijl, F. R. D., Kranenc, H. J. V. and Mullendersb, L. H. F. 2001. UV-induced DNA damage, repair, mutations and oncogenic pathways in skin cancer. *Journal of Photochemistry and Photobiology B: Biology*. 63(1–3): 19–27.

Guan GF1, Zhao M, Liu LM, Jin CS, Sun K, Zhang DJ, Yu DJ, Cao HW, Lu YQ, Wen LJ. 2013. Salmonella typhimurium mediated delivery of Apoptin in human laryngeal cancer. *International Journal of Medical Science*. 10(12):1639-48.

Guelen L1, Paterson H, Gäken J, Meyers M, Farzaneh F, Tavassoli M. 2004. TAT-apoptin is efficiently delivered and induces apoptosis in cancer cells. *Oncogene*. 23(5):1153-65.

Guo, P., Fang, Q., Tao, H-Q, Schafer, C.A., Fenton, B. M., Ding, I., Hu, B. and Cheng, S. Y. 2003. Overexpression of vascular endothelial growth factor by MCF-7 breast cancer cells promotes estrogen-independent tumour growth in *vivo*. *Cancer Research*. 63: 4684-4691.

Gupta, P., Hall, C. K. and Voegler, A. C. 1998. Effect of denaturant and protein concentrations upon protein refolding and aggregation: A simple lattice model. *Protein Science*. 7: 2642-2652.

Hall, P. A., Coates, P. J., Ansari, B. and Hopwood, D. 1994. Regulation of cell number in the mammalian gastrointestinal tract: the importance of apoptosis. *Journal of Cell Science*. 107: 3569-3577.

Hecht, S.S. 2012. Lung Carcinogenesis by Tobacco Smoke. *International Journal of Cancer*. 131(12): 2724–2732.

Heisler, I., Keller, J., Tauber, R., Sutherland, M. and Fuchs, H. 2003. A cleavable adapter to reduce nonspecific cytotoxicity of recombinant immunotoxins. *International Journal of Cancer.* 103(2): 277-82.

Hetzel, C., Bachran, C., Fischer, R., Fuchs, H., Barth, S. and Stöcker, M. 2008. Small cleavable adapters enhance the specific cytotoxicity of a humanized immunotoxin directed against CD64-positive cells. *Journal of Immunotherapy*. 31(4):370-6.

Hooper, C. Accessed on 02/06/2016. EGFR interactions, roles and cancer therapy options by Dr. Claudie Hooper (KCL). Abcam. URL: http://www.abcam.com/index.html?pageconfig=resource&rid=10723#affil.

Huo, D. H., Yi, L. N. and Yang, J. 2008. Interaction with Ppil3 leads to the cytoplasmic localization of apoptin in tumour cells. Interaction with Ppil3 leads to the cytoplasmic localization of Apoptin in tumor cells. *Biochemical and Biophysical Research Communication*. 372(1): 14-18.

Hyder, A., Ehnert, S., Hinz, H., Nüssler, A.K., Fändrich, F. and Ungefroren, H. 2012. EGF and HB-EGF enhance the proliferation of programmable cells of monocytic origin (PCMO) through activation of MEK/ERK signaling and improve differentiation of PCMO-derived hepatocyte-like cells. *Cell Communication and Signalling*. 10(1):23.

Ivana, S. and David, P. 2016. ALK inhibitors in non-small cell lung cancer: the latest evidence and developments. *Therapeutic Advances in Medical Oncology*. 8(1): 32–47.

James, E.A., Wang, C., Wang, Z., Reeves, R., Shin, J.H., Magnuson, N.S. and Lee, J.M. 2000. Production and characterization of biologically active human GM-CSF secreted by genetically modified plant cells. *Protein expression and purification*. 19(1):131-8.

Jeurissen, S. H., Wagenaar, F., Pol, J, M., Van der Eb, A. J., and Noteborn, M. H. 1992. Chicken anemia virus causes apoptosis of thymocytes after in vivo infection and of cell lines after in vitro infection. *Journal of Virology*. 66(12): 7383-7388.

Jin, T.C., Wang, J., Zhu, X.J., Xu, Y.N., Zhou, X.F. and Yang, L.P. 2015. A new transient expression system for large-scale production of recombinant proteins in plants based on air-brushing an Agrobacterium suspension. *Biotechnology Reports*. 6: 36–40.

Kanoria, S. and Burma, P. K. 2012. A 28 nt long synthetic 5′UTR (synJ) as an enhancer of transgene expression in dicotyledonous plants. *BMC Biotechnology*. 12:85.

Keller, J., Heisler, I., Tauber, R., Fuchs, H. 2001. Development of a novel molecular adapter for the optimization of immunotoxins. *Journal of controlled release*. 74(1-3): 259-61.

Kerr, J. F., Wyllie, A. H. and Currie, A. R. 1972. Apoptosis: a basic biological phenomenon with wide-ranging implications in tissue kinetics. *British Journal of Cancer*. 26(4):239-257

Kim, M.Y., Li, J.Y., Tien, N.Q. and Yang, M.S. 2016. Expression and assembly of cholera toxin B subunit and domain III of dengue virus 2 envelope fusion protein in transgenic potatoes. *Protein Expression and Purification*. PII: S1046-5928(16)30105-X. DOI: 10.1016/j.pep.2016.06.006.

Kim, T. G., Lee, H. J., Jang, Y. S., Shin, Y. J., Kwon, T. H., Yang, M.S. 2008. Co-expression of proteinase inhibitor enhances recombinant human granulocyte-macrophage colony stimulating factor production in transgenic rice cell suspension culture. *Protein Expression and Purification*. 61(2): 117-21.

Kingsbury, N.J. and McDonald, K.A. 2014. Quantitative Evaluation of E1 Endoglucanase Recovery from Tobacco Leaves Using the Vacuum Infiltration-Centrifugation Method. *BioMed Research International.* 2014(1):483596.

Kittur, F.S., Arthur, E., Nguyen, M., Hung, C.Y., Sane, D.C., Xie, J. 2015. Two-step purification procedure for recombinant human asialoerythropoietin expressed in transgenic plants. *International Journal of Biological Macromolecules*. 72:1111-6.

Komarnytsky, S., Borisjuk, N.V., Borisjuk, L.G., Alam, M.Z., Raskin, I. 2000. Production of recombinant proteins in tobacco guttation fluid. *Plant Physiology*. 124(3): 927-34.

Kopito, R. R. 2000. Aggresomes, inclusion bodies and protein aggregation. *Trends in Cell Biology*. 10(12): 524–530

Kuusisto, H. V., Wagstaff, K. M., Alvisi, G., Jans, D. A. 2008. The C- terminus of apoptin represents a unique tumour cell-enhanced nuclear targeting module. *International Journal of Cancer*. 123(12): 2965-9

Lacorte, C., Lohuisa, H., Goldbacha, R., and Prinsa, M. 2007. Assessing the expression of chicken anemia virus proteins in plants. *Virus Research*. 129(2): 80–86.

Lamkanfi, M. and Dixit, V. M. 2010. Manipulation of Host Cell death pathways during microbial infection. *Cell Host and Microbe*. 8(1): 44-54.

Lawen, A. 2003. Apoptosis – an introduction. *Bioessays*. 25(9): 888-896.

Lee, J.H., Kim, N.S., Kwon, T.H., Jang, Y.S. and Yang, M.S. 2002. Increased production of human granulocyte-macrophage colony stimulating factor (hGM-CSF) by the addition of stabilizing polymer in plant suspension cultures. *Journal of biotechnology*. 96(3):205-11.

Lee, L. Y. and Gelvin, S. B. 2008. T-DNA Binary Vectors and Systems. *Plant Physiology*. 146(2): 325–332

Lee, M. S., Sun, F. C., Huang, C. H., Lien, Y. Y., Feng, S. H., Lai, G. H., Lee, M. S., Chao, J., Chen, H. J., Tzen, J. T. and Cheng, H.Y. 2012. Efficient production of an engineered apoptin from chicken anemia virus in a recombinant E. coli for tumor therapeutic applications. *Biomed Central (BMC) biotechnology*. 12:27.

Lee, M.S., Sun, F. C., Huang, C.H, Lien, Y.Y., Feng, S.H., Lai, G. H., Lee, M. S., Chao, J., Chen, H. J. and Tzen, T. C. 2012. Efficient Production of an Engineered Apoptin from Chicken Anemia Virus in a Recombinant E. coli for Tumor Therapeutic Applications. *BMC Biotechnology*. 12:27.

Leibly, D.J., Nguyen, T.N., Kao, L.T., Hewitt, S.N., Barrett, L.K. and Van Voorhis, W.C. 2012. Stabilizing additives added during cell lysis aid in the solubilization of recombinant proteins. *Peer-reviewed open access scientific journal*. 7(12): e52482. doi: 10.1371.

Leliveld, S. R., Dame, R. T., Rohn, J. L., Noteborn, M. H. and Abrahams, J.P. 2004. Apoptin's functional N- and C-termini independently bind DNA. *FEBS Letter*. 557(1-3):155-158.

Leliveld[a], S. R., Zhang, Y. H., Rohn, J. L., Noteborn, M. H. M. and Abrahams, J. P. 2003. Apoptin induces tumour-specific apoptosis as a globular multimer. *The Journal of Biology and Chemistry*. 278(11): 9042-9051

Leliveld[b], S. R., Noteborn, M. H., Abrahams, J. P. 2003. Prevalent conformations and subunit exchange in the biologically active apoptin protein multimer. *European Journal of Biochemistry*. 270(17): 3619-27.

Leliveld[c], S. R., Dame, R. T., Mommaas, M. A., Koerten, H. K., Wyman, C., Danen-van Oorschot, A. A., Rohn, J. L., Noteborn, M. H., Abrahams, J.P. 2003. Apoptin protein multimers form distinct higher-order nucleoprotein complexes with DNA. *Nucleic Acids Research*. 31(16): 4805-13.

Leuzinger, K., Dent, M., Hurtado, J., Stahnke, J., Lai, H., Zhou, X., and Chen, Q. 2013. Efficient Agroinfiltration of Plants for High-level Transient Expression of Recombinant Proteins. Journal of visualized experiments. (77): 50521.

Li Xi, Jin N, Mi Z, Lian H, Sun L, Li X, Zheng H. 2006. Antitumor effects of a recombinant fowlpox virus expressing Apoptin in vivo and in vitro. *International journal of cancer*. 119(12):2948-57.

Li, F., Srinivasan, A., Wang, Y., Armstrong, R.C., Tomaselli, K.J. and Fritz, L.C. 1997. Cell-specific induction of apoptosis by microinjection of cytochrome c. Bcl-xL has activity independent of cytochrome c release. *The Journal of Biological Chemistry*. 272(48): 30299-305.

Li, L. Y., Luo, X. and Wang, X. D. 2001. Endonuclease G is an apoptotic DNase when released from mitochondria. *Nature*. 412: 95-99

Lico, C., Chen, Q., and Santi, L. 2008. Viral Vectors for production of Recombinant Proteins in Plants. *Journal of Cell Physiology*. 216: 366-377

Lim, S.N., Zeenathul, N. A., Mohd Azmi, M. L., Abas Mazni, O. and Fauziah, O. 2011. Effect of Protein Concentration and Injection Pressure in Microinjection Delivery of Maltose Binding Protein into Breast Cancer Cells. *Pertanika Journal of Science and Technology*. 19 (2): 273 – 283.

Lindbo, JA. 2007. TRBO: a high-efficiency tobacco mosaic virus RNA-based overexpression vector. *Plant Physiology* .145(4):1232-40.

Liotta, L. A. 1986. Tumour invasion and metastases- role of the extracellular matrix: Rhoads memorial award lecture. *Cancer research*. 46: 1-7

Liu SS1, Ben SB, Zhao HL. 2008. Construction of apoptin gene delivery system and its effect on apoptosis of A375 cells. *Xi Bao Yu Fen Zi Mian Yi Xue Za Zhi*. 24(2):133-5.

Lodish, H., Berk, A., Zipursky, S. L., Matsudaira, P., Baltimore, D. and Darnell, J. 2004. Section 17.3: Overview of the secretory pathway. Molecular Cell Biology, 5th edition. New York, NY. W.H. Freeman and Company.

Los, M., Panigrahi, S., Rashedi, I., Mandal, S., Stetefeld, J., Essmann, F. and Schulze-Osthoff, K. 2009. Apoptin, a tumour-selective killer. *Biochimistry Biophysic Acta.* 1793(8): 1335-42

Ma JL, Han SX, Zhao J, Zhang D, Wang L, Li YD, Zhu Q. 2012. Systemic delivery of lentivirus-mediated secretable TAT-apoptin eradicates hepatocellular carcinoma xenografts in nude mice. *International Journal of oncology*. 41(3):1013-20.

Maddika, S., Bay, G.H., Kroczak, T. J., Ande, S. R., Maddika, S., Wiechec, E., Gibson, S.B., Los, M. 2007. Akt is transferred to the nucleus of cells treated with apoptin, and it participates in apoptin-induced cell death. *Cell Proliferation*. 240(6): 835-848.

Maddika, S., Booy, E. P., Johar, D., Gibson, S. B., Ghavami, S., Los, M. 2005. Cancer-specific toxicity of apoptin is independent of death receptors but involves the loss of mitochondrial membrane potential and the release of mitochondrial cell-death mediators by a Nur77-dependent pathway. *Journal of Cell Science*. 118(9): 4485-4493.

Maddika, S., Wiechec, E., Ande, S. R., Poon, I. K., Fischer, U., Wesselborg, S., Jans, D. A., Schulze-Osthoff, K. and Los, M. 2010. Interaction with PI3-kinase contributes to the cytotoxic activity of Apoptin. *Oncogene*. 27(21): 3060–3065.

MAKNA-National Cancer Counsil. URL: http://www.makna.org.my/. Accessed date: 1th March 2013

Mansour, N.M. and Abdelaziz, S.A. 2016. Oral Immunization of Mice with Engineered Lactobacillus gasseri NM713 Strain Expressing Streptococcus pyogenes M6 Antigen. *Microbiology and Immunology*. DOI: 10.1111/1348-0421.12397D.

Marsian, J. and Lomonossoff, G. P. 2016. Molecular pharming - VLPs made in plants. Current *Opinion in Biotechnology*. 37: 201-6.

McIlwain, D. R., Berger, T. and Mak, T.W. 2013. Caspase functions in cell death and disease. *Cold Spring Harbour Perspective Biology*. 5(4):a008656. doi: 10.1101/cshperspect.a008656.

Michaud, D. S., Giovannucci, E., Willett, W. C., Colditz, G. A., Stampfer, M. J., Fuchs, C. S. 2001. Physical Activity, Obesity, Height, and the Risk of Pancreatic Cancer. *The Journal of the American Medical Association*. 286(8): 921-929.

Mochizuki, H., Goto, K., Mori, H. and Mizuno, Y. 1996. Histochemical detection of apoptosis in Parkinson's disease. *Journal of Neurological Sciences*. 137(2): 120-3.

Mohammadi Vida1,2, Takhshid Mohammad Ali1,2, Behzad-Behbahani Abbas 1,2, Hosseini Seyed Younes3, Rafiei Dehbidi Golamreza1,2, Taheri Mohammad Naser1,2, Seyyedi Noorossadat. 2016. In vitro Targeting of Prostate Cancer Cells Using Adenoviral Vector Containing Apoptin Gene under PSA Promoter. 2nd international and 14th Iranian Genetic Congress.

Mohanty, C., Das, M., Kanwar, J.R., Sahoo, S.K. 2011. Receptor mediated tumor targeting: An emerging approach for cancer therapy. *Current Drug Delivery*. 8: 45-58.

Mohd-Azmi,M.L., Ghrissi,M., Raha,R.A., Yusof,K. and Aini,I. 1997. The complete DNA sequence of VP3 gene of Chicken Anemia Virus (Malaysian Isolate). Veterinary Pathology & Microbiology, Faculty of Veterinary Medicine & Animal Science, Universiti Putra Malaysia, UPM, Serdang, Selangor 43400, Malaysia.

Musiychuk, K., Stephenson, N., Bi, H., Farrance, C. E., Orozovic, G., Brodelius, M., Brodelius, P., Horsey, A., Ugulava, N., Shamloul, A. M., Mett, V., Rabindran, S., Streatfield, S. J., and Yusibov, V. 2007. A launch vector for the production of vaccine antigens in plants. *Influenza and Other Respiratory Viruses.* 1: 19–25.

Nishimura, A., Aichi, I. and Matsuoka, M. 2007. A protocol for Agrobacterium-mediated transformation in rice. A protocol for Agrobacterium-mediated transformation in rice. *Nature Protocols*. 1: 2796 – 2802.

Nogueira-Dantas, E. O., Ferreira, A. J., Astolfi-Ferreira, C. S., Brentano, L. 2007. Cloning and expression of chicken anemia virus VP3 protein in Escherichia coli. *Comparative Immunology, Microbiology and Infectious Diseases*. 30(3):133-42.

Normanno, N., De Luca, A., Bianco, C., Strizzi, L., Mancino, M., Maiello, M.R., Carotenuto, A., De Feo, G., Caponigro, F. and Salomon, D.S. 2006. Epidermal growth factor receptor (EGFR) signaling in cancer. *Gene*. 366(1): 2-16.

Noteborn, M. H. M., Danen-van Oorschot, A. A. A. M. and Van der Eb, A. 1998. The Apoptin gene of chicken anemia virus in the induction of apoptosis in human tumorigenic cells and in gene therapy of cancer. *Gene Therapy Molecular Biology*. 1: 399-406.

Noteborn, M.H., Todd, D., Verschueren, C.A., de Gauw, H.W., Curran, W. L., Veldkamp, S., Douglas, A.J., McNulty, M.S., van der EB, A.J. and Koch G. 1994. A single chicken anemia virus protein induces apoptosis. Journal of Virology. 68(1): 346–351.

Noteborn, M.H.M. and Koch, G. 1995. Chicken anemia virus infection: molecular basis of pathogenicity. *Avian Pathology*. 24(1): 11-31

Olijslagers, S. J., Zhang, Y. H., Backendorf, C. and Noteborn, M. H. 2006. Additive cytotoxic effect of apoptin and chemotherapeutic agents paclitaxel and etoposide on human tumour cells. *Basic Clinical Pharmacology and Toxicology*. 100(2):127-31.

Oltval, Z. N., Milliman, C. L. and Korsmeyer, S. J. 1993. Bcl-2 heterodimerizes in vivo with a conserved homolog, Bax, that accelerates programed cell death. *Cell*. 74(4): 609-619

Outsourcing-Phama.com. 2004. Sigma-Aldrich to distribute animal-free aprotinin. Acess link: http://www.outsourcing-pharma.com/Preclinical-Research/Sigma-Aldrich-to-distribute-animal-free-aprotinin. Accessed on 25 December 2016.

Paez JG1, Jänne PA, Lee JC, Tracy S, Greulich H, Gabriel S, Herman P, Kaye FJ, Lindeman N, Boggon TJ, Naoki K, Sasaki H, Fujii Y, Eck MJ, Sellers WR, Johnson BE, Meyerson M. 2004. EGFR mutations in lung cancer: correlation with clinical response to gefitinib therapy. *Science*. 304(5676):1497-500.

Parijs, L. V., Biuckians, A. and Abbas, A. K. 1998. Functional roles of Fas and Bcl-2-regulated apoptosis of T lymphocytes. *The Journal of Immunology*. 160(5): 2065-2071

Peters, M. A., Jackson, D. C., Crabb, B. S. and Browning, G. F. 2002. Chicken Anemia Virus VP2 is a novel dual specificity protein phosphatase. *The Journal of Biological Chemistry*. 277(42):39566-39573.

Pietersen AM1, Rutjes SA, van Tongeren J, Vogels R, Wesseling JG, Noteborn MH. 2004. The tumor-selective viral protein apoptin effectively kills human biliary tract cancer cells. *Journal of molecular medicine*. 82(1):56-63

Pietersen AM1, van der Eb MM, Rademaker HJ, van den Wollenberg DJ, Rabelink MJ, Kuppen PJ, van Dierendonck JH, van Ormondt H, Masman D, van de Velde CJ, van der Eb AJ, Hoeben RC, Noteborn MH.. 1999. Specific tumor-cell killing with adenovirus vectors containing the apoptin gene. *Gene Therapy*. 6(5):882-92.

PlantForm. Accessed on 26th December 2016. http://www.plantformcorp.com/products.aspx.

Pogue GP1, Vojdani F, Palmer KE, Hiatt E, Hume S, Phelps J, Long L, Bohorova N, Kim D, Pauly M, Velasco J, Whaley K, Zeitlin L, Garger SJ, White E, Bai Y, Haydon H, Bratcher B. 2010. Production of pharmaceutical-grade recombinant aprotinin and a monoclonal antibody product using plant-based transient expression systems. *Plant Biotechnology Journal*. 8(5):638-54.

Poon, I. K., Oro, C., Dias, M. M., Zhang, J., Jans, D. A. 2005. Apoptin nuclear accumulation is modulated by a CRM1-Recognised Nuclear export signal that is active in normal but not in tumor cells. *Cancer Research*. 65(16): 7059-64.

Prasetyo, A. A., Kamahora, T., Kuroishi, A., Murakami, K. and Hino, S. 2009. Replication of chicken anemia virus (CAV) requires apoptin and is complemented by VP3 of human torque teno virus (TTV). *Virology*. 385(1): 85–92

Puigbo P, Bravo IG and Garcia-Vallve S. 2008. CAIcal: a combined set of tools to assess codon usage adaptation. *Biology Direct*. 3:38.

Qian, Y. C., Qiu, M., Wu, Q. Q., Tian, Y. Y., Zhang, Y., Gu, N., Li, S. Y. Xu, L. and Yin, R. 2014. Enhanced cytotoxic activity of cetuximab in EGFR-positive lung cancer by conjugating with gold nanoparticles. *Nature Science Report*. 4: 7490.

Quax, T.E.F., Claassens, N.J., So, D. and Van der Oos, J. 2015. Codon bias as a means to fine-tune gene expression. *Molecular Cell*. 59: 149-161.

Raha, S., Paunesku, T. and Woloschak, G. 2011. Peptide mediated cancer targeting of nanoconjugates. *Wiley Interdisciplinary Reviews: Nanomedicine and Nanobiotechnology*. 3(3): 269-281.

Rajkumar, T. 2001. Growth factors and growth factor receptors in cancer. *Current Science*. 81 (5):535-541.

Rang, H.P., Dale, M. M., Ritter, J. M. and Flower, R. J. 2007. Section 5: Cancer chemotherapy. In: Rang and Dale's pharmacology. 6th edition. *Churchill Livingstone Elsevier*. Pg: 718-738.

Riedl, S. J. and Salvesen, G. S. 2007. The apoptosome: signalling platform of cell death. *Nature Reviews Molecular Cell Biology*. 8: 405-413.

Rohn, J. L., Zhang, Y. H., Aalbers, R. I., Otto, N., Den Hertog, J., Henriquez, N. V., Van De Velde, C. J., Kuppen, P. J., Mumberg, D., Donner, P., Noteborn, M. H. 2002. A tumour specific kinase activity regulates the viral death protein apoptin. *The Journal of Biological Chemistry*. 277(52): 50820-50827.

Rollano Peñaloza, O. M., Lewandowska, M., Stetefeld, J., Ossysek, K., Madej, M., Bereta, J., Sobczak, M., Shojaei, S., Ghavami, S. and Los, M. J. 2014. Apoptins: selective anticancer agents. Trends Molecular Medicine. 20(9):519-28.

Roy, G., Weisburg, S., Rabindran, S. and Yusibov, V. 2010. A novel two-component Tobacco mosaic virus-based vector system for high-level expression of multiple therapeutic proteins including a human monoclonal antibody in plants. *Virology*. 405: 93-99

Ruberti, C., Kim, S. J., Stefano, G. and Brandizzi, F. 2015. Unfolded protein response in plants: one master, many questions. *Current Opinion in Plant Biology*. 27: 59-66.

Russell, J. W., Sullivan, K. A., Windebank, A. J., Herrmann, D. N. and Feldman, E. L. 1999. Neurons undergo apoptosis in animal and cell culture models of diabetes. *Neurobiology of Disease*. 6(5):347-363

Sainsbury, F. and Lomonossoff, G. P. 2014. Transient expressions of synthetic biology in plants. *Current Opinion in Plant Biology*. 19: 1–7

Santra, M., Reed, C.C., and Lozzo, R.V. 2002. Decorin Binds to a Narrow Region of the Epidermal Growth Factor (EGF) Receptor, Partially Overlapping but Distinct from the EGF-binding Epitope. *The Journal of Biological Chemistry*. 277, 35671-35681.

SBIRSource. 2014. A MERS-CoV Receptor Decoy. Access link: https://sbirsource.com/sbir/awards/149909-a-mers-cov-receptor-decoy. Accessed on 25 December 2016.

Scheller, J., Henggeler, D., Viviani, A. and Conrad. U. 2004. Purification of spider silk-elastin from transgenic plants and application for human chondrocyte proliferation. *Transgenic Research*. 13(1):51-7.

Schlessinger, J., Shechter, Y., Willingham, M. C. and Pastan, I. 1978. Direct visualization of binding, aggregation, and internalization of insulin and epidermal growth factor on living fibroblastic cells. *Proceedings of the National Academy of Sciences*. 75(6):2659-63.

Scopes, R. K. 1994. Chapter 1: Protein purification laboratory. Protein Purification: Principles and Practice. Pg: 3-4.

Shah, K.H., Almaghrabi, B. and Bohlmann, H. 2013. Comparison of Expression Vectors for Transient Expression of Recombinant Proteins in Plants. *Plant Molecular Biology Reporter*. 31:1529-1538.

Sharp, P. M. and Li, W. H. 1987. The codon adaptation index - a measure of directional synonymous codon usage bias and its potential applications. *Nucleic Acids Research*. 15: 1281-1295.

Shay, J. W. 1997. Telomerase in human development and cancer. *Journal of cellular physiology*. 173: 266-270.

Slater, A., Scott, N. W. and Fowler, M. R. 2003. Plant Biotechnology: The Genetic Manipulation of Plants. Oxford. UK. Pp: 63.

Sparks CA1, Doherty A, Jones HD. 2014. Genetic transformation of wheat via Agrobacterium-mediated DNA delivery. *Methods in Molecular Biology*. 1099:235-50.

Stahnke, B., Thepen, T., Stocker, M., Rosinke, R., Jost, E., Fischer, R., Tur, M.K. and Barth, S. 2008. Granzyme B-H22 (scFv), a human immunotoxin targeting CD64 in acute myeloid leukemia of monocytic subtypes. *Molecular cancer therapeutics*. 7(9):2924-32.

Streatfield, S. J. 2007. Approaches to achieve high-level heterologous protein production in plants. *Plant Biotechnology Journal*. 5: 2–15.

Streatfield, S.J., Lane, J.R., Brooks, C.A., Barker, D.K., Poage, M.L., Mayor, J.M., Lamphear, B.J., Drees, C.F., Jilka, J.M., Hood, E.E. and Howard, J.A. 2003. Corn as a production system for human and animal vaccines. *Vaccine*. 21(7-8):812-5.

Sun, J., Wang, Y. Z., Zong, Y. Q. and Qu, S. 2003. Cloning of chicken anemia virus VP3 gene and apoptosis inductive effect of VP3 gene *in vitro*. *Journal of Huazhong University of Science and Technology*. 23(4): 329-331.

Sun, J., Yan, Y., Wang, X.T., Liu, X.W., Peng, D.J., Wang, M., Tian, J., Zong, Y.Q., Zhang, Y.H., Noteborn, M. H. and Qu, S. 2009. PTD4-apoptin protein therapy inhibits tumor growth in vivo. *International Journal of Cancer*. 124(12): 2973-81.

Teodoro, J. G., Heilman, D. W., Parker, A. E., and Green, M. R. 2004. The viral protein apoptin associates with the anaphase-promoting complex to induce G2/M arrest and apoptosis in the absence of p53. *Genes and Development*. 18: 1952-1957.

Terpe, K. 2003. Overview of tag protein fusions: from molecular and biochemical fundamentals to commercial systems. *Applied Microbiology and Biotechnology*. 60:523–533.

Torchilin, V. 2008. Intracellular delivery of protein and peptide therapeutics. *Drug discovery today: Technologie*s. 5(2-3): e95-e103.

Urh, M., Simpson, D., Zhao, K. 2009. Chapter 26 Affinity Chromatography: General Methods. Methods in Enzymology. 463: 417–438.

Van der Pola, L. and Tramperb, J. 1998. Shear sensitivity of animal cells from a culture-medium perspective. *Trends in Biotechnology*. 16(8): 323–328.

Van Loo, G., Schotte, P., Van Gurp, M., Demol, H., Hoorelbeke, B., Gevaert, K., Rodriguez, I., Ruiz-Carrillo, A., Vandekerckhove, J., Declercq, W., Beyaert, R. and Vandenabeele, P. 2001. Endonuclease G: a mitochondrial protein released in apoptosis and involved in caspase-independent DNA degradation. *Cell Death and Differentiation*. 8(12):1136-1142.

Verma, R., Boletia, e., and Georgea, A. J. T. 1998. Antibody engineering: Comparison of bacterial, yeast, insect and mammalian expression systems. *Journal of Immunological Methods*. 216(1–2): 165–181.

Vitale, A. 2013. More players in the plant unfolded response. *Proceedings of the National Academy of Sciences*. 110(48): 19189-19190.

Vogler, H., Akbergenov, R., Shivaprasad, P.V., Dang, V., Fasler, M., Kwon, M.-O., Zhanybekova, S., Hohn, T. and Heinlein, M. 2007. Modification of small RNAs associated with suppression of RNA silencing by tobamovirus replicase protein. *Journal of Virolog*y. 81: 10379–10388.

Walboomers, J. M. M., Jacobs, M. V., Manos, M. M., Bosch, F. X., Kummer, J. A., Shah, K. V., Snijders, P. J. F., Peto, J., Meijer, C. J. L. M., Muñoz, N. 1999. Human papillomavirus is a necessary cause of invasive cervical cancer worldwide. *The Journal of Pathology*. 189(1): 12–19

Walker, P. R., Leblanc, J., Smith, B., Pandey, S., and Sikorska, M. 1999. Detection of DNA Fragmentation and Endonucleases in Apoptosis. *Methods*. 17(4): 329-338.

Walker, P. R., Weaver, V. M., Lach, B., LeBlanc, J. and Sikorska, M. 1994. Endonuclease activities associated with high molecular weight and internucleosomal DNA fragmentation in apoptosis. *Experimental Cell Research*. 213(1): 100–106.

Ward, C.W. and Garrett, T. P. J. 2001. The relationship between the L1 and L2 domains of the insulin and epidermal growth factor receptors and leucine-rich repeat modules. *BMC Bioinformatics*. 2:4.

Wattel, E., Preudhomme, C., Hecquet, B., Vanrumbeke, M., Quesnel, B., Dervite, I., Morel, P. and Fenaux, P. 1994. p53 mutations are associated with resistance to chemotherapy and short survival in hematologic malignancies. *Blood*. 84(9): 3148-3157.

Weinberg, R. A. 2007. The biology of cancer. Garland Science, Taylor & Francis Group, LLC. USA.

Widlak, P. 2000. The DFF40/CAD endonuclease and its role in apoptosis. *Acta Biochimia Polonica*. 47(4):1037-44.

Wilken, L.R. and Nikolov, Z.L. 2012. Recovery and purification of plant-made recombinant proteins. *Biotechnology advances*. 30(2):419-33.

Wolk, A., Gridley, G., Svensson, M., Nyrén, O., McLaughlin, J. K., Fraumeni, J. F., Adami, H. O. 2001. A prospective study of obesity and cancer risk (Sweden). *Cancer Causes & Control*. 12(1): 13-21.

World Health Organisation (WHO). URL: http://www.who.int/mediacentre/factsheets/fs297/en/ Accessed date: 1th March 2013.

Wroblewski,T., Tomczak, A. and Michelmore, R. 2005. Optimization of Agrobacterium-mediated transient assays of gene expression in lettuce, tomato and Arabidopsis. *Plant Biotechnology Journal.* 3(2):259-73.

Wu Y1, Zhang X, Wang X, Wang L, Hu S, Liu X, Meng S. 2012. Apoptin enhances the oncolytic properties of Newcastle disease virus. *Intervirology*. 55(4):276-86.

Xu, H., Montoya, F. U., Wang, Z., Lee, J.M., Reeves, R., Linthicum, D.S., Magnuson, N.S. 2002. Combined use of regulatory elements within the cDNA to increase the production of a soluble mouse single-chain antibody, scFv, from tobacco cell suspension cultures. *Protein Expression and Purification.* 24(3):384-94.

Yang, J., Barr, L.A., Fahnestock, S.R., Liu, Z. B. 2005. High yield recombinant silk-like protein production in transgenic plants through protein targeting. *Transgenic Research*. 14(3): 313-24.

Yang, L., Wang, H., Liu, J., Li, L., Fan, Y., Wang, X., Song, Y., Sun, S., Wang, L., Zhu, X., Wang, X. 2008. A simple and effective system for foreign gene expression in plants via root absorption of agrobacterial suspension. *Journal of Biotechnology*. 134(3-4):320-4.

Yao,J., Weng, Y.Q., Dickey, A. and Wang, Y.J. 2015. Plants as Factories for Human Pharmaceuticals: Applications and Challenges. *International Journal of Molecular Sciences*. 16(12): 28549–28565.

Yina, J. C., Lib, G. X., Rena, X. F. and Herrlerc, G. 2007. Select what you need: A comparative evaluation of the advantages and limitations of frequently used expression systems for foreign genes. *Journal of Biotechnology*. 127(3): 335–347

Yuasa, N., Taniguchi, T. and Yoshida, I. 1979. Isolation and some characterization of an agent inducing anemia in Chicken. *Avian Disease*. 23(2): 366-385

Zhang, Y. and Yu, L.C. 2008. Single-cell microinjection technology in cell biology. *BioEssays*. 30:606–610.

Zhang, Y.H., Leliveld, S.R., Kooistra , K., Molenaar, C., Rohn, J.L., Tanke, H.J., Abrahams, J.P. and Noteborn, M.H. 2003. Recombinant Apoptin multimers kill tumor cells but are nontoxic and epitope-shielded in a normal-cell-specific fashion. *Experimental Cell Research*. 289: 36–46.

Zhuang, S. M., Shvarts, A., van Ormondt, H., Jochemsen, A. G., van der Eb, A. J., Noteborn, M. H. 1995. Apoptin, a protein derived from chicken anemia virus, induces p53-independent apoptosis in human osteosarcoma cells. *Cancer Research*. 55(3): 486-489.

Chapter 9

Appendices

Appendices for Chapter 3

3.1 Nucleotide and amino acid sequences of synthetic apoptin gene cassette, PR-VP3-HK

Nucleotide sequence

TGTACATTAATTAAATGGGTTTCGTGCTGTTCAGCCAGCTGCCTTCTTTCCTTCTTGT
GTCTACCCTTCTGCTGTTCCTGGTGATCTCTCATTCTTGCAGGGCTATGGATGCTCTG
CAAGAGGATACTCCTCCTGGTCCTTCTACTGTTTTCAGGCCTCCTACTTCTAGCAGGC
CTCTTGAAACTCCTCACTGCAGAGAGATCAGGATCGGTATCGCTGGTATTACCATCA
CCCTTTCTTTGTGCGGTTGCGCTAATGCTAGGGCTCCTACTCTTAGATCTGCTACCGC
TGATAACAGCGAGAGCACCGGTTTCAAGAACGTGCCAGATCTTAGGACCGATCAGC
CTAAGCCTCCAAGCAAGAAGAGAAGCTGCGATCCTTCTGAGTACAGGGTGAGCAAG
CTGAAAGAGAGCCTTATCACTACCACCCCTTCTAGGCCAAGGACTGCTAAGAGAAG
GATTAAGCTTCATCACCATCACCACCACAAGGATGAGCTGTAGCTCGAGGGCGCGC
CGCTAGC

Amino acid sequence

MGFVLFSQLPSFLLVSTLLLFLVISHSCRAMDALQEDTPPGPSTVFRPPTSSRPLETPHCRE
IRIGIAGITITLSLCGCANARAPTLRSATADNSESTGFKNVPDLRTDQPKPPSKKRSCDPSE
YRVSKLKESLITTTPSRPRTAKRRIKLHHHHHHKDEL*

Features

Signal peptide PR1a	: (nucleotide) 15…104	(amino acid) 1…30
VP3-A	: (nucleotide) 105…467	(amino acid) 31…151
Hexahistidine	: (nucleotide) 468…485	(amino acid) 152…157
ER retention signal	: (nucleotide) 486…497	(amino acid) 158…161

3.2 Nucleotide and amino acid sequences of synthetic apoptin gene cassette, PR-GFP-VP3-HK

Nucleotide sequence

TGTACATTAATTAAATGGGTTTCGTGCTGTTCAGCCAGCTGCCTTCTTTCCTTCTTGT
GTCTACCCTTCTGCTGTTCCTGGTGATCTCTCATTCTTGCAGGGCTGCTTCTAAGGGT
GAGGAACTTTTCACTGGTGTGGTGCCTATTCTGGTTGAGCTGGATGGTGATGTGAAC
GGTCACAAGTTCTCTGTGTCTGGTGAAGGTGAGGGTGATGCTACCTACGGTAAGCTG
ACCCTTAAGTTCATCTGTACCACCGGAAAGTTGCCTGTGCCTTGGCCTACTCTTGTGA
CCACTTTCTCATACGGTGTGCAGTGCTTCAGCAGGTATCCTGATCATATGAAGAGGC
ACGATTTCTTCAAGAGCGCTATGCCTGAGGGTTACGTGCAAGAGAGGACCATCTTCT
TCAAGGATGATGGTAACTACAAGACCAGGGCTGAGGTGAAGTTCGAAGGTGATACC
CTTGTGAACAGGATCGAGCTGAAGGGTATCGATTTCAAAGAGGATGGAAACATCCT
GGGTCACAAGCTTGAGTACAACTACAACAGCCACAACGTTTACATCACCGCTGATA
AGCAGAAGAACGGTATCAAGGCTAACTTCAAGATCAGGCACAACATCGAGGATGGT
AGCGTGCAGCTTGCTGATCATTACCAGCAGAACACCCCTATCGGTGATGGTCCTGTT
CTGCTTCCTGATAACCACTACCTGTCTACCCAGTCCGCTCTGTCTAAGGATCCTAACG
AGAAGAGGGATCACATGGTGCTGCTTGAGTTCGTTACCGCTGCTGGTATTACCCACG
GTATGGATGAGCTGTATAAGGACGATGATGATAAGATGGATGCTCTGCAAGAGGAT
ACCCCTCCTGGTCCTTCTACTGTTTTTAGGCCTCCTACCTCTAGCAGGCCTCTTGAAA
CTCCACACTGCAGAGAGATCAGGATCGGTATCGCTGGAATTACCATCACCCTGTCTT
TGTGCGGTTGCGCTAATGCTAGGGCTCCTACTCTTAGATCTGCTACCGCAGATAACA
GCGAGAGCACCGGTTTCAAGAACGTGCCAGATCTTAGGACCGATCAGCCTAAGCCT
CCAAGCAAGAAGAGAAGCTGCGATCCTTCTGAGTACAGGGTGAGCAAGCTGAAAGA
GAGCCTTATTACCACCACCCCTTCAAGGCCTAGGACTGCTAAGAGAAGGATTAAGCT
TCATCACCACCACCATCACAAGGATGAGCTTTAGCTCGAGGGCGCGCCGCTAGC

Amino acid sequence

MGFVLFSQLPSFLLVSTLLLFLVISHSCRAASKGEELFTGVVPILVELDGDVNGHKFSVSG
EGEGDATYGKLTLKFICTTGKLPVPWPTLVTTFSYGVQCFSRYPDHMKRHDFFKSAMPE
GYVQERTIFFKDDGNYKTRAEVKFEGDTLVNRIELKGIDFKEDGNILGHKLEYNYNSHN

VYITADKQKNGIKANFKIRHNIEDGSVQLADHYQQNTPIGDGPVLLPDNHYLSTQSALSK
DPNEKRDHMVLLEFVTAAGITHGMDELYKDDDDKMDALQEDTPPGPSTVFRPPTSSRP
LETPHCREIRIGIAGITITLSLCGCANARAPTLRSATADNSESTGFKNVPDLRTDQPKPPSK
KRSCDPSEYRVSKLKESLITTTPSRPRTAKRRIKLHHHHHHKDEL*

Features

Signal peptide PR1a	: (nucleotide) 15…104	(amino acid) 1…30
GFP	: (nucleotide) 105…818	(amino acid) 31…268
VP3-A	: (nucleotide) 834…1196	(amino acid) 274…394
Enterokinase site	: (nucleotide) 819…833	(amino acid) 269…273
Hexahistidine	: (nucleotide) 1197…1214	(amino acid) 395…400
ER retention signal	: (nucleotide) 1215…1226	(amino acid) 401…404

3.3 Nucleotide and amino acid sequences of synthetic apoptin gene cassette, PR-Lic-VP3-HK

Nucleotide sequence

TGTACATTAATTAAATGGGTTTCGTGCTGTTCAGCCAGCTGCCTTCTTTCCTTCTTGT
GTCTACCCTTCTGCTGTTCCTGGTGATCTCTCATTCTTGCAGGGCTCAGAACGGTGGT
TCCTACCCTTATAAGTCTGGTGAGTACAGGACCAAGAGCTTCTTCGGTTACGGTTAC
TACGAGGTGAGGATGAAGGCTGCTAAGAACGTGGGTATCGTGTCCAGCTTCTTTACC
TACACCGGTCCAAGCGATAACAACCCTTGGGATGAGATTGATATCGAGTTCCTGGGT
AAGGATACCACCAAGGTGCAGTTCAACTGGTACAAGAATGGTGTGGGTGGTAACGA
GTACCTGCACAACCTTGGTTTCGATGCTTCCCAGGATTTCCACACCTACGGTTTTGAG
TGGAGGCCTGATTACATCGATTTCTATGTGGATGGTAAGAAGGTTTACAGGGGTACT
AGGAACATCCCTGTGACCCCTGGTAAGATCATGATGAACCTTTGGCCTGGTATCGGT
GTGGATGAGTGGCTTGGTAGATACGATGGTAGGACTCCTCTGCAGGCTGAGTACGA
GTACGTTAAGTACTACCCTAACGGTAGGTCCGAGTTCAAGCTTGTGGTGAATACTCC
TTTCGTGGCTGTGTTCAGCAACTTCGATTCTAGCCAGTGGGAGAAGGCTGATTGGGC
TCAGGGTTCTGTTTTCAACGGTGTGTGGAAGCCTTCTCAGGTGACCTTCTCTAACGGT
AAGATGATCCTGACCCTGGATAGGGAATACGACGATGATGATAAGATGGATGCTCT
GCAAGAGGATACCCCTCCTGGTCCTTCTACTGTTTTTAGGCCTCCTACCTCTAGCAGG
CCTCTTGAAACTCCACACTGCAGAGAGATCAGGATCGGTATCGCTGGTATTACCATC
ACCCTTTCTTTGTGCGGTTGCGCTAATGCTAGGGCTCCTACTCTTAGATCTGCTACCG
CTGATAACAGCGAGAGCACCGGTTTCAAGAACGTGCCAGATCTTAGGACCGATCAG
CCTAAGCCTCCAAGCAAGAAGAGAAGCTGCGATCCTTCTGAGTACAGAGTGAGCAA
GCTGAAAGAGTCCCTTATCACCACTACCCCTTCTAGGCCAAGGACAGCTAAGAGAA
GGATTAAGCTTCATCACCATCACCACCACAAGGATGAGCTGTAGCTCGAGGGCGCG
CCGCTAGC

Amino acid sequence

MGFVLFSQLPSFLLVSTLLLFLVISHSCRAQNGGSYPYKSGEYRTKSFFGYGYYEVRMK
AAKNVGIVSSFFTYTGPSDNNPWDEIDIEFLGKDTTKVQFNWYKNGVGGNEYLHNLGF
DASQDFHTYGFEWRPDYIDFYVDGKKVYRGTRNIPVTPGKIMMNLWPGIGVDEWLGRY

DGRTPLQAEYEYVKYYPNGRSEFKLVVNTPFVAVFSNFDSSQWEKADWAQGSVFNGV
WKPSQVTFSNGKMILTLDREYDDDDKMDALQEDTPPGPSTVFRPPTSSRPLETPHCREIR
IGIAGITITLSLCGCANARAPTLRSATADNSESTGFKNVPDLRTDQPKPPSKKRSCDPSEY
RVSKLKESLITTTPSRPRTAKRRIKLHHHHHHKDEL*

Features

Signal peptide PR1a	: (nucleotide) 15…104	(amino acid) 1…30
Lichenase	: (nucleotide) 105...773	(amino acid) 31…253
VP3-A	: (nucleotide) 789...1151	(amino acid) 259…379
Enterokinase site	: (nucleotide) 774…788	(amino acid) 254…258
Hexahistidine	: (nucleotide) 1152…1169	(amino acid) 380…385
ER retention signal	: (nucleotide) 1170…1181	(amino acid) 386…389

3.4 Nucleotide and amino acid sequences of synthetic gene, mCherryNuc

Nucleotide sequence

ATGGTGAGCAAGGGTGAAGAGGATAACATGGCTATCATCAAAGAGTTCATGAGGTT
CAAGGTGCACATGGAAGGTAGCGTGAACGGTCACGAGTTTGAGATTGAAGGTGAGG
GTGAGGGTAGGCCTTATGAGGGTACTCAAACCGCTAAGCTGAAGGTTACAAAGGGT
GGTCCTCTTCCTTTCGCTTGGGATATTCTGAGCCCTCAGTTCATGTACGGTAGCAAGG
CTTACGTTAAGCACCCTGCTGATATCCCTGATTACCTGAAGCTGTCTTTCCCAGAGG
GTTTCAAGTGGGAGAGGGTGATGAATTTCGAGGATGGTGGTGTGGTGACTGTGACC
CAGGATTCTTCACTTCAGGATGGTGAGTTCATCTACAAGGTGAAGCTGAGGGGTACT
AACTTCCCTTCTGATGGTCCTGTGATGCAGAAAAAGACTATGGGTTGGGAGGCTTCA
AGCGAGAGAATGTATCCTGAAGATGGTGCTCTGAAGGGTGAGATCAAGCAGAGGCT
GAAGCTGAAAGATGGTGGTCACTACGATGCTGAGGTTAAGACCACCTACAAGGCTA
AGAAGCCTGTTCAGCTTCCTGGTGCTTACAACGTGAACATCAAGCTGGATATCACCA
GCCACAACGAGGATTACACCATCGTTGAGCAGTATGAGAGGGCTGAGGGAAGGCAT
TCTACTGGTGGTATGGATGAGCTTTACAAAGATCCTAAGAAGAAGAGGAAAGTTGA
TCCAAAGAAAAAAAGAAAAGTTGATCCTAAAAAGAAGAGAAAGGTTTAG

Amino acid sequence

MVSKGEEDNMAIIKEFMRFKVHMEGSVNGHEFEIEGEGEGRPYEGTQTAKLKVTKGGP
LPFAWDILSPQFMYGSKAYVKHPADIPDYLKLSFPEGFKWERVMNFEDGGVVTVTQDS
SLQDGEFIYKVKLRGTNFPSDGPVMQKKTMGWEASSERMYPEDGALKGEIKQRLKLKD
GGHYDAEVKTTYKAKKPVQLPGAYNVNIKLDITSHNEDYTIVEQYERAEGRHSTGGMD
ELYKDPKKKRKVDPKKKRKVDPKKKRKV

Features

mCherry	: (nucleotide) 1…708	(amino acid) 1…236
Nuclear localisation signal (Nuc)	: (nucleotide) 709...783	(amino acid) 237…260

3.5 Nucleotide and amino acid sequences of synthetic gene, H22 single chain antibody

Nucleotide sequence

CAGGTTCAGCTGGTTGAGTCTGGTGGTGGTGTTGTTCAACCTGGAAGATCTCTGAGG
CTGAGCTGCTCATCTAGCGGTTTCATCTTCAGCGATAACTACATGTACTGGGTGAGG
CAGGCTCCTGGTAAGGGTCTTGAATGGGTGGCAACCATTTCCGATGGTGGTAGCTAC
ACCTACTACCCTGATTCTGTGAAGGGAAGGTTCACCATCAGCAGGGATAACAGCAA
GAACACCCTGTTCCTTCAGATGGATAGCCTGAGGCCTGAAGATACCGGTGTTTACTT
TTGCGCTAGAGGATATTACAGGTACGAGGGTGCTATGGATTACTGGGGTCAAGGTA
CTCCTGTGACCGTTTCTAGCGGAGGTGGTGGATCAGGTGGTGGTGGAAGTGGTGGTG
GTGGTTCTGATATTCAGCTTACCCAGAGCCCTAGCAGCCTTTCTGCTTCTGTTGGTGA
TAGGGTGACCATTACCTGCAAGTCCTCTCAGTCTGTGCTGTACTCCAGCAACCAGAA
GAACTACCTGGCTTGGTATCAGCAGAAGCCTGGAAAGGCTCCTAAGCTGCTTATCTA
CTGGGCTTCCACTAGGGAATCTGGTGTGCCTTCTAGGTTCTCCGGTTCTGGTTCTGGT
ACTGATTTCACCTTCACCATCTCCAGCCTTCAGCCTGAGGATATCGCTACTTACTACT
GCCACCAGTACCTGTCCTCTTGGACTTTTGGTCAGGGTACTAAGCTTGAGATCAAA

Amino acid sequence

QVQLVESGGGVVQPGRSLRLSCSSSGFIFSDNYMYWVRQAPGKGLEWVATISDGGSYT
YYPDSVKGRFTISRDNSKNTLFLQMDSLRPEDTGVYFCARGYYRYEGAMDYWGQGTP
VTVSSGGGGSGGGGSGGGGSDIQLTQSPSSLSASVGDRVTITCKSSQSVLYSSNQKNYLA
WYQQKPGKAPKLLIYWASTRESGVPSRFSGSGSGTDFTFTISSLQPEDIATYYCHQYLSS
WTFGQGTKLEIK

Feature

H22 single chain antibody : (nucleotide) 1…741 (amino acid) 1…247

3.6 Nucleotide and amino acid sequences of synthetic gene, epidermal growth factor (EGF)

Nucleotide sequence

AACAGCGATAGCGAGTGCCCTCTGTCTCATGATGGTTACTGCTTGCATGATGGTGTG
TGCATGTATATCGAGGCTCTGGATAAGTACGCTTGCAACTGCGTGGTGGGTTACATT
GGTGAGAGATGCCAGTACAGGGATCTGAAGTGGTGGGAACTTAGA

Amino acid sequence

NSDSECPLSHDGYCLHDGVCMYIEALDKYACNCVVGYIGERCQYRDLKWWELR

Feature

Epidermal growth factor (EGF)	: (nucleotide) 1…159	(amino acid) 1…53

3.7 Nucleotide and amino acid sequences of synthetic gene, bZIP17

Nucleotide sequence

ATGCTGTACAATGGCTGAACCAATCACCAAGGAGCAGCCTCCTCCACCTGCTCCGGA
CCCTAATTCCACCTACCCTCCTCCGTCCGATTTTGATTCCATCTCGATCCCTCCGTTA
GATGATCATTTCTCCGATCAGACTCCGATTGGTGAACTAATGTCCGATCTGGGGTTT
CCCGATGGTGAATTCGAGCTCACTTTCGACGGTATGGACGATCTTTACTTCCCTGCTG
AGAATGAGTCGTTTCTCATCCCTATCAATACGTCCAATCAAGAACAGTTTGGTGATT
TCACTCCGGAGTCTGAAAGTTCTGGAATTTCCGGTGATTGTATTGTTCCCAAAGATG
CAGATAAGACTATTACAACTTCCGGTTGCATTAACCGGGAATCTCCTAGAGATTCCG
ATGATCGTTGCTCCGGTGCTGACCATAATTTAGATCTACCGACTCCATTGTCCTCTCA
GGGTTCGGGTAATTGCGGTTCTGATGTTTCGGAAGCTACAAATGAATCGTCGCCTAA
ATCGAGAAACGTTGCGGTCGACCAGAAGGTTAAAGTGGAAGAAGCTGCTACGACGA
CGACGTCTATTACCAAGAGGAAGAAAGAGATCGATGAGGATTTGACTGACGAGTCT
AGGAACAGTAAGTACAGGAGATCGGGAGAGGATGCTGACGCTAGTGCTGTTACCGG
TGAAGAAGATGAGAAAAAGAGAGCTAGACTCATGAGAAACCGTGAAAGTGCTCAG
CTTTCTAGGCAGAGGAAGAAGCATTACGTCGAGGAGCTTGAAGAAAAGGTTAGGAA
TATGCATTCTACGATTACGGATTTGAACGGTAAGATATCGTATTTCATGGCTGAGAA
TGCTACTCTAAGGCAGCAATTGGGTGGCAATGGAATGTGCCCGCCGCATCTTCCACC
ACCTCCGATGGGAATGTATCCACCTATGGCTCCAATGCCTTATCCATGGATGCCTTG
TCCTCCTTATATGGTGAAGCAACAAGGATCTCAAGTGCCTTTGATTCCTATTCCTAGG
TTGAAACCACAGAACACCCTTGGAACATCCAAGGCTAAGAAGTCCGAGAGTAAGAA
GAGTGAAGCTAA

Amino acid sequence

MAEPITKEQPPPPAPDPNSTYPPPSDFDSISIPPLDDHFSDQTPIGELMSDLGFPDGEFELTF
DGMDDLYFPAENESFLIPINTSNQEQFGDFTPESESSGISGDCIVPKDADKTITTSGCINRE
SPRDSDDRCSGADHNLDLPTPLSSQGSGNCGSDVSEATNESSPKSRNVAVDQKVKVEEA
ATTTTSITKRKKEIDEDLTDESRNSKYRRSGEDADASAVTGEEDEKKRARLMRNRESAQ
LSRQRKKHYVEELEEKVRNMHSTITDLNGKISYFMAENATLRQQLGGNGMCPPHLPPPP

MGMYPPMAPMPYPWMPCPPYMVKQQGSQVPLIPIPRLKPQNTLGTSKAKKSESKKSEA
KT*

Feature

bZIP17 : (nucleotide) 1…1092 (amino acid) 1…363

3.8 Nucleotide and amino acid sequences of synthetic gene, bZIP28

Nucleotide sequence

ATGACGGAATCAACATCCGTGGTTGCTCCTCCGCCGGAGATACCTAATCTGAACCCT
AGCATGTTTTCTGAGTCCGATTTGTTTTCTATTCCGCCGCTAGATCCTCTTTTCCTATC
TGATTCTGATCCGATTTCAATGGATGCGCCAATCTCCGATCTCGACTTCTTACTCGAC
GATGAGAACGGAGATTTCGCTGATTTTGATTTCTCGTTTGATAATTCTGATGATTTCT
TCGATTTCGATTTATCGGAGCCCGCGGTGGTGATCCCTGAGGAGATCGGTAACAATC
GTTCGAATTTGGACTCATCGGaAAACAGAAGCGGCGATGGAGGTTTAGAAGGAAGA
TCTGAGTCTGTTCATTCACAGGTTTCATCTCAAGGCTCCAAGACTTTTGTGTCCGACA
CCGTTGACGCATCATCCTCCCCTGAATCAAGCAATCACCAGAAATCTTCTGTTAGCA
AGAGGAAGAAGGAAAATGGAGACTCCAGTGGCGAATTAAGGAGCTGCAAGTACCA
AAAGTCCGATGATAAATCAGTCGCTACGAACAACGAAGGTGATGATGACGACGACA
AGAGGAAGTTGATAAGGCAGATTAGGAACCGTGAAAGTGCTCAGCTTTCGAGGTTG
AGGAAGAAGCAACAAACTGAGGAGCTTGAAAGAAAAGTGAAGAGTATGAATGCTA
CCATTGCTGAATTGAATGGTAAGATTGCTTATGTTATGGCTGAGAATGTCGCTTTAA
GGCAACAAATGGCTGTTGCTTCTGGTGCTCCTCCTATGAATCcTTATATGGCTGCCCC
GCCTTTACCGTATCAATGGATGCCGTATCCGCCGTATCCTGTTAGGGGATATGGATC
ACAGACACCTTTGGTTCCCATTCCTAAGTTAAATCCTAAGCCTGTATCGAGTTGTAG
ACCGAAGAAGGCAGAGAGTAAGAAGAATGAGGGTAAAAGTAAGCTCTGA

Amino acid sequence

MTESTSVVAPPPEIPNLNPSMFSESDLFSIPPLDPLFLSDSDPISMDAPISDLDFLLDDENGD
FADFDFSFDNSDDFFDFDLSEPAVVIPEEIGNNRSNLDSSENRSGDGGLEGRSESVHSQVS
SQGSKTFVSDTVDASSSPESSNHQKSSVSKRKKENGDSSGELRSCKYQKSDDKSVATNN
EGDDDDDKRKLIRQIRNRESAQLSRLRKKQQTEELERKVKSMNATIAELNGKIAYVMAE
NVALRQQMAVASGAPPMNPYMAAPPLPYQWMPYPPYPVRGYGSQTPLVPIPKLNPKPV
SSCRPKKAESKKNEGKSKL*

Feature

bZIP28 : (nucleotide) 1…960 (amino acid) 1…320

3.9 Nucleotide and amino acid sequences of synthetic gene, bZIP60

Nucleotide sequence

ATGGTGGATGACATCGATGATATCGTTGGACACATCAATTGGGACGATGTAGATGA
CCTCTTCCACAACATTCTAGAGGATCCCGCCGACAATCTCTTCTCTGCTCATGATCCG
TCCGCGCCGTCTATCCAGGAGATCGAGCAGCTTCTCATGAACGATGATGAAATCGTC
GGTCACGTGGCTGTCGGAGAGCCTGATTTTCAACTTGCTGACGACTTTCTCTCCGAC
GTGCTAGCCGATTCTCCTGTTCAGTCCGATCTTTCTCACTCTGATAAAGTCATTGGAT
TCCCCGATTCCAAGGTTTCAAGTTGCTCAGAGGTTGATGATGACGACAAAGACAAG
GAGAAGGTTTCCCAGTCGCGGATTGACTCTAAGGACGGCTCTGACGAACTAAACTGT
GATGATCCCGTCGATAAAAAGCGTAAGAGGCAATTGAGAAACAGAGATGCAGCTGT
CAGGTCACGAGAGCGGAAGAAGTTGTATGTTAGGGATCTTGAGTTGAAGAGTAGAT
ACTTTGAATCAGAGTGCAAGAGGTTGGGGTTAGTTCTCCAGTGCTGTCTTGCAGAAA
ATCAAGCTTTGCGCTTCTCTTTGCAGAATGGCAATGCTAATGGTGCTTGTATGACCA
AGCAGGAGTCTGCTGTGCTCTTGTTGGAATCCCTGCTGTTGGGTTCCCTGCTTTGGTT
CCTGGGCATCATATGCCTGCTCATTCTTCCCAGCCAACCCTGGTTAATTCCAGAAGA
AAATCAACGAAGCAGAAACCACGGTCTTCTGGTTCCGATAAAGGGAGGAAATAAGG
CTGGTCGGATTTTTGAGTTCCTGTCCTTCATGATGGGCAAGAGATGCAAAGCTTCAA
GATCGAGGATGAAGTTCAATCCCCATTCTTTGGGAATTGTTATGTGA

Amino acid sequence

MVDDIDDIVGHINWDDVDDLFHNILEDPADNLFSAHDPSAPSIQEIEQLLMNDDEIVGHV
AVGEPDFQLADDFLSDVLADSPVQSDLSHSDKVIGFPDSKVSSCSEVDDDDKDKEKVSQ
SRIDSKDGSDELNCDDPVDKKRKRQLRNRDAAVRSRERKKLYVRDLELKSRYFESECK
RLGLVLQCCLAENQALRFSLQNGNANGACMTKQESAVLLLESLLLGSLLWFLGIICLLIL
PSQPWLIPEENQRSRNHGLLVPIKGGNKAGRIFEFLSFMMGKRCKASRSRMKFNPHSLGI
VM*

Feature

bZIP60 : (nucleotide) 1…900 (amino acid) 1…300

3.10 List of primers

Primers	Sequences
pVP3-F	TGTACATTAATTAAATGGGTTTCGTGCTGTT
VP3H-R	GCTAGCGGCGCGCCCTCGAGCTAGTGGTGGTGATGGT GATGAAGCTT
VP3-F	TGTACATTAATTAAATGGATGCTCTGCAAGAGGATAC
gVP3H-R	GCTAGCGGCGCGCCCTCGAGCTAGTGATGGTGGTGGT GATGAAGCTT
gVP3-F	TGTACATTAATTAAATGGCTTCTAAGGGTGAGGAACT
LicVP3-F	TGTACATTAATTAAATGCAGAACGGTGGTTCCTACCC
PRH22-F	TGTACATTAATTAAATGGGTTTCGTGCTGTTCAGCCAG CTGCCTTCTTTCCTTCTTGTGTCTACCCTTCTGCTGTTC CTGGTGATCTCTCATTCTTGCAGGGCTCAGGTTCAGCT GGTTGAGTCTGGTG
HCatVP3-R	GGTATCCTCTTGCAGAGCATCCATAGGACCCCTATC
HCatVP3-40-121-R	GGTGATGGTAATAGGACCCCTATCAACTTCATCGTG
HCatVP3-60-121-R	ATCTGCGGTAGCAGGACCCCTATCAACTTCATCGTG
HCatVP3-80-121-R	AGGCTTAGGCTGAGGACCCCTATCAACTTCATCGTG
HCatVP3-F	CACGATGAAGTTGATAGGGGTCCTATGGATGCTCTG
VP3-HK_R	GCTAGCGGCGCGCCCTCGAGCTAAAGCTCA
HCatVP3-40-121-F	GATAGGGGTCCTATTACCATCACCCTGTCTTTGTGC

HCatVP3-60-121-F	GATAGGGGTCCTGCTACCGCAGATAACAGCGAGAGC
HCatVP3-80-121-F	GATAGGGGTCCTCAGCCTAAGCCTCCAAGCAAGAAG
PREGF-F	TGTACATTAATTAAATGGGTTTCGTGCTGTTCAGCCAGCTGCCTTCTTTCCTTCTTGTGTCTACCCTTCTGCTGTTCCTGGTGATCTCTCATTCTTGCAGGGCTAACAGCGATAGCGAGTGCCCTCTGT
ECatVP3-R	CAGAGCATCCATAGGACCTCTATCAACTTCATCGTG
ECatVP3-F	GATAGAGGTCCTATGGATGCTCTGCAAGAGGATACC
YFE-1-T-F	TGTACATTAATTAAATGGGTTTCGTGCTGTTCAGCCAGCT
ECatVP3-40-121-R	GGTGATGGTAATAGGACCTCTATCAACTTCATCGTG
ECatVP3-60-121-R	ATCTGCGGTAGCAGGACCTCTATCAACTTCATCGTG
ECatVP3-80-121-R	AGGCTTAGGCTGAGGACCTCTATCAACTTCATCGTG
ECatVP3-40-121-F	GATAGAGGTCCTATTACCATCACCCTGTCTTTGTGC
ECatVP3-60-121-F	GATAGAGGTCCTGCTACCGCAGATAACAGCGAGAGC
ECatVP3-80-121-F	GATAGAGGTCCTCAGCCTAAGCCTCCAAGCAAGAAG

3.11 Codon usage table of *Nicotiana benthamiana* (*N. benthamiana*)

This data was adopted from URL: http://www.kazusa.or.jp/codon/cgi-bin/showcodon.cgi?species=4100

Features: [codon] [frequency: per thousand] ([number])

UUU 23.7 (1036)	UCU 22.3 (974)	UAU 15.8 (690)	UGU 9.2 (404)
UUC 17.6 (771)	UCC 10.4 (453)	UAC 12.8 (562)	UGC 7.2 (315)
UUA 12.8 (559)	UCA 17.2 (752)	UAA 0.7 (32)	UGA 0.9 (39)
UUG 24.3 (1062)	UCG 5.6 (247)	UAG 0.7 (29)	UGG 12.4 (542)
CUU 24.9 (1091)	CCU 18.9 (826)	CAU 12.9 (566)	CGU 7.7 (335)
CUC 12.5 (545)	CCC 6.4 (278)	CAC 8.2 (360)	CGC 4.2 (183)
CUA 9.2 (404)	CCA 16.8 (734)	CAA 18.1 (790)	CGA 5.8 (253)
CUG 11.9 (522)	CCG 6.5 (284)	CAG 17.0 (745)	CGG 5.3 (233)
AUU 26.7 (1170)	ACU 17.4 (762)	AAU 29.1 (1272)	AGU 14.7 (642)
AUC 13.9 (610)	ACC 10.1 (443)	AAC 16.9 (741)	AGC 10.7 (469)
AUA 12.1 (530)	ACA 15.2 (665)	AAA 29.0 (1269)	AGA 15.8 (690)
AUG 23.9 (1044)	ACG 5.4 (236)	AAG 38.0 (1662)	AGG 13.0 (569)
GUU 26.1 (1142)	GCU 33.2 (1452)	GAU 38.5 (1686)	GGU 24.3 (1065)
GUC 10.6 (465)	GCC 12.6 (550)	GAC 16.4 (719)	GGC 11.4 (500)
GUA 9.9 (435)	GCA 23.5 (1029)	GAA 35.2 (1541)	GGA 22.5 (986)
GUG 15.6 (684)	GCG 6.5 (283)	GAG 30.9 (1351)	GGG 11.1 (485)

Appendices for Chapter 4

4.1 Expression profile for mock infected plant sample

Protein expression profile of plants infected with recombinant vector without gene insert (as a negative control/ pGR-D4) was analysed using western blotting. No band was detected from total protein (TP) and total soluble protein (with triton) (TSP-T) fraction from protein samples extracted from plants infected with recombinant vector without gene insert.

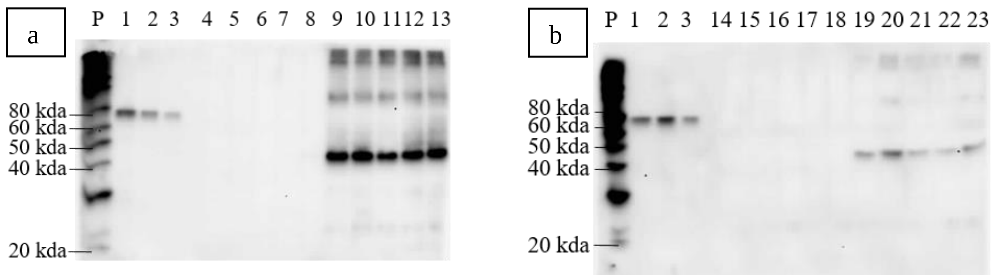

Lane	Sample	Expression vector	Estimated size
P	MagicMark™ XP Western Protein Standard		
1-3	60 ng, 30 ng and 15 ng of HAI standard		~ 70 kDa
4-8	TP extracts from leaf samples harvested from 4, 5, 6, 7 and 8 dpi	pGR-D4	
9-13	TP extract from leaf samples harvested on 4, 5, 6, 7 and 8 dpi	pGR-D4:: GFP-VP3-H	~ 42 kDa
14-18	TSP-T extract from leaf samples harvested on 4, 5, 6, 7 and 8 dpi	pGR-D4	
19-23	TSP-T extract from leaf samples harvested on 4, 5, 6, 7 and 8 dpi	pGR-D4:: PR-GFP-VP3-H	~ 42 kDa

Figure A4.1: Protein expression profile of mock infected plants. (a) Western profiles showed the detection of TP from mock infected (pGR-D4) plants and plants infiltrated with recombinant pGR-D4:: PR-GFP-VP3-H using Tetra-His mouse monoclonal antibody. (b) Western profiles showed the detection of TP from mock infected (pGR-D4) plants and plants infiltrated with recombinant pGR-D4:: PR-GFP-VP3-H using Tetra-His mouse monoclonal antibody.

Appendices for Chapter 5

5.1 IMAC purification of recombinant apoptin from leaves infiltrated with recombinant vector pGR-DN:: PR-VP3-HK__bZIP60

Total protein (TP) harvested from leaf materials infiltrated with recombinant vector, pGR-DN:: PR-VP3-HK__bZIP60 yielded ~ 20 mg/kg (Figure A5.1-a*:* Lane 4); however, amount of total soluble protein (TSP) (Figure A5.1-a*:* Lane 5) was ~ 4 mg/kg. Recovery of soluble recombinant apoptin in eluent containing 300 mM imidazole was ~ 10% of TSP. Protein eluent contained high amount of unspecific protein (Figure A5.1-a*:* Lane 15).

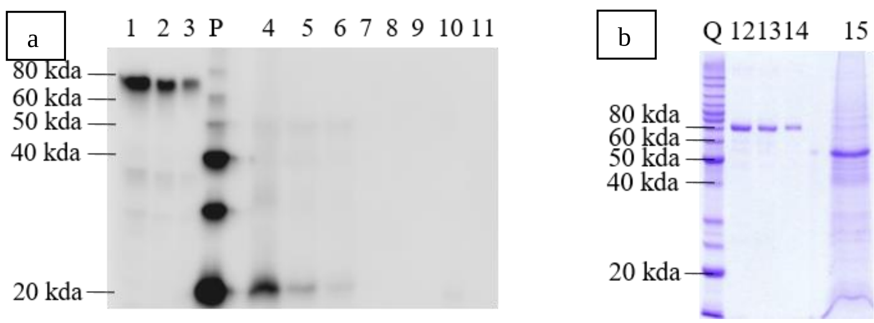

Lane	Sample	Estimated size
P	MagicMark™ XP Western Protein Standard	
Q	Benchmark™ Protein Ladder	
1-3	60 ng, 30 ng and 15 ng of HAI standard	~ 70 kDa
4	TP extract from leaf sample	~ 18 kDa for recombinant VP3-HK
5	TSP extract from leaf sample	~ 18 kDa for recombinant VP3-HK

6	Flow through fraction from IMAC	~ 18 kDa for recombinant VP3-HK
7-11	IMAC eluent containing 20, 40, 60, 300 and 500 mM imidazole	~ 18 kDa for recombinant VP3-HK
12-14	900 ng, 600 ng and 300 ng of BSA standard	~ 66.5 kDa
15	IMAC eluent containing 300 mM imidazole	~ 18 kDa for recombinant VP3-HK

Figure A5.1: IMAC protein purification profiles of recombinant apoptin alone from leaves infiltrated with recombinant pGR-DN:: PR-VP3-HK__bZIP60. (a) Western profiles showed the detection of recombinant apoptin at a molecular size of ~ 18 kDa reacted with Tetra-His mouse monoclonal antibody in each step of IMAC. All sample volume was adjusted to the volume of starting material and subsequently loaded into gel at the same volume for all fractions. (b) Protein sample from IMAC eluent containing 300 mM imidazole was electrophoresed in SDS-PAGE and stained with coomassie blue.

5.2 Ion exchange chromatography (IEX) of IMAC purified recombinant GFP-apoptin using HiTrap SP column

IMAC purified recombinant GFP-apoptin (GFP-VP3-HK) was further purified with HiTrap SP column at pH 7.7 (Figure A5.2-b), pH 8.5 (Figure A5.2-a) and pH 8.0 (Figure A5.2-c and -d). Among these three conditions, purification using HiTrap SP column gave the highest purification yield (~ 40% recovery) at pH 8.0 using eluent buffer containing 0.6 M NaCl. However, unspecific plant protein at ~ 50 kDa still remained as a major contaminant in this purified product.

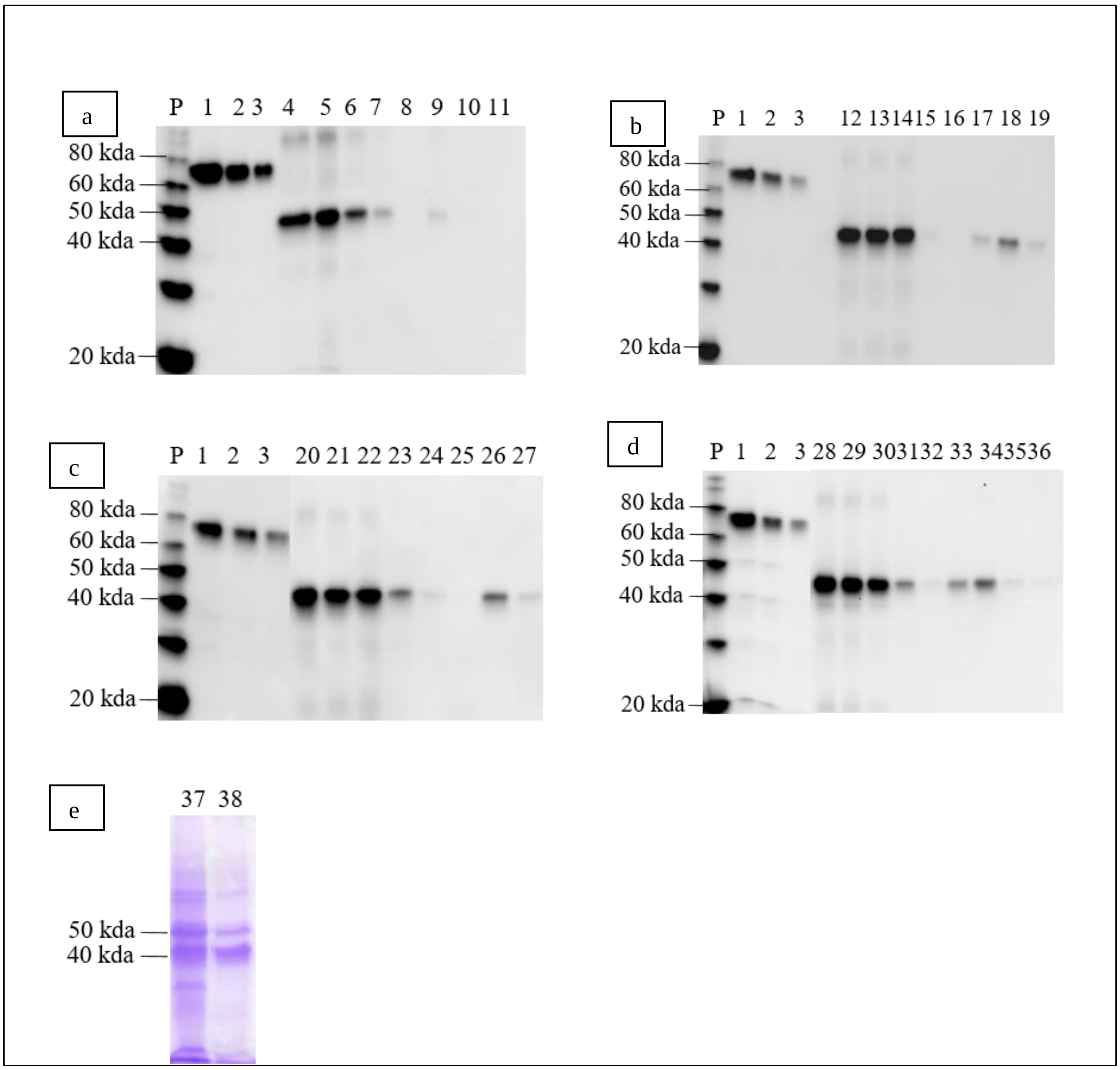

Lane	Sample	Estimated size
P	MagicMark™ XP Western Protein Standard	
1-3	60 ng, 30 ng and 15 ng of HAI standard	~ 70 kDa
4, 13, 21 and 29	Supernatant of IMAC Eluent after centrifuged at 40, 000 xg	~ 45 kDa for recombinant GFP-VP3-HK
5	Buffer exchange IMAC eluent to IEX Starting Buffer C	~ 45 kDa for recombinant GFP-VP3-HK
6	Flow through fraction from HiTrap SP column at pH 8.5	~ 45 kDa for recombinant GFP-VP3-HK
7	HiTrap SP column washed using IEX Starting Buffer C	~ 45 kDa for recombinant GFP-VP3-HK
8-11	Eluent with 0.2, 0.4, 0.6 and 0.8 M NaCl containing buffer using IEX Elution Buffer C	~ 45 kDa for recombinant GFP-VP3-HK
12, 20, 28 and 37	IMAC eluent containing 300 mM imidazole buffer	~ 45 kDa for recombinant GFP-VP3-HK
14	Buffer exchange IMAC eluent to IEX Starting Buffer D	~ 45 kDa for recombinant GFP-VP3-HK
15	Flow through fraction from HiTrap SP column at pH 7.7	~ 45 kDa for recombinant GFP-VP3-HK
16	HiTrap SP column washed using IEX Starting Buffer D	~ 45 kDa for recombinant GFP-VP3-HK
17-19	Eluent with 0.2, 0.4 and 0.6 M NaCl containing buffer using IEX Elution Buffer D	~ 45 kDa for recombinant GFP-VP3-HK
22	Buffer exchange IMAC eluent to IEX Starting Buffer E	~ 45 kDa for recombinant GFP-VP3-HK

23	Flow through fraction from HiTrap SP column at pH 8.0	~ 45 kDa for recombinant GFP-VP3-HK
24	HiTrap SP column washed using IEX Starting Buffer E	~ 45 kDa for recombinant GFP-VP3-HK
25-27	Eluent with 0.2, 0.4 and 0.6 M NaCl containing buffer using IEX Elution Buffer E	~ 45 kDa for recombinant GFP-VP3-HK
30	Buffer exchange IMAC eluent to IEX Starting Buffer F	~ 45 kDa for recombinant GFP-VP3-HK
31	Flow through fraction from HiTrap SP column at pH 8.0	~ 45 kDa for recombinant GFP-VP3-HK
32	HiTrap SP column washed using IEX Starting Buffer F	~ 45 kDa for recombinant GFP-VP3-HK
33-36	Eluent with 0.4, 0.6, 0.8 and 1.0 M NaCl containing buffer using IEX Elution Buffer E	~ 45 kDa for recombinant GFP-VP3-HK
38	Eluent with 0.6 M NaCl containing buffer (pH 8.0)	~ 45 kDa for recombinant GFP-VP3-HK

Figure A5.2: Protein purification profiles of IMAC purified recombinant GFP-apoptin (GFP-VP3-H). All sample volume was adjusted to the volume of starting material and subsequently loaded in the same volume for all fractions. Western profiles showed the detection of recombinant GFP-apoptin at a molecular size of ~ 45 kDa reacted with with Tetra-His mouse monoclonal antibody in each step of purification performed at (a) pH 8.5. (b) pH 7.7 (c) pH 8.0 and (d) pH 8.0 with 0.2 M of NaCl in starting buffer. (e) Protein samples from IMAC eluent containing 300 mM imidazole and IEX eluent containing 0.6 M NaCl were electrophoresed in SDS-PAGE and stained with coomassie blue.

5.3 IMAC purification of recombinant GFP-apoptin from insoluble extract

Recombinant GFP-apoptin (GFP-VP3-H) purified using IMAC under denaturing condition showed a recovery of ~ 50% (Figure A5.3). IMAC eluent containing GFP-apoptin required subsequent buffer exchange step to remove and refold protein. It was noticed that refolded recombinant protein showed a weak GFP signal compared to protein purified using method described in Chapter 5 (section 5.3.1.2) (Figure A5.4).

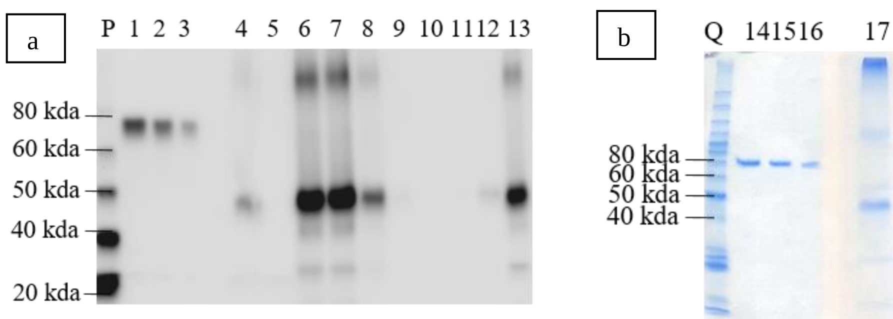

Lane	Sample	Estimated size
P	MagicMark™ XP Western Protein Standard	
Q	Benchmark™ Protein Ladder	
1-3	60 ng, 30 ng and 15 ng of HAI standard	~ 70 kDa
4	TP extract from leaf sample	~ 45 kDa for recombinant GFP-VP3-H
5	TSP-T extract from leaf sample	~ 45 kDa for recombinant GFP-VP3-H
6	Insoluble protein extract from leaf sample with triton	~ 45 kDa for recombinant GFP-VP3-H
7	Insoluble protein extract filtered with 0.2 µm filter	~ 45 kDa for recombinant GFP-VP3-H

8	Flow through fraction from IMAC	~ 45 kDa for recombinant GFP-VP3-H
9-13	IMAC eluent containing 20 (+0.5% triton), 20, 40, 60 and 300 mM imidazole	~ 45 kDa for recombinant GFP-VP3-H
14-16	900 ng, 600 ng and 300 ng of BSA standard	~ 66.5 kDa
17	IMAC eluent containing 300 mM imidazole	~ 45 kDa for recombinant GFP-VP3-H

Figure A5.3: IMAC protein purification profiles of recombinant GFP-apoptin (GFP-VP3-H). (a) Western profiles showed the detection of recombinant GFP-apoptin at a molecular size of ~ 45 kDa reacted with Tetra-His mouse monoclonal antibody in each step of IMAC. All sample volume was adjusted to the volume of starting material and subsequently loaded into gel at the same volume for all fractions. (b) Protein sample from IMAC eluent containing 300 mM imidazole was electrophoresed in SDS-PAGE and stained with coomassie blue.

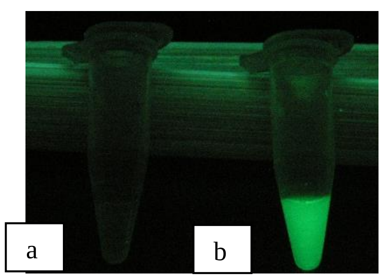

Figure A5.4: Fluorescence signal of recombinant GFP-apoptin (GFP-VP3-H) under UV lamp. (a) Refolded recombinant GFP-apoptin purified under denaturing condition as described in this section showing unapparent green fluorescence. Protein concentration was estimated as 0.1 mg/ml. (b) Refolded recombinant GFP-apoptin purified under native condition as described in Chapter 5 (section 5.3.1.2) showing green fluorescence. Protein concentration was estimated as 0.07 mg/ml.

5.4 Extraction of recombinant GFP-apoptin and EGF-apoptin

Recombinant GFP-apoptin was extracted from leaf materials infiltrated with recombinant vector, pGR-D4:: PR-GFP-VP3-HK using buffer at pH 5.5-9.0 (Figure A5.5: Lane 4-8). Similarly, recombinant EGF-apoptin was extracted from leaf materials infiltrated with recombinant vector, pGR-D4:: PR-EGF-CatAD-VP3-HK using similar condition (Figure A5.5: Lane 9-13). It was noticed that both proteins had high solubility at pH 8.0 and most of the proteins were precipitated at acidic condition.

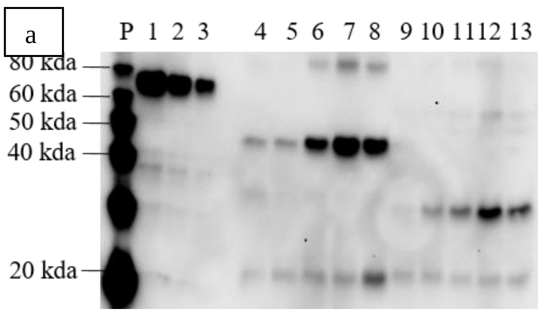

Lane	Sample	Estimated size
P	MagicMark™ XP Western Protein Standard	
1-3	60 ng, 30 ng and 15 ng of HAI standard	~ 70 kDa
4-8	Protein extract of recombinant GFP-apoptin at pH 5.5, 6.0, 7.0, 8.0 and 9.0	~ 45 kDa for recombinant GFP-VP3-HK
9-13	Protein extract of recombinant EGF-apoptin at pH 5.5, 6.0, 7.0, 8.0 and 9.0	~ 30 kDa for recombinant EGF-VP3-HK

Figure A5.5: Protein extraction profiles of recombinant GFP-apoptin (GFP-VP3-HK) and EGF-apoptin (EGF-VP3-HK) using buffer at pH 5.5-9.0. Western profiles showed the detection of recombinant GFP-VP3-HK (a molecular weight of ~ 45 kDa) and EGF-VP3-HK (a molecular weight of ~ 30 kDa) reacted with Tetra-His mouse monoclonal antibody.

5.5 IMAC purification of recombinant EGF-apoptin in denaturing condition

Total protein (TP) harvested from leaf material infiltrated with recombinant vector, pGR-D4:: PR-EGF-CatAd-VP3-HK yielded ~ 30 mg/kg (Figure A5.6-a*: Lane 4).* Recovery of recombinant EGF-apoptin in eluent containing 300 mM imidazole was ~ 50% of total protein extract in denaturing condition (Figure A5.1-a*: Lane 9*). Unspecific host protein ~ 50 kDa was detected in IMAC eluent (Figure A5.1-a*: Lane 16*).

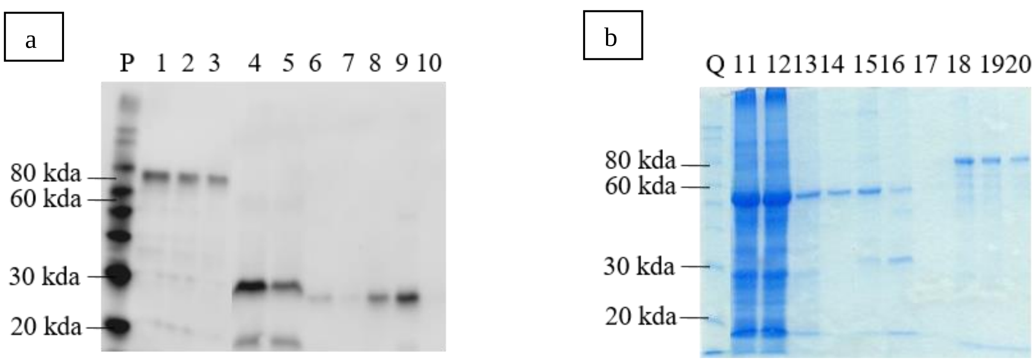

Lane	Sample	Estimated size
P	MagicMark™ XP Western Protein Standard	
Q	Benchmark protein standard	
1-3	60 ng, 30 ng and 15 ng of HAI standard	~ 70 kDa
4 and 11	Insoluble protein extract from leaf sample	~ 30 kDa for recombinant EGF-VP3-HK
5 and 12	Flow through fraction from IMAC	~ 30 kDa for recombinant EGF-VP3-HK
6-10 and 13-17	IMAC eluent containing 20, 40, 60, 300 and 500 mM imidazole	~ 30 kDa for recombinant EGF-VP3-HK

18-20	900ng, 600 ng and 300 ng BSA standard	~ 66.5 kDa

Figure A5.6: IMAC protein purification profiles of recombinant EGF-apoptin (EGF-VP3-HK) in denaturing condition. (a) Western profiles showed the detection of recombinant EGF-apoptin at a molecular size of ~30 kDa reacted with anti- Tetra-His mouse monoclonal antibody in each step of IMAC. All sample volume was adjusted to the volume of starting material and subsequently loaded into gel at the same volume for all fractions. (b) Protein samples from each step of IMAC were electrophoresed in SDS-PAGE and stained with coomassie blue.

Appendices for Chapter 6

6.1 Activity of ectopically expressed apoptin in A549 cells

Activity of ectopically expressed apoptin was assessed in A549 cells in order to identify for the susceptibility of A549 cells towards apoptin. Gene sequence of GFP, GFP-VP3, VP3-A and EGF-VP3 were synthesized by GeneArtTM Gene Synthesis, Thermo Scientific (USA). Besides, GFP and EGF gene sequences were optimised based on codon usage of *Homo sapiens*. Gene sequence of apoptin (VP3) was synthesised based on sequence of Mohd-Azmi *et al.* (1997) (Malaysia isolate) (GenBank accession number: AAB86420.1). Synthesised genes were cloned into mammalian expression vector pCDNA3.0(+) and generated recombinant vectors, pCDNA3.0(+):: GPF, pCDNA3.0(+):: GFP-VP3-A, pCDNA3.0(+):: VP3-A and pCDNA3.0(+):: EGF-VP3-A. All recombinant vectors were delivered into A549 cells using Lipofectamine 3000 (Thermo Scientific, USA) by following the instruction provided by the manufacturer. Expression of proteins in A549 cells were evaluated using IF (described in section 6.2.4) on 2, 4, 5 and 6 days post transfection. For evaluation of activity of apoptin in A549 cells, ~50 cells were examined for cells expressed each recombinant protein. Survival of apoptin or GFP expressed cells were quantified by checking the morphology of cell nucleus stained by SYB Green or PI. Data collected were analysed by statistical analysis ANOVA by using GraphPad Prism. Significance of cell death was evaluated by comparing cells expressing GFP to cells expressing GFP-VP3, VP3-A and EGF-VP3.

Significant cell death was not observed on apoptin expressed cells on 2 days post transfection; but instead, it was observed on 4, 5 and 6 days post transfection (Figure A6.3). DNA condensation and nucleus fragmentation occurred in cells expressing apoptin (Figure A6.4). Instead of quantifying the viability of cells expressing apoptin, localisation of protein was also studied. GFP protein expressed in A549 cells was distributed evenly within the cells; however, ectopically expressed apoptin was relocalised into cell nucleus (Figure A6.5). Relocalisation of apoptin into cell nucleus was reported in various kinds of cancer cells and this activity of protein was mainly due to the bipartite nuclear localisation signal residing in C-terminal of apoptin (Los, 2009).

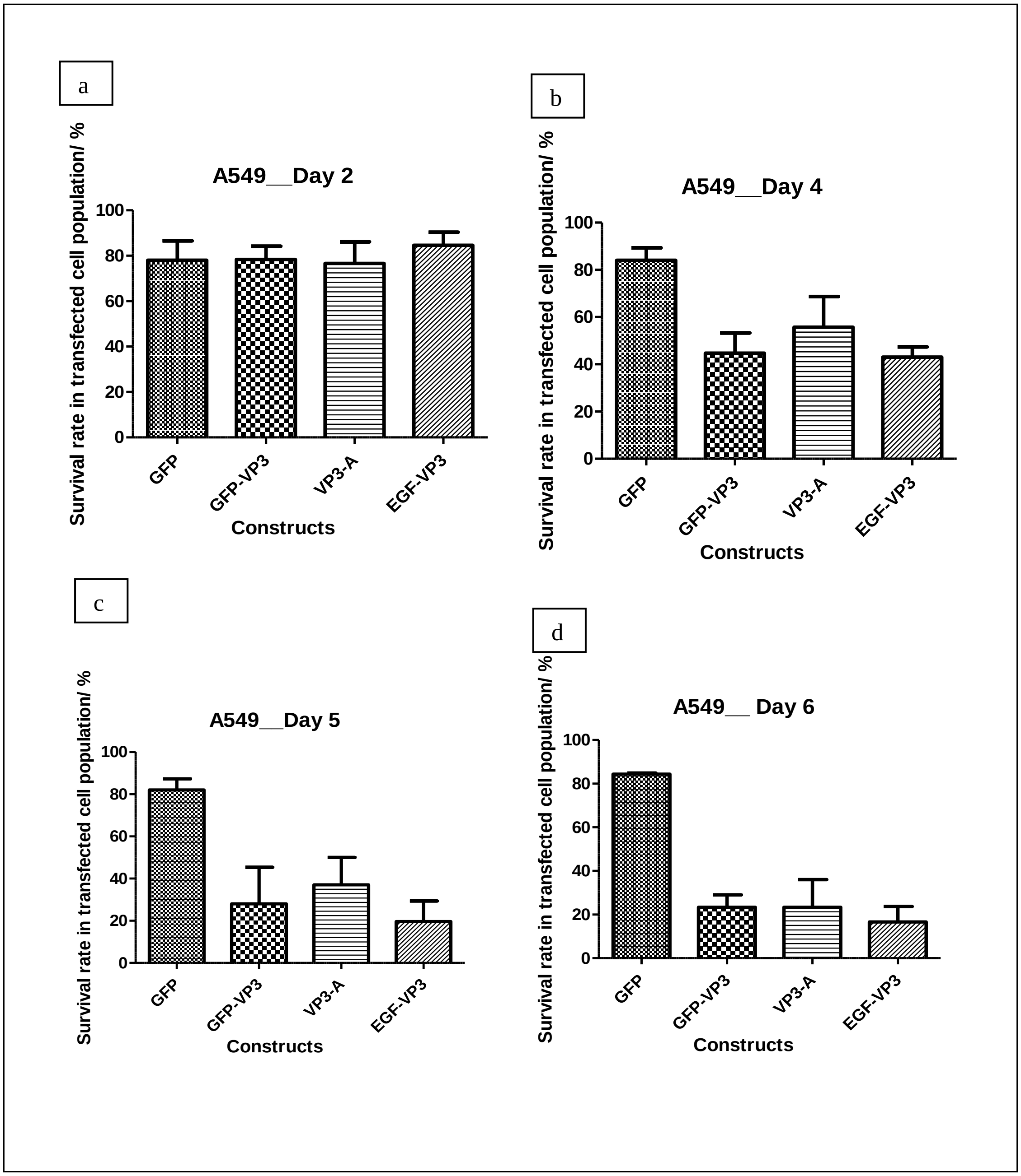

Figure A6.1: Evaluation of survival rate of ectopically expressed apoptin in A549 cells. Cells expressing recombinant GFP, GFP-apoptin (GFP-VP3), apoptin alone (VP3-A) and EGF-apoptin (EGF-VP3) were firstly confirmed by using indirect immunofluorescent assay (IF). Viability of cells expressing recombinant proteins was quantified by evaluating morphology of cells using propidium iodide (PI) or SYBGreen. Cells expressing recombinant GFP and apoptin showed similar rate of survival (p=0.67) on 2 days post transfection; however, cells expressing apoptin showed significant cell death in relative to cells expressing GFP protein on 4 (p= 0.0008), 5 (p= 0.0003) and 6 (p< 0.0001) days post transfection.

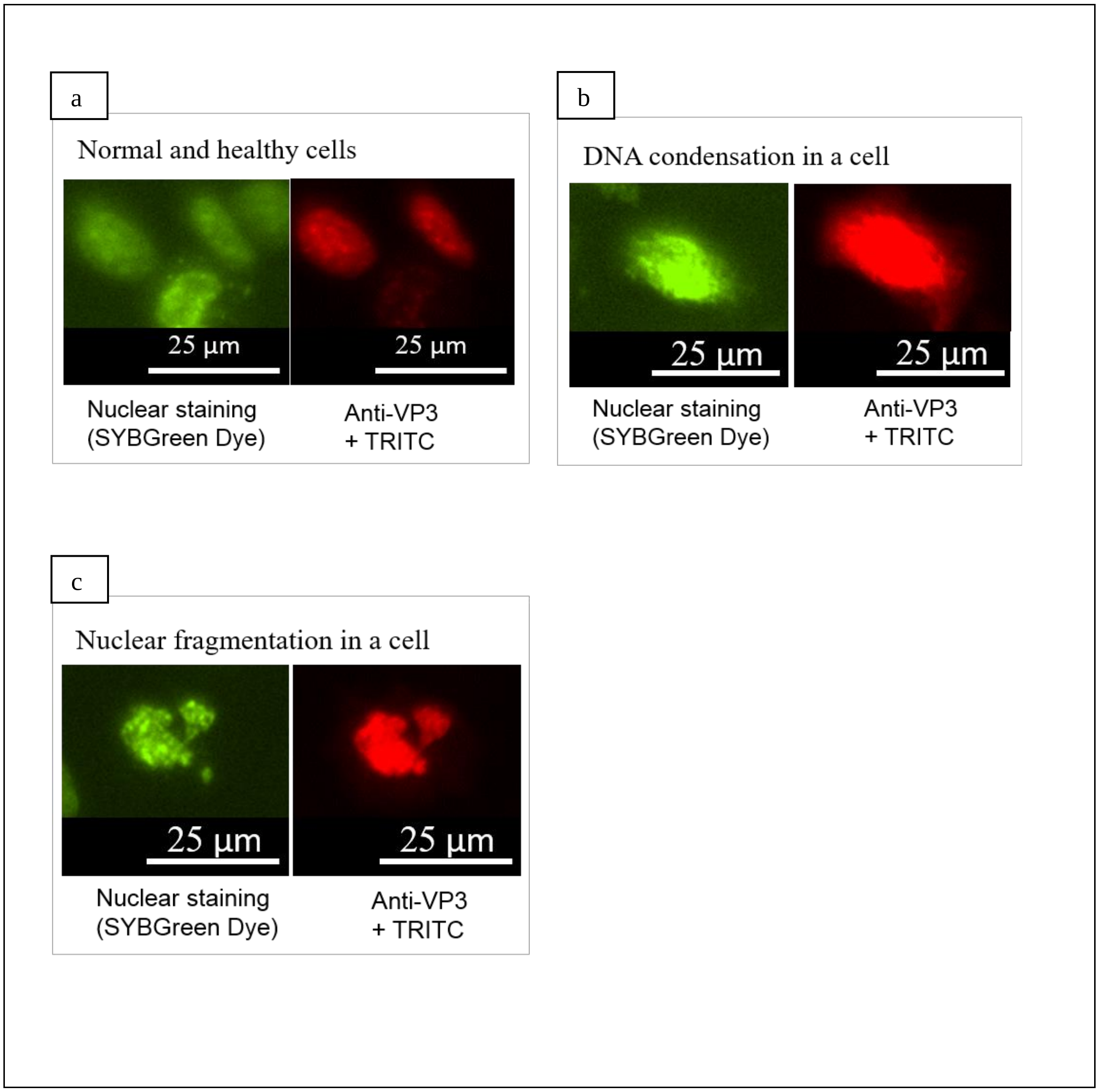

Figure A6.2: Fluorescence microscopic observation of ectopically expressed apoptin in A549 cells captured using Nikon Instruments Eclipse Ti-E inverted microscopes. (a) Cells expressing apoptin showed normal and healthy conditions. Cell nuclei remained round and intact. (b) Cells expressing apoptin showed chromatin condensation with evidence of bright green fluorescence stained DNA. (c) Cells expressing apoptin showed nuclear fragmentation morphology. Nucleus of cells was no longer intact and had been broken into pieces.

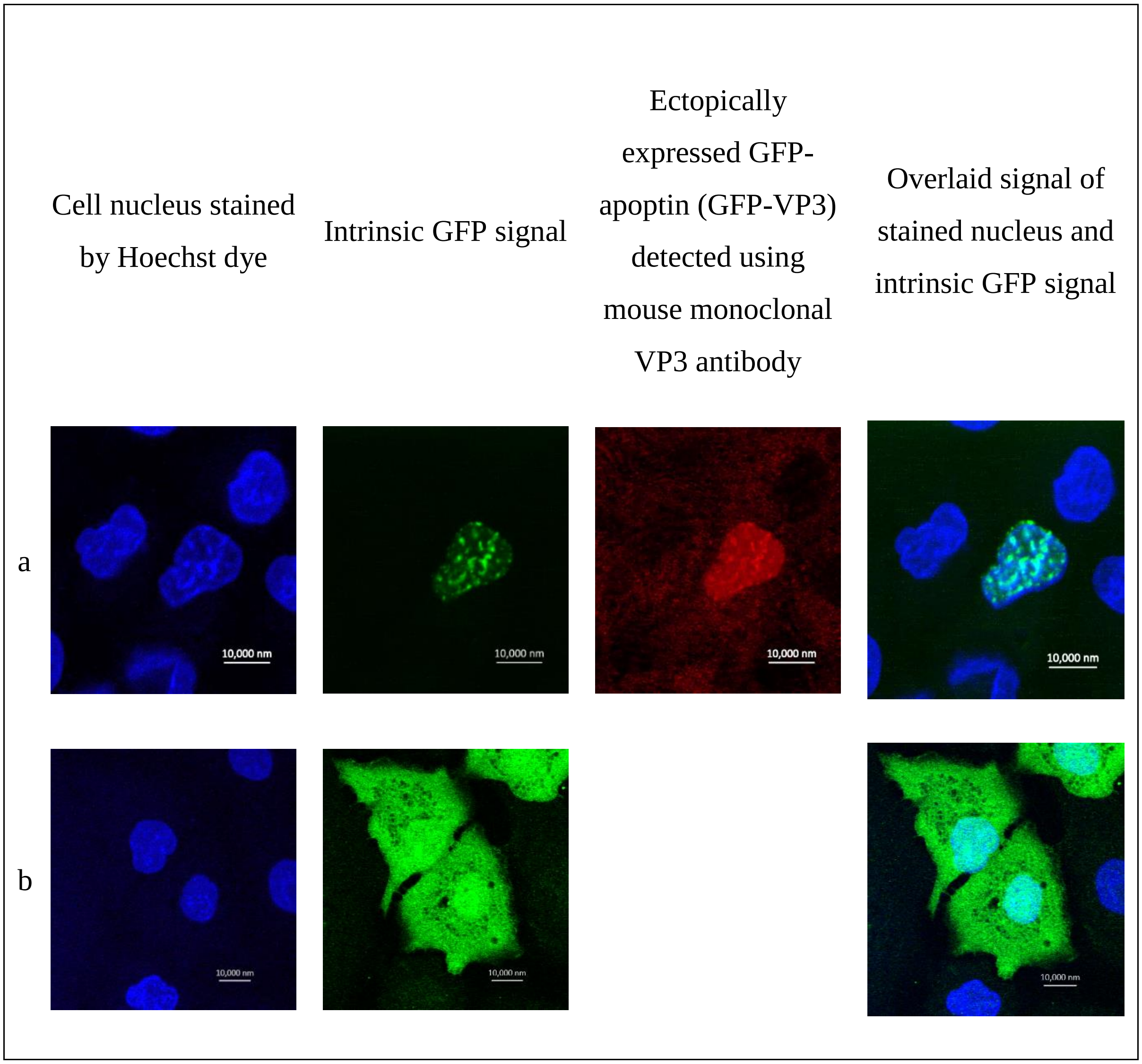

Figure A6.3: Fluorescence microscopic observation of ectopically expressed apoptin in A549 cells captured using Zeiss Observer Z1 microscope and Zeiss LSM 510 META highspeed confocal microscope. (a) Cells expressing apoptin (red) (detected using mouse monoclonal VP3 antibody) showed protein aggregation in cell nucleus (stained by Hoechst dye). (b) Cells expressing GFP protein showed even distribution of protein in A549 cells.

6.2 Delivery of recombinant GFP-VP3-HK into A549 cells using Pulsin protein transfection reagent

Since recombinant GFP-VP3-HK did not harbor cell penetrating peptide, refolded GFP-VP3-HK was transfected into A549 cells using PULSin® protein delivery reagent (Polyplus transfection, France) based on the protocols provided by the manufacturer. PULSin® protein delivery reagent is a kind of cationic amphiphile molecule that forms non-covalent complexes with proteins. Complexes are internalized via anionic cell-adhesion receptors and are released into the cytoplasm where they are disassembled. In this study, cells were incubated with recombinant GFP-VP3-HK and PULSin® protein delivery reagent for 4 hours. Subsequently, fresh culture medium was used to replace medium containing recombinant GFP-VP3-HK and transfection reagent. IF (described in section 6.4) was performed to identify for the location of recombinant GFP-VP3-HK. Fluorescence microscopic images showed that positive control R-Phycoerythrin (~ 240 kDa), as provided by manufacturer, was successfully delivered into A549 cells as shown in Figure A6.6. However, delivery of recombinant GFP was not as efficient as R-Phycoerythrin since limited green fluorescent signal was observed from transfected cells. For recombinant GFP-VP3-HK, huge aggregates were observed on A549 cells and these aggregates were proven to be recombinant GFP-VP3-HK by IF using mouse monoclonal VP3 antibody.

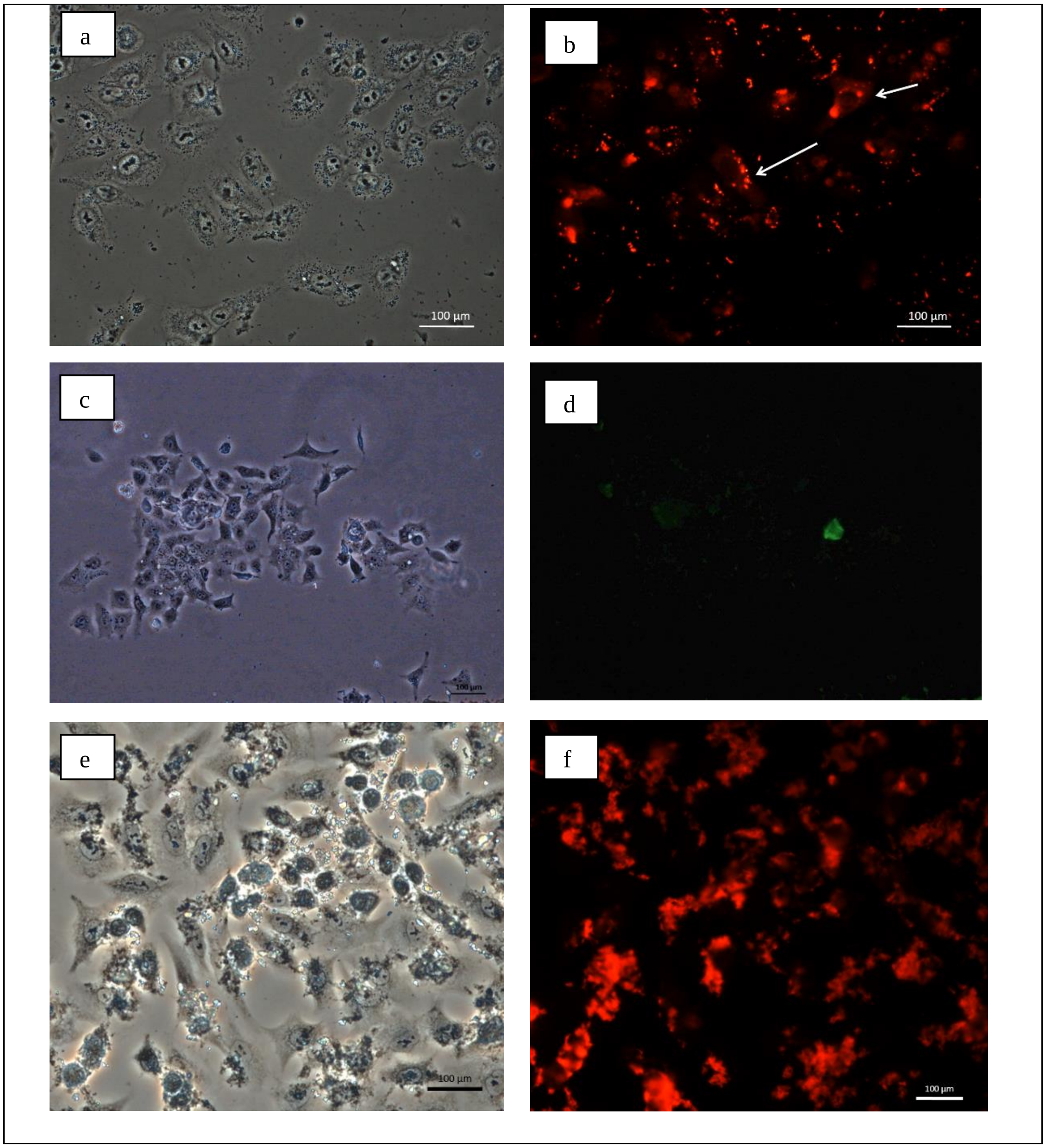

Figure A6.4: Fluorescence microscopic observation of A549 cells transfected with R-Phycoerythrin, GFP and recombinant GFP-VP3-HK. (a and b) Images of A549 cells transfected with R-Phycoerythrin. R-Phycoerythrin (fluorescent in red) was successfully delivered into A549 cells as shown in image (b) (white arrows). (c and d) Images of A549 cells transfected with recombinant GFP protein. Limited numbers of cells (d) were successfully transfected with recombinant GFP protein. (e and f) Images of A549 cells transfected with recombinant GFP-VP3-HK protein. Huge amount of aggregates was noticed locating on A549 cells (e) and these aggregates were proven to be recombinant GFP-VP3-HK as shown in image (f), by which IF was performed using Mouse monoclonal VP3 antibody.

6.3 Scoring for microinjection efficiency and viability of A549 cells microinjected with recombinant GFP and GFP-VP3-H

Microinjection was chosen as delivery tool to transfer recombinant GFP-VP3-H into A549 cells since the protein did not have cell penetrating peptide. Efficiency as well as viability of cells microinjected with recombinant GFP and GFP-VP3-H was scored and presented as in Table A6.1. Efficiency of microinjection for recombinant GFP was scored based on the detected intrinsic signal of GFP present in the microinjected cells; however, microinjected cells turned up with signal from indirect immunofluorescence (IF) staining of recombinant GFP-VP3-H using mouse monoclonal VP3 antibody and Rhodamine (TRITC) AffiniPure Goat Anti-Mouse IgG (H+L) which was calculated as the efficiency of microinjection. The nuclei of cells microinjected with recombinant GFP were stained with propidium iodide (PI) while nuclei of cells microinjected with recombinant GFP-VP3-H were stained with SYB Green. Staining of cell nuclei allowed for the identification of the nuclear morphology of cells and determination of the survival of injected cells (Figure 6.6). Only those with intact and round nucleus were considered as survived cells, which did not include cells with condensed chromatin or fragmented nuclei.

Table A6.1: Survival of cells microinjected with recombinant GFP and GFP-VP3-H.

Recombinant Proteins	Efficiency and viability of microinjected cells	Time (hours)				
		2	4	6	12	24
GFP	Detected cells	60 %	58 %	66 %	68 %	41 %
	Survived cells	55 %	52 %	61 %	58 %	37 %
GFP-VP3-H	Detected cells	40 %	57 %	17 %	7 %	1 %
	Survived cells	18 %	34 %	11 %	4 %	0 %

Note: Detected cells - Cells detected after 2-24 hours post microinjection based on intrinsic signal of recombinant GFP or fluorescent signal shown in IF of cells microinjected with recombinant GFP-VP3-H were classified as detected cells. The calculation was

	performed by [(detected cell numbers/ total injection number) x 100].
Survived cells	- Microinjected cells with intact and normal nuclear features were considered as survived cells. The calculation was performed by [(survived cell numbers/ total injection number) x 100].

Data shown in Table A6.1 were calculated from a single experiment. Cells microinjected with recombinant GFP showed survival rate of more than 50% during the period of 2-12 hours post microinjection. Survival of cell microinjected with recombinant GFP decreased starting at 24 hours post microinjection and this most likely due to the decrease of detected cells that caused by the overturn of recombinant protein in live cells. Decrease of cells microinjected with recombinant GFP-VP3-H was also observed. The lower cell numbers might be caused by the overturn of apoptin protein as well as cell killing effect from recombinant GFP-VP3-H.

6.4 Mitochondrial membrane permeability (MMP) evaluation of A549 cells using carbonyl cyanide 3-chlorophenylhydrazone (CCCP)

MMP evaluation for A549 cells using a reversible proton gradient uncoupling agent, carbonyl cyanide 3-chlorophenylhydrazone (CCCP), was performed as a positive control for MMP assay, which would be performed for microinjected A549 cells with recombinant GFP as well as recombinant EGF-VP3-HK treated A549 cells. In untreated and normal cells, positively charged MitoPT TMRM dye was accumulated in mitochondria and red fluorescent signal was detected (Figure A6.1 -b). By using CCCP as low as 50 μM, mitochondrial membrane potential of A549 cells was disturbed and red fluorescent signal was depleted (Figure A6.1 -f).

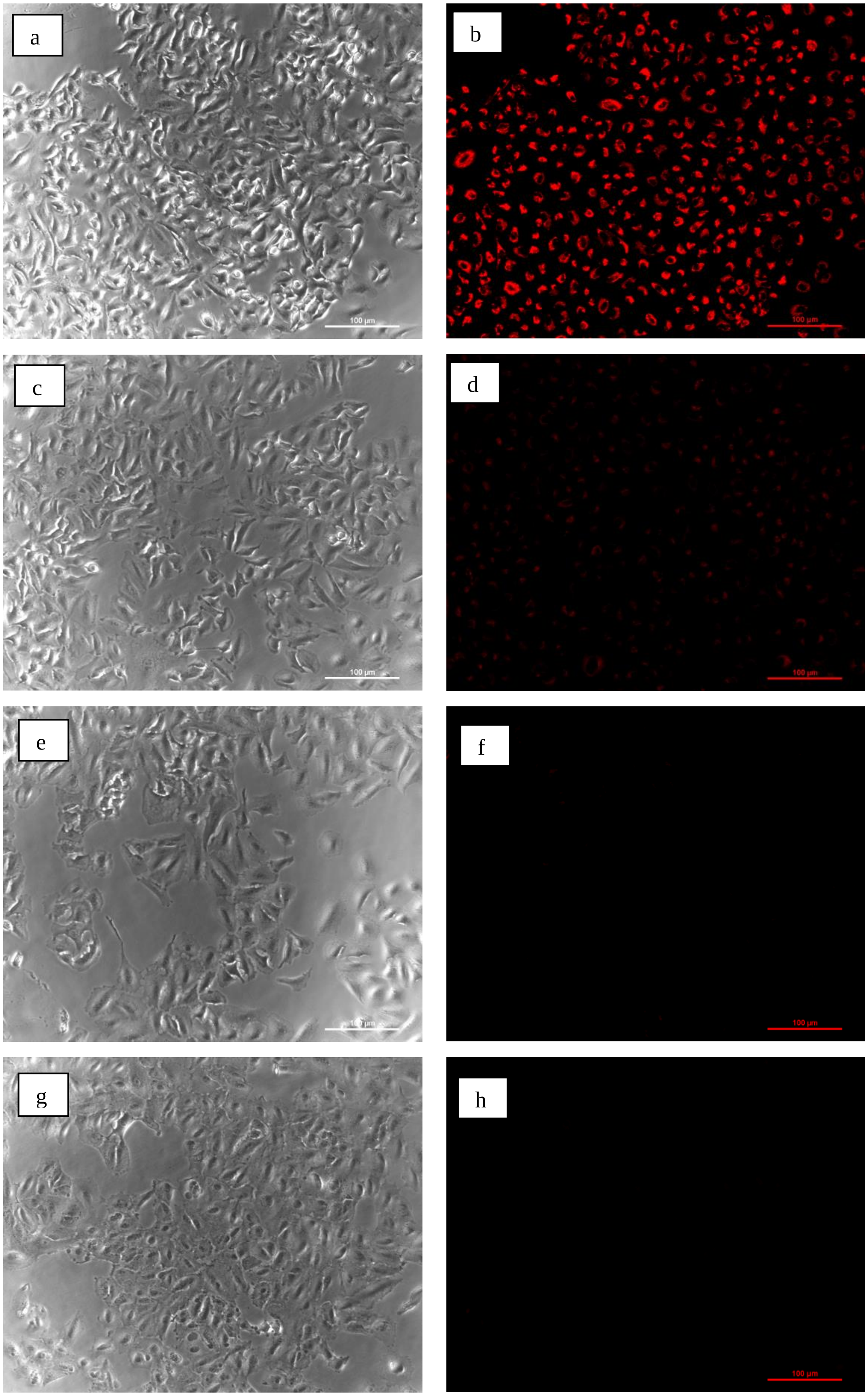
a
b
c
d
e
f
g
h

Figure A6.5: Mitochondrial membrane permeability activity of A549 cells treated with carbonyl cyanide 3-chlorophenylhydrazone (CCCP) for an hour. (a and b) Untreated A549 cells. (c and d) A549 cells treated with 5 µM of CCCP. (e and f) A549 cells treated with 50 µM of CCCP. (g and h) A549 cells treated with 500 µM of CCCP. Loss of mitochondrial membrane potential (represented by the loss of red fluorescent signal) was observed as dose-dependent of CCCP effect.

6.5 Caspase 3/7 activity of A549 cells treated with Camptothecin

Commercially available Camptothecin is a cytotoxic drug that induces apoptosis in mammalian cells via activation of caspases activity. In this study, Camptothecin was employed to be a positive control used to examine for the activation of caspase 3/7 using MagicRed Caspase 3/7 kit in A549 cells. No fluorescent signal was detected for untreated A549 cells indicating no activation of caspase 3/7. While activation of caspase 3/7 causes the cleavage of MagicRed Caspase 3/7 substrate and releasing of cresyl violet fluorophore, which will cause the cells fluoresced in red. A549 cells showed red fluorescent signal (Figure A6.2 -d) as the cells were treated with 0.625 µg/ml of Camptothecin.

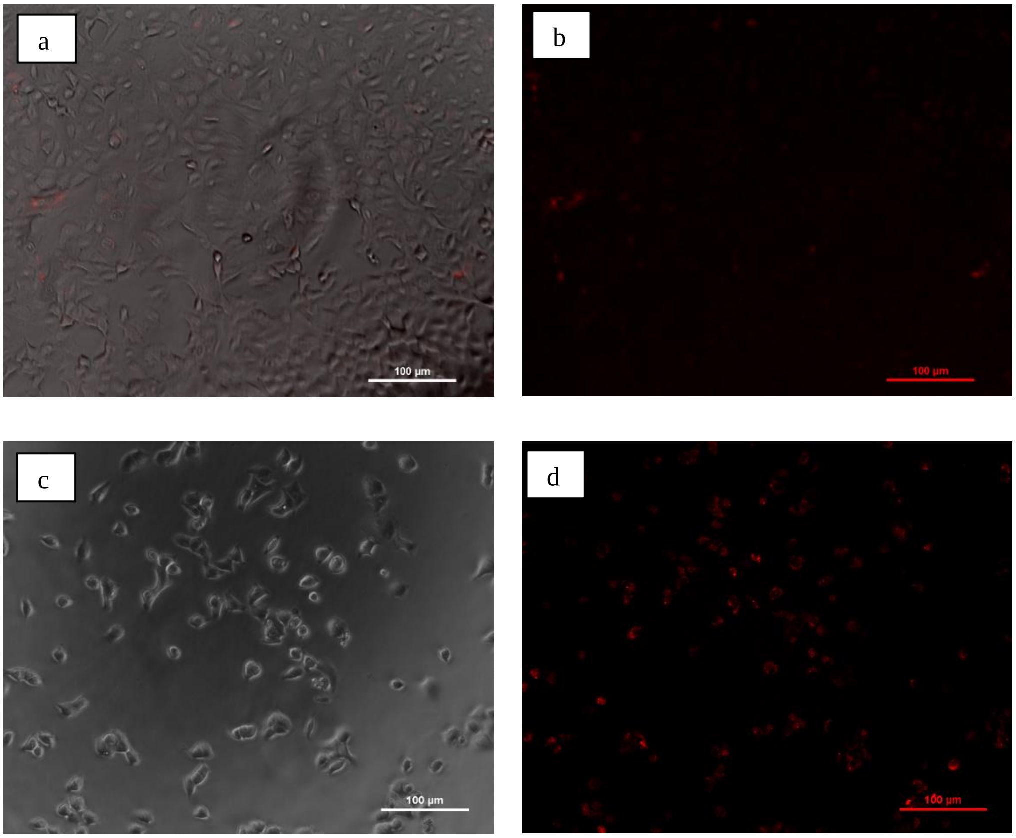

Figure A6.6: Caspase 3/7 activity of A549 cells treated with 0.625 µg/ml of Camptothecin for 2 days post incubation. (a and b) Untreated A549 cells. (c and d) A549 cells treated with 0.625 µg/ml of Camptothecin. Activation of caspase 3/7 was detected on A549 cells (red fluorescence) treated with Camptothecin.